

Stratigraphy and facies architecture of the uppermost fan system in the Tanqua sub-basin, Permian Ecca Group, South Africa

By

Willem C. van der Merwe



**Thesis presented in partial fulfilment of the requirement for the degree of Master of
Geology at the University of Stellenbosch.**



Geology
Stellenbosch University

**Study leader
Dr H. de V. Wickens**

December 2005

Declaration:

I, the undersigned, hereby declare that the work contained in this thesis is my own original work and that I have not previously in its entirety or in part submitted at any university for a degree.

W.C. van der Merwe

Abstract

Fan System 5 forms the uppermost submarine fan system of the Permian-age Tanqua Fan Complex (Ecca Group) of the southwestern Karoo Basin. It is the most widespread system and represents the final phase of fan deposition in the Tanqua sub-basin. Depositional characteristics differ markedly from the rest of the fan systems, mainly because it lacks sedimentary features indicative of a single point source basin floor fan. The entire system consists of six different stages of fan growth and development in the lower slope settings.

A hypothetical model was composed for Fan System 5 to understand the spatial/temporal distribution of reservoir and seal facies in slope turbidite settings. The facies vary from massive amalgamated sandstone beds to thin-bedded, ripple cross-laminated sand and siltstone beds. A thick shale unit identified as a regional marker layer overlies Fan System 5. Its base is defined by the presence of a regionally developed 20 cm thick hemipelagic shale unit.

Six sand-rich units with channel-complexes are present in the Klein Hangklip, Groot Hangklip, Kalkgat, Tongberg, Skoorsteenbergr and Blauwkoop localities. The facies characteristics in the southernmost outcrops of Fan System 5 (Groot Hangklip, Tongberg and Kalkgat) reflect deposition in a lower slope setting where local structural control seems to have played a major role in the distribution and regional development of channel-fill and overbank depositional elements.

The channel-fills are arranged in vertical to off-set stacking patterns and are comprised of massive, amalgamated fine to very fine-grained sandstone units up to 30 m in thickness. They are separated by thinner sandstone/siltstone units of varying thickness. The channelization displayed by the more proximal outcrops are interpreted to represent an upper fan, deposited in a lower- to mid-slope setting. In contrast to the channel-fill deposits at Skoorsteenbergr, Klein Hangklip and Groot Hangklip, ripple cross-laminated overbank deposits, associated with smaller channel-fill units, predominate in the northeastern and eastern parts of the outcrop area. Massive- and thin-bedded frontal sheet sandstones constitute the down-dip extensions to the most northern outcrops of Fan System 5.

Highly erosive, stacked base-of-slope channel complexes, seemingly controlled by subtle early structural features, were able to construct significant thicknesses of regionally well-developed overbank deposits, marginal to the channel complexes. These facies changes occur over relatively short distances, which hold significant implications for the prediction of and the heterogeneity of reservoir facies in slope settings.

Gradients are much steeper in the lower slope to mid-slope area than on the proximal basin floor. The occurrence of soft-sediment deformation in the overbank and upper parts of the channel-fill deposits supports a slope origin. Weakly developed wave-ripple marks in the uppermost layers of Fan System 5 further indicate that water depths approached wave base prior to deposition of the upper markerbed shales.

Paleotransport for Fan System 5 was towards the north, northeast and east. The palaeocurrent directions of the channel-fill complexes in Klein- and Groot Hangklip seem to roughly correspond to the structural trend of synclinal depressions in this area. However, the effect and influences of basin floor topography and structural features on deposition were determined to be minimal on the regional development and local facies control of the fan.

Uittreksel

Waaiersisteam 5 vorm die laaste submarine waaiersisteam van die Perm-ouderdom Tankwa Waaierkompleks (Ecca Groep) in die suidwestelike Karoo-kom. Dit vorm die mees wydverspreide sisteem en verteenwoordig ook die finale fase van waaierafsetting in die Tankwa sub-kom. Afsettingseienskappe verskil aansienlik van die onderliggende waaiersisteme, omdat kenmerkende sedimentêre eienskappe van 'n enkele toevoer bron ontbreek. Die hele sisteem bestaan uit ses verskillende periodes van waaiergroei en ontwikkeling in die laer komhelling omgewings.

'n Voorspellingsmodel is opgestel vir Waaiersisteam 5 om die ruimtelike/temporele verspreiding van die reservoir en seël fasies in komhelling turbidiet omgewings te kan verstaan. Hierdie fasies varieer van massiewe, geamalgameerde sandsteen tot dun gelaagde riffel- lamineerde sand- en sliesteenlae. 'n Dik regionale skalie eenheid oorkê Waaiersisteam 5 en vorm die boonste merkerlaag. Die basis word onderlê deur 'n 20 cm dik regionaal ontwikkelde hemipelagiese skalie laag wat die onderste merkerlaag vorm.

Ses sandige eenhede met geassosieerde kanaalkomplekse is onderskeidelik teenwoordig in: Klein Hangklip, Groot Hangklip, Kalkgat, Tongberg, Skoorsteenberg en Blauwkop omgewings. Die fasies-eienskappe van die mees suidelike dagsome van Waaiersisteam 5 (Tongberg, Groot Hangklip en Kalkgat) toon afsetting in 'n laer komhelling omgewing, waar plaaslike tektoniese effekte moontlik 'n groot rol gespeel het in die verspreiding en regionale ontwikkeling van die kanaalvulsels en geassosieerde oewerwal-afsettings.

Die gestapelde, wegstand kanaalvulsels-afsettings bestaan uit massiewe, geamalgameerde fyn tot baie fynkorrelrige sandsteen eenhede, wat diktes tot ongeveer 30 m kan bereik. Dit word van mekaar geskei deur dun sandsteen/sliesteen eenhede van afwisselende diktes. Die kanaal komplekse in die mees proksimale dagsome word interpreteer as 'n bo-waaier, wat afgeset is in 'n laer- tot middel komhelling omgewing. In teenstelling met die kanaalvulsels in die Skoorsteenberg, Klein Hangklip en Groot Hangklip omgewings, domineer riffel kruis-gelamineerde oewerwal-afsettings, geassosieer met klein kanaalvulsels, die noordoostelike en

oostelike dagsome van Waaiersisteam 5. Massiewe en dungelaagde frontale plaat sandstene, kom voor in die distale helling-omgewings in die mees noordelike dagsome van Waaiersisteam 5.

Hoogs eroderende, gestapelde kanaalkomplekse, aan die basis van die komhelling wat moontlik beheer is deur vroeë komvloer topografie, was die oorsaak vir regionaal goed-ontwikkelde oewerwalafsettings. Hierdie fasies-verandering vind plaas oor 'n baie kort afstand wat betekenisvolle gevolge inhou vir die voorspelling van heterogeniteit van petroleum reservoir fasies in komhelling afsetting-omgewings.

Die gradiënt vir die laer komhelling tot mid-komhelling omgewings is baie steiler as die distale komvloer omgewings. Die voorkoms van sagte-sediment deformasies in die oewerwal en bo-liggende dele van die kanaalvulsels weerspeël 'n moontlike komhelling omgewing. Swak-ontwikkelde golfriffelmerke in die boonste lae van Waaiersisteam 5 dui 'n waterdiepte aan wat naby aan golf-basis is, voordat dit deur diepmariene skalies oorlê word.

Paleovloeirigtings vir Waaiersisteam 5 was in 'n noord, noordoostelike en oostelike rigting. Die paleovloeirigting vir die Klein- en Groot Hangklip kanaalkomplekse stem min of meer ooreen met die strukturele grein van die sinklinale laagtes in die omgewing. Die effek en beheer van komvloer topografie en ander strukturele faktore op afsetting was minimaal op die regionale ontwikkeling en plaaslike fasies verspreiding van die waaier.

Acknowledgements

The fieldwork for this project was carried out from May to September 2004 under the precise guidance of Dr. H. de V. Wickens in the Ceres/Tanqua Karoo. Few students have had the opportunity to do research for six years under the supervision of an expert such as Dr Wickens. His support and patience are highly appreciated. I also wish to thank him for the financial support concerning the renovation of the field house, which was used as base camp for the duration of my fieldwork.

I would not have been able to complete my studies without the support of my family and friends. I wish to thank my parents Marié and Bennie van der Merwe for their help and encouragement over the years and specially my mother for her love, patience and support through all these years. She always helped me to stay focused. Special thanks to uncle and aunt Hannes and Elmarie Theron for their encouragement and the lending of field equipment.

I am grateful towards my brother, Schalk, who visited me while I was doing my fieldwork and towards my sisters, Hannelie and Cila, for their loving support. To my dearest friends: Etienne, Ruhan, Annemarie, Elistea, Leandrie, Liezel, Ryno, Jeandré, Christiaan, Corlie, Marko and Jaco, your encouragement and true friendship meant a lot to me. A special word of thanks to Johan and Cornelia de Kock for moral support over a period of three years and to my landlady Mrs Mathee for her interest in my project.

I sincerely appreciate the fact that Dawie le Roux and his family accommodated me on their farm Bizansgat for the five months of my fieldwork. The cups of hot coffee during cold winter evenings will not be easily forgotten.

To all the farm owners in the area where I did my research, a very special word of thanks. They always received me with typical Afrikaner warmth and hospitality and this changed the mapping during the cold winter months into a long summer holiday.

The project was carried out with the financial support (bursaries and other funds) from the Department of Geology of the University of Stellenbosch.

Bedankings

Die veldwerk vir hierdie projek is gedoen onder die noukeurige leiding van Dr H. de V Wickens, oor 'n periode van 5 maande (Mei tot September) gedurende 2004 in die Ceres/Tankwa Karoo. Min studente het die geleentheid om vir ses jaar onder die leiding en aanmoediging van so 'n meester in veldgeologie te kon wees. U ondersteuning en geduld vir al die jare word opreg waardeer en sal altyd onthou word. Dr Wickens word ook bedank vir sy persoonlike befondsing vir herstel van die veldwerkhuis wat as basiskamp vir die duur van die projek gedien het.

Om 'n tesis van enige formaat te skryf, verg baie geduld en ondersteuning van jou familie, vriende en geliefdes. Daarom wil ek graag my Ma (Marié) en Pa (Bennie) bedank vir al hul belangstelling en aanmoediging. 'n Spesiale woord van dank vir my Ma vir haar geduld, liefde, ondersteuning en bystand deur al die jare, dit het my baie gehelp het om my fokus te behou. Spesiale dank gaan ook aan my broer (Schalk) en sy kuier in die veld en ook vir al ons genotvolle geselsies. Ook vir my twee susters, Hannelie en Cila baie dankie vir jul aanmoediging en liefdevolle ondersteuning. Vir Oom Hannes en Tannie Elmarie wil ek bedank vir die leen van veldtoerusting en ook vir hul aanmoediging met die projek.

Aan naby vriende: Etienne, Ruhan, Annemarie, Leandrie, Liezel, Ryno, Jeandré, Christiaan, Corlie, Marko en Jaco wat regtig baie geduld vir my en die projek gehad het, wil ek opreg bedank, julle vriendskap sal altyd onthou word. Spesiale dank gaan aan Annemarie se ouers (Oom Johan en Tannie Cornelia) vir hul morele ondersteuning en belangstelling die afgelope drie jaar. My opregte dank gaan ook aan Tannie Mathee by wie ek loseer het in Stellenbosch vir haar ondersteuning.

Spesiale dank ook aan Dawie le Roux en sy familie vir die verblyf op sy plaas (Bizansgat) tydens die 5 maande veldwerk, en sy warm welkom en koffie tydens die koue winter maande.

Laastens wil ek graag al die plaaseienaars in my veldwerkgebied opreg bedank vir hul tipiese warm Boereontvangs. 'n Geselsie en 'n koffie hier, en 'n bietjie boerreraat daar, het die kartering deur die winter, 'n somervakansie gemaak.

Die skrywer bedank die Departement van Geologie van die Universiteit van Stellenbosch met die verskaffing vir die nodige beurse en befondsing van hierdie projek.

Table of Contents

Abstract.....	iii
Uittreksel.....	v
Acknowledgements.....	vii
Bedankings.....	viii
Table of Contents.....	x
1. Introduction.....	1
1.1 General.....	1
1.2 Geological setting.....	2
1.3 Stratigraphic evolution of the Tanqua sub-basin.....	3
1.4 Sedimentation in the Tanqua depocentre.....	4
1.5 Previous research on FS 5.....	5
1.6 Aims and objectives of this study.....	7
1.7 Data set and methodology.....	7
2. Tectonic setting and structural evolution.....	13
2.1 General.....	13
2.2 Structure in the study area.....	14

3. Current models for deep-water fans.....	22
3.1 General.....	22
3.2 Brief review of turbidite models.....	23
3.3 Comparison of fan models.....	25
3.4 Facies associations and architectural elements of the Tanqua Fan Complex: A Review.....	25
3.4.1 Facies associations.....	25
3.4.2 Architectural elements.....	26
3.5 Distribution of architectural and facies elements for the lower four submarine Fans.....	27
4. Sedimentary characteristics of Fan System 5 (FS 5).....	40
4.1 General.....	40
4.2 Paleogeography.....	41
4.2.1 Interpretation of paleoflow patterns.....	41
4.3 Regional fan evolution.....	46
4.3.1 Klein Hangklip.....	46
4.3.2 Tongberg.....	46
4.3.3 Skoorsteenbergr.....	47
4.3.4 Blauwkoop.....	47
4.3.5 Groot Hangklip.....	47
4.3.6 Kalkgat.....	48
4.4 Lithofacies description and interpretation.....	51
4.4.1 Lithofacies 1 (Massive-bedded sandstones).....	51
4.4.2 Lithofacies 2 (Parallel- and ripple cross-laminated sandstones).....	52
4.4.3 Lithofacies 3 (Sigmoidally and wavy ripple cross-laminated sand- and siltstones).....	54
4.4.4 Lithofacies 4 (Parallel- and ripple cross-laminated siltstones).....	55

4.4.5 Lithofacies 5 (Thin-bedded sandstone, siltstones and shales).....	56
4.4.6 Lithofacies 6 (Erosional and bypass facies).....	57
4.4.7 Lithofacies 7 (Convolute laminated sandstones).....	58
4.4.8 Lithofacies 8 (Slumped units).....	59
4.4.9 Lithofacies 9 (Hemipelagic shales).....	61
4.4.10 Lithofacies 10 (Micaceous and carbonaceous siltstones).....	62
4.5 Measured sections and correlation framework.....	75
4.5.1 General.....	75
4.5.2 First-order correlation (regional markerbeds).....	76
4.5.3 Second-order correlation (stratigraphic entities).....	77
4.5.4 Third-order correlation (high-resolution internal bed architecture).....	77
4.6 Vertical and lateral facies development and correlation.....	78
4.6.1 Klein Hangklip complex.....	78
4.6.2 Tongberg complex.....	79
4.6.3 Skoorsteenbergs complex.....	80
4.6.4 Blauwkop complex.....	82
4.6.5 Groot Hangklip complex.....	83
4.6.6 Kalkgat complex.....	84
4.7 Internal architecture and geometry.....	101
4.7.1 Channel development.....	101
4.7.1.1 General.....	101
4.7.1.2 Klein Hangklip complex.....	104
4.7.1.3 Tongberg complex.....	106
4.7.1.4 Skoorsteenbergs complex.....	108
4.7.1.5 Blauwkop complex.....	109
4.7.1.6 Groot Hangklip complex.....	111
4.7.1.7 Kalkgat complex.....	112
4.7.2 Lateral accretion deposits (LADs).....	128
4.7.3 Overflow deposits (overbanks).....	131
4.7.4 Levee deposits.....	135
4.7.5 Frontal splays (sheet sands).....	138
4.7.6 Slump elements.....	142

4.8 Influence of basin floor topography on deposition.....144

5. Sequence Stratigraphy.....145

5.1 General.....145

5.2 Fan System 5.....146

 5.2.1 Sequence framework.....146

 5.2.2 Key surfaces.....147

 5.2.3 Condensed intervals.....147

 5.2.4 Flooding surfaces.....148

 5.2.5 Systems tract.....150

 5.2.6 A sequence stratigraphic model for FS 5.....150

 5.2.7 Summary.....153

6. Discussion.....166

6.1 Architectural elements.....166

6.2 Stages of fan development.....168

6.3 Depositional model.....170

 6.3.1 Type of slope setting.....170

 6.3.2 Multi-source versus point-source.....171

 6.3.3 Sequence stratigraphy.....172

7. Conclusions.....176

References.....179

Appendix.....198

Chapter 1

Introduction

Chapter 1

Introduction

1.1 General

The name “Tanqua” originated from Sanqua, a old name for the nomadic Bushmen ethnic group of people who originally lived in this area. The name was first given to the main river (Tanqua River) flowing westward through the middle of the Tanqua Karoo. The western Karoo is characterized by a dry, semi-desert climate with low rainfall (less than 100mm per annum) and very low vegetation (less than 1m). This makes the area unique for geological research because of the good exposure. The study area in the Ceres/Tanqua Karoo stretches from the farm Lower Roodewal in the south to the foot of Ouberg Pass, 55km to the north (Fig 1.1 + Fig. A).

There has been a rapid growth of interest in research and exploration for deep-water clastic depositional systems in slope settings by the oil industry in recent years. The main focus is on passive margin settings, such as the deep-water exploration fields along the West-African coast, where good reservoirs have been proven to exist. The Tanqua Fan Complex (TFC), which constitutes the Skoorsteenberg Formation of the Ecca Group in the western Karoo (Wickens, 1994), hosts one of the world’s best examples of well-exposed slope to basin-floor turbidites (Figs 1.3-5). These exceptional exposures allow detailed studies in both vertical and lateral sections, thereby providing the opportunity to evaluate the temporal and spatial evolution of the turbidite systems within the basin-fill succession (Figs 1.5-6).

The Tanqua sub-basin contains five regionally extensive submarine fan systems, deposited between 260 and 250 Ma (Fig. 1.2+5). Recently obtained data suggest a Mesoproterozoic age for the source material (Andersson *et al.*, 2003; Van Lente, 2004). Wickens *et al.* (1992) indicate that transport into the southwestern Karoo Basin were from the south, southwest and west (Fig. 1.2). Recent projects in the Tanqua have concentrated mainly on the 3D digital mapping (Petrel models) of the lower 4 fan systems (Hodgson *et al.*, 2006) and the lower slope setting (Wild *et al.*, 2004).

The uppermost fan system of the TFC, referred to as Fan System 5 (FS 5) in this thesis, represents the final phase of fan deposition in the Tanqua sub-basin, with sedimentary characteristics indicative of a deposition in a base-of-slope to basin floor setting. Of all fan systems, FS 5 is regionally most extensively developed, covering an area of more than 610 km² (Fig. A). It is separated from the underlying fan unit (Fan 4) by a thin, hemipelagic shale succession and overlain by a dark shale unit that clearly defines the top of the succession on a regional scale. Fan thickness is consistent throughout most of the outcrop area with gradual thinning towards the northeast. The area of fan termination (pinch out) gives the impression of a progressive thinning from a more sandy unit to a silty-shale and eventually, dark hemipelagic shales.

FS 5 comprises six sand-rich units of fan construction, occupying clearly defined stratigraphic intervals. Each of these units is characterized by channel complexes comprising vertically and laterally stacked sandstones and overflow deposits that are genetically linked to the channel complexes. Palaeoflow varies from east to northeast. The grain-size of the sandstone varies from fine to very fine-grained. The Kalkgat, Groot Hangklip, Tongberg and Klein Hangklip exposures form the southernmost sand-rich units of FS 5. The Blauwkop and Skoorsteenbergs exposures form the northern sand-rich units of FS 5.

FS 5 was previously known as Fan 5 (Wickens, 1994; Johnson *et al.*, 2001) and also recently presented as Unit 5 by Hodgson *et al.* (2006). On account of new evidence, which will be presented in this thesis, "Fan 5" consists of 6 major sand-rich units which, combined, constitute Fan System 5.

1.2 Geological setting

The Tanqua sub-basin is situated in the western part of the south-western Karoo Basin (Figs 1.1.a+b+c). With a 2-4° dip to the east, cover the TFC outcrops an area of approximately 650 km², and are almost structural undisturbed. The TFC comprises five individual fine-grained, sand-rich fan systems that are from 20 to 70 m thick, which alternate with shale-rich interfan units of similar thicknesses (Wickens, 1994). The Cape Fold Belt (CFB) consists of two branches, which flank the main Karoo Basin, namely the westward trending Swartberg Branch

and the northward trending Cedarberg Branch (Figs 1.1+2). The Swartberg and Cedarberg branches have undergone crustal shortening of 40% and 10% respectively (De Beer, 1990, 1992). Both these mountain ranges coalesce (or ‘amalgamate’) in the Hex River Mountains between the towns of Worcester and Ceres (Fig. 1.2). During the coalescence of the two branches, two major NE-trending anticlinal structures, namely the Hex River and Baviaanshoek, developed. During the development of the southwestern Karoo Basin, the two regional scale anticlines acted as an early basin floor high which separated the Tanqua sub-basin in the west from the Laingsburg sub-basin in the east (Fig. 1.2).

1.3 Stratigraphic evolution of the Tanqua sub-basin

The Ecca Group basin-fill succession ranges in age from Late Carboniferous (Visser, 1997) to Late Permian (Anderson and Cruickshank, 1978), i.e. from ± 310 to ± 250 Ma on the time scale of Haq and Van Eysinga (1987). The fan deposits in the northern part of the basin are tectonically almost undeformed, remarkably well exposed, and easily accessible.

According to Wickens (1994), the following tectono-sedimentary and stratigraphic properties characterise the Tanqua sub-basin-fill sequence:

- Almost no structural deformation of the turbidite, deltaic and fluvial sequences, except in the southern part.
- Deposition of five discrete fine-grained individual fan systems alternating with thick basin shale units.
- Development of laterally extensive “lobe/sheet” turbidite deposits, channel-fill complexes and associated overbank deposits.
- Mudstone-rich fluvial-dominated deltaic deposits are abruptly succeeded by high-sinuosity meander belt and floodplain deposits.
- Pinch-out areas of fans are characterised by sheet sands displaying lateral variation in thickness, which suggest an uneven finger-like outer fan margin.
- The Tanqua basin-fill deposits have an overall low sandstone/shale ratio and a fine to very fine grain-size for all the sands throughout the entire turbidite, deltaic and fluvial deposits of the lower Beaufort Group.

- Outcrops of the fan complex are laterally continuous and represent a basin floor to slope setting.
- Outcrops in the southern and northern part of FS 5 are tectonically disturbed and poorly exposed in some areas, which makes stratigraphic mapping very difficult (Van der Merwe, 2003) (Fig. A).

The above mentioned attributes are atypical of most active margin settings. It is suggested that the tectonic activities that predominated during submarine fan and deltaic deposition reflected conditions more typical of passive margin settings (Wickens, 1994). The diagnostic features of a passive margin setting are: a distal source, wide coastal plain and shelf, low depositional gradient, low sand/mud ratio and a large basin (Shanmugam and Moiola, 1988). The spatial and temporal distribution of the Tanqua submarine fan deposits, as well as the overlapping relationship of the western and southern deltaic systems are directly related to the structural development of the Cape Fold Belt (CFB) (Wickens *et al.*, 1990; De Beer, 1990, Wickens, 1994).

1.4 Sedimentation in the Tanqua depocentre

The Karoo Basin developed from a retro-arc basin, which relates to accretionary tectonics along the southern margin of Gondwana. Deposition in the basin commenced with the glaciogenic deposits of the Dwyka Group. This glaciation period, an event of an intensity and extent unparalleled in the Phanerozoic history of the earth, marked the onset of Karoo sedimentation in the Late Carboniferous (300-310 Ma, Westphalian). It was preceded by a hiatus of approximately 30Ma after the termination of the Witteberg Group sedimentation (Fig. 1.3) (Wickens, 1994). Ecca Group sedimentation commenced with rapid basin subsidence indicated by the succession of transgressive marine shales of the Prince Albert Formation (Bangert *et al.*, 1999), the carbonaceous shales of the Whitehill Formation, and the very fine-grained turbiditic sandstones of the Collingham Formation (Wickens, 1994; Turner, 1999) (Fig. 1.3). The Whitehill Formation accumulated in water with restricted circulation in depths of up to 150 metres. Surface waters hosted pelagic organisms, e.g. mesosaurid reptiles and palaeoniscid fishes. A benthic fauna, e.g. *Notocaris tapscottii*, and numerous insect fossils, which are the oldest in Africa is also present (Cole and Mclachlan, 1991; Geertsema and Van den Heever, 1996, 2000). The high concentration of tuff beds in the Collingham Formation indicates an important contribution from

volcanic ash clouds, derived from a Permian arc, speculated to have been situated in what is known today as northern Patagonia (Breitkreutz *et al.*, 1989).

In the Tanqua sub-basin, the Collingham Formation is overlain by Tierberg Formation. The latter represents deep-water suspension deposition that was periodically interrupted by deposition of five arenaceous submarine fan systems that constitute the Skoorsteenberg Formation (Bouma and Wickens, 1991; Wickens, 1994; Johnson *et al.*, 2001 – Figs 1.4+5+6).

Fan deposition is believed to have been controlled by fluctuations in relative sea-level, probably caused by local tectonic or isostatic factors rather than eustatic changes. The duration of cyclic deposition for the entire basin-fill may be as little as 3-5 Ma (Visser, 1990, 1993), favouring eustatic dominance over high-frequency or pulsating tectonism. Continuous volcanic activity in the magmatic arc is reflected by occasional tuff beds present in the shale units. Regression continued after deposition of FS 5 with the Kookfontein Formation becoming more bedded, changing into pro-delta and delta front deposits. The final phase of Ecca deposition was reached when large, highly constructive deltas of the Waterford Formation prograded from the south, west and north-west into the basin (Figs 1.3-5). The deltaic deposits overlap along the north-east trending anticlinal structures.

Different rates of sub-basin subsidence and sub-basin geometry could have had an influence on the rate of delta progradation and volume of sediment accumulation. More rapid subsidence of the Laingsburg sub-basin probably created more accommodation space that retarded deltaic progradation. The more stable western margin may account for the thickness and more rapid progradation of the Koedoesberg deltas (Wickens, 1994). Extensive, sub-aerially exposed, upper delta plain sediments were deposited behind the prograding delta lobes, mainly as aggrading overbank splays. The upper delta plain soon became a typical fluvial environment where sediments accumulated under arid to semi-arid conditions. The fluvial succession hosts abundant caliche horizons, silicified gypsum rosettes (Wickens, 1994) and the oldest land-living mammal-like reptiles known in South Africa (Rubidge, 1991).

1.5 Previous research on FS 5

Several studies have documented the regional stratigraphy and sedimentology of FS 5 over the last few years. The initial studies on this fan complex by Wickens *et al.* (1992), Wickens (1994); Wickens and Bouma (2000) concluded that Fan 5 (FS 5) consists of two major depositional phases, namely the Skoorsteenberg and Blauwkop phase, and a third depositional phase in the south, called 'Fan 6'. The latter was interpreted as a separate fan due to the uncertain stratigraphic relationships caused by structural complexities in the southern outcrop region.

Wickens (1994) interpreted the Blauwkop channel-fills to be a channel complex with associated levee/overbank deposits. A detailed study by Kirschner and Bouma (2000) and Basu and Bouma (2000) concluded that the Blauwkop channel complex is a distributary channel system with seven individual channel-fills, levee, and crevasse splay deposits.

Winters *et al.* (1995) studied the outcrops of FS 5 in the Skoorsteenberg area. Their interpretation concluded that the outcrop represents an amalgamated channel complex with individual channel-fills at the base with non-amalgamated channels and interchannel/overbank deposits in the upper part. They also noted that classic levee deposits, which are commonly associated with channels, are absent in these outcrops.

Johnson *et al.* (2001) characterized FS 5 in the Skoorsteenberg area as a fan with a major channelised depocentre with limited lateral extent and therefore were the first to identify FS 5 as a slope fan. The depositional characteristics of the Hangklip Fan or "Fan 6" are revealed in detailed work by Bouma and Wickens (1991, 1994), Wickens and Bouma (1998), Neethling (1992), Wach *et al.* (2000) and Johnson *et al.* (2001).

These fan systems have been the focus of a recent comprehensive, integrated outcrop-core-log study, namely the EU/Industry co-funded 'NOMAD' (Novel Modelling Analogue Data for more efficient exploitation of deepwater hydrocarbon reservoirs) project. Drilling and full coring and logging of seven wells (NS1, NS2, NS3, NS4, NB2, NB3, and NB4) in locations identified as being strategically important in developing an accurate and extensive 3D geologic and reservoir model, provided significant additional data. A total length of 1247 m of core was recovered and

logged at a 0.5 cm scale (Hodgson *et al.*, 2006). Present research falls under the Slope-project, a joint venture between the Universities of Liverpool and Stellenbosch, sponsored by the international petroleum industry. Hodgson *et al.* (2006) concluded from NOMAD core data that 'Unit 5' comprises several channel-fill, sheet and overbank elements on different stratigraphic levels.

Wickens (1994), Van der Merwe (2003) and Van der Merwe and Wickens (2004) were the first to describe an additional channel complex in the Klein Hangklip area as consisting of vertical and laterally stacked channel-fills. Van der Merwe (2003) also noted that the "Hangklip Fan" is part of FS 5 and that the Hangklip channel-fill complex represents deposition in a lower base-of-slope setting. Wild *et al.* (2005) also noted this additional system.

1.6 Aims and objectives of this study

The primary aims of this study are:

- A detailed sedimentological and stratigraphic analysis of the uppermost turbidite system of the Tanqua deep-water fan complex, in order to understand the spatial/temporal distribution of lithofacies in slope turbidite settings;
- To develop predictive sedimentological and stratigraphic models for application to petroleum exploration/exploitation by interpreting key surfaces, stacking patterns, internal architecture, facies distribution, and stages of fan growth in slope settings;
- To determine the effect of structural and depositional basin floor topography on regional fan development and local facies control;
- To create a comprehensive dataset on facies characteristics and continuity, channel-fill stacking patterns, channel-fill and sheet morphology, internal channel and overbank architecture, and vertical and horizontal relationships between sandstone units.

1.7 Data set and methodology

Field work was conducted during a six month period in 2004 and involved mainly detailed regional mapping and logging of vertical sections. FS 5 crops out over $\approx 410 \text{ km}^2$ and provides

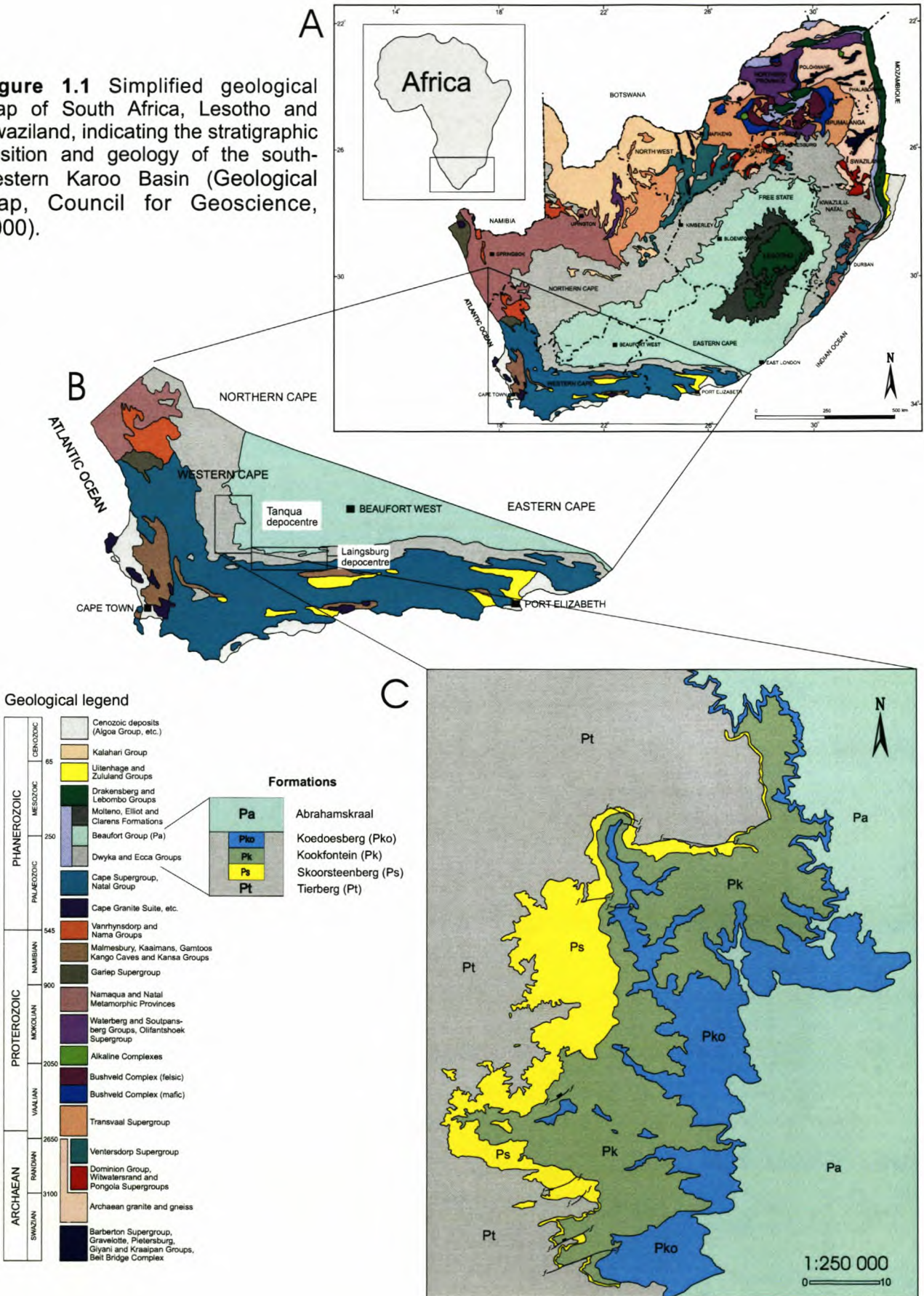
areas of near-continuous outcrop exposure up to 55 km in length. Vertical exposure allows continuous measurement of sections up to 110 m thick. More than 150 vertical sections (6.5 km) were logged in this study at centimetre scale and plotted on aerial photographs, including GPS positions. The excellent quality of outcrops enables “walk-out” of internal architecture as well as individual bedding surfaces. Four slim-hole cores (Hole width = 97mm with core width = 64mm, NOMAD Project) have also been logged and the data have been integrated with the field measurements. Three of the four core sections contain base to top information on FS 5.

Standard geological tools, such as a Jacobs’s staff, Abney level, geological compass, measuring tape, hammer, GPS-equipment (Garmin 12), digital camera (Nikon Coolpix 5.7M with 200mm zoom) and a 35mm camera were used. Throughout the photographs in this thesis has the Jacob staff been used, which consists of 10 cm divisions. Detailed mapping of structural and stratigraphic features was carried out on enlarged (1: 16 000) aerial photographs and subsequently compiled on a 1:50 000 topographical map. All diagrams, schematic figures, vertical sections, fence diagrams and photomontages were edited and compiled with the computer program Corel Draw 12. Over 1610 paleocurrent measurements were recorded from primary sedimentary structures such as groove casts, prod marks, ripple cross-lamination and current lineation. Rose diagrams were constructed from these measurements.

The lithofacies associations and architectural elements of FS 5 have been distinguished by Johnson *et al.* (2001) on the basis of grain-size and primary sedimentary structures. Field mapping and description also included post-depositional features such as soft-sediment deformation and clastic dyke intrusions. The stratigraphic and geographic position of the disturbed intervals and the physical extent and orientation of folds, faults and dykes were recorded.

The 3D lithological variability of the studied system was further characterised by the construction of a series of correlation panels and fence diagrams. Correlations were carried out between the different measured sections in order to describe and interpret the facies associations and internal architecture of FS 5. A detailed field map with interpretations of main channel flow patterns, architectural elements, structure and logged section localities is also included. The combination of field mapping, vertical sections and the interpretation of ground and aerial photomontages enabled a high-resolution stratigraphical correlation framework for FS 5.

Figure 1.1 Simplified geological map of South Africa, Lesotho and Swaziland, indicating the stratigraphic position and geology of the south-western Karoo Basin (Geological map, Council for Geoscience, 2000).



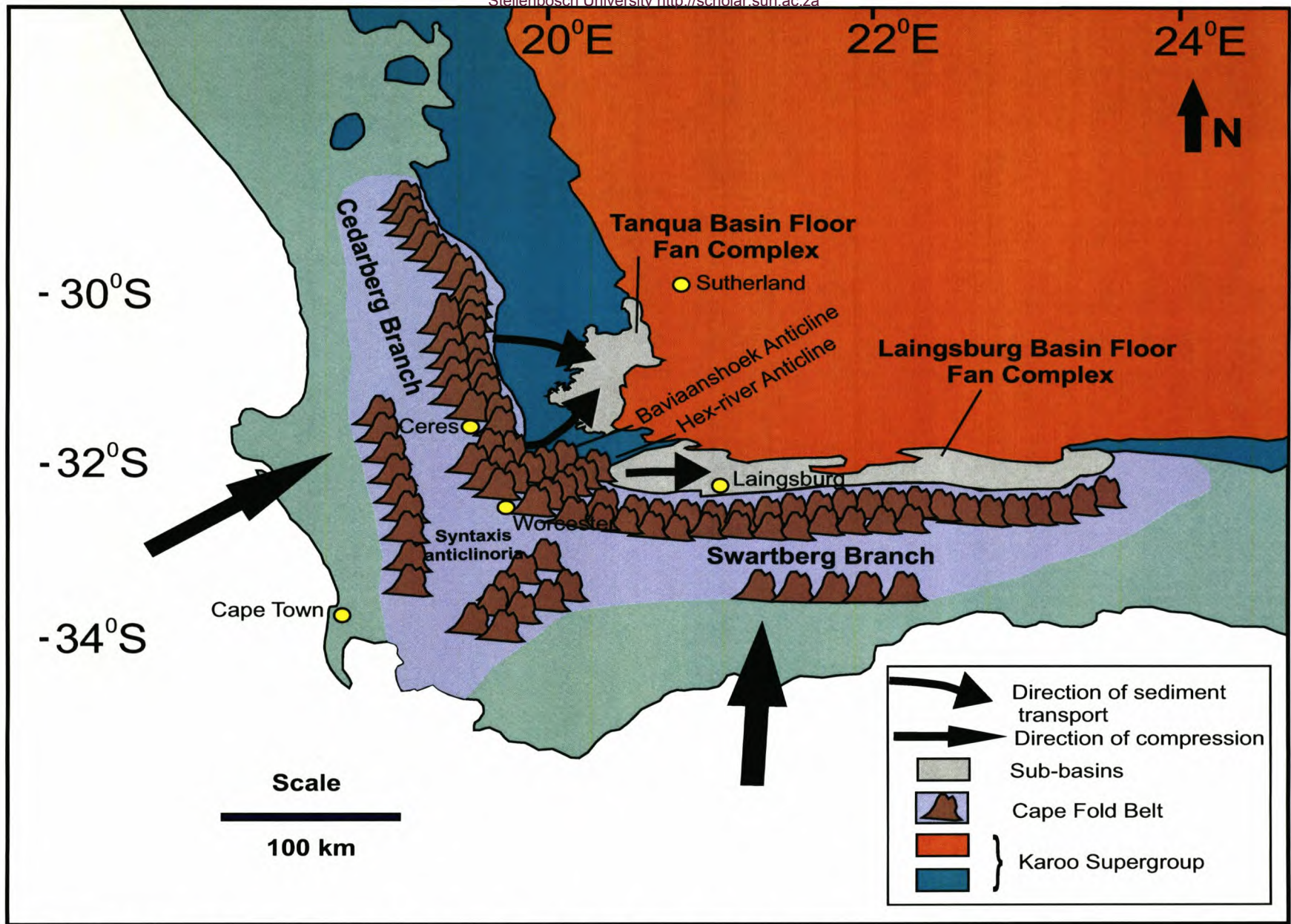


Figure 1.2 Schematic representation of fan deposition in the Laingsburg and Tanqua sub-basins. Main compression and sediment directions are indicated. Only the regional outlines of the Tanqua and Laingsburg fan complexes are shown (redrawn and modified from Wickens, 1994).

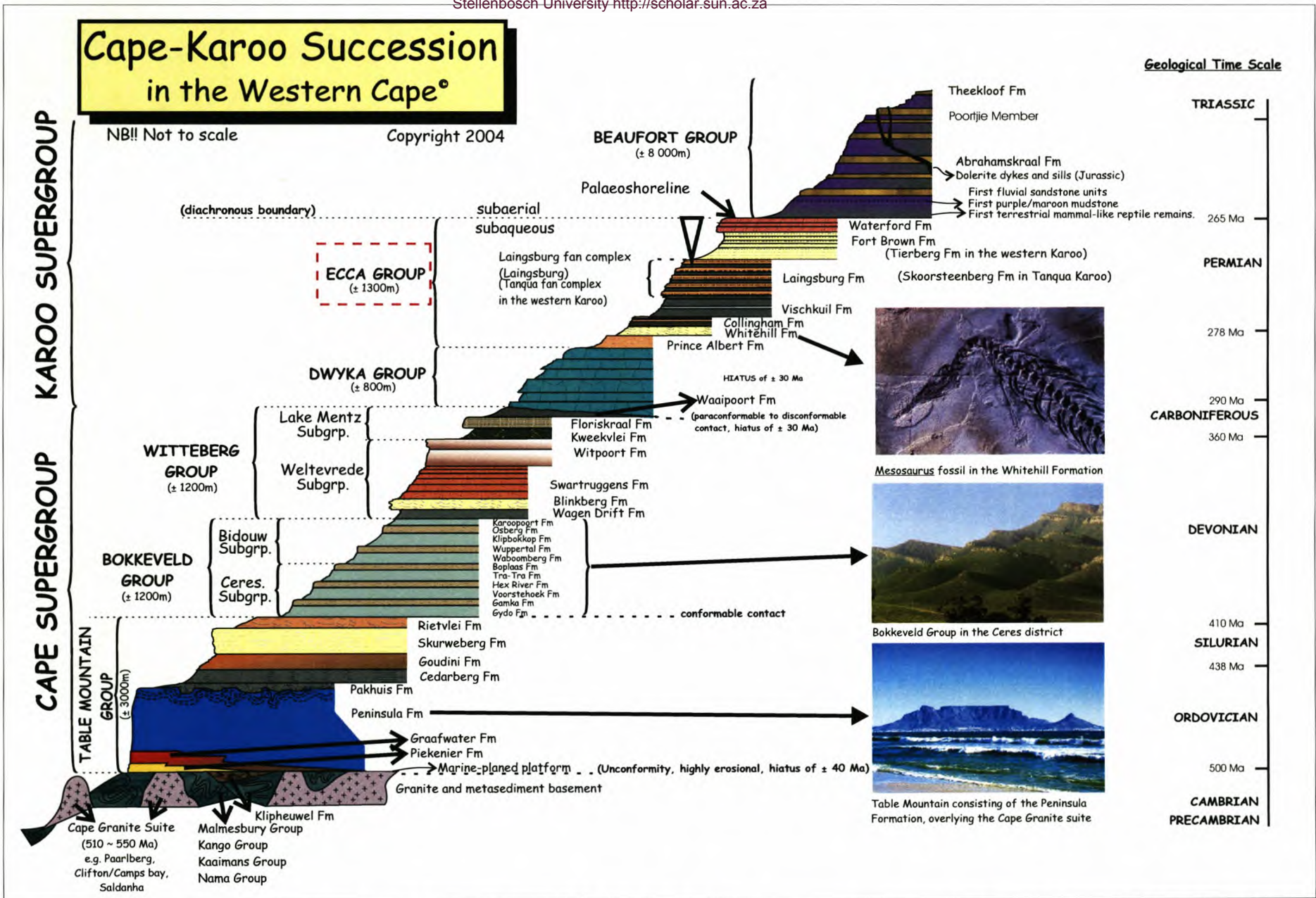


Figure 1.3 Schematic representation of the stratigraphy of the Cape and Karoo Supergroups (compiled by Wickens 1994, modified by Van der Merwe, 2003)

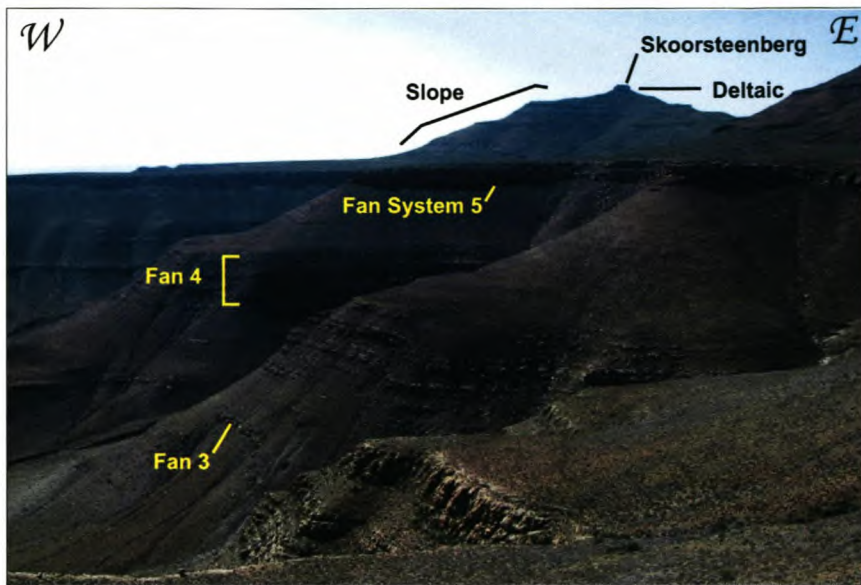


Figure 1.4 Upper part of the Skoorsteenberg Formation in the Tanqua Karoo.

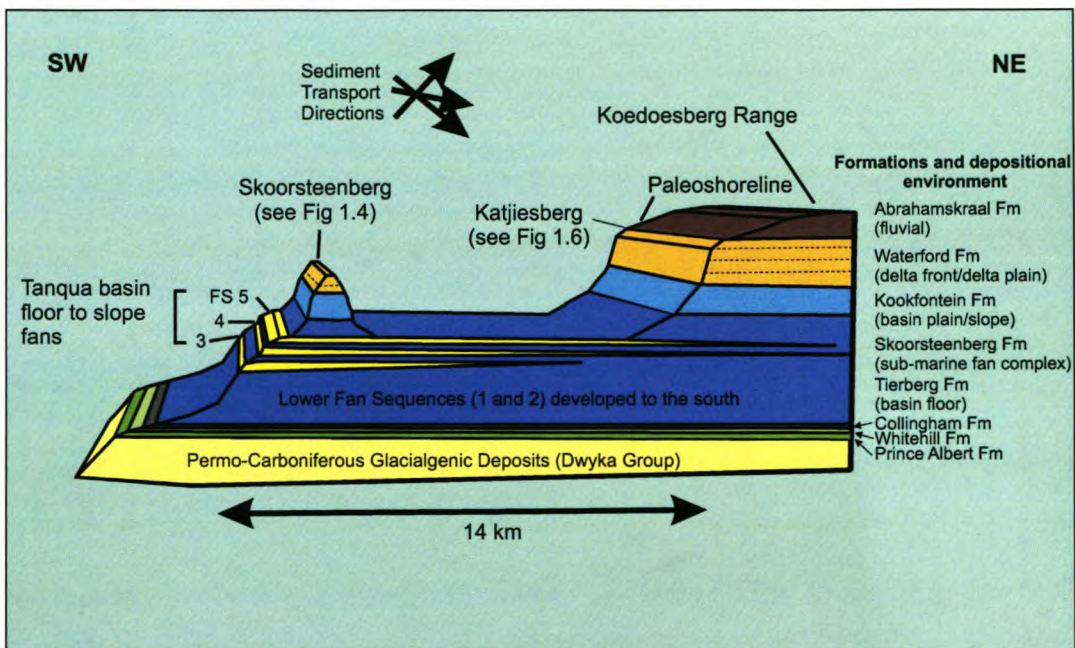


Figure 1.5 Schematic cross-section in the Katjiesberg area (northern outcrop) of the Tanqua sub-basin (modified after Wickens, 1994).

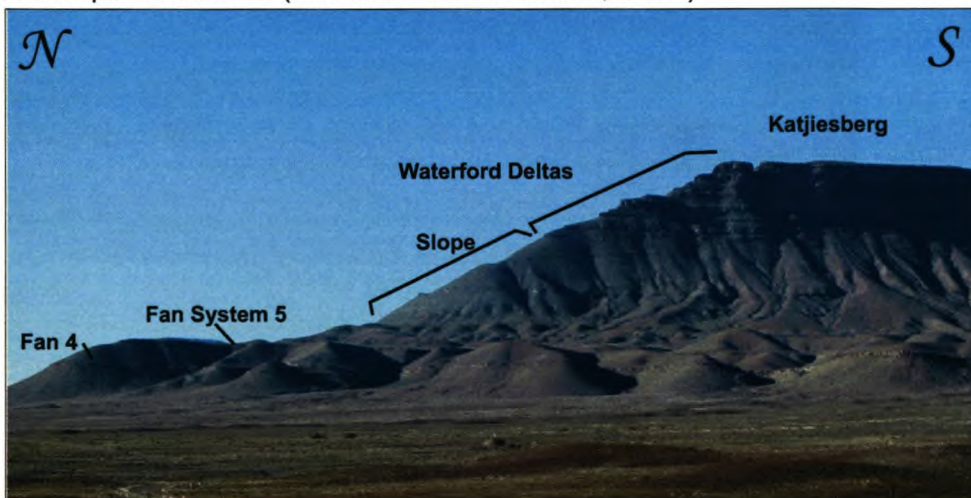


Figure 1.6 Outcrop on Bovenste Wagendrift at Katjiesberg showing distal submarine fans, slope deposits and delta deposits.

Chapter 2

Tectonic setting and structural evolution

Chapter 2

Tectonic setting and structural evolution

2.1 General

The Karoo Basin developed as a retro-arc foreland basin with subduction along the paleo-pacific margin of Gondwana (Johnson, 1991; Visser, 1992; Cole, 1992; Veevers *et al.*, 1994; Gamundi López and Rossello, 1998; Wickens, 2001) (Figs 2.1+2). The orogenic development of the Cape Fold Belt (CFB), which reflects major compressional paroxysms at 278, 258, 247 and 230 Ma, played a vital role in the construction and syn-tectonic sedimentary history of the Karoo foreland trough (Hälbich *et al.*, 1983; Wickens, 1992). The spatial distribution of the Tanqua sub-basin fans as well as their general transport directions, prove the early existence of a well-defined basin margin to the west and southwest. Northeasterly trending anticlinal structures clearly diverted the sediment gravity flows to the different sub-basins (Fig. 1.2). The north-northwesterly orientation of the paleo-coastline for the Tanqua sub-basin (Wickens, 1984) and the generally east-west coastline orientation along the southern margin of the basin (Theron, 1973; Kingsley, 1977; Visser *et al.*, 1980), fully reflect the arc of the CFB-syntaxis.

The development of the Laingsburg and Tanqua sub-basins resulted from the formation of the mega-anticlinal structures. The primary control for the distribution of the Tanqua fan systems was the structural amplification of these mega-anticlinoria, the Hex River and Baviaanshoek anticlines, which form part of the CFB (Fig. 1.2). The Laingsburg submarine fan deposits wedge out exactly along the north-eastward extension of the Hex River anticline, whereas the Tanqua fan deposits were only deposited north of the NW limb of the Baviaanshoek anticline (Fig. 1.2) (De Beer, 1992, 1995; Wickens, 1994).

In the Tanqua sub-basin, the strata are structurally almost undisturbed, except for gentle folding, occasional reverse, and thrust faulting with minor displacements over the southern and central area. Structural vergence illustrates the dominance of northward compression. Scott (1997) suggests that deposition of the submarine fans in both sub-basins took place during a period of

tectonic quiescence between the 278 Ma and 258 Ma tectonic events with deposition of the sediment infill irregularly switching from one sub-basin to the other.

2.2 Structure in the study area

Reconstruction of FS 5 (present and previous studies) indicates that the areal distribution and direction of fan growth were primarily controlled by the rate and amount of sediment supply, as well as the position of the point source. It is widely accepted that local basin tectonics, for example the shortening and folding north of the Baviaanshoek and Hex River anticlines, could also have influenced the distribution and flow direction of this fan. The southernmost outcrop of FS 5 is located just north of the Baviaanshoek anticline and displays features indicating unstable lower- and base-of-slope conditions. The distribution and lithofacies change of FS 5 in this area indicate that the sediments might have been confined to an elongated synformal depression and unconfined in the northern part of the basin. The major part of the northern outcrop area is largely undeformed. The structural complexities of the study area are, however, of much larger extent and obliterate important aspects of the stratigraphy that have been overlooked in the past (Van der Merwe, 2003).

Faulting in the basin was post-depositional and, therefore, did not influence any fan deposition. Thirty major faults and numerous smaller faults and fault-splays occur in the study area (Fig. B). Apart from displacements, faults have been identified in the field by the presence of extensive breccia zones containing secondary quartz and calcite (Fig 2.3 + Figs 2.4.1+2). Shortening was predominantly from the south, which resulted in reverse and thrusts faults striking east-west. Three structural 'provinces' have been highlighted namely the Brandhoek, Brakke Rivier and Droogekloof provinces (Fig. B). These areas are characterized by a concentration of reverse and low-angle thrust faulting, and gentle folding (Fig. B).

Two major east-west trending reverse faults occur in the Droogekloof province (Fig. B + Fig. 2.5.1). These faults dip at angles of $\pm 35^\circ$ to the south (Droogekloof 400 and Kalkgat 170), displacing FS 5 by a few hundred metres (Fig. B + Fig. 2.5.1). Common to most faults in the study area is the overfolding of strata northwards, followed by fracturing and sliding to form thrust-planes and breccia (Figs 2.3 + 2.4.1). In places, thrusting has resulted in the formation of imbricate complexes. Six thrusts occur in the southern outcrop area of FS 5; one is interpreted as

a high-angle, overlying reverse fault in the area where the former Fan 6 downlaps onto FS 5 (Fig. 2.5.2) (Van der Merwe, 2003). Minor thrust and reverse fault displacements of no more than 20 m occur in the Brakke Rivier province. A major thrust fault with a displacement of 22m occurs in the Skoorsteenberg outcrop area. It forms part of the Brakke Rivier province (Fig. B). The northernmost outcrop (Brandhoek province), in the vicinity of Katjiesberg and Blaauwheuwel, is greatly influenced by thrust and reverse faulting (Fig. 2.5.3). Here, the main shortening was from the south, as indicated by an overthrust plane, with associated fault-bend folding (Suppe, 1985) (Fig. 2.3). In places, clastic sandstone dykes give the impression that they are associated with some of these major faults (Van der Merwe, 2003).

East-west trending anticlines and synclines, plunging eastward throughout the study area, are present in all the three structural provinces (Fig. B). The dip of bedding varies from 10° to 42° on the fold limbs. In places, plunge of the fold axis implies domal structures (paraclines, Hodgson *et al.*, 2006). The Ongeluks River for example, flows along an anticlinal axis (Ongeluks anticline) (Fig. B), with a dip of 15° for the northern limb and 47° for the southern limb. Overtured folding is also present with the axial planes of the folds verging southwards. The double plunging trendy folds, which open to the west in the southern outcrop area (Hanglip 150, Droogekloof 400) comprise fold limbs with dip angles of 5° – 20° .

Deposition and concentration of the channel complexes in the southern part of FS 5 (Hanglip, Tongberg, Droogekloof and Kalkgat), suggest that the main Palaeoflow direction of the channel complexes had been predisposed by subtle anticlinal and synclinal basin floor structures. These subtle basin floor structures can also be verified by the deposition of the overflow (overbank) deposits in areas of possible raised topography. Structurally induced basin floor topography structures seem to have been absent from the north-western outcrop area (Skoorsteenberg), because the channels in the Skoorsteenberg area are low width:depth ratio channels with very subtle confinement along their margins.

Prominent dolerite dykes and sheets of Early Jurassic age occur in the northern part of the outcrop area (Figs 2.6.1+2) (Wickens, 1994). The large dykes, as seen on Waterlemoen Fontein 17, have northwest-southeast trend (Fig. B). These intrusive magmas intruded into tensional joint sets that formed parallel to the main break-up stress directions of Gondwana (Truswell, 1970).

Late Palaeozoic
300 +/- 75 Ma

Major foreland basins

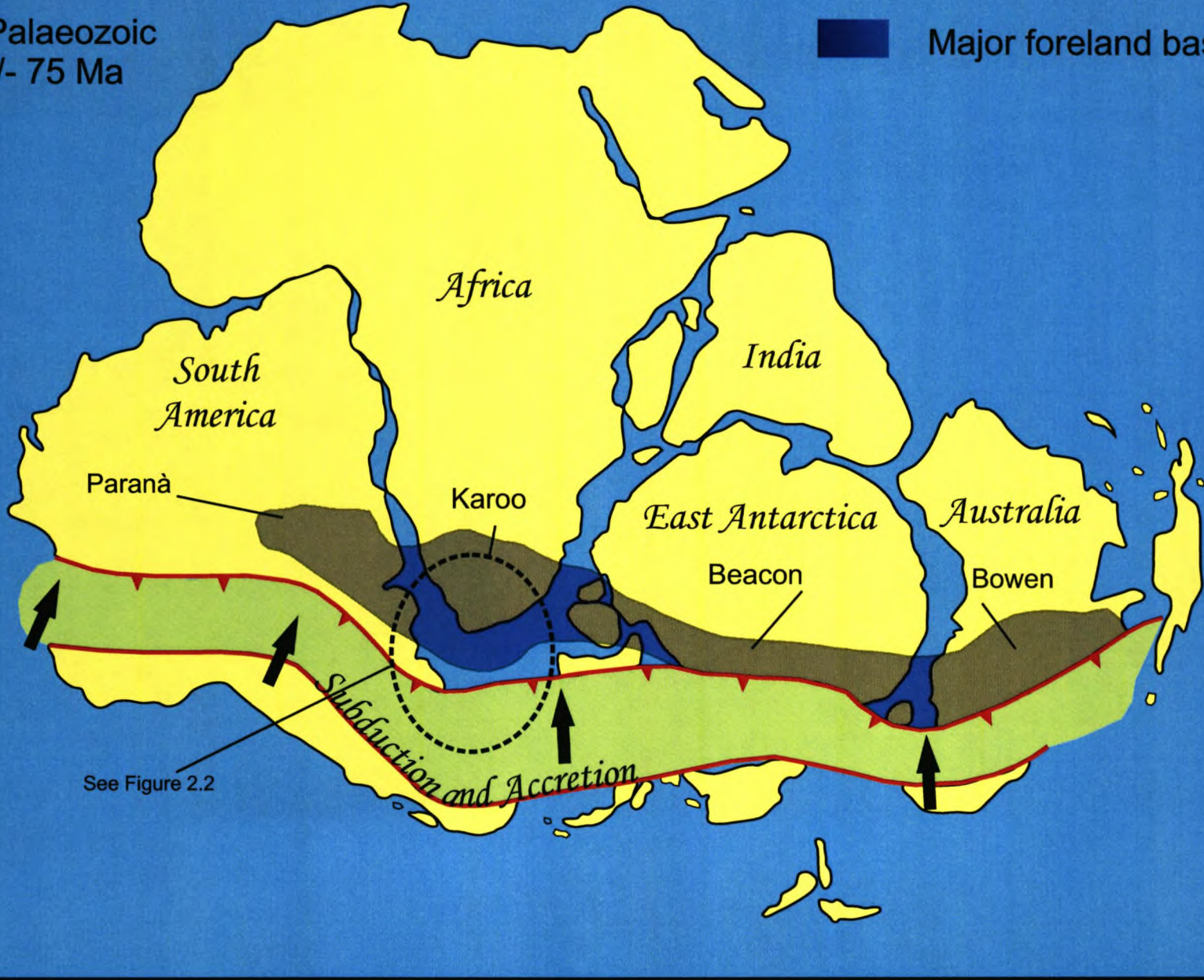


Figure 2.1 Karoo, Paraná, Beacon and Bowen Basins during accretionary tectonics along the southern margin of Gondwana (modified from De Wit and Ransome, 1992).

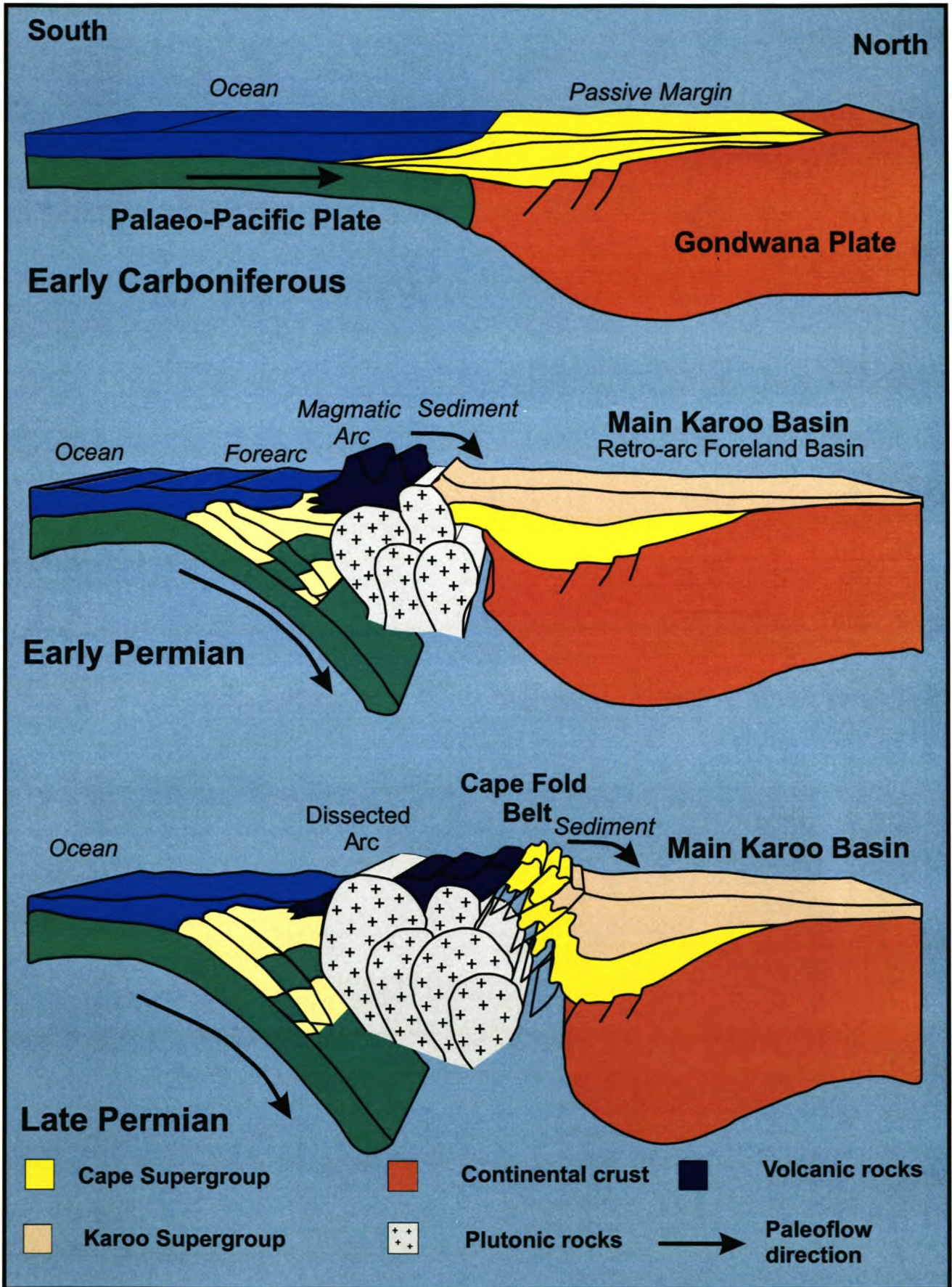


Figure 2.2 Schematic sections across southwestern Gondwana, illustrating the evolution of the main Karoo Basin and Cape Fold Belt (modified from Johnson, 1991).

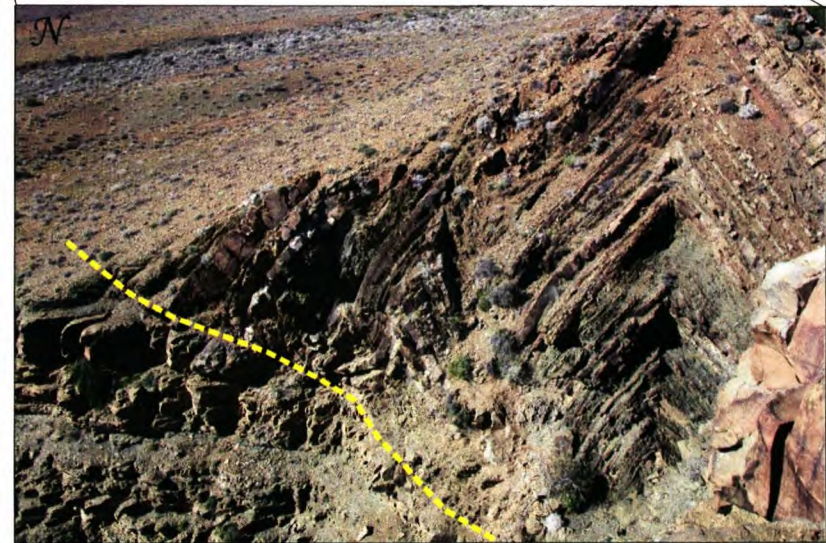
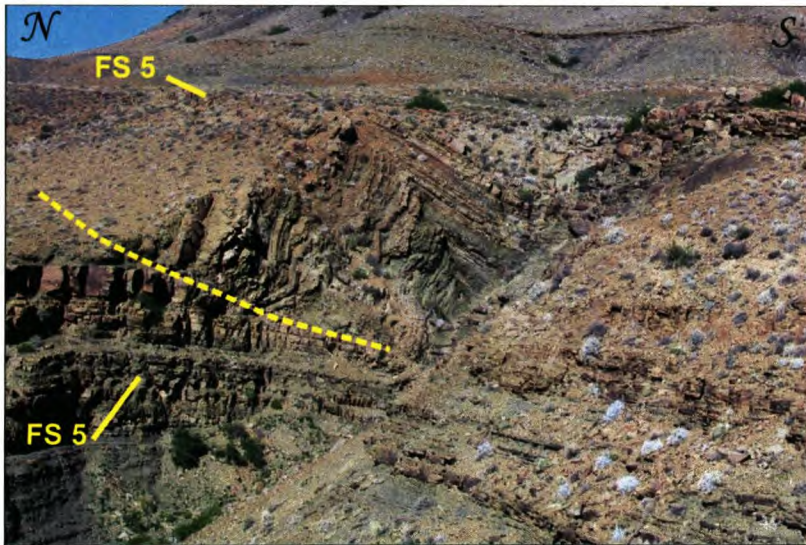
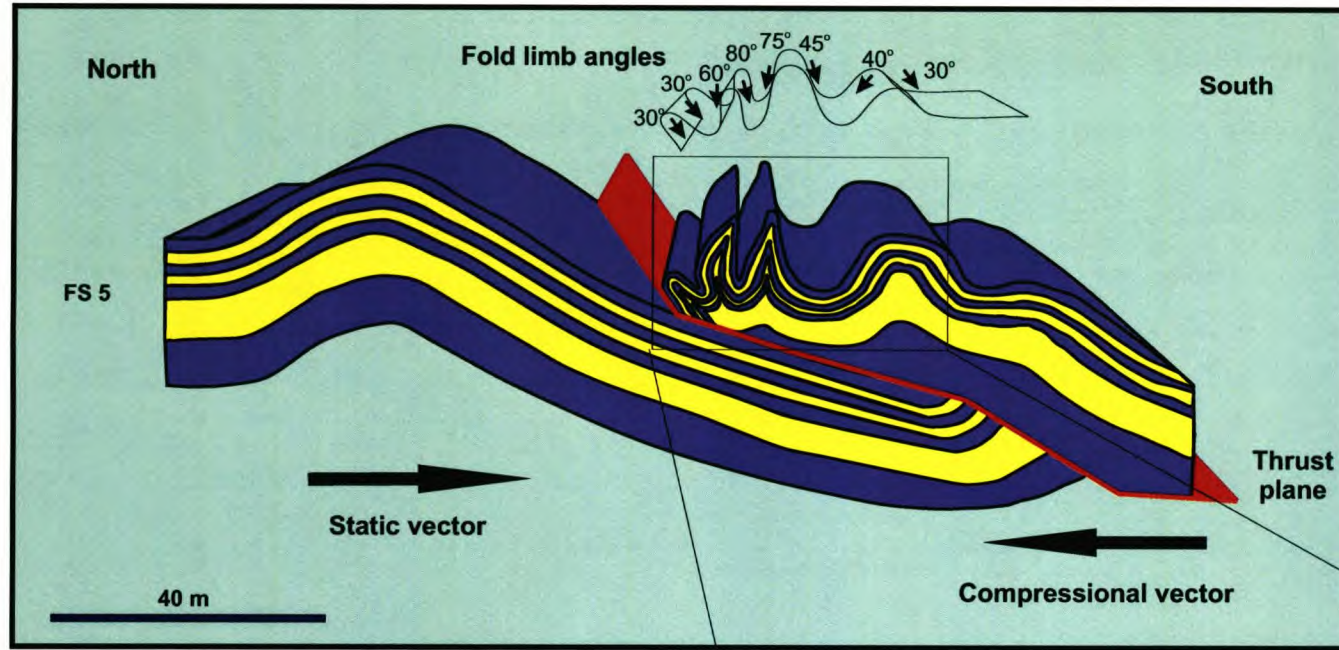


Figure 2.3 Schematic representation of an overthrust or fault-bend fold at the foot of Katjiesberg on Bovenste Wagendrift. Thrust faulting associated with folding is a common phenomenon in the study area. Thrust plane indicated by yellow dashed line on photos.

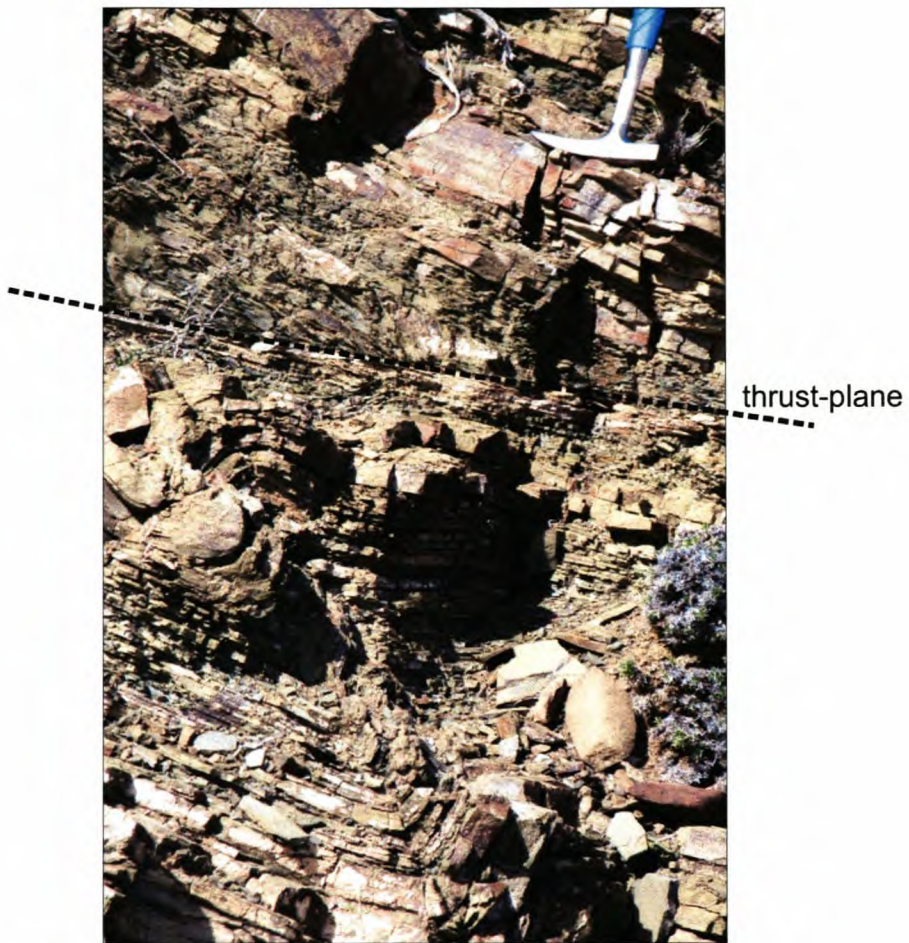


Figure 2.4.1 Fractured thrust-plane associated with breccia. Bizansgat 84 locality (from Van der Merwe, 2003).



Figure 2.4.2 Breccia containing secondary quartz and calcite. Miniature overfold associated within the thrust-plane in Figure 2.4.1 (from Van der Merwe, 2003).

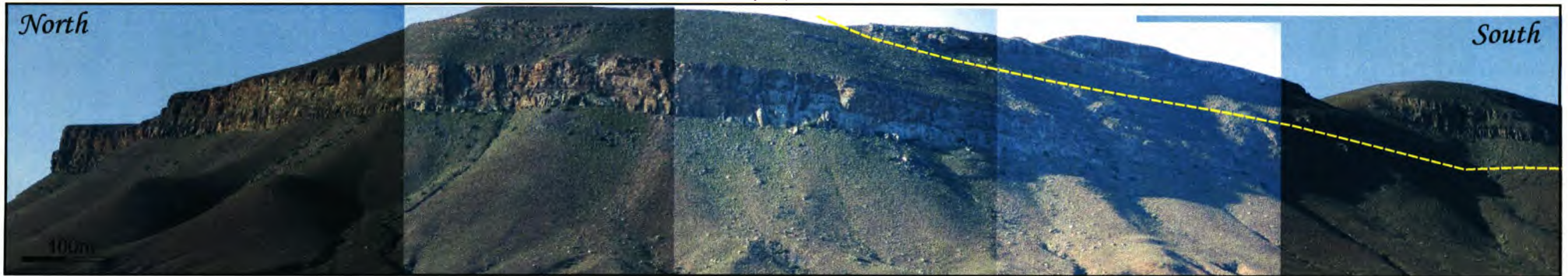


Figure 2.5.1 The Hangklip thrust in the Droogekloof province. Dashed line indicates the fault plane. Overall displacement of this fault is about 2 km towards the north.



Figure 2.5.2 The large red arrows indicate the fault plane of a major, low-angle thrust fault. The smaller arrows indicate the position of a clastic dyke, which suggests an unstable depositional environment.

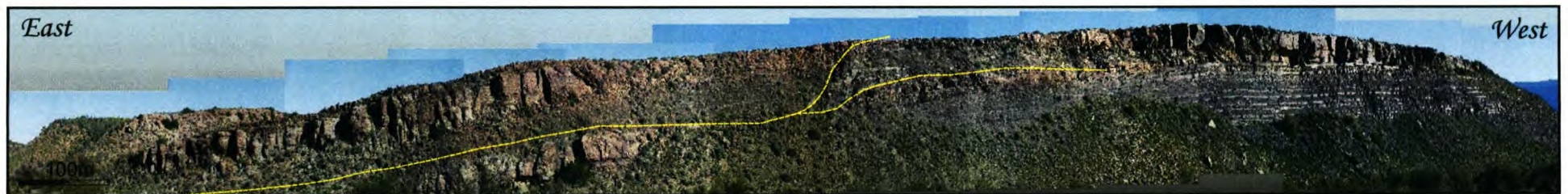


Figure 2.5.3 Thrust splay from the major Brandhoek fault in the Brandhoek province. Dashed line indicates fault planes.

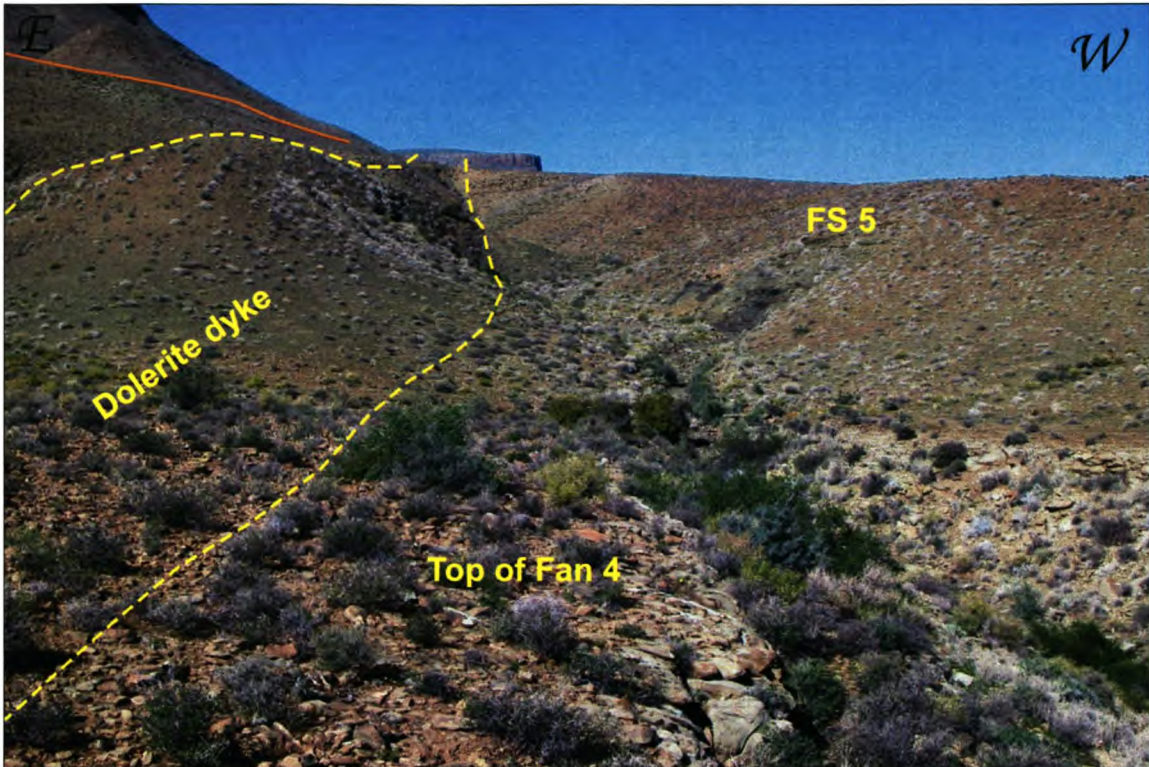


Figure 2.6.1 Late Jurassic dolerite dyke intrusion on the farm Waterlemoen Fontein 17.

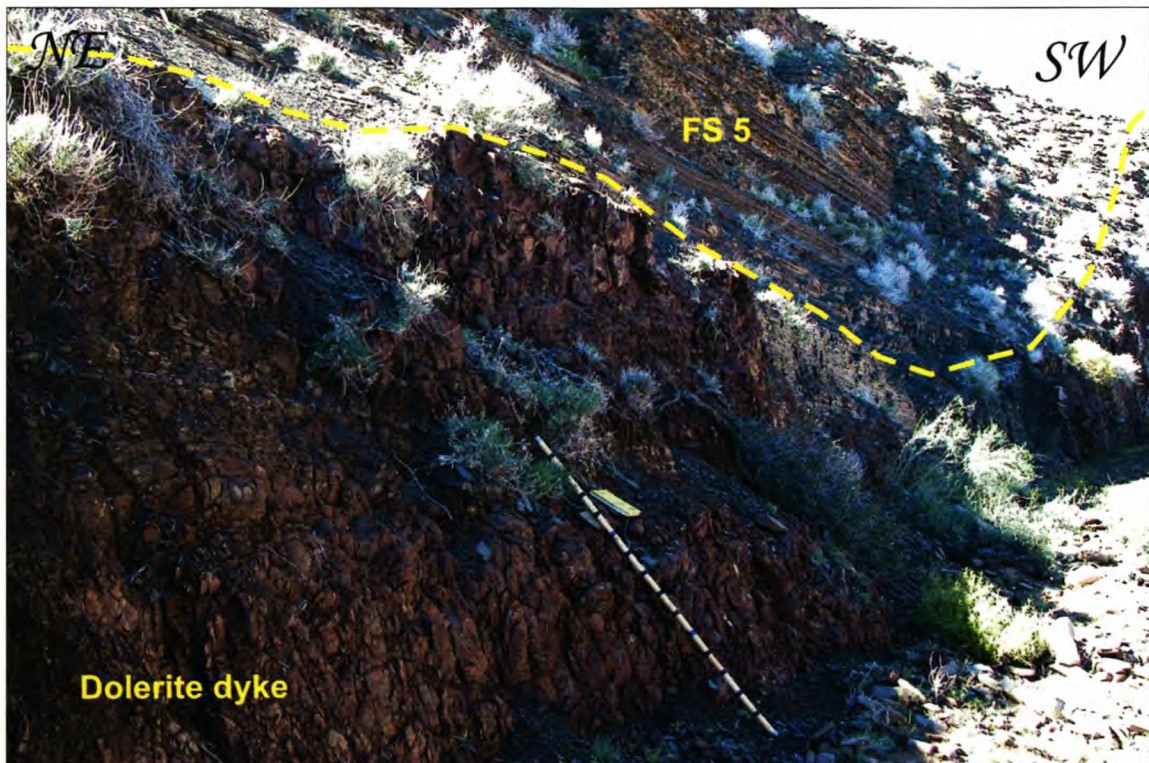


Figure 2.6.2 Dolerite dykes are mostly black in colour but due to weathering show a dark-brown to red colour in the field.

Chapter 3

Current models for deep-water fans

Chapter 3

Current models for deep-water fans

3.1 General

One of the main objectives of research projects on ancient marine slope or base-of-slope deep-water systems is to compare their depositional characteristics with those of modern turbidite systems. The knowledge gained from both ancient and modern systems are, however, limited and incomplete due to insufficient data from diverse sets of data. There are also several important factors that affect each depositional system, whether it is an ancient or modern system. These factors include: basin morphology and topography, tectonics, sediment type and supply, sea level fluctuations, climate, major flooding events, and the number of entry points into the basin. Different combinations of these factors therefore require great precautions to be taken when applying or comparing these models to ancient or modern systems.

The terms 'system' and 'complex' were defined by Mutti and Normark (1987). They defined a turbidite system as a body of genetically related mass-flow sediments deposited in stratigraphic continuity, commonly bound above and below by thick mudstones or by submarine erosional unconformities. The term turbidite complex is defined as several turbidite systems that are more or less stacked one upon the other in a basin floor or base-of-slope setting.

Eight popular models have been presented in the literature over the last 40 years. Nevertheless, one has to keep in mind that each of these models was proposed for a specific fan system or complex or as a generalized model. Therefore, these models are superb guides, but most of the basins around the world experienced numerous factors that influenced deposition. Great care should then be taken when applying any of the existing models to either ancient or modern deep-water systems.

3.2 Brief review of turbidite models

Bouma (1962) recognised five divisions characteristic of the deposition from true turbulent flows, i.e. a turbidite deposit (Fig. 3.1). He starts to classified the deposits from the base with a graded (or massive) interval which grades into an interval of parallel laminations. The third interval is characterized by ripple cross-lamination, the fourth by thin parallel laminations, followed by a mudstone interval deposited from the tail of the current. On top of this, a thin hemi-pelagic deposit may be present (Fig. 3.1).

Normark (1970) published the first model describing the entire body of a submarine fan (Fig. 3.2). He suggested that a deep-sea fan is divided into an upper, middle, and lower fan. Fan growth was described as follows: the upper fan is a single leveed fan valley that transports sediment onto the middle fan (Fig. 3.2). Progressively, the levees decrease in height and disappear downdip. The middle fan, originally called a suprafan) is a distributary system of numerous smaller channels that starts at the termination of the levee valley. Deposition in the lower fan changes from confined to unconfined flow and results in unchannelized sheet-like flow deposits.

The fan models of Mutti and Ricci Lucchi (1972) were the first to classify turbidite fan systems on the basis of facies characteristics of passive margin fans. Upper and lower slope, and inner, middle and outer-fan settings were defined and their typical sedimentary responses were shown (Fig. 3.3). Walker (1978) modified the morphological subdivisions (upper, lower, and middle fan) of Normark (1970) and interpreted various facies associated with each subdivision (Fig. 3.4). He distinguished five main facies of deep-water clastic rocks: classic turbidites, massive sandstones, pebbly sandstones, conglomerates, and debris flow deposits with slumps and slides. These lithofacies fit into the model proposed by Mutti and Ricci Lucchi (1972) with the addition of suprafan lobes and a preponderance of coarse-grained material (Fig. 3.4).

The submarine ramp model by Heller and Dickinson (1985) differs significantly from the canyon-fed submarine fan model described by Mutti and Ricci Lucchi (1972, 1975). The ramp model lacks a primary slope channel or canyon that acts as a conduit through which sediment is moved to the basin. The ramp model does not segregate facies into channel and overbank facies.

Submarine ramp development requires rapid sediment deposition in basins of shallow to moderate depth where deltaic progradation is high enough to mark the structural relief along the basin margin (Fig. 3.5). The inner and middle fan channelized sub-environments of the general models are missing (Fig. 3.5). The proximal ramp area is much sandier than known from other systems and is characterized by thick, massive sandstone beds. Bedding thicknesses are random, and thickening-upward and thinning-upward cycles are rare in occurrence.

Mutti and Normark (1987) recognized the difference in data sets for comparison between modern and ancient turbidite systems. They proposed a hierarchy based on physical scale and true scale for both modern and ancient systems to define turbidite complexes, systems, stages and sub-stages. Architectural element analysis was also introduced as a tool to sub-divide and spatially evaluate and define a turbidite fan system in terms of its constituent depositional elements such as channel-fills, overbank deposits, channel-lobe transitional zone and lobes.

A classification of a deep-water depositional system based on grain-size and feeder systems is achieved by Reading and Richard's (1994) models. They present twelve different models based on four grain-size ranges (mud-rich, mud/sand-rich, sand-rich and gravel-rich) that can originate from either a single point-source, a multiple source system, or a line source (Fig. 3.6).

The Bouma Fine-Grained model (Bouma, 1995, 2000) describes a fine-grained turbidite system that is separated into three zones: upper (inner) fan, middle (mid-) fan, and lower (outer) fan. This model identifies three major end-members with transition zones in-between. The transition from upper fan to middle fan is the base-of-slope, which is characterized by a channel/levee complex (Fig. 3.7). The middle fan comprises one or more leveed channels and overbank deposits. The third zone, the lower fan, is composed of sheet sand deposits (Fig. 3.7).

Prather (2003) presented a model for the classifications of slope settings. Three types were classified on the basis of slope topography (Fig. 3.8):

- above-graded slopes with well-developed ponded accommodation and large amounts of mid- to upper-slope healed-slope accommodation,
- above-grade slopes characterized by stepped profiles that lack well-developed ponded accommodation, and

- graded slopes that lack significant topography that are associated with immobile substrata.

3.3 Comparison of fan models

All the above models share the same general sub-divisions namely: upper/inner fan valley, middle fan, and lower/outer fan, except for the Heller and Dickinson (1985) model. The coarse-grained models are not applicable to the Tanqua submarine fans.

The most suitable type of model as a basis for studying the Tanqua Karoo submarine fans is one that describes a fine-grained, mud-rich environment, typically found in a passive margin setting (Bouma *et al.*, 1995). Although the Tanqua sub-basin represents a foreland basin setting, the fine-grained, mud-rich nature of the basin-fill is more indicative of a passive margin setting than an active one (Wickens, 1994). Deep-water siliciclastic deposits in tectonically active settings are typically characterized by medium- to coarse-grained sands and gravels. The passive margin setting is characterized by a more distal sediment source, a wide shelf, and the development of relatively large submarine fans (Reading and Richards, 1994).

The Heller and Dickinson (H&D) (1985) submarine ramp model has been proven incorrect for most depositional settings in most environments. However, a few valuable observations in this model could be considered for the FS 5 model. In this study, the FS 5 outcrops were mostly characterized by using the Bouma fine-grained/mud-rich depositional model, because the Tanqua deposits were used as basis for his fine-grained model.

3.4 Facies associations and architectural elements of the Tanqua Fan Complex: A Review

3.4.1 Facies associations

Wickens *et al.* (1990) recognized and described five major lithofacies for the TFC, which was later modified by Johnson *et al.* (2001) who added 5 additional lithofacies, based on their lithological composition and internal sedimentary structures. These lithofacies associations are based on outcrop observations only (See Table 1 for a detailed summary and description of the different facies associations).

3.4.2 Architectural elements

The Skoorsteenberg Formation architectural elements have been described in detail by Bouma and Wickens (1992), Wickens (1994) and Johnson *et al.* (2001). They recognised five types of elements, namely:

- 1) individual channel-fills and channel-fill complexes,
- 2) scouring,
- 3) channel-levee-overbank and crevasse splay elements,
- 4) sheet-sand deposits, and
- 5) slumps and debris flows.

Channel-fills in the Tanqua Karoo are variable in terms of style and geometry. Widths vary from 100m to 1.5 km and vertical thickness of individual channel-fills ranges from 1 m to 35 m (Bouma and Wickens, 1992; Van Antwerpen, 1992; Winters *et al.*, 1995). Johnson *et al.* (2001) identified five different channel forms (Fig. 3.9). These differ in geometry and style of infill (Fig. 3.9). Scours are isolated, roughly equidimensional cut-and-fill features where erosion and subsequent fills are most commonly produced by the same flows, but in different time periods (from a view days to millions of years). These features generally occur as relatively small and deeply incised structures at the bases of highly erosive channel-fill and thick sheet sandstone beds in the depositional lobes (Figs 3.10.1+2) (Morris *et al.*, 2001).

Deep-water levee/overbank deposits, such as those in non-marine fluvial environments, flank the main channels (Johnson *et al.*, 2001). Levee deposits form from turbiditic flows of sufficient magnitude that overtop the channel and deposit sediment adjacent to the channel by low-density turbidity flows and suspension sedimentation (Fig. 3.11). This gives rise to intensely interstratified, thinly-bedded intervals composed of alternating ripple cross-laminated and parallel-laminated sandstones and siltstones (Bouma T_{cd}) and graded muddy siltstones and mudstones (Bouma T_e) with highly variable net sand content. In deep-water settings, crevasse splay deposits are produced by significant overflow of low-density turbidity flows through a small breach in the levee (Fig. 3.11). As a result, are the channel-fills commonly interstratified with levee/overbank deposits.

Sheet sands are the preferred term for the non-channelized, laterally extensive sandstone units in the Tanqua. Johnson *et al.* (2001) divided and classified the sheet deposits into amalgamated sheets and layered sheets (Fig. 3.12.1). These deposits have typical tabular geometry with planar upper and lower surfaces (Figs 3.12.2+3).

Slumps and associated debris flows are common components of slope and basin-plain deposits and occur at multiple scales (Woodcock, 1979). Slump deposits are typically wedge-shaped in profile and amoeboid or tongue-shaped in plan view (Figs 3.13.1+2). They consist of different mass movement deposits varying from internally coherent slide blocks to debris flows. Slide blocks may show internal bedding highly deviating from that of the surrounding, non-slumped deep-water deposits (Hall, 1973). The size of slump deposits varies widely. In the submarine fans off large deltas, slumps may achieve great sizes of ± 50 km and more. Smaller slumps (5m-20m) often occur in channel/levee systems, where proximal levee deposits slump into the channel.

3.5 Distribution of architectural and facies elements for the lower four submarine Fans

Both Johnson *et al.* (2001) and Hodgson *et al.* (2006) developed a detailed architectural model of deposition for the lower four fans. Johnson *et al.* (2001) compiled a genetic fan model in which the relation of the geometries and distribution of architectural elements within the successive fans are shown (Fig. 3.14). This model shows the down-dip evolution of channels, from erosive/bypass to the depositional types. Hodgson *et al.* (2006) combine the existing models of Johnson with the NOMAD core dataset, which led to the identification of three broad phases of fan development, i.e. phases of progradation, aggradation and retrogradation. The progradational phase records active basin-ward stepping of the zones during the early stratigraphic evolution of the fans. The aggradational phase records only limited basin-ward and/or land-ward stepping of the fan and the retrogradational phase preserves significant hinterland shifts in the position of the limit of turbidite sedimentation. The distribution of facies and architectural elements in FS 5 forms part of the Hodgson model, but it is still characterized by the basic fan geometries suggested by Johnson *et al.* (2001).

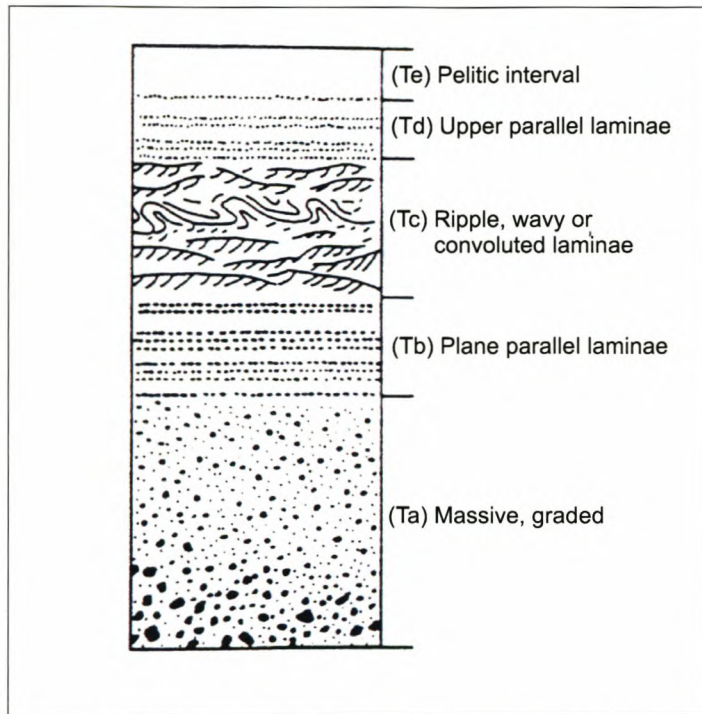


Figure 3.1 Diagram of the Bouma Sequence (T_a-T_e). (after Bouma, 1962).

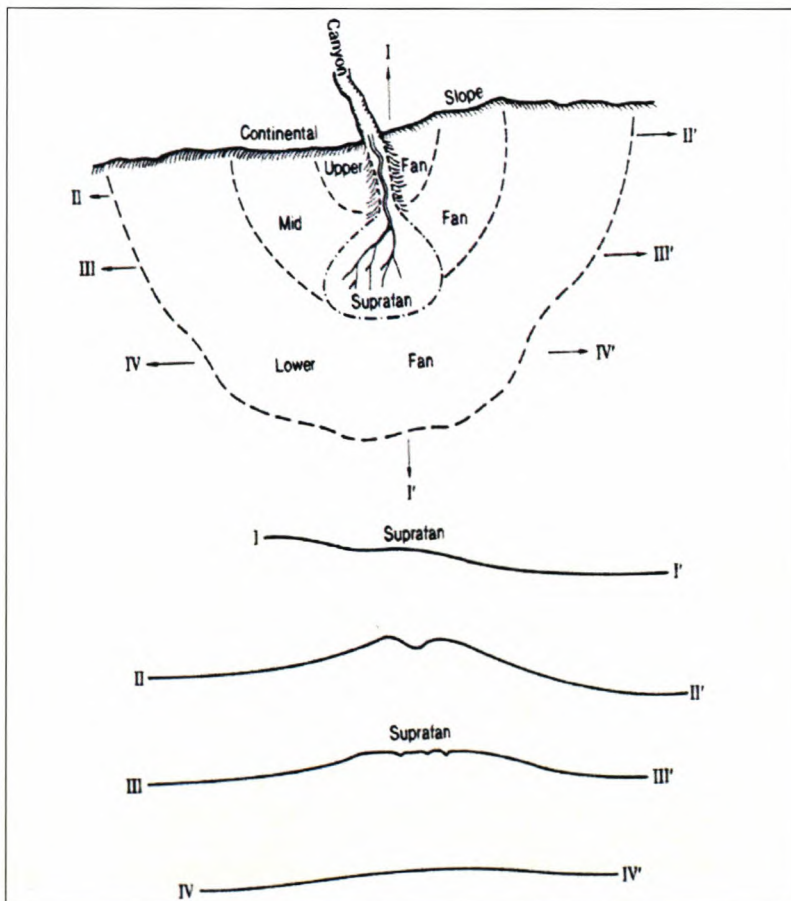


Figure 3.2 Schematic representation for the growth of a sand-rich submarine fan, emphasizing fan zonation, the most active depositional area (suprafan) and morphological shapes in cross sections (after Normark, 1978).

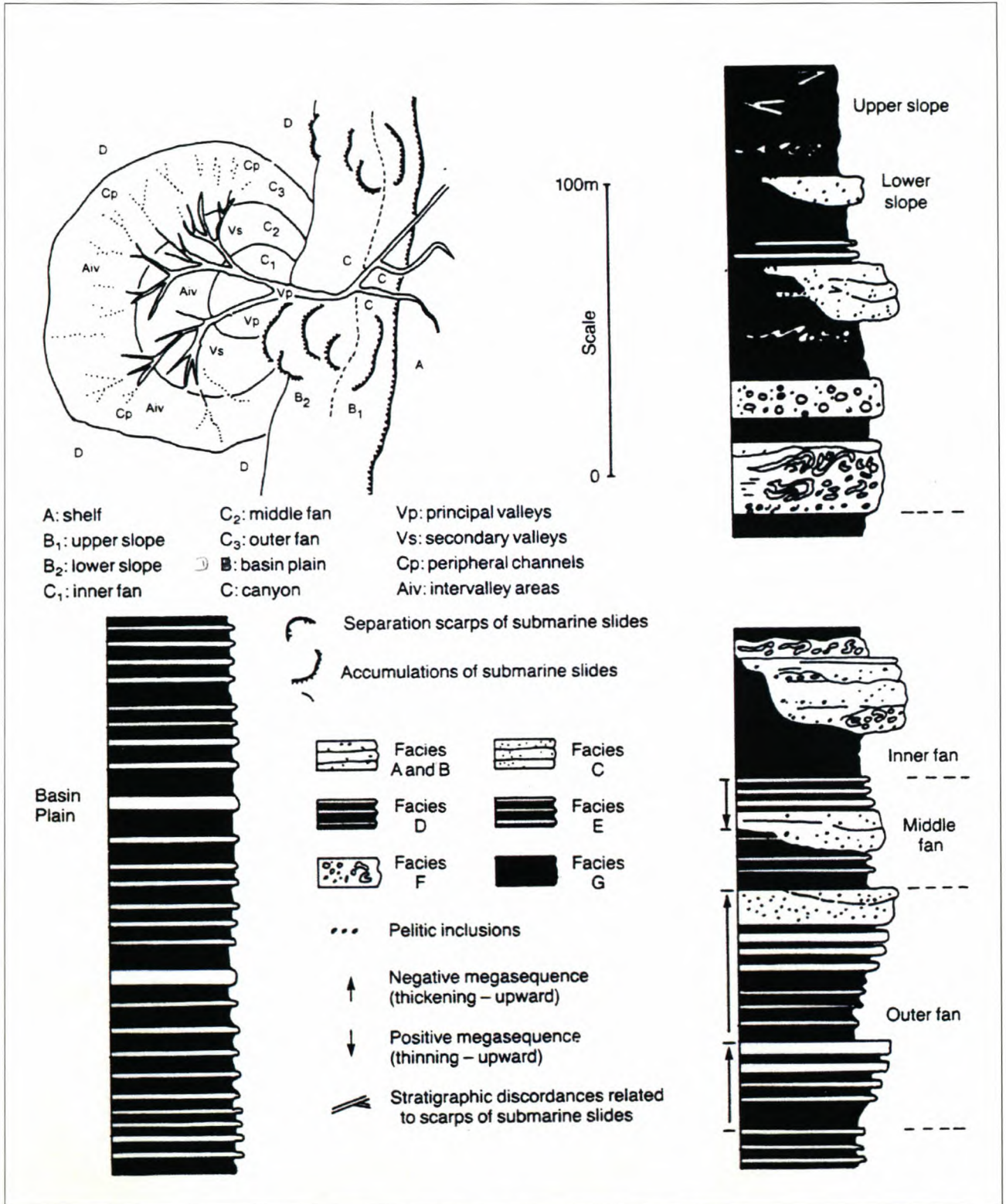


Figure 3.3 Diagram showing three distinct intervals of a submarine fan system and schematic cross sections and related facies within the three intervals (from Mutti and Ricci Lucchi, 1972).

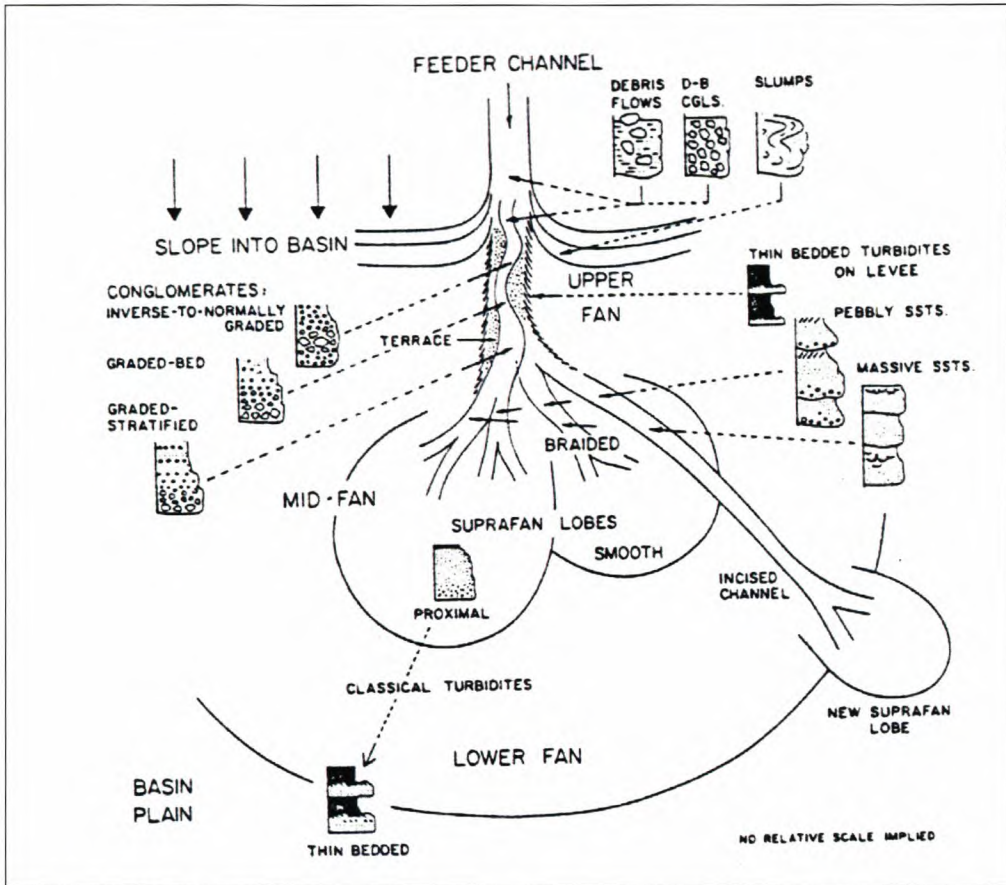


Figure 3.4 Schematic presentation of a coarse-grained, conglomerate-rich submarine fan model (after Walker, 1978).

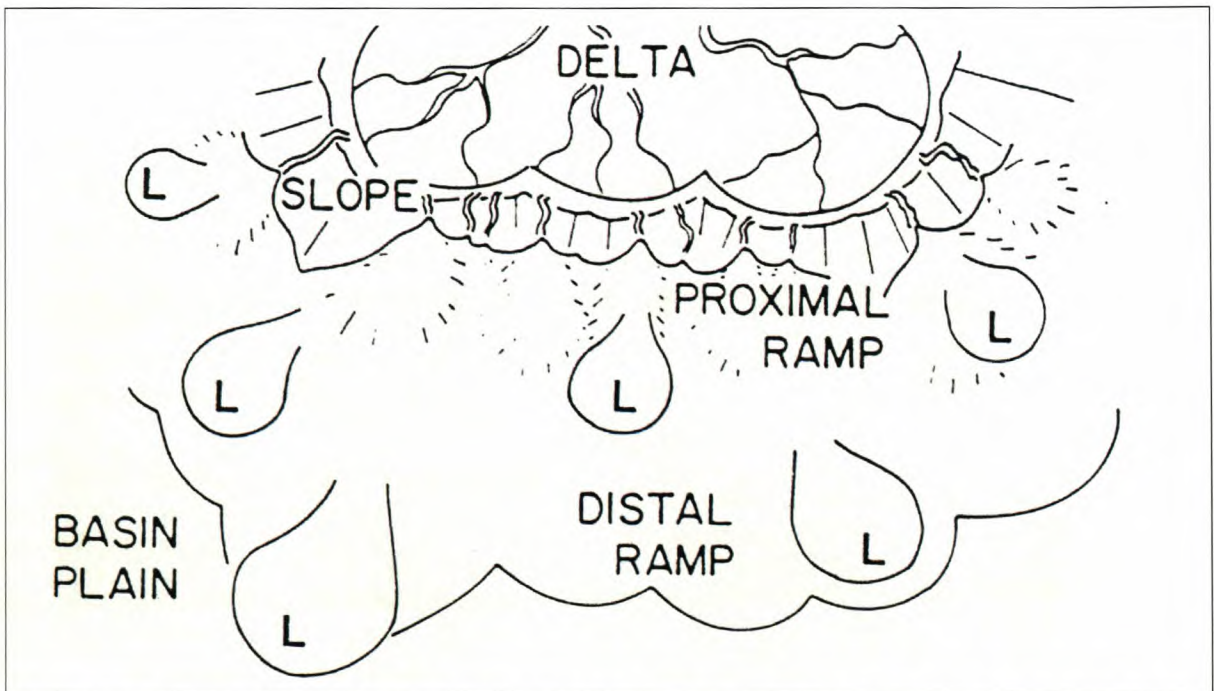


Figure 3.5 The submarine ramp model by Heller and Dickinson (1985). The ramp model lacks a primary slope channel or canyon that acts as a conduit through which sediment is moved to the basin.

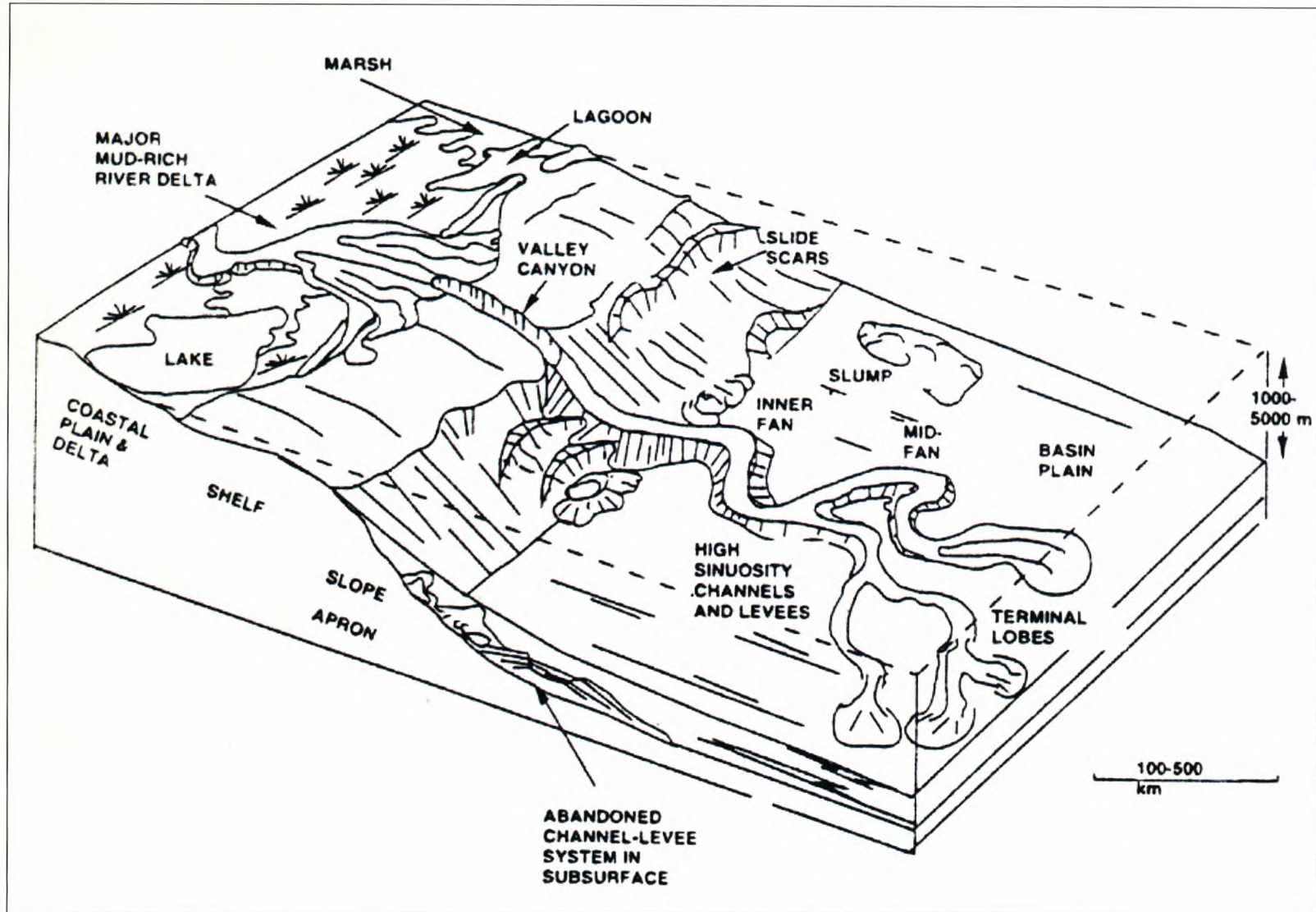


Figure 3.6 A point-source, mud-rich depositional submarine fan model (from Reading and Richards, 1994).

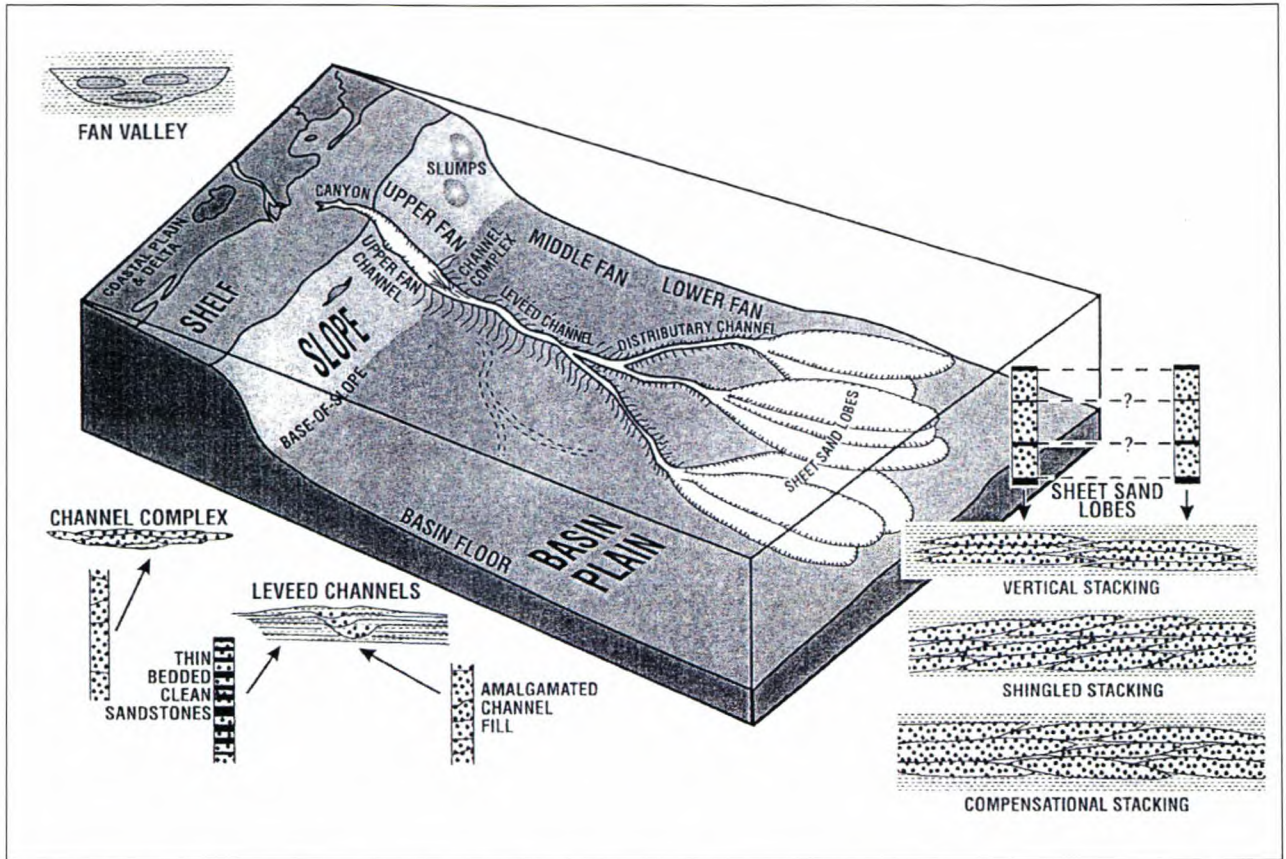


Figure 3.7 Fine-grained fan model with three major end-member components: 1) channel complex at the base-of-slope, 2) leveed channel with overbank areas on the middle fan, and 3) lower fan sheet sand deposits. Generalized cross sections and vertical sections represents three possible stacking patterns and compensational bedding of lower fan sheet sands (from Bouma, 2000).

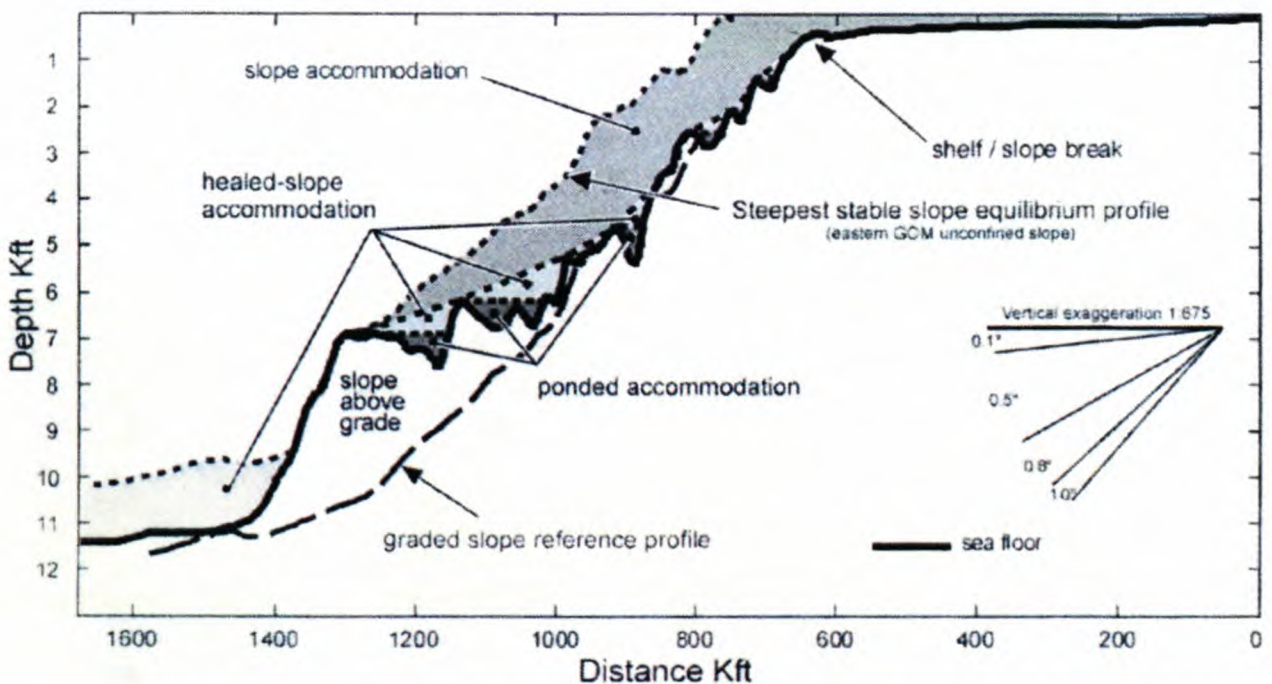
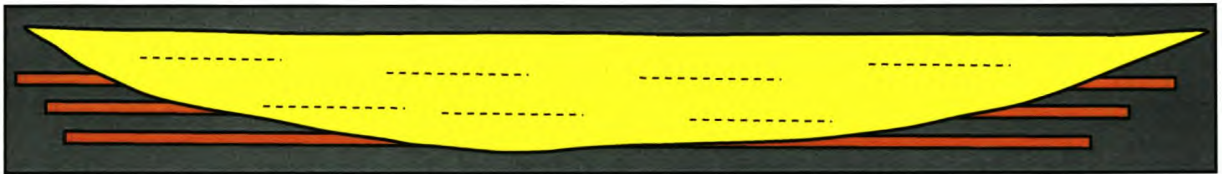


Figure 3.8 A seafloor profile showing the distribution of three types of accommodation in a slope setting (from Prather, 2003).

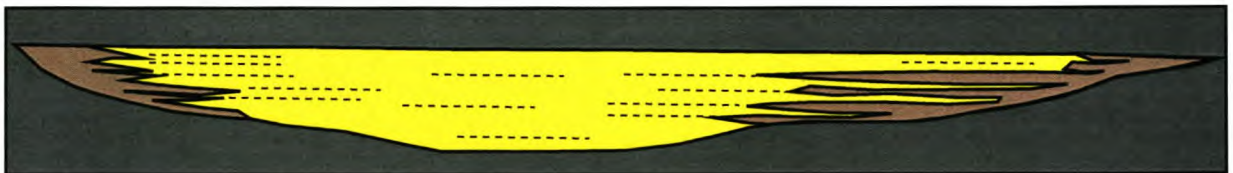
1) Erosive, multi-event channel with a complex fill: Significant erosion and truncation of underlying strata are followed by thick-bedded turbidity current deposits in axial and marginal areas. Subsequently the upper parts of the channel-fill contain components of thin-bedded turbidites in channel margins and axial thick-bedded turbidites. Finally a 'drape' fill of thin-bedded turbidites occur over the full channel width.



2) Erosional multi-event channel with simple fill. Significant erosion and truncation of underlying strata followed by multiple event fill of thick-bedded turbidites. Zero to minor amounts of thin-bedded channel margins facies.



3) Depositional and minor erosional channel. Clear internal partitioning of sand-rich axial facies and heterolithic channel margin facies.



4) Erosional channel with heterolithic thin-bedded fill. Significant erosion followed by fill of alternating thin-bedded turbidites, siltstones and minor amounts of thick-bedded turbidites.



5) Channel complex. Variable architecture consisting of channel-fills which stack in an offset lateral and vertical arrangement. Slumped material is observed in channel types 1 to 4. Most common are complex erosional and depositional channel types.



Figure 3.9 Schematic summary of the five main channel types of the TFC (redrawn from Johnson *et al.*, 2001).



Figure 3.10.1 Scour in channel-fill sandstone (dashed line). Scours are cut-and-fill features where erosion and subsequent fill are commonly produced by the same flows, but in different time periods. Located on the farm Pienaarsfontein 414.



Figure 3.10.2 Rip-up clasts associated with a scour. Hammer for scale. Located on the farm Pienaarsfontein 414.

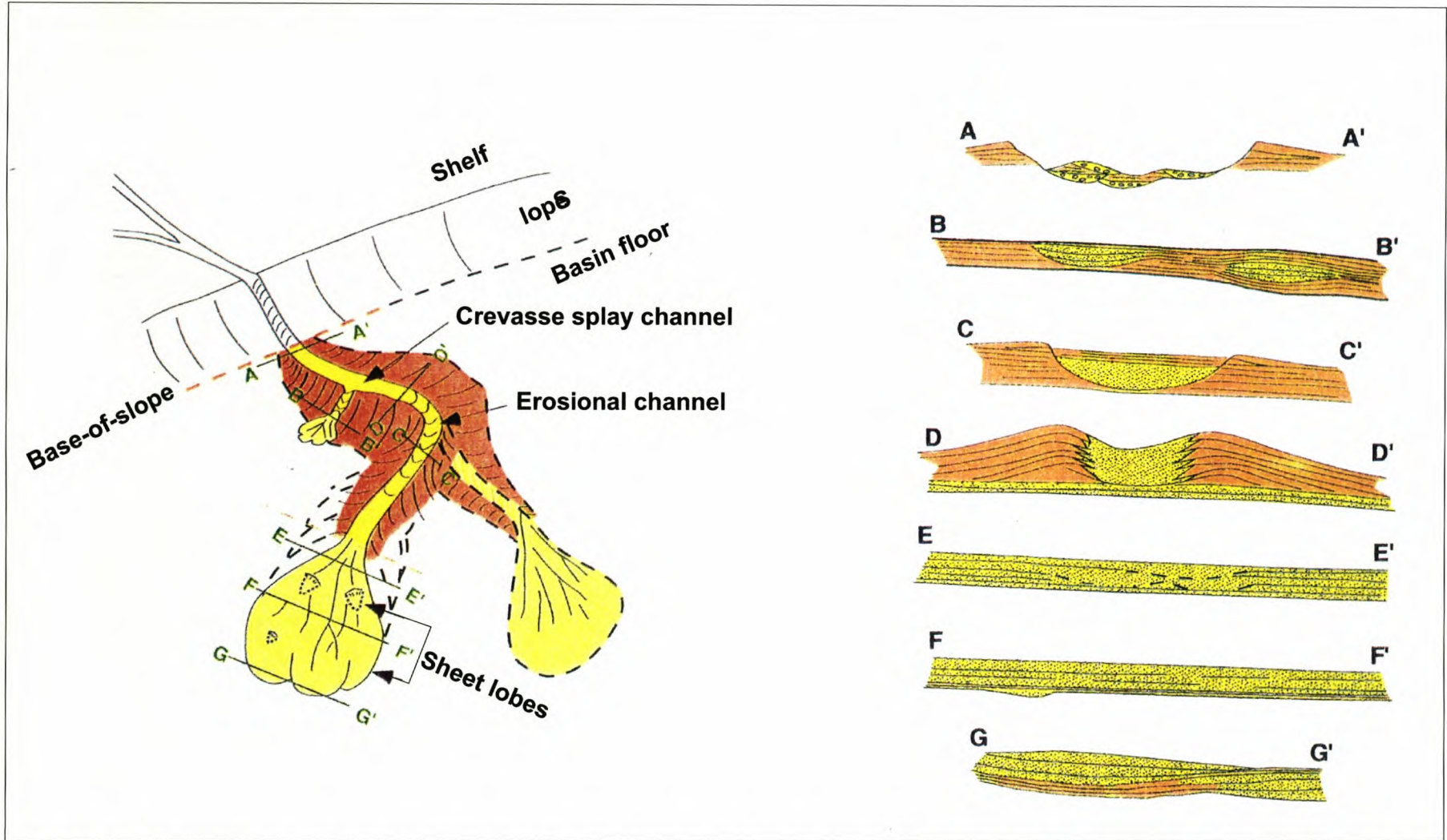


Figure 3.11 Depositional model of major architectural and facies elements in a turbidite setting. Cross-section **A** presents: Erosional channel complex; **B**) Crevasse channel & splay; **C**) Erosional channel; **D**) channel-levee-overbank deposits; **E,F** and **G**) Lobe-sheet sands form proximal to distal (from Morris *et al.*, 2001).

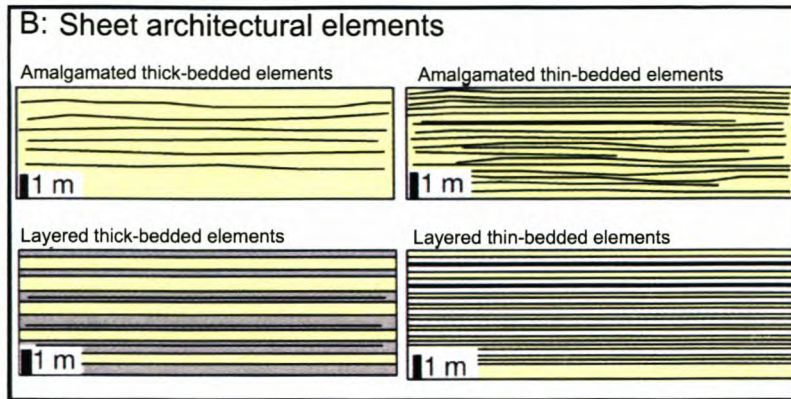


Figure 3.12.1 Schematic line drawings of basic non-channelized sheet sand architectural element (from Johnson *et al.*, 2001).



Figure 3.12.2 Layered sheet deposits are very similar to the amalgamated sheets. They are distinguished by the occurrence of thin, interbedded siltstone and claystone beds. Fan 4, located on the farm Rondavel 34.



Figure 3.12.3 Amalgamated sheet deposits with erosional surfaces. Indicated by arrows. Located on the farm Zoetmeisjes Fontein 75.

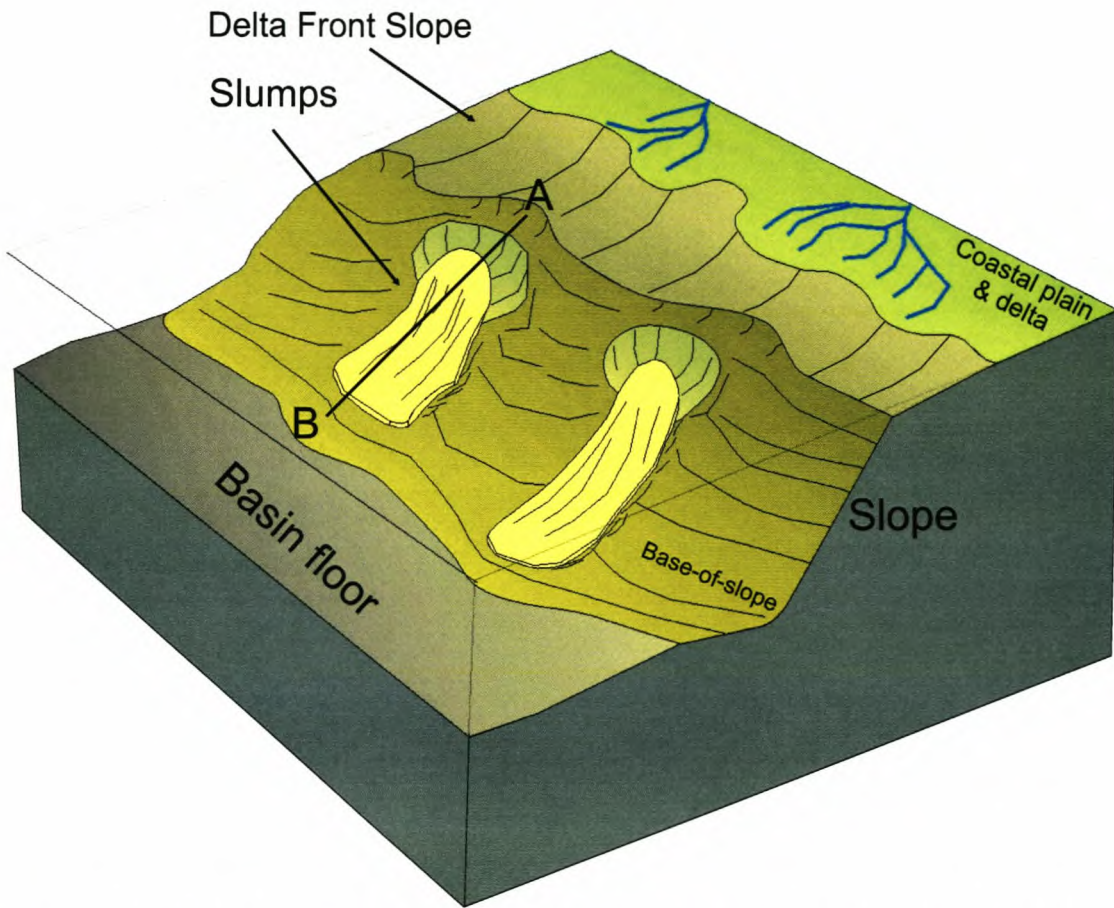


Figure 3.13.1 Slumps and associated debris flows are common components of slope and basin floor deposits. See cross-section A-B for more detail.

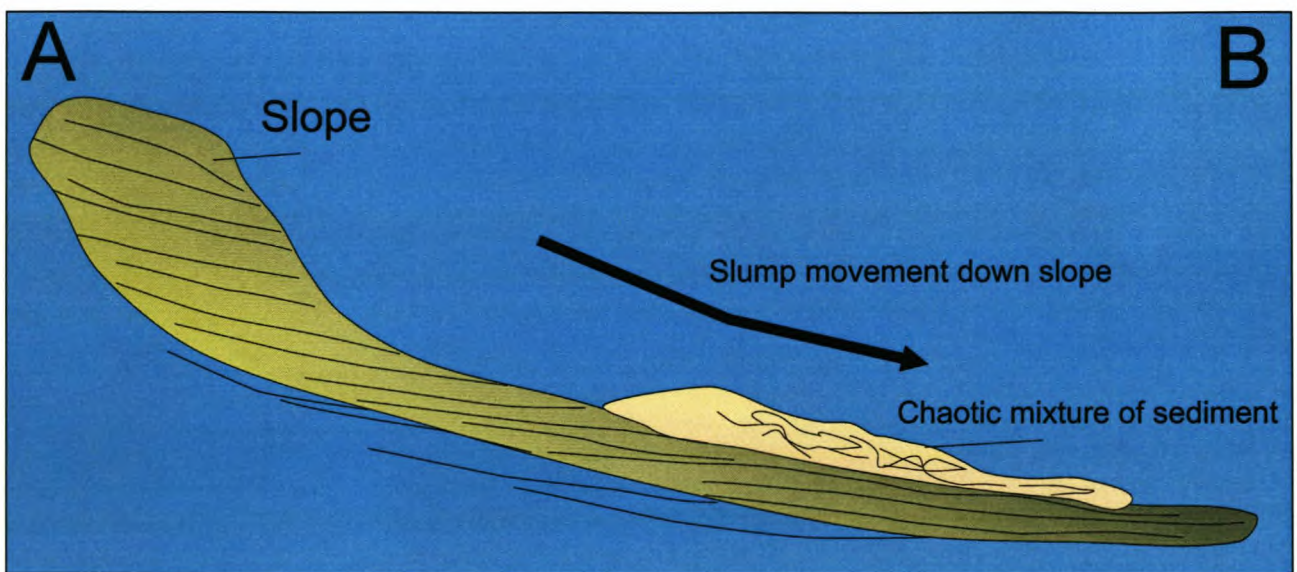


Figure 3.13.2 Slump deposits are typically wedge-shaped in profile and tongue-shaped in plan view.

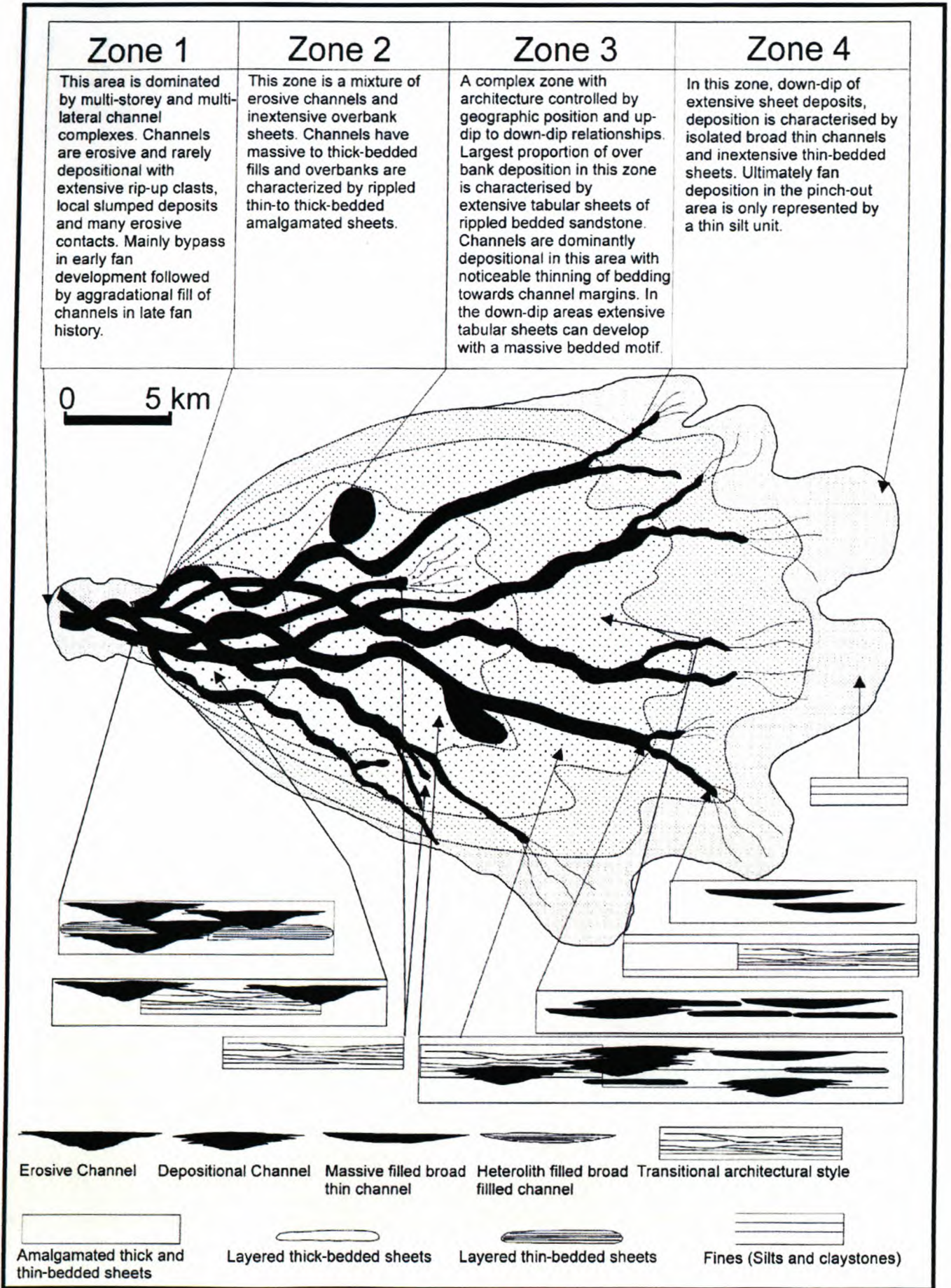


Figure 3.14 Model for spatial distribution of facies associations for the lower four fans in the Tanqua depocenter (from Johnson *et al.*, 2001).

Table 1: Characteristics of lithofacies defined by Johnson *et al.* (2001)

Lithofacies number	Lithology	Sedimentary structures	Bouma divisions	Bounding surfaces	Thickness	Geometry	Trace fossils and other notable features	Process of deposition
1	Claystone/silty claystone	Generally massive. Rare parallel lamination	None in claystone. T _{dec} in silt	Gradational	2-cm to > 10-m packages	Often laterally extensive sheets	Rare to present. <i>Chondrites</i> . Common concretionary horizons (lithofacies 10)	Deposition from hemipelagic suspension and low concentration turbidity currents
2	Claystone/silty claystone with mm to cm silt/vfs laminae	Generally massive to parallel lam. Starved ripple lamination	T _{de} rare T _{cde}	Laminae have sharp bases and gradational tops	Laminae 0.1–1 cm. Units 10 cm to 4 m	Laminae tabular to lenticular. Units often sheet-like	Rare to moderate. <i>Chondrites</i> , <i>Gordia</i> sp.	Hemipelagic and low-concentration turbidity current deposition
3	Silt–vfs/vfs–claystone couplets	Silt to vfs have starved ripples, parallel lamination and massive nature. Prods and grooves on base	Variable, common T _{cde} , T _{de} and T _{bc}	Sands have sharp bases, tops are gradational to sharp	1–5 cm	Individual beds tabular at the outcrop scale. Units display a sheet geometry	Common. <i>Chondrites</i> , <i>Helminthopsis</i> , <i>Helminthoida</i> , <i>Gordia</i> sp., <i>Lorenzina</i> , <i>Lophoctenium</i> , <i>Cosmorhapha</i> , <i>Palaeodyctyon</i>	Generally low concentration turbidity current and minor hemipelagic deposition
4	Vfs–fs/silt couplets	Variable, climbing ripples, parallel lamination, massive. Local sigmoid geometry and pinch and swell	T _{cde} , T _{ab} , T _{a–c} (T _{cde} most common)	Sharp bases to sands. Sharp to gradational tops. Upper fine layer (T _c) can be absent	Sands usually form units dominated by bedding of 5–10 cm, 10–20 cm and > 20 cm	Beds tabular. Sheet geometry to units		Low-high concentration turbidity currents
5	Medium to thick bedded sandstone	Commonly massive, parallel lamination, climbing ripples. Some scour and fill. Dewatering	T _{a–b} and T _{ac} common	Bases sharp and rarely erosional	20–60 cm	Tabular to locally lenticular. Units form sheet and channel geometries	Rare. <i>Helminthoides</i>	High-concentration turbidity currents. Variety of flow types but dominated by depletive steady flow
6	Masive sandstone	Massive, local parallel lamination. Local scour and fill. Dewatering	T _a	Sharp to erosive bases and sharp tops	20–80 cm, 10-m packages caused by amalgamation	Channel fills and some sheets	Wood fragments occur	High-concentration turbidity currents with depletive steady and unsteady flows
7	Intraclast-rich conglomerate	Chaotic		Sharp and sometimes erosive	< 50 cm	Lenticular pockets up to 20 m wide or thin beds at the top of lithofacies 5 and 6	No traces. Wood and organic debris common	Deposits of slurry flows and more localized deposition of rip-up clasts
8	Distorted heterolithic units	Small folds and thrusts at the 20 cm scale		Sharp often associated with erosive scour	Up to 5 m	Lenticular pockets up to 200 m wide		Local slumps of overbank and minor levee deposits
9	Tuffs	None if not reworked		Sharp	Up to 30 cm	Sheet		Suspension fall-out of volcanic ash
10	Concretionary horizon	Cone-in-cone structures		Sharp	Up to 50 cm	Lenticular to localized pans		Diagenetic concretions at times of maximum sediment starvation

Chapter 4

**Sedimentary characteristics of Fan System 5
(FS 5)**

Chapter 4

Sedimentary characteristics of Fan System 5 (FS 5)

4.1 General

Forming the uppermost system of the 400m thick Skoorsteenberg Formation, the gross thickness of FS 5 ranges from 112 metres in the proximal outcrops to less than 25 metres in the distal outcrops. The silty-shale package underlying FS 5 varies in thickness from 5 m in the south to 9 m in the north. The silty-shales overlying FS 5 form a regionally mappable unit varying between 15-20 m in thickness throughout the outcrop area. Overlying this silty-shale package are the pro-delta deposits, followed by delta front slope and delta plain deposits of the Waterford Formation (Wickens, 1994).

The majority of the exposures of FS 5 are cliff-type, with several broad exposures revealing lateral continuity. Palaeotransport indicates a general flow direction from the west-southwest. Stratigraphically, FS 5 can be subdivided into six different sand-rich units, based primarily on regional distribution/development of sandy channel-fill complexes, sheet splay deposits, and levee-overbank/overflow deposits. Although developed in different areas, these units occur within the same stratigraphic interval with complex vertical and lateral relationships of facies. The channel-fill complexes consist of massive amalgamated sandstones with erosive bypass basal sediments, whereas the overbank/overflow and splay units consist of thin-bedded siltstones, alternating with thin-bedded sandstones.

Four major channel complexes, occupying different stratigraphic levels and with SW-NE orientated axes characterize the southern part of the FS 5 outcrop. These channel complexes, representing base-of-slope in present-day outcrops, seem to extend basin-ward over a distance of 15-25 km into the subsurface. The northern channel complex at Skoorsteenberg is well exposed and extends for 18 km downdip before the most distal sand packages pinch out. Due to limited outcrop for the southern four channel complexes, mid-fan and lower-fan deposits have not been recognised. The Skoorsteenberg outcrop indicates well-developed mid-fan and lower-fan sheet deposits, which extend over an area of about 100 km². A few major channel-fills and sheet-splays

have been identified in the middle part of the studied outcrop, which are interpreted to be genetically related to the southern channel complexes. The areas in-between these major complexes are characterized by interchannel deposits of thin-bedded units.

4.2 Palaeogeography

Palaeoflow data are fundamental for accurate reconstruction of depositional patterns. Previous work in different areas of FS 5 (Wickens, 1994; Johnson *et al.*, 2001 and Hodgson *et al.*, 2006) indicates a palaeoflow direction from the west-southwest and west. Field observations of this study support those findings with the measurement of over 1600 directions. Palaeoflow directions were obtained from erosional sole structures, such as flute casts, prod casts and tool marks (Figs 4.1.1+2), traction structures, such as stream lineation, and ripple cross-lamination, seen in plan view as rib-and-furrow structures (Figs 4.2+3). Ripple cross-laminations occasionally show quite different current directions, probably due to deflections of bottom currents.

The different phases of active fan deposition show slightly different palaeoflow directions. Eleven palaeogeographical areas were compiled with rose diagrams (Fig. 4.4). The vector mean for the combination of these eleven different zones is 025° , i.e. towards a north-easterly flow direction (Fig. 4.4).

4.2.1 Interpretation of palaeoflow patterns

Lein *et al.* (2003) reconstructed a spill-over model from the interpretations of different flow directions of more confined channelized sands and related unconfined overflow deposits. A similar interpretation could be applied for the palaeoflow directions in the channelized and related overflow environments of FS 5 (Fig. 4.5). The spread of readings for the thin-bedded ripple cross-laminated facies varies much more than the readings obtained for the thick-bedded, more amalgamated facies from the different channelized regions (Fig. 4.5). It could be concluded that the thicker amalgamated sandstones from the channelized regions reflect a confined environment with palaeocurrent directions being more consistent. The thinner, more widely spread, sandstone/siltstone units of the spill-over area (overbank and sheet sand deposits), deviate

significantly from the main channel axis (Fig. 4.5). This occurrence is recorded from the outcrops of Skoorsteenberg, Blauwkop and Klein Hangklip (Fig. 4.4).

The two southernmost channel complexes, Kalkgat and Groot Hangklip, show a main palaeoflow direction to the northeast. The Tongberg complex consists of an upper, middle and lower unit; the lower channels flowed more to the east-northeast, the middle channels in a north-easterly direction and the uppermost channels show a north-northwestly direction (Fig. 4.4). The palaeoflow for the Klein Hangklip channel complex varies slightly from a more easterly ($067^{\circ} - 084^{\circ}$) to a north-easterly direction (Van der Merwe, 2003; Van der Merwe and Wickens, 2004; Wild *et al.*, 2005). The Blauwkop distributary channel complex's main current flow was to the north ($340^{\circ} - 015^{\circ}$).

The Skoorsteenberg channel complex's main palaeoflow varies from an easterly ($060^{\circ} - 080^{\circ}$) to a north-easterly direction ($014^{\circ} - 030^{\circ}$) (Fig. 4.4). Palaeocurrent directions of most of the overflow deposits related to the main channel feeder systems vary slightly from $005^{\circ} - 030^{\circ}$. The possibility that these different flow surges could have influenced each other's flow patterns, by subtle topography, seems to be possible for the southern units but not for the Skoorsteenberg unit because it occurs on a different stratigraphic level than the lower units.

Major structural highs and lows on the basin floor could also have played a role in the distribution of the units, but limited field evidence prevents any conclusive interpretation. The palaeoflow of FS 5 forms the fundamental understanding of deposition of each of the units.

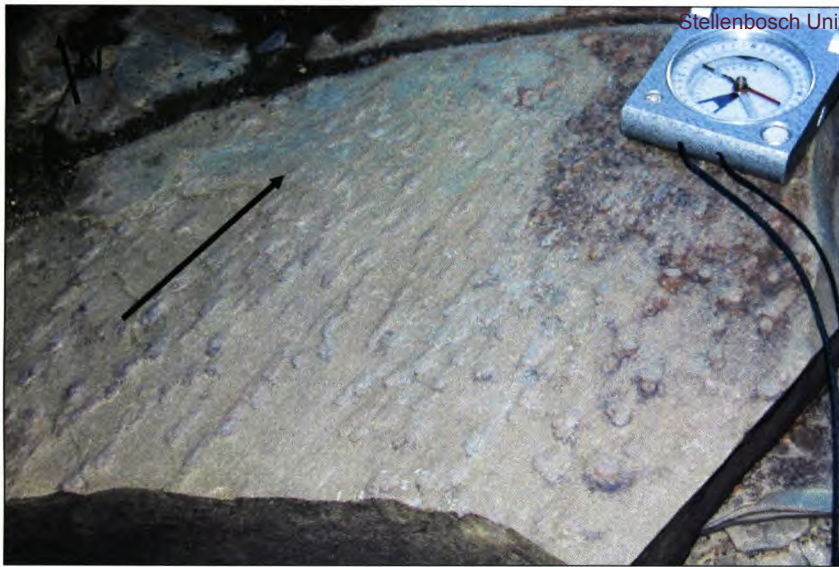


Figure 4.1.1 Flute cast structures on the underside of a bed. Bed in Log section M35. Palaeoflow indicated.



Figure 4.1.2 Groove casts on the underside of a bed. They are good palaeoflow indicators. From Log section M134. Palaeoflow indicated.



Figure 4.2 Parting lineation indicating a current orientation parallel to the pencil. Current flow direction indicated.

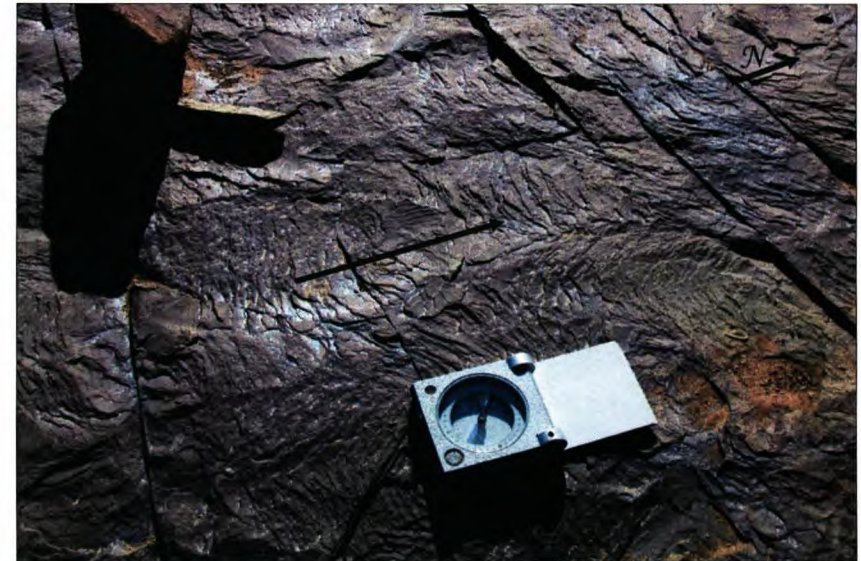


Figure 4.3 Rib-and-furrow structures displaying the steep, concave, down-dipping foreset laminae of linguoid current ripples. Palaeoflow indicated.

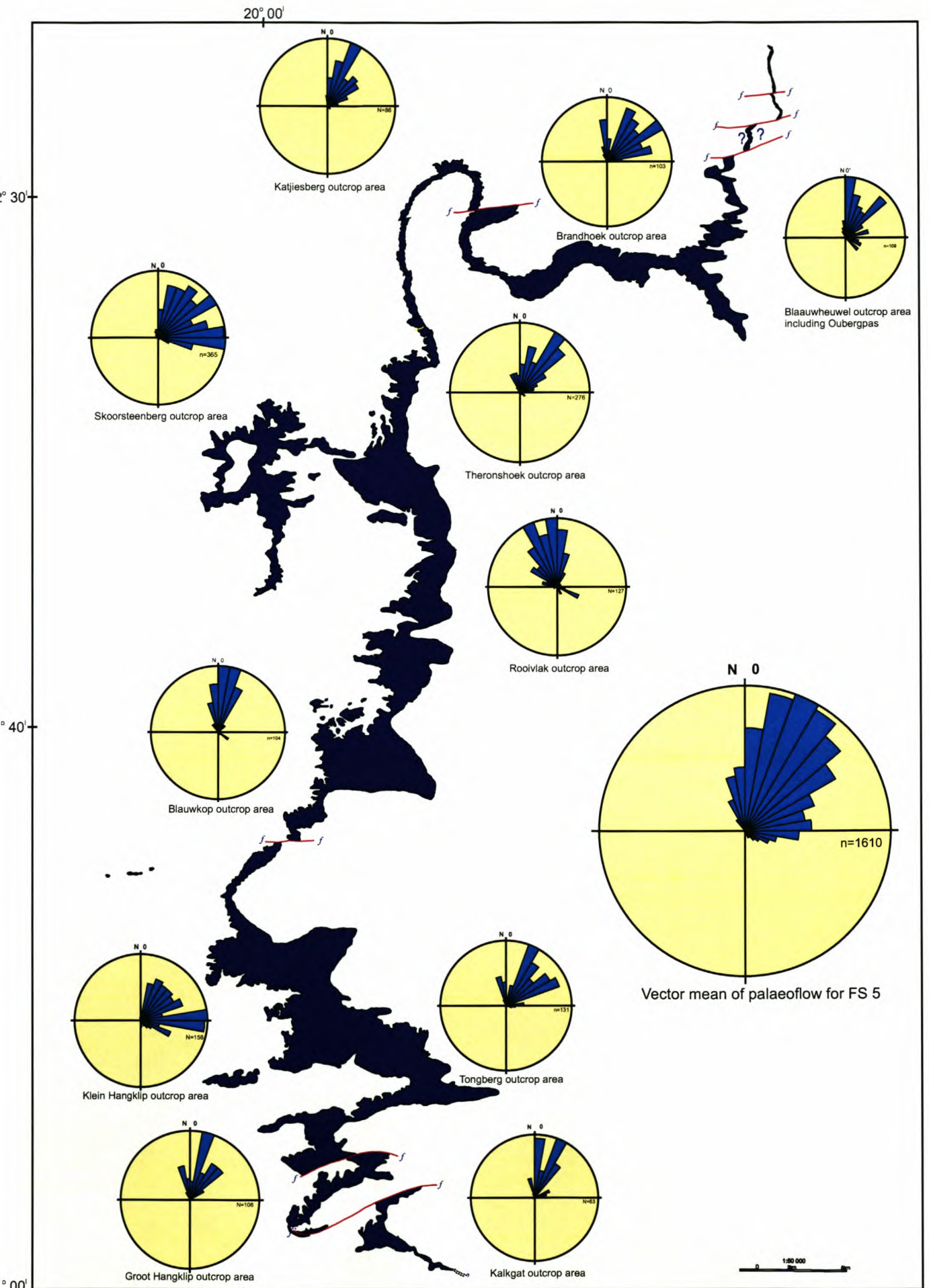


Figure 4.4 Paleoflow patterns for different areas of FS 5.

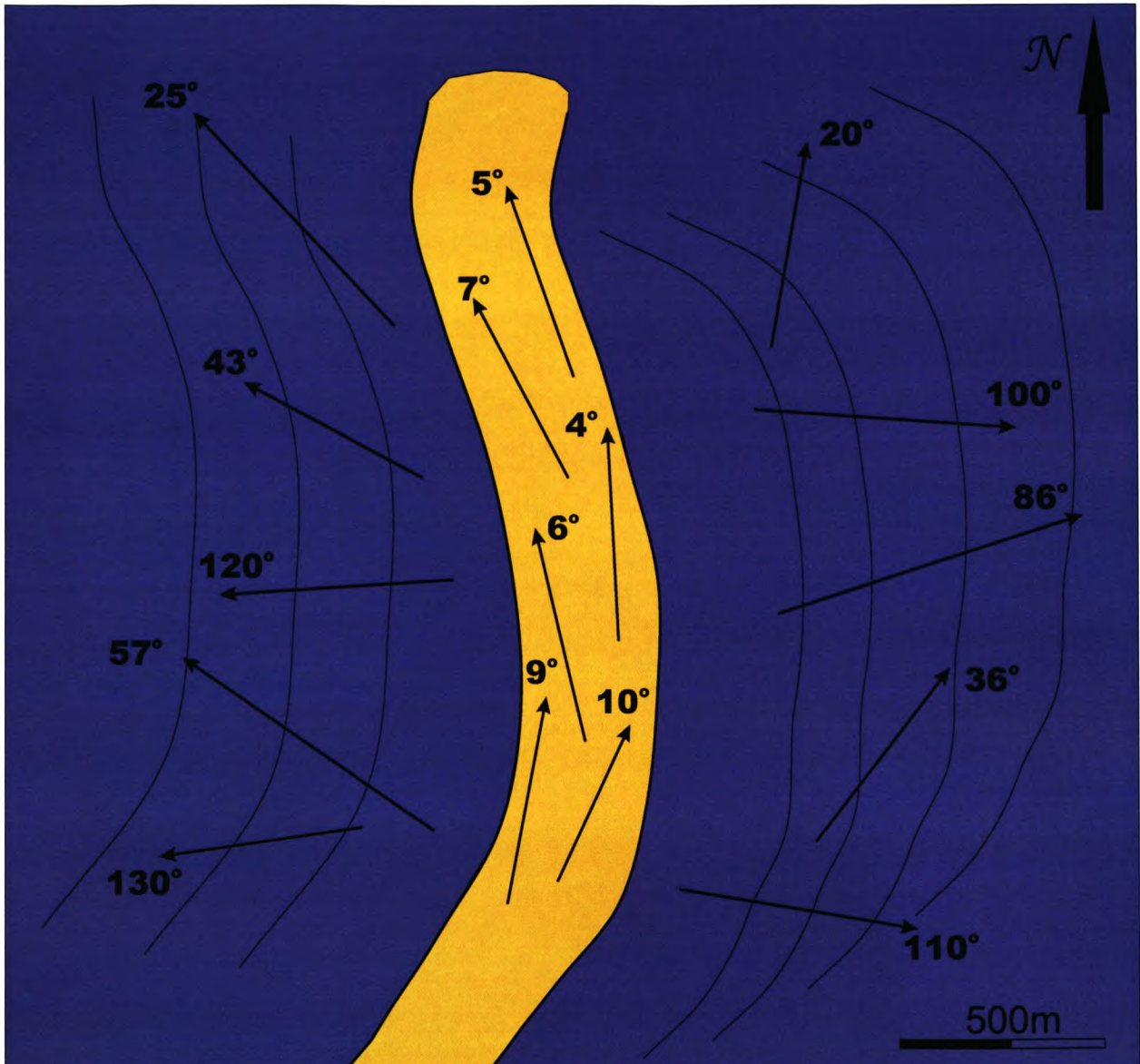


Figure 4.5 A schematic diagram indicating the palaeoflow for most of the FS 5 channel-fills. The thicker amalgamated sandstones constituting the channelized region are deposited in a more confined environment, with paleoflow directions that are more constant. The unconfined and more widely spread spillover area (overflow and sheet sand deposits) reveals paleoflow directions significantly different from the channel axis.

4.3 Regional fan evolution

This section describes the regional distribution and general thickness trends of the areally distinctive channelized zones of FS 5. The six sand-rich units of FS 5 were deposited at different times of fan construction but still form part of the same stratigraphic interval. FS 5 lies between two regionally developed silty-shale successions, which are relatively constant in thickness but with local variation in places. Evidence for erosion into the lower shale unit in the more proximal outcrop area may be due to high-density turbidity currents within channels and the deposition of mass transport slumps. A detailed geological field map has been compiled for the outcrop of FS 5 (Fig. A).

4.3.1 Klein Hangklip

Outcrops of this unit occur on the farms Hanglip 150, Meide Berg 153, Pienaarsfontein 414, Bizansgat 84, Oude Muur 81, Ongeluks Rivier 85 and Kopjes Kraal 86. It has a maximum thickness of 95 m in the westernmost outcrop, and is characterized by massive channel-fill deposits (Fig. 4.6.1). The latter outcrops occur mainly on the farms Hanglip 150, Pienaarsfontein 414 and Meideberg 153 (Fig. A). The channels tend to erode into the lower shales as well as into Fan 4.

Crevasse splay channels occur in the area between the main channel axes and overflow deposits on the farms Kopjes Kraal 86, Bizansgat 84 and Ongeluks River 85. Some of these splay channels are very large, such as the Blauwkoop complex, which forms part of a major distributary channel system that could be connected to the Klein Hangklip unit. A 112m thick succession of thin-bedded ripple-laminated beds (Kopjes Kraal 86) (Fig. A), interpreted as overflow units, occurs approximately 10 km north of the Klein Hangklip outcrops. The uppermost thin-bedded units, underlying the regional silty-shale unit, are slumped in places with ball-and-pillow and dewatering structures.

4.3.2 Tongberg

This unit outcrops mainly on the farms Hanglip 150, Droogekloof 400 and Meideberg 153. It maintains a regular thickness of approximately 85 m along an oblique strike section from the west to the east on the farm Hanglip 150 (Fig. A). A facies change occurs from west to the east.

The Tongberg area hosts three channelized depositional phases. These phases occur on different stratigraphic levels within FS 5, and consist of massive channel-fill sandstone, displaying dewatering features in places (Fig. 4.6.2). The middle phase consists of massive layers of slumped material displaying ball-and-pillow structures and dewatering features. Palaeoflow indicators vary from an easterly to northerly direction. Contacts with under- and overlying shales are relatively sharp.

4.3.3 Skoorsteenberg

The Skoorsteenberg outcrop partly represents a solitary, wide, unconfined channelized system. It outcrops on the farms Groot Fontein 35, Klipfontein 31, Rondavel 34, Zwartbosch 36, Vaalfontein 18 and Zoutrivier 32 (Fig. A). Laterally extensive, predominantly thick-bedded and amalgamated sandstone units, exhibiting large-scale channel-fills and sheet deposits, characterize the succession in this area. This unit consists of a vertical succession of 95 – 105 m of which the lower 60m comprises thin ripple-laminated turbidites and the upper units, massive sandstone beds (Fig. 4.6.3). Palaeoflow indicates an easterly to north-easterly flow direction. The contact with the overlying dark silty shale is abrupt. Weakly developed wave ripple marks occurring on the uppermost layers indicate shallower depths, i.e. at least storm wave base (± 100 m) (Winters *et al.*, 1995; Boggs, 2001). The fan is overlain by pro-delta shales and heterolithic beds, and is interpreted as slope deposits (Johnson *et al.*, 2001) (Fig. 4.6.4).

4.3.4 Blauwkop

This unit outcrops on the farms Krantzkraal 83, Blauwkop 76, Brakke Rivier 77, Kookfontein 78 and Zoetmeisjes Fontein 75. The thickness of the succession of this unit is 85 – 90m in the Blauwkop area and is constant towards the north (Fig. 4.6.5). Palaeoflow data indicates a northerly flow direction, compared to the overall north-easterly flow direction of FS 5. Kirschner and Bouma (2000) interpreted the Blauwkop outcrops as a distributary channel system, comprising seven individual channel-fills, levee, and crevasse splay deposits. In this thesis, the distributary channels systems of Blauwkop are interpreted as crevasse splay channels, which likely correlate with the major channel system of Klein Hangklip (see Section 4.6 for more detail).

4.3.5 Groot Hangklip

This outcrop area has been studied quite extensively over the last few years. Massive slump and channel deposits (Fig. 4.6.6) characterize the Groot Hangklip outcrop, which forms an impressive vertical cliff face of 60 m on the farms Droogekloof 400 and Kalkgat 170. Two major post-depositional thrust faults, namely the Kalkgat fault in the south and the Droogekloof fault in the north divide the Groot Hangklip outcrops (Fig. 4.6.7). The lower contact with the Tierberg Shale Formation is very sharp whereas the upper boundary tends to be gradational in places. A few thin units comprising thin-bedded sandstone and siltstone are present in the Tierberg shale just below this fan. These thin units could be correlated with the distal deposits of Fan 4.

4.3.6 Kalkgat

This unit constitutes the southernmost outcrops of FS 5 before it pinches out on the farm Lower Roodewal 169. These outcrops are the least known and little research has been done on them. It outcrops on Lower-Roodewal 169, Kalkgat 170, and Bakovens Kloof 152. The thickness of this unit is approximately 60m, which reduces to less than 5m in less than 1 km to the south (Fig. 4.6.8). It forms part of the Groot Hangklip outcrops, 4 km north of the Kalkgat locality. A major thrust fault with a displacement throw of 500m separates these two outcrop units. This unit displays massive slumped deposits; the latter being very similar to the Groot Hangklip outcrops. There is an indication of three major slump units in the Kalkgat outcrop. It is evident through this study that the Kalkgat channel-fills reflect a unique high-energy and highly unstable area in the FS 5 system. This could explain the formation of the massive slump deposits, a phenomenon that is common throughout the southern outcrops of FS 5.



Figure 4.6.1 Massive channel-fills characterize the Klein Hangklip area. Transport is away from the viewer in a northeasterly direction.



Figure 4.6.2 Three phases of sediment input characterize the Tongberg unit. Note the upper single channel-fill.

49



Figure 4.6.3 Massive, amalgamated sandstones discordantly overlying 60 m of thin-bedded overflow deposits of FS 5 at Skoorsteenberg.



Figure 4.6.4 Pro-delta shales and heteroliths overlying FS 5, interpreted as slope deposits. Skoorsteenberg in background.

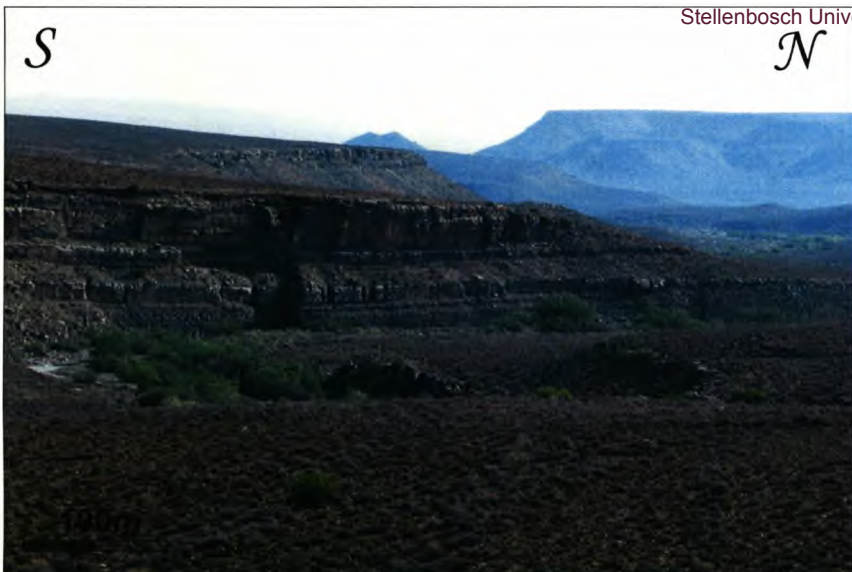


Figure 4.6.5 Outcrops of the Blauwkop unit, consisting of sheet-like massive sandstones alternating with parallel-laminated sandstones.



Figure 4.6.6 A 60 m vertical cliff of the Groot Hangklip outcrop. This is an oblique dip-section of this unit, facing to the west. 30 m of thin heteroliths underlie this unit.

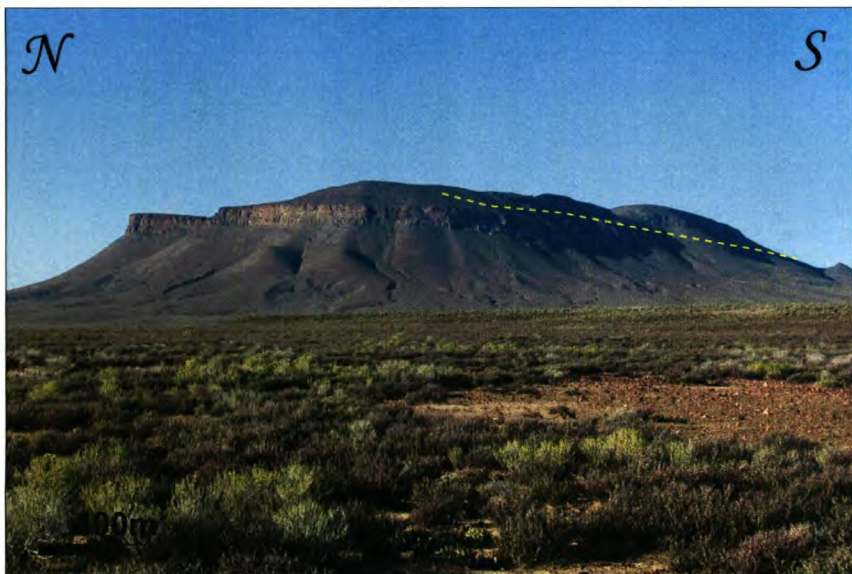


Figure 4.6.7 South-facing strike section of the Groot Hangklip unit. Major thrust fault on the right separates this unit from the Kalkgat unit.



Figure 4.6.8 Massive channel-fills characterize the Kalkgat unit. This is an oblique strike-section.

4.4 Lithofacies description and interpretation

The main types of facies in the Tanqua depocentre have already been mentioned in Section 3.4. This section discusses briefly the different lithofacies types in FS 5 and their interpretation. Ten major lithofacies types, based on lithological composition and internal sedimentary structures, were recognized as the building stones of FS 5. A summary (Table 2) has been compiled for the description and location of these lithofacies. A key for the logs is given in Figure 4.7.

4.4.1 Lithofacies 1 (Lf 1): Massive-bedded sandstones

Description:

This facies predominates in areas where major channel-fill deposits and sheet sand deposits occur. Throughout, the medium to thick beds are homogeneously fine-grained and the thinner beds are fine- to very fine-grained (Marot, 1992). Grain-size rarely exceeds fine sandstone. Amalgamation of beds is common, especially in the confined channel zones (Fig. 4.8.1). Contacts are usually sharp and horizontal (Fig. 4.8.2), but sometimes also irregular due to loading or local scouring (Figs 4.8.3+5). The massive sandstone beds are erosive at the base and some display load casts, fluid scouring and tool marks (Figs 4.1.1+2). The thickness of individual sandstone beds vary within the channel-fills, i.e. from 1 m to 6 m and even more (Fig. 4.8.4). The colour of these massive sandstones varies from a greenish-grey to grey when fresh.

Massive sandstone beds often have an upper component that is dominated by structures of tractive processes, such as parallel- or ripple cross-lamination. These beds often show a fining-upward trend into siltstone in the upper few centimetres, with plant fragments commonly preserved on top of some of these surfaces. Channelized sandstones vary in geometry within channel-fills and exhibit a lenticular geometry (Fig. 4.8.7). Dewatering structures (dish and pillar structures) are common phenomena in the massive sandstones, especially where rapid deposition took place as sheet sands, e.g. at Blaauwheuwel 121, or in the more unstable base-of-slope environments such as at Droogekloof 400 and Kalkgat 170 (see section 4.4.8 for more detail and figures).

Elongated or rounded calcareous concretions of various sizes (up to 1 m in diameter) are also present in some of the thicker sandstone beds. Loading is commonly associated with amalgamated contacts (Fig. 4.8.3). The best outcrops of this facies are concentrated in the six major channel feeder systems of FS 5 but also in the sheet sand deposits, especially at Blaauwheuwel 121 and Zoetmeisjes Fontein 75 (Figs 4.8.6+8).

Interpretation:

Structureless (massive) sandstones are deposited by high-density turbidity currents (Kuenen and Migliorini, 1950; Bouma, 1962; Pickering *et al.*, 1986, 1989; Kneller and Branney, 1995). They are interpreted in FS 5 as primary sand deposition from the parent or initial flow. The latter consists of a higher density sand/water mixture which is the main driving force in the turbidity current. Deposition can be in less than a few minutes, with no time for any internal structures to form. The remaining part of the flow has a low density and stays longer in suspension. This less dense material is deposited out of suspension some time after the massive parent flow, which could take hours or many years (Kneller and Branney, 1995). Amalgamation is common in the more confined channel environment, where most of the massive sands are deposited (Fig. 4.8.1).

Erosional structures and surfaces are caused by the high-density parent flow (Figs 4.8.5+7). Sole structures result from the impact on the muddy substrate by objects within the flow; i.e. mostly by mud-clasts and plant material. In turbulent flows, mud-clasts interact within a flow and will, on occasion, come into contact with the underlying substrate (Dzulynski and Sanders, 1962). This produces scour marks, such as flute casts and prod casts. Tool marks such as groove casts and chevron marks, are caused by the dragging of larger objects along the base of the flow (Dzulynski and Sanders, 1962). These structures are very useful palaeoflow indicators.

In conclusion, these massive structureless sandstone bodies are very good reservoirs for oil and gas and therefore sought after reservoir targets in hydrocarbon exploration. Geometry of sand bodies and their vertical and lateral connectivity within channel-fill environments and sheet-sand deposits are of key importance to understand the production of hydrocarbons from them.

4.4.2 Lithofacies 2 (Lf 2): Parallel- and ripple cross-laminated sandstones

Description:

Bed thickness of this facies varies from 10 cm up to 2 m. It is generally thinner than that of Lithofacies 1 but with similar grain-sizes. The colour is grey to light brown to yellow. Parallel-laminated sandstone beds, which represent deposition in the upper flow regime (Bouma Tb-division), generally overlie the massive sandstone facies (Fig. 4.9.1). The laminations vary in thickness from 1 mm up to 3cm (Fig. 4.9.2). The beds most commonly have flat, sharply defined bases and tops, but in places their contacts with either underlying or overlying beds are diffuse and not clearly defined (Fig. 4.9.3). Stream lamination and parting lamination on bedding surfaces provide for palaeoflow orientations (Fig. 4.9.4). Climbing-ripple structures, produced by the migration of linguoid ripples, are most abundant and commonly show the preserved stoss side lamination (Fig. 4.9.5). These ripple forms are characterized by a highly sinuous, asymmetrical crestline with irregular shallow troughs (Fig. 4.9.6). Successive beds commonly drape over underlying bedforms, resulting in lenticular to wavy bedding. Ripple height varies from 2 – 7 cm and their wavelengths are 10-20 cm. Rib-and-furrow structures reveal steep, concave, down-dipping foreset laminae with dip direction indicating current direction (Collinson and Thompson, 1989) (Fig. 4.9.6). Erosional surfaces are also present within some of the beds. Sole structures such as load casts, flute casts and tool marks occur on the underside of beds and correspond to those of Lithofacies 1 (Fig. 4.9.7).

Interpretation:

This facies is commonly found in the thin-bedded interval above the base of FS 5 and mainly constitutes the overbank deposits of FS 5 in the Krantz Kraal 83, Pienaarsfontein 414, Bizansgat 84, Oude Muur 81 and Meide Berg 153 areas. Deposition of Lithofacies 2 took place in a lower energy flow regime than that of Lithofacies 1. It occurs throughout the study area and forms part of the channel-fill deposits but predominates in the overflow settings. For the formation of parallel laminations the bed-load sediment concentrations and viscosity of the bed-load layer must be high, and the turbulent flows above the beds must also be largely suppressed (Bagnold, 1956; Simons *et al.*, 1965; Allen and Leeder, 1980; Lowe, 1988).

The occurrence of this lithofacies is regional, but it is much more concentrated as upper flow regime deposits of the confined channel-fill complexes and sheet sand localities. The cross-laminated facies is the most abundant facies type in the FS 5 outcrop area. Ripple cross-laminated sandstones occur mostly in the unconfined overflow environments adjacent to the main channel

axes. The variation in thickness of these packages give the impression that sediment input was continuous for a long period. Small shale-siltstone partings (less than 1 cm) reflect breaks in sediment input.

The thick successions with ripple and climbing ripple-lamination are interpreted as overflow deposits. These beds follow after deposition from the parent flow and are produced from a lower sedimentation rate. The type of cross-lamination, which is mainly a function of the angle of bedform climb, is directly proportional to the rate of sediment transfer and bedform height, and inversely related to the rate of bedload transport (Kuenen, 1967; Allen, 1982). Climbing ripple-lamination is a primary sedimentary structure produced by over-sedimentation, whereby the rate of fall-out from suspension is so great that the ripples have insufficient time to move laterally or migrate downstream - they rather aggrade vertically (Fig. 4.9.5).

4.4.3 Lithofacies 3 (Lf 3): Sigmoidal and wavy ripple cross-laminated sand- and siltstones

Description:

This type of ripple cross-laminated beds displays an unusual geometry. The ripple forms are asymmetrical with the stoss and lee side mostly preserved (Fig. 4.10.1). The wavy bedded or sinusoidal (Jopling and Walker, 1968) sandstones have an undulating bed shape which, in some cases, can be almost symmetrical (Fig. 4.10.2). The ripple form is commonly 'draped' by a silt interval (Fig. 4.10.3). The sandstone is commonly very fine- to fine-grained, and silty. The beds are thin to very thin, between 1-10 cm, with upper and lower contacts sharp and commonly non-erosive (Figs 4.10.1+4+5). In plan view, these wave ripple-forms display straight and laterally continuous crests (Fig. 4.10.6). Their amplitudes are similar (1-2 cm) and their wavelengths are also equal (5-10 cm). It gives the impression of miniature anti-forms and syn-forms (Fig. 4.10.2).

Interpretation:

This lithofacies type has been described in many turbidite successions. Mutti (1992) suggested that this facies occurs commonly in confined depositional settings, meaning smaller areas or smaller depositional systems and not in laterally extensive areas as in the case of the climbing ripples. Wavy bedding in other deep-water successions has been interpreted as short-wavelength anti-dunes (wavelength ~ 65 cm) (Skipper, 1971; Skipper and Bhattacharjee, 1978). Wild *et al.* (2005) interpreted this wave bedding as the deep-water effect from large storm events that

reworked the top surface of the turbidite beds by orbital bottom currents. The full preservation of the ripple form and drape by subsequent silt suggests a high suspension fall-out rate during traction deposition (Johnson *et al.*, 2001). The difference between sigmoidal and wavy geometry as described above, is interpreted as due to the difference in net sediment fall-out rate (medium for sigmoidal and very high for wavy) and whether the crests are symmetrical or asymmetrical.

Castro and Snyder (1993) based their explanation for these structures on what the downstream effects of topography could have on the turbulent current of sand particles during their flow and deposition. Flood (1988), McCave and Tucholke (1986) attributed their development to the formation of fine-grained sediment waves that occur in many slope, base-of-slope and levee settings. The wave bedded structures have wavelengths between 500-3000 m and heights of 10 – 100 m compared to the 3-20 cm in FS 5. Because of their close spatial association with the cross-laminated facies, the sigmoidal and wavy laminations could be explained by a period of low sediment supply and high bottom current flow. This high-energy bottom current reworks the upper silty-sand linguoid ripples into more symmetrical and asymmetrical wave crests before the following sand-rich unit is deposited onto the newly formed crests, and builds it onto the previous current ripple.

4.4.4 Lithofacies 4 (Lf 4): Parallel- and ripple cross-laminated siltstones

Description:

These finely laminated to micro-cross-laminated siltstones are normally interbedded with layers of sandstone and shale of a few centimetres in thickness (Fig. 4.11.1). Another characteristic of this facies is a rhythmic alternation of cross-laminated sandstone and siltstone (Fig. 4.11.2). The bed thickness of these units varies from 2-10 cm and the stacking thickness of these facies is up to 40 m in the Skoorsteenberg outcrop area (Fig. 4.11.3). The colour varies from dark grey to almost bluish-black when fresh (Fig. 4.11.4). Bounding surfaces are sharp, but in some environments, for example the sheet sand deposits, the contact surfaces are much more graded (Fig. 4.11.4). Small-scale flame and loading structures are quite common in this facies (Fig. 4.11.5). The regional extent of this facies, especially the thicker units, is large and beds gradually pinch out in the basin shales down-fan. Bioturbation and trace fossils are quite common on bedding planes (Fig. 4.11.6).

Interpretation:

Settling of silt-sized particles from suspension to form siltstone beds normally takes place after the deposition of turbidite sands. Silt particles remain longer in suspension and are deposited during the time of energy reduction in the turbidite current (Wickens *et al.*, 1990). The pronounced silty character suggests sediment supply from a relatively close adjacent source from a slope setting (Martinsen *et al.*, 2003; Friès and Parize, 2003). This facies results from the low concentration, low-density turbidity currents at the tail-end of sand-rich high-density turbidity currents. The isolated 'starved' ripples observed in this facies result from weak tractional processes (as discussed in Lithofacies 3). The bioturbation, arthropod trackways and fish trails suggest a relative calm environment (Figs 4.11.6+7). This facies is very dominant within the basal units of FS 5. These beds, as well as those to the northeast in the vicinity of Oude Muur 81 and Meide Berg 153 are interpreted as distal overflow deposits of the major channels in the Klein Hangklip and Tongberg areas.

4.4.5 Lithofacies 5 (Lf 5): Thin-bedded sandstones, siltstones and shales*Description:*

This facies type occurs as thick units of 1 – 20 m alternating with sheet-sand deposits of FS 5. Good examples occur on Zoetmeisjes Fontein 75 and Blaauwheuwel 121 (Figs 4.12.1+2). This facies consists of very thin sandstone layers (5-10 cm), alternating with siltstone (2-5 cm) layers and very fine dark shale (0.5-2 cm) layers (Figs 4.12.3+4). The more sandy layers are usually ripple-laminated and the siltstone and shale are parallel-laminated. In most cases lamination is absent (Fig. 4.12.5). The colour of these layers is greyish to brown, giving the impression that the sandstone layers are compositionally immature. The upper and lower contacts are sharp in the case of the more sand-rich layers but more gradual for the siltstone-shale layers (Fig. 4.12.6). Also associated with these layers are ichnofauna but no evidence of plant fossils could be found.

Interpretation:

Packages of this facies usually display an upward thickening or upward fining/thinning pattern and are associated with underlying or overlying thicker massive sandstone units (Figs 4.12.1+2). Both upward thickening and upward thinning packages are found in the sheet-sand deposits and do not occur in the channelized environments. A coarsening-upward character might indicate increasing proximity to the source, and thus progradation (Martinsen *et al.*, 2003). Thus, the

sandstone layers, which in some outcrops consist of parallel laminations, or ripple laminations were deposited in a distal unconfined environment which was also associated with the tail end of the turbidite flow. Erosional features are rare in this lithofacies. However, in some of these sandy units, small clay pebbles occur, which is an indication of occasional higher energy conditions. Deposition of the thin layers of shale could be ascribed to short periods of starvation in the basin.

4.4.6 Lithofacies 6 (Lf 6): Erosional and bypass facies

Description:

This facies consist of different sizes of mud-clasts intermixed with sand. The mud-clasts are round and spherical balls of clay before compaction and sub-angular and often fragmented after compaction. The size of the clay-clast pebbles varies from 5 mm up to 300 mm in diameter (fine pebbles to small boulders). These rip-up clay/mud clasts are associated with the massive sandstone units of the high-energy environments (Fig. 4.13). This facies is mostly chaotic and in some localities associated with slump-like structures (Fig. 4.13.1). Field evidence indicates that an alignment of the pebbles in a certain direction, which could indicate flow direction, is absent. The clay clasts are usually embedded in a mixture of shale, siltstone and sandstone (Fig. 4.13.2). Internal structures are absent except for typical hook-shaped, twisted bedding form (designated as miniature slump overfolds by Cromwell, 1957) and alternating thin sandstone stringers (Fig. 4.13.3). The colour of these pebbles is purple to greyish-black i.e. the same colour as the surrounding hemipelagic shales of the basin. The bypass facies occurs in very small areas and forms cigar, ellipsoid and finger type geometries (Fig. 4.13.4). The occurrence of rip-up clasts at the base of channel-fill erosional surfaces is very inconsistent and could form down-stepping erosional surfaces within the adjacent layers without any clay clasts or lag deposits (Figs 4.13.5+6).

Interpretation:

The bypass facies is associated with erosional surfaces and miniature slump-like structures, interpreted as lag deposits (Figs 4.13.1+3+4). This facies is not only associated with the basal erosional zones of channels but with any high-energy environment, even in the most distal sheet sand units (Fig. 4.13.7). Mud/clay is deposited during a sediment starved period in a basin and is eroded during the first parent sand flow surges, which originate from the source. This eroded clay sticks together in small clusters and is rolled up in small balls by the overflowing sand. These

clay balls are denser and tend to concentrate at the base of the flow (Fig. 4.13.8). Rip-up clasts are commonly associated with amalgamated surfaces in the thalwegs, especially where local scouring occurs, e.g. the channel-complex at Klein Hangklip (Figs 4.13.8+9) (Wickens *et al.*, 1990). These rip-up clast clusters (lag deposits) are an indication of flows that have bypassed a specific area within the thalweg.

The differences between rip-up clasts in channel deposits and in sheet-sand deposits are minimal. Their composition is similar, only the mode of deposition differs. At the bases of the channels the clay clasts form big cigar-type clusters or pockets whereas in the sheet-sand layers, clasts are more solitary and collected in small pockets (Fig. 4.13.4).

4.4.7 Lithofacies 7 (Lf 7): Convolute laminated sandstones

Description:

Convolute lamination was first referred to as “convolute bedding” by Keunen (1953). He described it as a structure characterized by marked crumpling or intricate folding of the laminations within well-defined, tectonically undeformed sediments. The convoluted layers occur in finely laminated sandstones and siltstone deposits (Fig. 4.15.1). The colour of this facies is dirty brown-grey in fresh samples. The layers display laminae that have been folded in irregular, small-scale, sharp-crested anticlines and rounded to box-shaped synclines (Fig. 4.15.2). The amplitudes and wavelengths vary from a few millimetres up to 2 m. It did not originate from chaotic slumping, because the original bedding and laminae are still present and very clearly visible on the weathered surfaces due to a slight contrast in colour and relief (Figs 4.15.1+2).

Interpretation:

Convolute bedding is one of the most difficult primary sedimentary structures to define and to explain. If the folds indicate transport direction, the process producing convolutions must develop during deposition (Boggs, 2001). However, in agreement with Boggs (2001), it is believed that the process that controls the formation of convoluted layers is liquefaction of the sediment due to processes such as differential overloading, earthquakes, wave action and bottom currents. Some convoluted beds are laterally continuous in some parts of the study area and at some localities, merge with ripple cross-lamination. There is no evidence of any dislocation of the thin layers,

although the deformation is complex in some of these layers. Some of the convoluted layers form folds that resemble ball-and-pillow structures, suggesting load deformation.

Potter & Pettijohn (1977) and Boggs (2001) believe that the axes of the convoluted fold orientations coincide with the palaeocurrent direction. There was however, locally not enough exposure to determine current direction. Micro-faulting is absent, even in the most complicated fold structures, although some laminations are truncated by small internal unconformities which are themselves involved in convolutions. This facies seems to be restricted to the base-of-slope environments such as interpreted for the southern outcrop areas of FS 5. The best exposed examples are in the Droogekloof locality, which forms part of the Groot Hangklip slump channel complex. Very large-scale convoluted structures are also present below the upper regional shale of FS 5. The amplitudes and wavelength are up to 4 m and are thus much larger.

Other structures that are sometimes associated with the convoluted layers are flame structures and sand volcanoes (Fig. 4.15.3). These structures are due to sediment loading by more dense material such as rapid deposition of sand over water-saturated mud. Some of the structures display overturned orientations, suggesting that the loading resulted from horizontal movement of the mud or sand (Boggs, 2001) or by current drag (Wickens pers.comm).

4.4.8 Lithofacies 8 (Lf 8): Slumped units

Description:

More than 65% of the Kalkgat, Groot Hangklip and Tongberg deposits display soft-sediment deformation, particularly slumping and sliding. These deposits consist of thick sandstone units displaying dewatering and ball-and-pillow structures (Fig. 4.15.1). The upper contacts of these disturbed beds are sharp (Fig. 4.15.2). These packages of slump material are interbedded with thin undeformed turbidite deposits (Fig. 4.15.2). Overlying strata sometimes are undeformed without any signs of thrusting between them. Irregularities in the upper surface of slump sheets commonly show infill by the overlying bed. This facies is generally sharp-based, but seldom erosive. The outcrops of slump deposits in the Groot Hangklip (Fig. 4.15.3) and Kalkgat areas display a sheet-like geometry over most of this area.

Ball-and-pillow structures are characteristic of this facies and confined to the bed without causing any disturbance in the over- or underlying beds (Fig. 4.15.2). The sandstones display hemispherical to kidney-shaped geometries with sandstone balls ranging from 10 cm up to 150 cm in diameter (Figs 4.15.1+4). These structures are associated with an overlying dewatered mudstone unit with a sharp upper boundary in the Tongberg locality (Fig. 4.15.5); the overlying beds are undisturbed sandstones. Shale associated with these structures is deformed and appears to be wrapped around the pillows, squeezed in between them and extending as thin tongues up into the sandstone bed (Figs 4.15.1+4). In some cases the original lamination can still be detected in the pillow sandstones. The massive, dewatered sandstones which are closely associated with overlie ball-and-pillow structures, are up to 6 metres in thickness. They have a very peculiar brittle weathering pattern which makes them easy to identify in outcrop (Fig. 4.15.5). Numerous dish and pillar structures are present in fresh samples (Fig. 4.15.6). No preferred orientations were found in any of these structures.

The dewatering structures are mostly dish and pillar structures, of which the concave upward dishes are the most common (Fig. 4.15.8). Unique examples of such structures are found in the Blaauwheuwel sheet sand deposits of FS 5. The pillar structures are absent here but the dish structures are very large and show well-defined upward migration (Figs 4.15.8+9). These are very special dewatering features and not typical 'dish' structures. They almost resemble worm burrows and are concave upward (Fig. 4.15.9). Some of them are vertical but most of them "migrate" at an angle of 30° or more.

Interpretation:

Slump structures are most likely caused by either earthquakes, which would have caused a foundering of the unconsolidated sand bed (Potter and Pettijohn, 1977), or slope sediment failure. Kuenen (1958) was able to reproduce ball-and-pillow structures experimentally. He deposited a layer of unconsolidated sand over clay and applied a shock which caused the sand layer to founder and to break up into kidney-shaped segments. This led him to the conclusion that earthquake shocks might be a triggering mechanism.

The large-scale slumps observed in the field area could have been caused by tectonic syn-depositional growth structures that disturbed the sediment, causing localised movement. The small-scale slumps and slides are interpreted to be the result of locally induced factors, such as

small-scale overbank collapse in response to topographic readjustment. The small-scale slumps are then most likely to occur in local areas of channel systems (Fig. 4.15.7). The large-scale slumps occur in areas that were tectonically active during deposition. The slump deposits could have derived from a lateral slope and not from the same source as the turbidites. Thus, it is likely that turbidite sedimentation occurred at the same time as slumping so that these events were not temporally but rather spatially separated.

4.4.9 Lithofacies 9 (Lf 9): Hemipelagic shales

Description:

The colour of the shale varies from dark-grey to blackish with some sections containing calcareous concretions. Thicknesses range from 0.2 cm to 15 m. The basal contact of FS 5 is sharp with the underlying mudstone (Fig. 4.16.1). The thickness of the shale unit between the top of Fan 4 and the base of FS 5 varies from 3 m in the southern outcrops to 9 m in the northern outcrops (Fig. 4.16.2). All the shales display soft flaky weathering with the silty shale weathering more pencil-like (Fig. 4.16.3). The shale facies present in the upper unit of FS 5 is much siltier and convoluted than the other shale facies in the Tanqua sub-basin (Fig. 4.16.4). Round and spherical calcareous concretions of yellowish-brown colour are abundant in this facies. These structures cause a distortion of the shale during compaction of the over-lying shale. It forms typical ellipsoid single bodies with a diameter of 10 – 150 cm (Fig. 4.16.5).

The shale interval between Fan 4 and FS 5 changes in thickness and character from the south of the study area to the north. The true shale unit becomes thinner (< 1.5 m) and the remainder is siltier and shows ripple cross-lamination. The fine hemipelagic shale units are very thin, maximum 3 m, the rest of the beds associated with these shales are mostly parallel-laminated siltstone units. The base of FS 5 consists of a regionally developed shale layer of 20-50 cm (Fig. 4.16.6). This thin shale unit forms a laterally extensive marker bed between Fan 4 and FS 5. The first sandy-siltstone units at the base of FS 5 form a sharp basal contact with the underlying marker bed (Fig. 4.16.7). Overlying FS 5 is a regionally developed shale marker bed with a constant thickness of approximately 25 m. This bed consists of 80% siltstone and 20% mudstone (Fig. 4.16.4). It seems that the time period of zero sediment input into the basin was short, from the last sand flow at the top of Fan 4 to the first hemipelagic shale unit.

Interpretation:

This facies represents background sedimentation in an environment where sand- and silt-rich turbidite flows were absent. It accumulates by slow suspension settling of mud through the water column. This facies is deposited as interfan units when the fan system is no longer active, or between sand-rich turbidity currents if intervening time allows it.

Concretionary horizons occur as a result of sediment starvation (Fig. 4.16.5). The lack of sedimentation allows a form of diagenesis to operate on the sea floor just below the sediment-water interface (Raiswell, 1987). These horizons reflect times when even background sedimentation is lower than normal. The size of the concretions is interpreted to be a direct result of the length of sediment starvation (Sixsmith, 2000).











4.4.10 Lithofacies 10 (Lf 10): Micaceous and carbonaceous siltstones*Description:*

This facies is commonly found at the top of massive sandstones in both channel-fill and sheet deposits as well as overbank deposits. These beds are mostly silt-dominated and frequently occur as parallel-laminated beds. Lf 10 consists of abundant, grey, coalified plant material, fine sand, silt, mica flakes and small shale clasts (Wickens *et al.*, 1990) (Fig. 4.17.1). The average thickness is 5 – 40cm, and it is associated with Lf 1, 4 and 5. The upper beds of FS 5 comprise ‘dirty’, soft, greyish-weathering layers with plant fossils (Figs 4.17.2+3).

Interpretation:

Less dense plant material and other finer materials remain in suspension after the sandy part of the turbidite flows has been deposited. This facies forms the tail deposits of a turbidite flow and therefore occur in the uppermost part of the bed.

Table 2: Summary of the main depositional lithofacies which comprise Fan System 5.

Lithofacies (Lf)	Image	Name	Description	Bounding surfaces and structures	Location	Ichnofauna and fossils
1		Massive bedded sandstone	Massive sandstones with abundant amalgamation contacts. Grey in fresh sample and very fine-grained. Rip-up clay clasts associated with erosive contacts	Very sharp and erosive. Tops gradual to sharp. Groove-, flute-, prod-, and load casts abundant on basal contacts.	Channel-fills and sheet and lobe sand deposits	Absent
2		Parallel- and ripple cross-laminated sandstone	Structured sandstones with primary sedimentary structures such as, parallel laminations and ripple - and climbing-cross laminations.	Basal contacts are gradual but sharp in certain areas and even erosive. Tops are sharp. Groove-, flute-, prod-, and load casts abundant on the basal contacts.	Upper fill of channels, overflow and levee areas.	Infrequent, but plant fossils are abundant on parallel-laminated beds in the upper channel-fills.
3		Sigmoidally and wavy ripple cross-laminated sand- and siltstone	Sigmoidal ripple forms are asymmetrical with the stoss and lee side of ripples preserved. Wavy ripple forms are symmetrical with straight and laterally continuous crests.	Very sharp bases and tops. Basal structures are infrequent but mostly absent	Overflows and levees	Infrequent
4		Parallel- and ripple cross-laminated siltstone	Very fine micro-cross- and parallel-laminated siltstones interbedded with the thicker sandstone beds. Deposited in a low-energy environment.	Sharp bases and tops, mostly eroded by denser material. Contains imprints of erosional structures.	Most of the depositional environments.	Depends on the depositional environment. Abundant in the overflow and sheet depositional areas. Absent in channel areas
5		Thin-bedded sandstone, siltstone and shale	Very thin layered (2-5 cm) sandstones interbedded with siltstones and shales. Mostly laminated.	Very sharp, bases and tops. Sole structures infrequent.	Overflow and sheet sands	Abundant
6		Erosional and bypass facies	Abundant mud rip-up clasts. Chaotic sediment fills. Intermixture of sand, silt and shale. Lateral accretion packages form in this areas of active channel migration and erosion.	Chaotic upper and lower contacts, mostly erosive or in erosive zones. Sole structures absent	Mostly in the erosional cuts of primary channel-fills. Or in high-energy sheet sands deposits	Absent
7		Convoluted laminated sandstones	Crumpling or intricate folding of laminations within undeformed sediments. Sharp-crested anticlines and box-shaped synclines	Sharp lower and upper contact surfaces. Groove marks occasionally present.	Overflow and sheet sands	Infrequent, plant fossils in some occurrences.
8		Slump structures	Chaotic overturned and deformed beds. Abundant dewatering and ball-and-pillow structures interbedded with shale. High-energy and unstable environments	Large slump structures eroded into lower units. The dewatered beds form sharp contacts. Bottom drag apparent in some places	Base-of-slope	Absent
9		Hemipelagic shales	Very low-energy environments. Dark pencil weathering, often with thin beds of highly bioturbated silty siltstones. Calcareous concretions are interbedded in the shale.	Graded bases and tops, except if high-density sandstones been deposited very sharply on these shales	Interfan and basin floor deposits. Typical background sedimentation.	Abundant
10		Micaceous and carbonaceous siltstones	Very fine laminated siltstones with a high percentage of organic matter, such as plant fragments.	In most cases it forms graded beds. Sole structures are absent.	On the tops of massive channel-fills and in overflow and sheet deposits	Absent

Key for the sedimentary logs

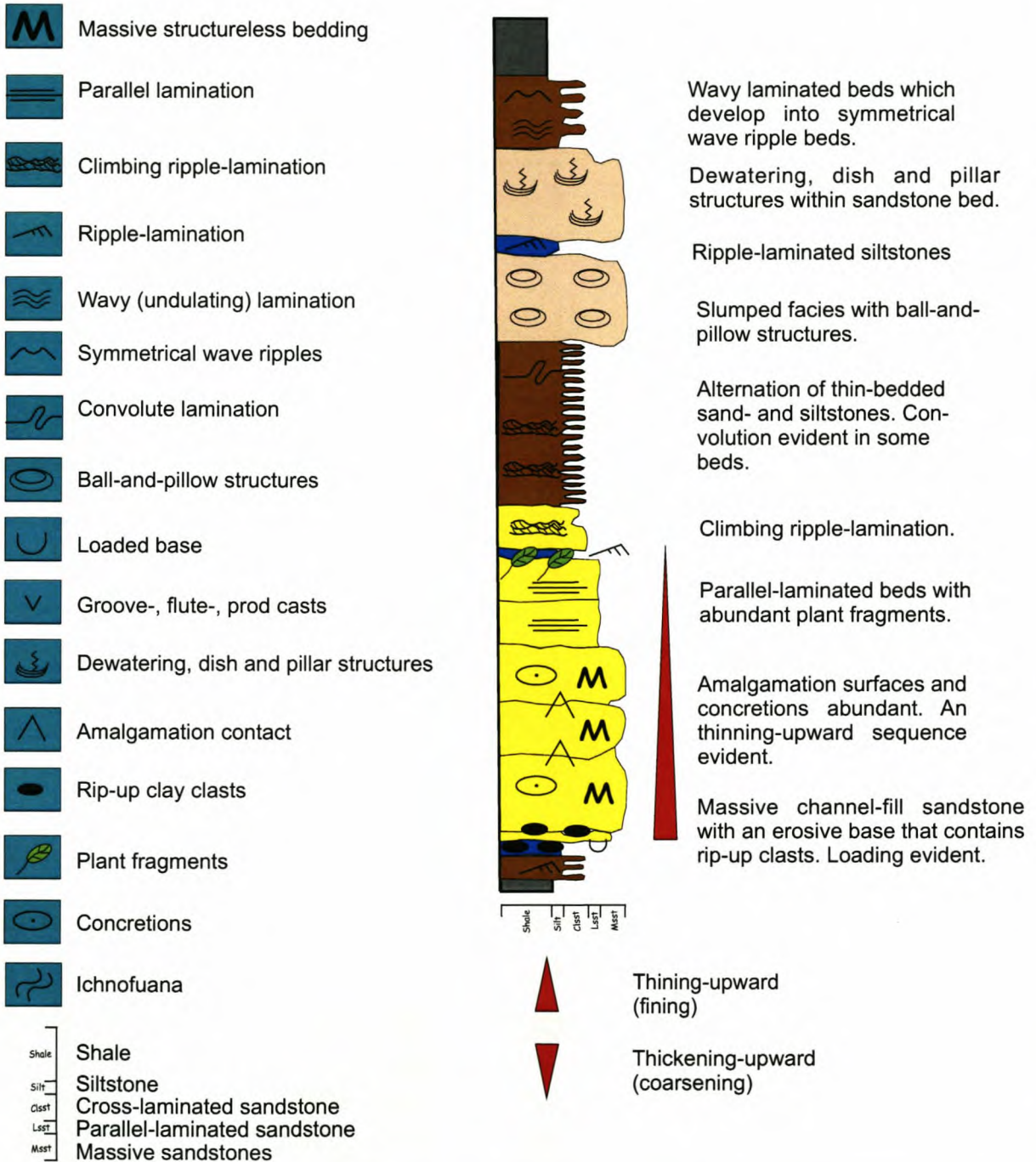


Figure 4.7 Key symbols used in the sedimentary logs.

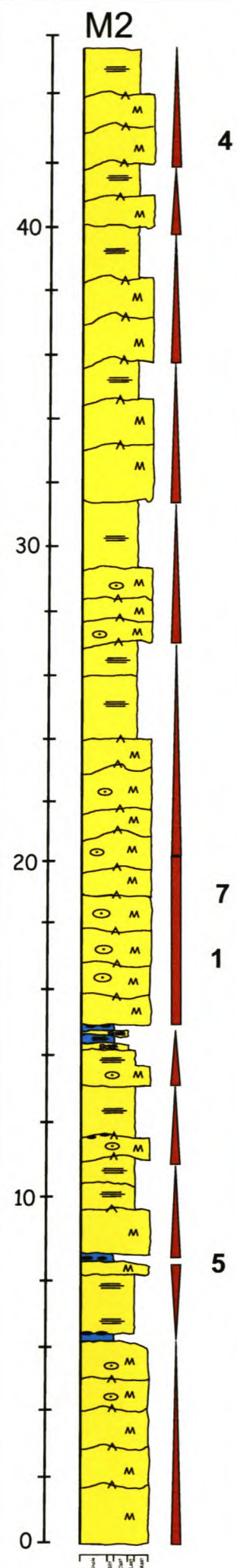
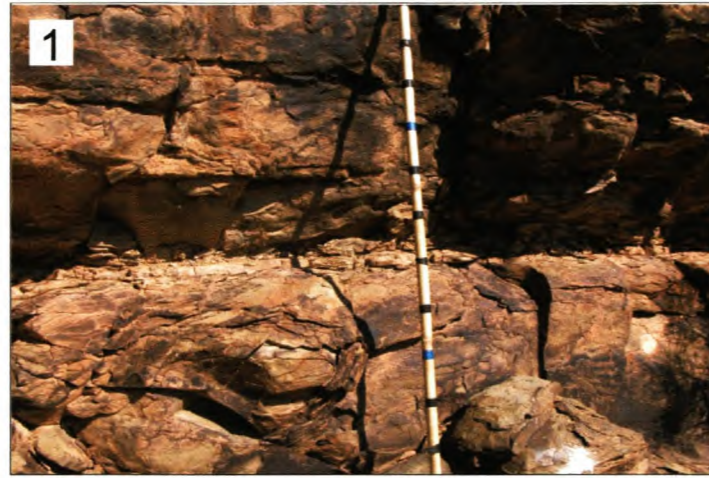


Figure 4.8 Lithofacies 1. Example of a vertical section through a succession of dominantly massive sandstones (MSS). Located at Hanglip 150. Photographs represent examples from the study area. (1) Amalgamation contact between two MSS units. (2) MSS loaded into, and forming a sharp contact with a bed of thin, alternating facies of sandstone and siltstone. (3) Loading structures at the base of a MSS. (4) 5 m thick MSS unit in a channel-fill. (5) Amalgamation contact with erosional features. Note the lenticular rip-up clast unit, indicating an erosive contact between these two units. (6) MSS units deposited as sheet sands at Zoetmeisjes Fontein 75. (7) Scouring surface in MSS beds. Strike-section through a small channel-fill which forms part of a larger channel complex. (8) Massive sheet sand at Blaauwheuwel 121.



D13

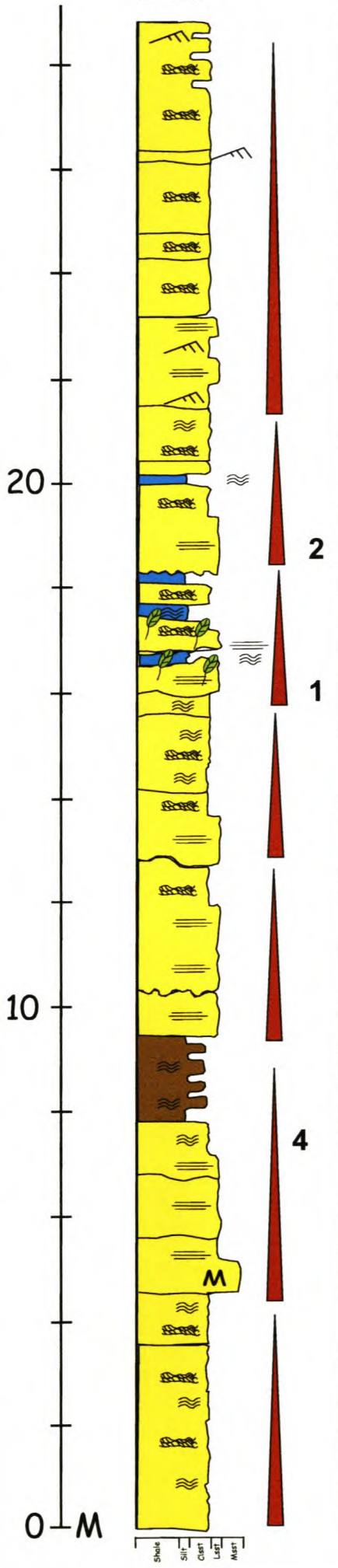


Figure 4.9 Lithofacies 2. This vertical section consists predominantly of parallel- and ripple cross-laminated sandstones. Located at Skoorsteenberg. (1) Parallel-laminated sandstone bed. Laminations are clearly shown by weathering. (2) Fine, parallel laminations. (3) Graded bedding. Note the different colours of each sand layer. (4) Stream lineation and parting lineation on bedding surfaces of parallel-laminated beds. (5) Climbing ripple-lamination. Ripples gradually die out and the lamination becomes sub-horizontal. (6) Rib-and-furrow structures on the surface of a ripple cross-laminated layer. (7) Groove marks as sole structures.

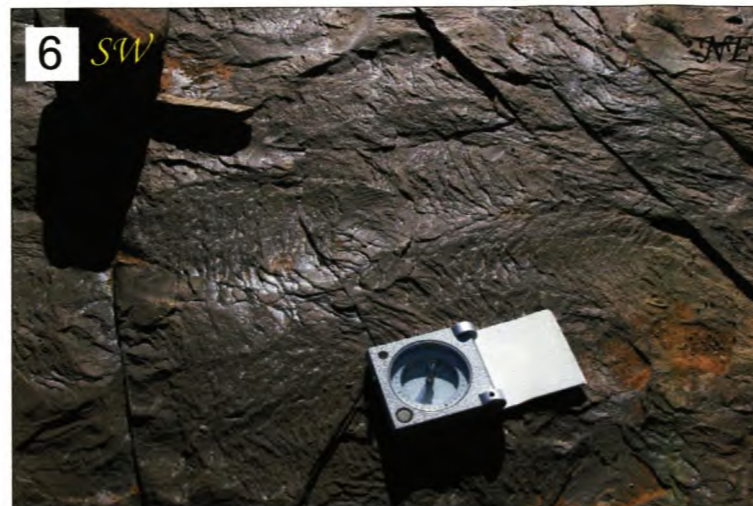
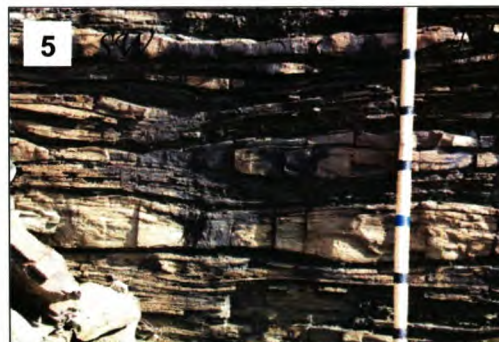
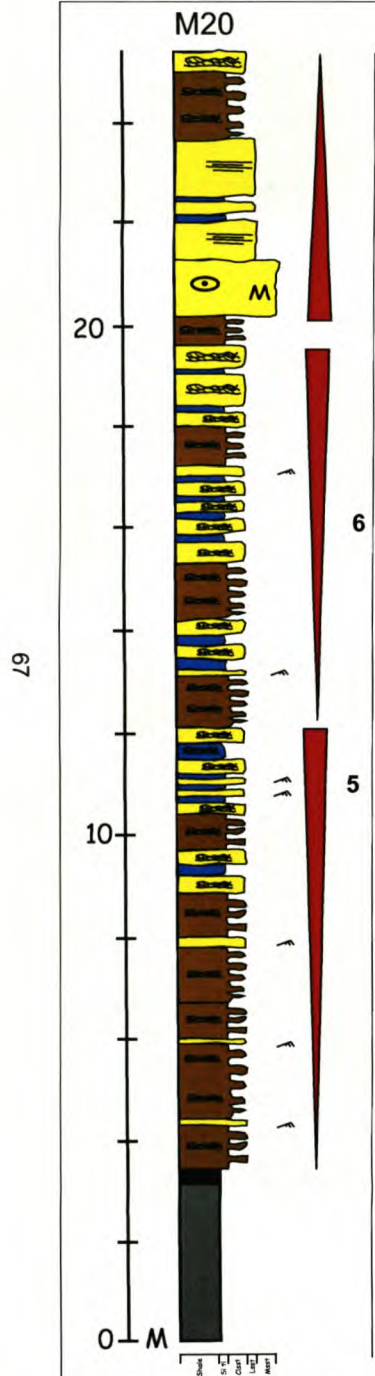


Figure 4.10 Lithofacies 3. Vertical section with characteristic features of the sigmoidal and wavy bedded lithofacies. Located at Blauwkop 76. (1) A succession of sigmoidally cross-laminated sandstones. The forms are asymmetrical with the stoss and lee side preserved. (2) Wavy laminated layers are symmetrical and indicate an undulating bed shape. (3) Directly after deposition of the first sigmoidal structure a second started to build itself over the previous underlying one, with thin silt layers in-between. (4) Thin-beds with sharp upper and lower contacts. (5) Sharp upper and lower contact sigmoidal-laminations. (6) In plan view the wave ripple forms display, straight and laterally continuous crests.



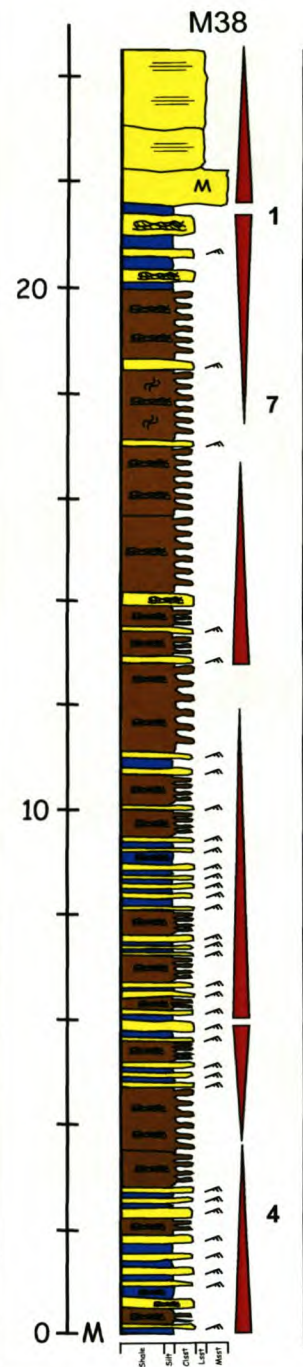
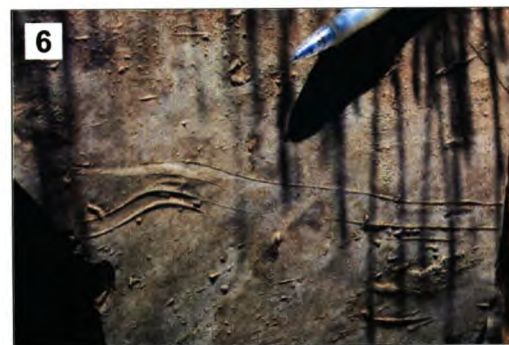


Figure 4.11 Lithofacies 4 A vertical section consisting mostly of parallel- and cross-laminated siltstones. Located at Rondavel 34. (1) Finely parallel-laminated siltstones, interbedded with thinner sandstone units. (2) A very good example of rhythmic climbing ripple-laminated siltstone and sandstone units. (3) The siltstone facies which are characteristically the dominant facies beneath the sand units in the Skoorsteenberg outcrop of FS 5. (4) Shale and siltstone interbedded as fine parallel-laminated units. (5) Loading structures, caused by denser sand unit deposited onto a soft, very fine-grained siltstone layer. (6) Trace fossils are common features on the bedding planes/bottoms of the siltstone facies, like these fish trails. (7) Arthropod trackways in a siltstone layer.



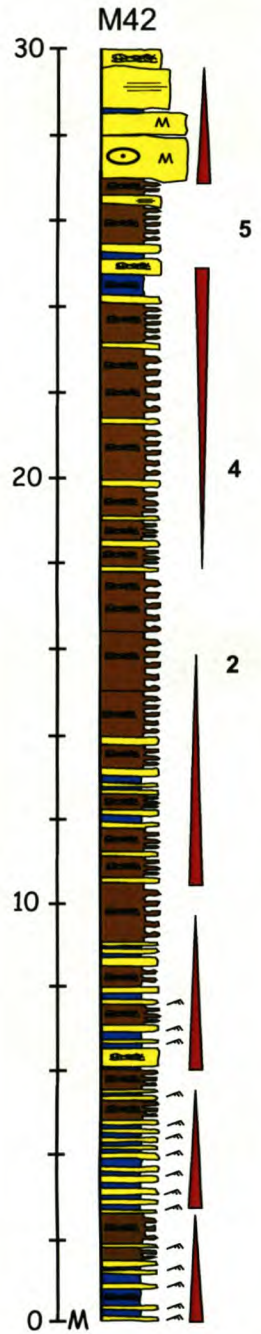
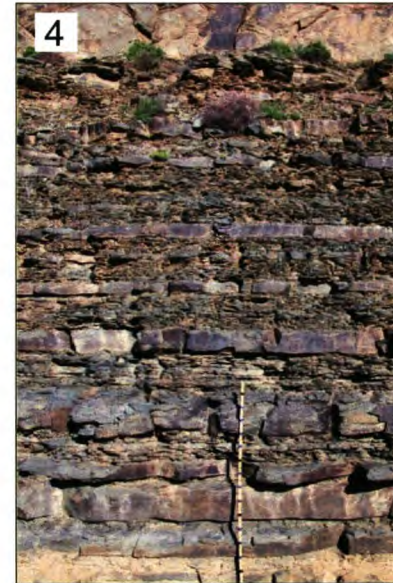


Figure 4.12 Lithofacies 5. Vertical section which consists of layered sandstone alternating with siltstone and shale. Located at Zoetmeisjes Fontein 75. (1) A 25m thick sheet sand outcrop section of FS 5. Note that the lower 14m consists of Lithofacies 5. (2) Horizontal sheet sand deposits. Note the lower 6 m consists of lithofacies 5. (3) Alternation of parallel-bedded siltstone and shale. (4) Alternation of 10cm thick sandstone layers with 5 cm thick siltstone and shale layers. Jacob staff for scale. Note the upward-thinning trend. (5) A close-up of alternating sandstone and siltstone layers. Note the upward thickening pattern. (6) Laterally continuous sandstone beds displaying sharp bases and tops.



M6

Figure 4.13 Lithofacies 6. An example of a vertical section in an erosive channel environment with lag deposits. Located at Hanglip 150. (1) Steep erosional surface overlain by massive sandstones and rip-up clasts associated with the base of the upper channel-fill (indicated by arrows). (2) Cluster of clay clasts above an erosional contact (3) Typical hook-shaped and twisted bedding of the bypass facies. There is no orientation of layers or pebbles. (4) A large cluster of rip-up clasts in a channel erosional zone. (5) Wedge-out of unit above an erosional contact between two massive sandstone units. Note the clay-clasts. (6) Erosional truncation of horizontal ripple-laminated sandstone beds. Jacob staff for scale. (7) Different erosional surfaces associated with rip-up clasts. This outcrop forms part of the high-energy sheet sands. Pencil for scale. (8) Major erosional contact with overlying thick bypass facies unit, consisting of clusters of rip-up clasts and slump material. (9) Sharp erosional contact with a small channel in layered beds.

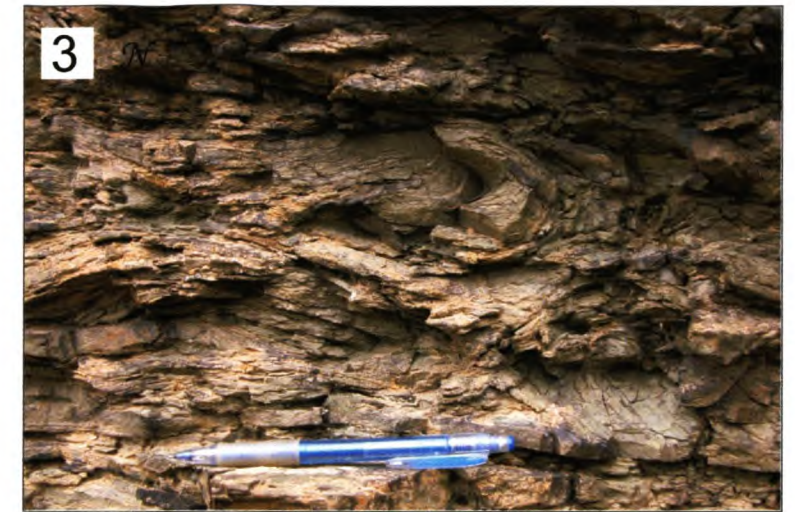
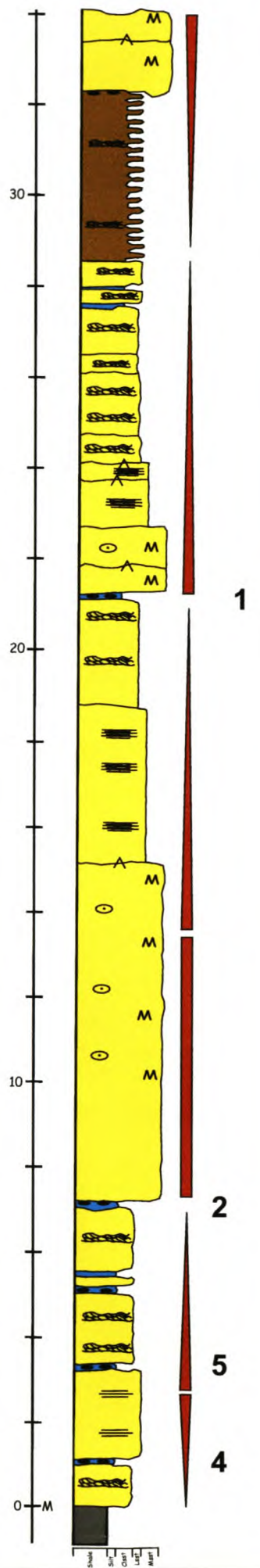




Figure 4.14 Lithofacies 7. Soft-sediment deformation structures, characteristic of Lithofacies 7. Located at Droogekloof 400. (1) Convoluted lamination characterized by marked crumpling or intricate folding of the laminations. (2) Sharp anticlinal and open box-like synclinal forms are characteristic of the convoluted bedding. (3) Small siltstone flame structures associated with convoluted layers. Indicated by the dashed line.

M145

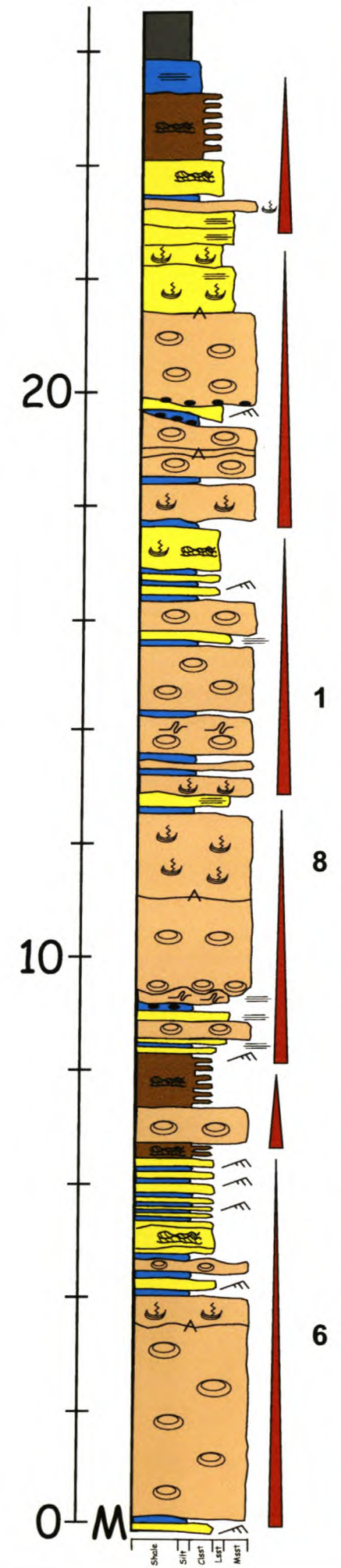
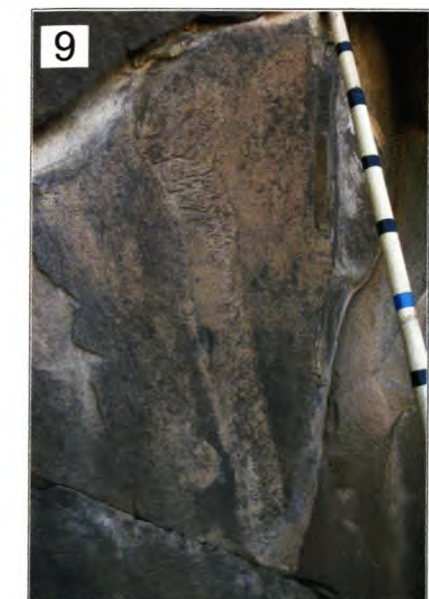
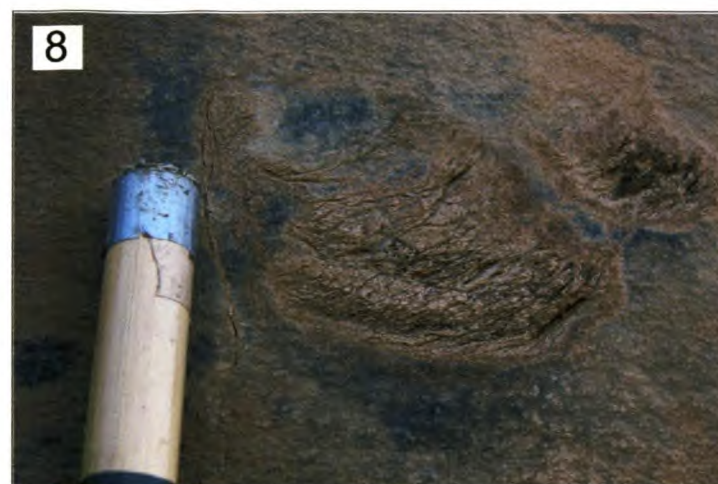
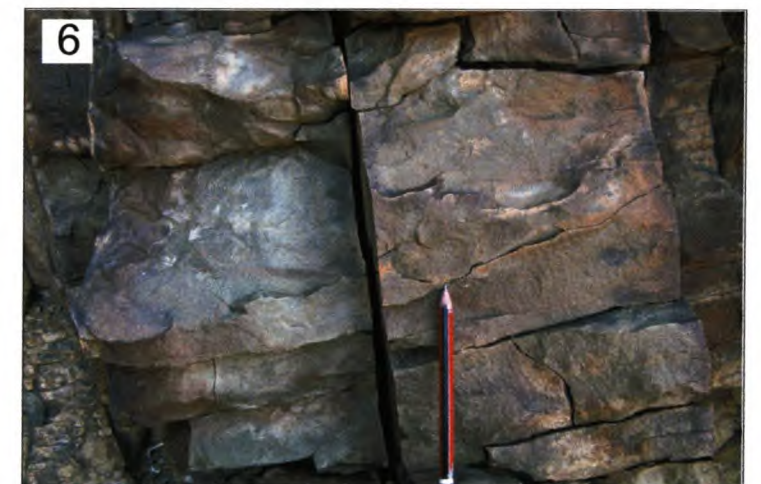
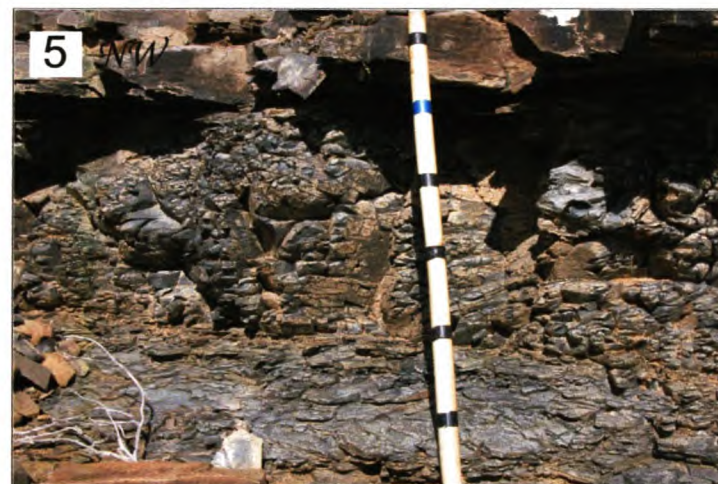


Figure 4.15 Lithofacies 8. Vertical section of a slump succession. Located at Droogekloof 400. (1) Typical ball-and-pillow structures associated with slump facies. Sandstones displaying hemispherical to kidney-shaped geometries. The associated shale is deformed and appears to be wrapped around the pillows. (2) Layer of ball-and-pillow structures overlain by a layer of undeformed turbidite deposits. Note the sharp contact. (3) Extensive slump deposition characterizing the Groot Hangklip outcrop. (4) Ball-and-pillow structures with deformed silty-shale wrapped around them. (5) Dewatered sandstones overlying the slump deposits, forming a sharp contact with upper undeformed layers. Note the weathering pattern. (6) Dewatered sandstones, associated with slump deposits. Note the dish structures. (7) Slump layer on the margin of a channel-fill. (8) Large dish type dewatering structures in a thick sheet sandstone bed. Note the concave upward bending of laminae. The scale is 10 cm for the upper section of stick. (9) Upward 'migration' of dish-structures for nearly 80 cm. It gives the impression of a burrow.



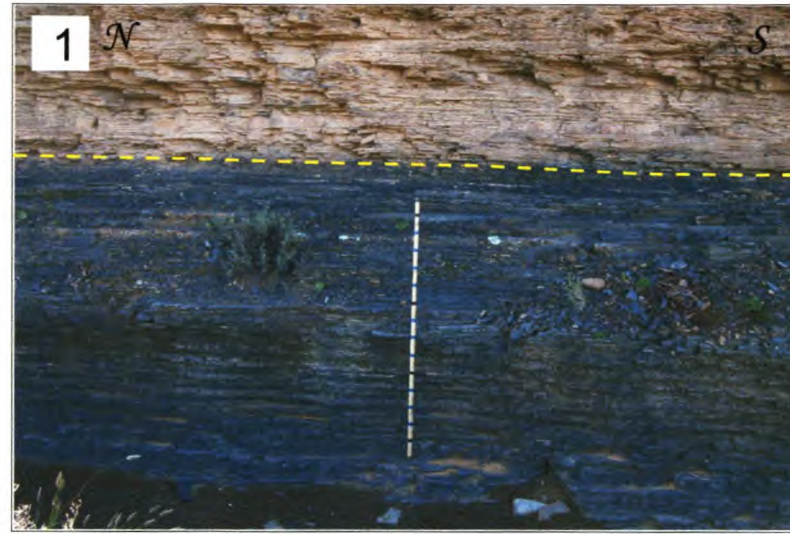
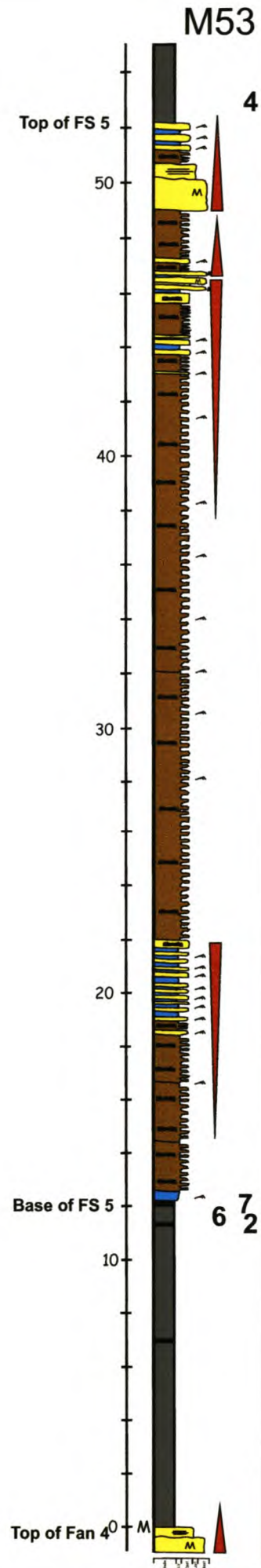


Figure 4.16 Lithofacies 9. A vertical section from the top of Fan 4 to the top of FS 5. The shales between the two fan systems and the overlying silty-shale regional marker of FS 5 consist of Lithofacies 9. Located at Zoutrivier 32. (1) Note the colour difference of the shale-rich unit beneath the base of FS 5. Dashed line indicate base of FS 5. (2) Outcrop of the base of FS 5 (indicated by dashed line) and the silty-shale between Fan 4 and FS 5 (indicated by green arrow). (3) True hemipelagic shales are softer and weather more easily. They forms a sharp contact with the siltstone beds. (4) Silty-shale unit above FS 5. (5) Calcareous concretion in hemipelagic shale. (6)+(7) The markerbed below the base of FS 5 consisting of 20-30 cm hemipelagic shale. Note the typical flaky weathering and sharp upper contact with overlying siltstones. Pencil for scale.

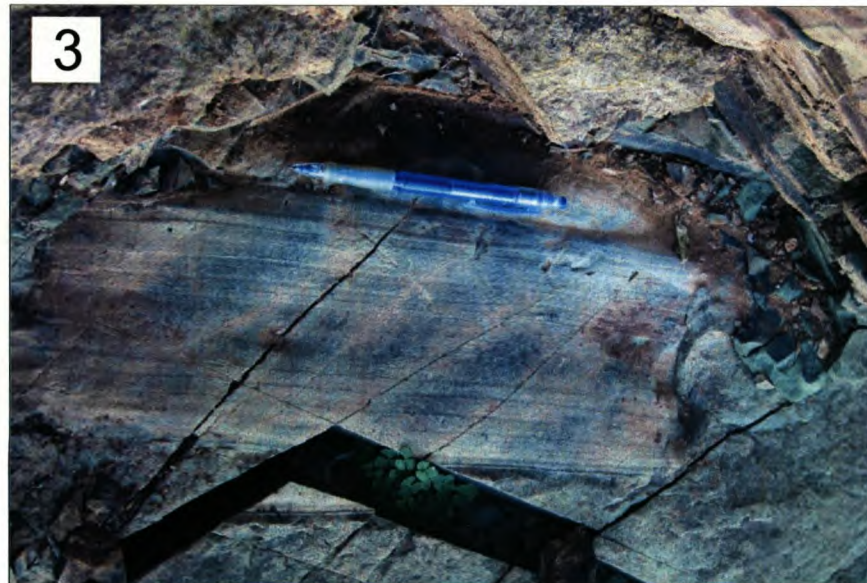


Figure 4.17 Lithofacies 10. Plant fragments associated with silty sandstones in the FS 5. (1)+(2) Plant fragments in a silty matrix. (3) Large leaves and stems of *Glossopteris* and *Gangamopteris* are quite common (Visser and Loock, 1978) and seem to be the most general plant fossil type.

4.5 Measured sections and correlations framework

4.5.1 General

Fully reliable correlations, i.e. unequivocal demonstration of time equivalence of beds, require physical lateral tracing of such beds. However, with FS 5, lateral tracing of beds was not always possible over long distances because of the limited exposures in some areas, the weathered conditions of the outcrops and the variation in depositional elements. The correlation frameworks for FS 5 are based on the method presented by Remacha and Fernández (2003). They divide their framework from the lowest-frequency (basin-fill) scale up to the highest-frequency scale (bed-by-bed correlation), i.e. defining progressively smaller groups of beds.

First-order correlation is based on mapping of large-scale stratigraphic units whereas second- and third-order correlations are based on matching small-scale data from geographically separated stratigraphic sections within the same time-equivalent first-order units. Sub-divisions for the second- and third-order are characterised by particular attributes including lithology, texture, thickness, geometry, sedimentary structures and gradational or sharp contacts between successive divisions. Detailed vertical sections provide a serial data set, which forms the backbone for high-frequency correlations.

Over 150 logs were measured in the field as well as four slim-well core sections from the NOMAD project. The core sections, which include a section from the top of Fan 4 up to the silty-shale package above FS 5, are very good reference logs for correlation of field-logs and the compilation of fence diagrams. An outcrop distribution map of FS 5 shows the location of the logged sections and correlation panels (Fig. 4.18).

Detailed fence diagrams (Figs C+D) were compiled from the first-, second- and third-order correlation sections for the main sand-rich units of FS 5. Certain colours were used in the sections for the identification of these different order correlative units.

4.5.2 First-order correlation (regional marker beds)

First-order correlation relies on the mapping of large-scale stratigraphic features of the turbidite succession, thus providing direct lateral tracing of stratigraphic units. These units are traceable at basin scale. The two most significant regional marker horizons associated with FS 5 are 1) the upper silty-shale unit overlying FS 5 and 2) the 20-50 cm shale bed, which forms part of the silty-shale interfan unit between Fan 4 and FS 5. The thin basinal shale unit is interpreted as the base of FS 5. These two regional marker horizons bound the turbidite system, because they represent the bounding surfaces of the depositional sequence (Fig. C).

The silty-shale unit, which overlies FS 5, reaches a thickness of up to 30 m (Fig. 4.19.1). The silty-shale layers display very fine parallel-lamination and starved ripple-lamination (Fig. 4.19.2). Thin shale layers (0.2 - 0.5 cm) alternate with thin siltstone layers (Fig. 4.19.3). The interval between the top of FS 5 and the first silty-shale layers comprises a sharp contact with beds of wave-rippled thin sandy turbidites (Fig. 4.19.4).

Very thin-laminated (1-2 cm) silty-shale layers characterize the interfan unit between the top of Fan 4 and the base of FS 5 (Fig. 4.20.1). This unit varies quite significantly from the interfan units of the underlying fan systems, which consist predominantly of dark hemipelagic shales. Two thin units of very fine hemipelagic shales (about 20-40 cm) are present in the interfan unit between Fan 4 and FS 5 (Fig. 4.20.2). These two units are laterally extensive throughout the outcrop area. The basal silty-sand units of FS 5 in the northern outcrop area were deposited directly on this upper hemipelagic layer (Fig. 4.20.3). The initial channel complexes of the southern outcrop area were deposited onto, directly or in some places eroded into the interfan unit (Fig. 4.20.4). The weathering pattern of the interfan unit compared to the first thin-bedded turbidites of FS 5 is also quite significant (Fig. 4.20.3).

All the measured sections in the second- and third-order were correlated from the basal shale unit or the upper silty-shale marker. The thickness of FS 5 seems to be more or less constant between the regional marker beds. Only in the north-eastern outcrop area of FS 5 is there an indication of pinching-out of the lower beds of the system.

4.5.3 Second-order correlation (stratigraphic entities)

Within first-order packages, second-order correlation relies on the matching of a series of stratigraphic entities, which normally characterise a fan system (Remacha *et al.*, 1998). Such entities provide the second-order correlation framework. FS 5 consists of six stratigraphic sand-rich units comprising channel-fills with interbedded overflow and spreading sheet flows that are clearly distinguishable in the correlated units (Fig. C). The Kalkgat and Groot Hangklip correlation sections consist of massive sandy units at the base, which form part of two separate channel flows. The most distinguishable feature of these two outcrop localities are the slump units (LF 6) which are concentrated only in this area and localized to certain beds. Only in the Kalkgat vicinity are the slump units more massive and seem to be concentrated in highly erosional channel scars. These slumps do not correlate with any of the turbidite flows in the channel environments (Fig. C).

Massive sandstone units dominate the Klein Hangklip (KHK) outcrops, which form part of the main channel complex of FS 5. This unit correlates with the Tongberg unit and in turn forms part of the Blauwkoop sand-rich unit. The Skoorsteenberg system was identified as the uppermost second-order correlation sand-rich unit of FS 5 (Fig. C).

4.5.4 Third-order correlation (high-resolution internal bed architecture)

The third-order correlation relies on the same matching principle as the second-order correlation, although in the third-order correlation, the number, vertical arrangement and facies characteristics test the coherence of the down-current evolution of facies (textural and structural divisions) within single beds. Packages of beds within third-order intervals show thickening- and coarsening- or thinning- and fining-upward trends, at scales from a few metres in thickness down to less than a metre, with less frequent cases of uniform vertical stacking. Such packages usually form cycles comprising a lower coarsening-upward group of beds followed by a fining-upward package. Based on the above, matching within third-order packages is a multi-step task that leads to the definition of smaller groups of time-equivalent beds, up to reaching the bed-by-bed correlation (Remacha *et al.*, 1998).

Most of the third-order correlation in FS 5 has been done on small areas and variations on these correlations are possible. Correlation between the different channel-fills within channel complexes and the overflow units is difficult, because most of the outcrop sections are oblique to the main palaeoflow direction and interpretation of bed continuity is impossible. The sheet sand units for example, in the Zoetmeisjes Fontein 75 and Blaauwheuwel 121 localities, are more or less continuous and can be traced and correlated for a radius of more than 15 km from the main channel systems (Fig. C).

4.6 Vertical and lateral facies development and correlation

The different lithofacies summarised in Table 2 occur as distinctive assemblages that constitute certain depositional elements, such as lobes, overflows and channel-fills. In this section, each sand-rich unit is described in terms of its regional development, its facies arrangement, and distribution, primarily to distinguish between channelized and non-channelized parts and to illustrate possible cyclicity in deposition.

In this section, the vertical (temporal) and lateral (spatial) associations of lithofacies are illustrated and described by means of the correlation framework for each sand-rich unit in FS 5. A detailed fence diagram was compiled for the whole of the outcrop of FS 5 (Fig. C). Some of the sections in this fence diagram are oblique representatives of the palaeoflow direction of FS 5. The four slim well logs (NS 1-4) serve as basic connection points for this diagram (Fig. C). The basal shale first-order marker bed varies in thickness in certain areas in the basin and thickens considerably where FS 5 thins out in the far northern outcrops. The upper marker shale bed is constant throughout the area.

4.6.1 Klein Hangklip complex (KHK)

The Klein Hangklip complex (KHK) consists predominantly of Lithofacies 1 (Table 2). Lf 2, 3 and 4 also occur and form part of the abandonment channel-fill and overflow facies. The thickness of this unit is constant between 80-90 m in this area (Fig. 4.21). The overflow (overbank) facies occur less than 10 km to the north of the main channel system (Van der Merwe, 2003). Individual beds and amalgamated units of up to 4 m in thickness can be traced for short distances before they are eroded or truncated by successive channel-fills (Fig. 4.21). The channel

deposits in the KHK section were deposited directly on the interfan shale between Fan 4 and FS 5 and are interpreted as the initial deposits of FS 5. Downward erosion into the interfan shale occurs where large and steep erosive channels are present in this complex (Fig. 4.20.4). Fan 4 in this locality consists of two small units, 4A and 4B, which are the last remnants of this fan system before final pinch-out to the south (Van der Merwe, 2003).

A NW – SE trending correlation diagram was compiled for 20 measured log sections, which include the well log of NS 4 (Fig. 4.21). First-order correlation units form the top and basal bounding units of FS 5 and comprise two silty-shale packages below FS 5 and above FS 5. Second-order correlation forms the main framework of the KHK sand-rich unit (Fig. 4.21). Third-order correlation was applied to some of the channel-fill units and there possible related overflow units, which are located more or less 10km away from the main channel axis (Fig. 4.21). Small crevasse splay channels occur within the overflow deposits, northwest of the main channel axis. The development and preservation of levee deposits are difficult to prove because most of the channels are stacked and eroded laterally into the underlying previous fill.

4.6.2 Tongberg complex (TB)

The Tongberg sand-rich unit is located on the farm Droogekloof 400 and outcrops in two back-to-back cliff sections with exceptional exposure. The Tongberg channel complexes comprise Lf 1 and Lf 8 and to a certain extent Lf 2, 4, 5 and 7 (Table 2). The correlation section consists of 15 vertical sections, measured along an oblique dip section of outcrop (Fig. 4.22). The section is bounded by the two first-order marker beds at the top and base of FS 5. The second-order correlation reveals three units: 1) the lower primary channel-fill complex, 2) the middle unit comprising sandstone layers with ball-and-pillow and dewatering structures, 3) an upper smaller, distributary channel-fill located in-between thin-bedded deposits. Lf 7 predominates in the upper 10 m of thin-bedded units of FS 5 (Fig. 4.22).

The massive channel sands, which form part of the second primary channel complex, were deposited directly onto the lower basal shale unit. Two large conduits and a third smaller conduit to the east of the section have been identified (M 121 and M 120). Vertical section M134, which is located more or less 1km to the south of these large conduits, contains no evidence of this large primary channel complex (Fig. 4.22). Stacked, predominantly thin-bedded ripple cross-laminated sandstones (Lf 2, 4 and 5), constitute the outcrop 2 km east of the main channel axis. Profiles

M122 and M123 illustrate the dominance of this facies in this area, and its relationship with the larger channel-fills (Fig. 4.22). The overlying slump deposits are restricted and interbedded with Lf 5. The palaeoflow direction for these slump units is very unidirectional and the mean value was towards the northeast. These beds form part of the larger slump system towards the south, i.e. the Kalkgat and Groot Hangklip units. The third and overlying single channel-fills consist mostly of Lf 2 and the palaeoflow direction for these sands is to the north (Fig. 4.22). These conduits seem to have been more open and less erosive than those of the lower channel complex units were.

TB is characterized by architectural elements such as channel-fill complexes, overflow deposits, slump deposits and single 'splay' channels. The lower primary channel complex correlates with the primary channel complex of the Klein Hangklip area. The TB and KHK depositional areas seem to be divided by an earlier syn-depositional anticlinal structure, which might have had an influence on the depositional patterns for the primary complex (Fig. B). No evidence could however, be found that this anticline separated the two different channel systems. A wide-open channel-complex at the base-of-slope seems to be the most likely model for both these systems.

4.6.3 Skoorsteen complex (SB)

FS 5 consists of a variety of facies assemblages in different parts of the outcrop area in the vicinity of Skoorsteen. Thick, wedge-shaped sandstone units, interbedded with thin sandstone/siltstone couplets and amalgamated channelized Lf 1 and Lf 2 sandstones (Table 2) dominate the outcrops of this unit. The latter constitute the upper 30 m of the FS 5 stratigraphical succession. Johnson *et al.* (2001) interpreted the Skoorsteen unit as a major slump scar, which was later filled up with sediment. This interpretation was made for the upper 30m of the succession, but the true base of FS 5 is 45 m below this sandy upper unit. This succession of 45 m consist of alternating, thin, ripple-laminated sandstone and siltstones (Lf 4 and Lf 5) (Table 2), which are interpreted as the distal expression of overflows and spreading sheet sands of the KHK and BK sand-rich units or possibly other sand-rich units which have been removed by later erosion.

The main architectural elements in the SB sand-rich unit are two wide non-erosive (350m:30m) channel complexes at Skoorsteen, spreading and sheet sand deposits in the Brandhoek 119 and Blaauwheuwel 121 areas and smaller channel-fills in the Katjiesberg outcrops (Fig. D). Thus,

SB represents, similar to BK, a lower mid-fan to upper lower fan depositional environment. It comprises low width:depth ratio distributary channels, which deposited large amounts of sediment in the more distal areas of Blaauwheuwel 121 and Brandhoek 119. Most of these deposits form spreading sheet sand lobes, which outcrop at Blaauwheuwel 121 (Fig. 4.23.1). This figure also indicates the gradual thinning of the lower thin-bedded units of FS 5 towards the NE of the basin (Fig. 4.23.1). See more detail in Section 4.7.

Over 103 vertical sections were measured and 15 redrawn from Winters *et al.* (1995) for this sand-rich unit and compiled in six correlation sections and a fence diagram (Fig. D). The vertical section of NS 1 was used as the reference point for most of the correlation sections in the fence diagram. The upper and basal shale first-order correlation marker beds are prominent in this area (Fig. D). The basal shale is overlain by the approximately 45 m of thin-bedded Lf 4 and Lf 5. The thin, sand-rich unit, 25 m below the SB sand-rich unit in M118, M108, M81 and M82, represents the last thin-bedded sheet sand deposits from the BK sand-rich unit (Fig. 4.23.2).

The SB sand-rich unit forms the second-order correlation entity. This unit is divided into several third-order channel-fills, overflow and sheet sand deposits. The low width:depth ratio channel-fills consist of numerous smaller channel-fills, which consist predominantly of Lf 1 and 2 (Fig. 4.23.2). The palaeoflow directions for these smaller channels vary from north to east whereas the main palaeoflow direction for this unit is east-northeast. The north-facing outcrop of Skoorsteenberg displays an oblique dip-section of the channel-fills and their levee overflow deposits (Fig. 4.23.2), whereas the western outcrop face is an oblique strike section of the channelized deposits (Fig. 4.23.3). The southern outcrop of the SB unit on the farm Grootfontein aan Schoorsteenberg 35, consists of smaller channel-fills with collapsed marginal slump deposits in some of the channel-fills (Fig. 4.23.4).

The distance over which lithofacies variation takes place, i.e. from the main channel-fills to the sheet sand deposits, is less than 10 km. The sheet sands consist predominantly of dewatered massive sandstones, which are interbedded with siltstone layers (Lf 1 and 4). Smaller channel-fills are present in the most northern outcrops of FS 5 at Katjiesberg (Fig. 4.23.5). These channel-fills are interpreted as bypass systems, which originated from the main depositional area in the Skoorsteenberg locality. The fence diagram indicates the main sand concentration of the

Skoorsteenbergr unit (Fig. D). Well logs NS 1 and NS 2 serve as reference points in the compilation of the fence diagrams for the SK unit (Fig. D).

4.6.4 Blauwkop complex (BK)

The Blauwkop complex has been described and discussed in detail by Basu (1992) and Kirschner and Bouma (2000). Only a summary of their conclusions and a few new ideas will be provided in this thesis.

The Blauwkop sand-rich unit mainly outcrops on the farms Blauwkop 76, Brakke Rivier 77 and Zoetmeisjes Fontein 75. Kirschner and Bouma's study focused on the outcrops on Blauwkop, where approximately 1.5 km² of FS 5 is exposed. They concluded that this outcrop is composed of four different architectural elements: two types of channel-fills, levee deposits, and crevasse splay deposits. The association of these four architectural elements forms the distributary channel system presented by Kirschner and Bouma. They also suggest deposition in the lower mid-fan to lower fan environment of fine-grained submarine fan systems. The dominant lithofacies types in the two types of channels are Lf 1 and Lf 2, in the levee deposits, it is Lf 2 and Lf 4, and in the overflow deposits, it is Lf 3, Lf 4 and Lf 5 (Table 2).

The BK unit forms the middle stratigraphical unit of the FS 5 succession (Fig. C). The second-order correlation units are the distributary channel system but also the spreading/sheet sand deposits (Fig. 4.24.1). A thin-bedded unit (Lf 5) comprises the lower 10m between the shale base and the first sandy turbidite units. These thin-bedded units are interpreted as overflow deposits, genetically linked to the KHK channel complex (Fig. 4.24.1). The interpretation of Kirschner and Bouma that the BK channel system forms part of the lower mid-fan to lower fan, is well supported by additional field evidence.

The distributary channel system forms the area of confined sand-flow, because less than 1 km down-current (north) the outcrop consists mainly of unconfined sheet sand units that eventually pinch out 15 km down-current, i.e. north from BK (Fig. 4.24.1). They represent the lower fan environment and form the major part of the second-order correlation unit. Thus, the BK unit was deposited on the transition zone between the mid-fan and lower fan environments. Lf 1 and Lf 2 predominate in the sheet sand zones (Table 2). The units approximately 10 km west of the main BK channel axis are characterized by small single crevasse splay channels, interbedded with

overflow units (Fig. 4.24.2). Some of the beds can be correlated, in the third-order, for almost the entire distance from the BK channels until they pinch-out in the northern outcrops (Zoutrivier 32 and Waterlemoen Fontein 17) (Fig. 4.24.1). The palaeoflow direction for this system varies from northwest to northeast.

Direct correlation with the KHK unit, indicates that the BK unit forms the down-current equivalent of the channelized outcrops in KHK and TB. However, most of the outcrop in-between these two units is in the subsurface and direct correlation could only be achieved by the correlation of the core logs NS 3 and NS 4 with the field logs. The regional extent of this system is indicated in the fence diagram (Fig. C).

4.6.5 Groot Hangklip complex (GHK)

GHK consists the southern outcrops of FS 5 and comprises predominantly unstable and chaotic slump deposits. These slump sediments form part of a different flow system but still within the boundaries of FS 5. Wach *et al.* (2000) interpreted the GHK as a slope fan, with a channel complex and slump deposits of the mid-upper slope that shallows upward into deltaic deposits, capping the basin-fill succession. The most likely depositional setting for these deposits is at the base-of-slope (Wild and Hodgson pers. comm.).

The GHK sand-rich unit consists predominantly of stacked, amalgamated, dewatered, and slumped sandstone beds (Lf 8, Table 2). The sandstones show gradual lateral wedging and can be traced for tens of metres in the vertical cliff sections of M135, M136 and M137 (Fig. 4.25). Ball-and-pillow structures and dewatering dish structures are characteristic of these slumped beds. The thickness of the channel-fills is between 15 and 22 m (Fig. 4.25). Thin-bedded units with interbedded ball-and-pillow and dewatering layers are present in section M134, the latter being 1km north of the main axis of the GHK flow (Fig. 4.25). Dark basin shales containing several thin units (1-3m thick) of alternating siltstone and sandstone underlie GHK. They are interpreted to be the distal siltstones of Fan 4A and 4B (Fig. 4.25).

The upper and lower shale beds form part of the first-order marker beds. In total, seven vertical logs were measured and correlated in this section (Fig. 4.25). The second-order correlations involve two channelized sections. The lower section comprises two massive channel-fills, which consist of deformed and dewatered massive sandstones (Lf 1 and Lf 8) (Fig. 4.25). It might have

been deposited during the same period as the upper complexes of KHK and BK. The second unit is the massive soft-sediment deformed slump deposits overlying and even eroded into the underlying channel-fill. The channel-fill pinches out, to the south and to the north of the GHK locality. This channelized unit could be divided into three periods of flow within the third-order correlative division (Fig. 4.25). The slump succession could also be divided in several different sub-units within the third-order division (Fig. 4.25).

The main architectural elements in this study area are slump deposits and channel-fills. Overflow deposits are recorded for up to 2km to the north of the main depositional axis. Vertical logs M144 and M145 have been measured 4km down-current from the main outcrop of the GHK and are characterized by the lower slump channel-fill and the overlying slump deposits (Fig. 4.25).

A change in depositional style is marked by a recessive break at top of the last slump-type deposits. This succession comprises of sheet-like, planar laminated, medium-bedded fine-grained sandstone (Lf 5) and ripple laminated, very fine siltstone interbeds (Lf 4) (Table 2).

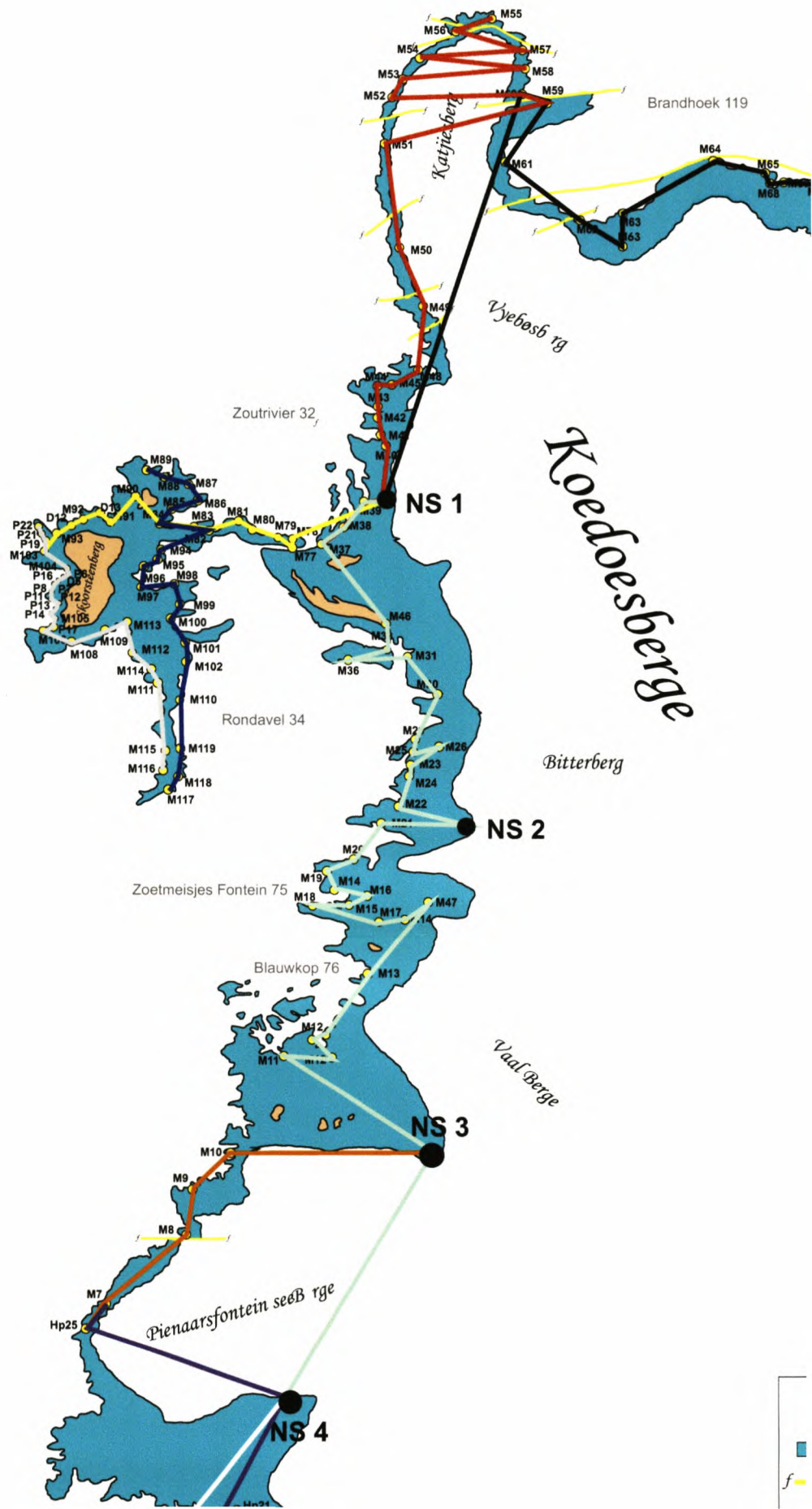
4.6.6 Kalkgat complex

This fan unit consists mainly of Lf 8 and to some extent Lf 2 (Table 2). The Kalkgat outcrops are the southernmost outcrops of FS 5 before it pinches out on the farm Lower Roodewal 169 (Fig. A). They are characterized by a high-energy and unstable environment of deposition. That is the main reason for the abundant slump and dewatered deposits. An extensively developed thrust separates the Kalkgat outcrops from the Groot Hangklip outcrops (Fig. B)

Five vertical logs were correlated in this area (Fig. 4.26.1). The first-order correlations are based on the regionally developed silty-shale units overlying and underlying FS 5 (Fig. 4.26.1). Second-order correlation involves the slump channel-fills in the measured sections. A vertical section, M143 is the most representative section for the second-order correlations, because most of the slump units are present (Fig. 4.26.1). For the third-order correlation, four separate slump units were identified within the second-order entity (Fig. 4.26.1). Several large channel-fills with erosional surfaces in-between the fills, were identified. Most of these channels wedge out, in less than 2 km, towards the north, as indicated by section M139 (Fig. 4.26.1). In the Kalkgat and Groot Hangklip vicinity, the slumps are directly overlain by the regional shale, whereas in the TB

it is overlain by thin-bedded turbidites and single channel-fills. This indicates a more proximal depositional area, because the KG and GHK are not overlain by later turbidite flows (Fig. 4.26.1).

The second-order sand-rich slump units of KG correlate directly with the GHK slumps on the farm Droogekloof 400, and with the thin-bedded slump layers in the Tongberg area (Fig. 4.26.2). The formation of the two southern slump-rich units suggests a separated depositional flow system, which forms part of the FS 5 succession (Fig. 4.26.2 + Fig. C). Thus, it might be that there was a major slope failure and that a separate system of mostly chaotic sediment was initiated and deposited directly in the same environment as the channel-complex of FS 5. The palaeoflow direction for the slump material is also the same as the mean direction (towards the northeast) of FS 5.



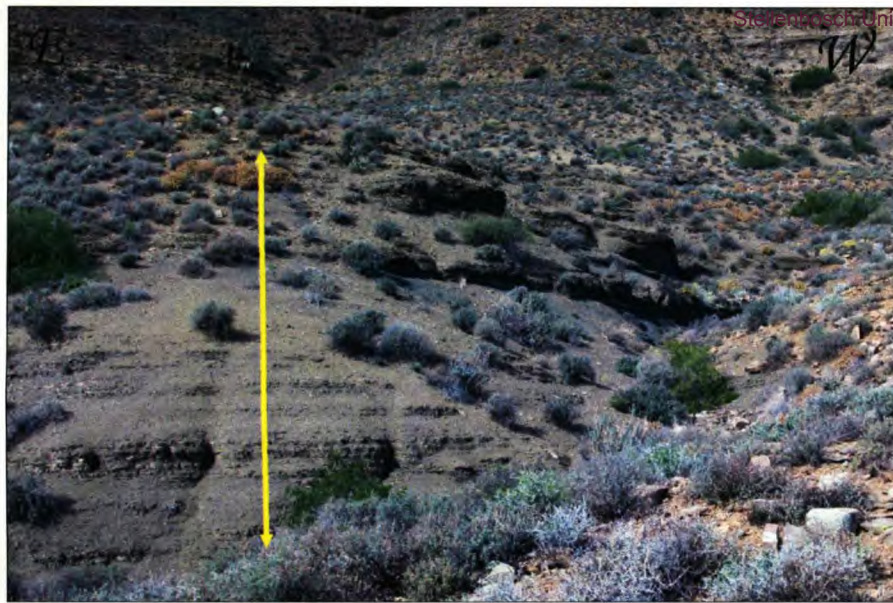


Figure 4.19.1 A 30 m thick silty-shale unit overlying FS 5, indicated by arrow. Located on Pienaarsfontein Mountain.



Figure 4.19.2 Finely laminated silty-shale layers at Skoorsteenbergr.



Figure 4.19.3 Thin layers of shale interbedded with silty layers, in the upper part of FS 5. Located on the farm Krantzkraal 83.



Figure 4.19.4 Sharp contact between the top of FS 5 (wavy bedding) and the overlying silty-shale layers. This indicates deposition under different conditions. Located on the farm Klipfontein 31.



Figure 4.20.1 The interfan unit between the top of Fan 4 and the base of FS 5 is characterized by very thinly laminated silty-shale layers. Located on the farm Zoetmeisjes Fontein 75.



Figure 4.20.3 The lowermost silty-sand layers at the base of FS 5. Note the colour and textural difference between the two types of deposits. Located on the farm Zoetmeisjes Fontein 75.



Figure 4.20.2 Two thin, (about 20-40 cm) very fine hemipelagic shale layers are present in the interfan unit between Fan 4 and FS 5. The upper shale layer in the photo is the base of FS 5, indicated by arrow. Located on the farm Blauw-kop 76.

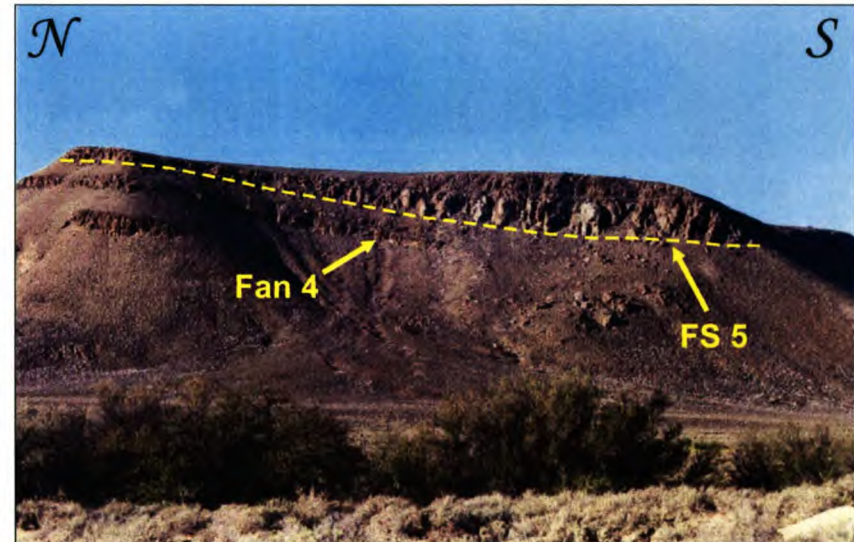


Figure 4.20.4 A channel-fill deposit in the KHK area. Note the erosion into the lower units and Fan 4. See image D in Fig A.

Figure 4.21 Characterization of the Klein Hangklip Unit
(A) Strike section from northwest to southeast showing the development from the main channel-fill axis to thin overflow units less than 10 km to the northwest. Massive (Lf 1) sandstones and erosional contacts are characteristic for the complex. Third-order correlation indicates numerous channel-fills. **(B)** Position of section indicated on locality map. Main flow direction is to the ENE.

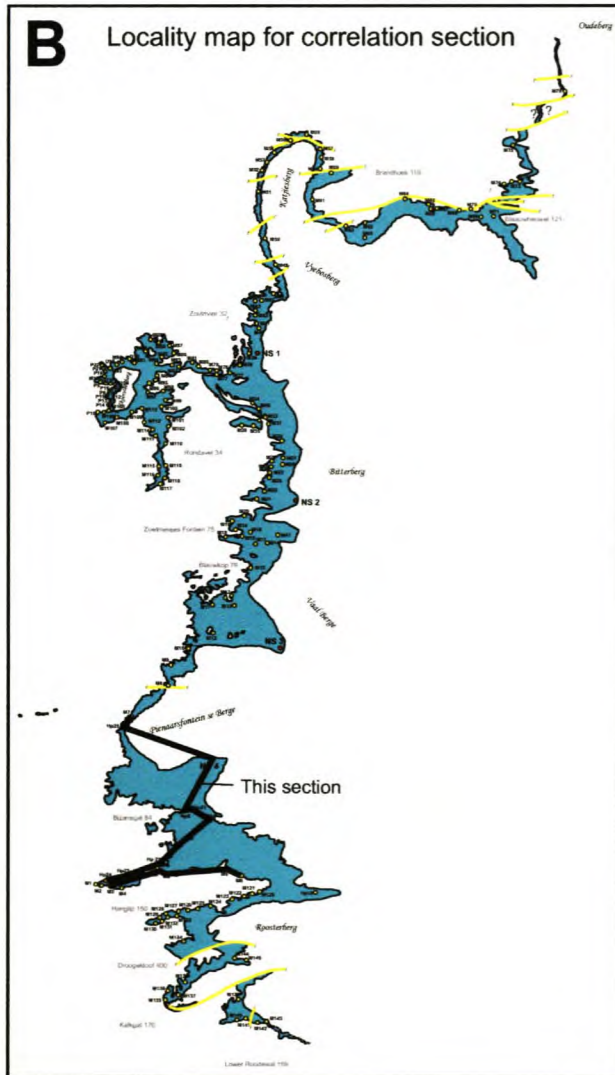
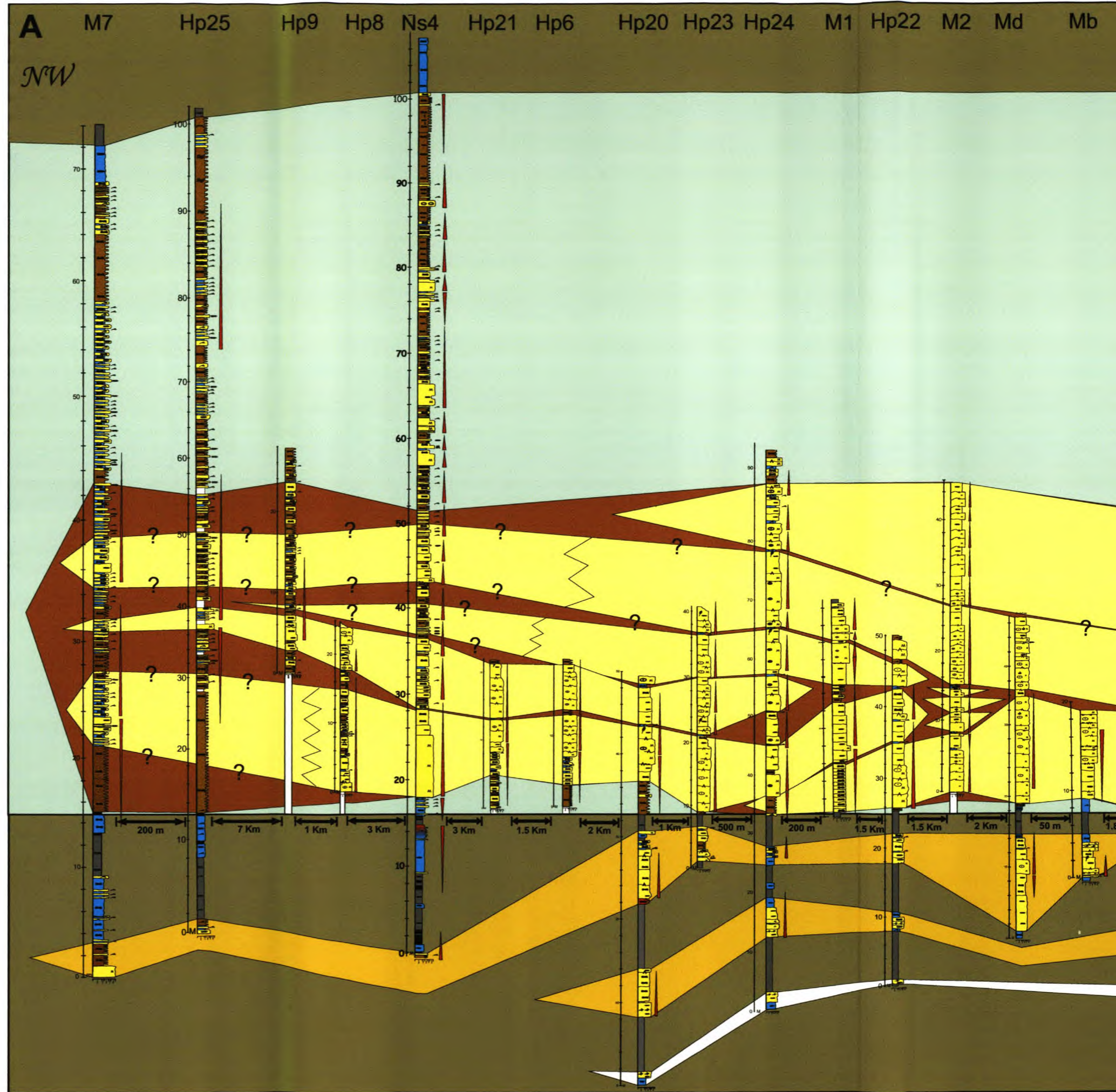
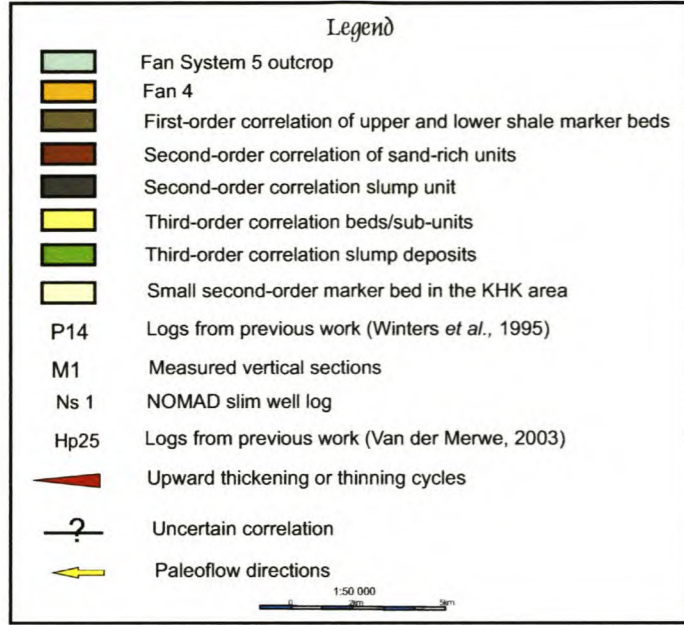


Figure 4.23.1 (A) This section represents an oblique dip orientation of the SB sand-rich unit and was hung from the top of FS 5. The main architectural element in this section is the sheet sands. This is the lower-fan depositional area of the SB unit. This section indicates a thinning of the lower beds of FS 5 from west to east. Pinch out of FS 5 occurs in the most north-easterly outcrop. **(B)** Locality map for the Blaauwheuvel correlation section.

SOUTH-WEST

Legend

- Fan System 5 outcrop
- Fan 4
- First-order correlation of upper and lower shale marker beds
- Second-order correlation of sand-rich units
- Second-order correlation slump unit
- Third-order correlation beds/sub-units
- Third-order correlation slump deposits
- Small second-order marker bed in the KHK area
- P14 Logs from previous work (Winters *et al.*, 1995)
- M1 Measured vertical sections
- Ns 1 NOMAD slim well log
- Hp25 Logs from previous work (Van der Merwe, 2003)
- Upward thickening or thinning cycles
- Uncertain correlation
- Paleoflow directions

1:50 000

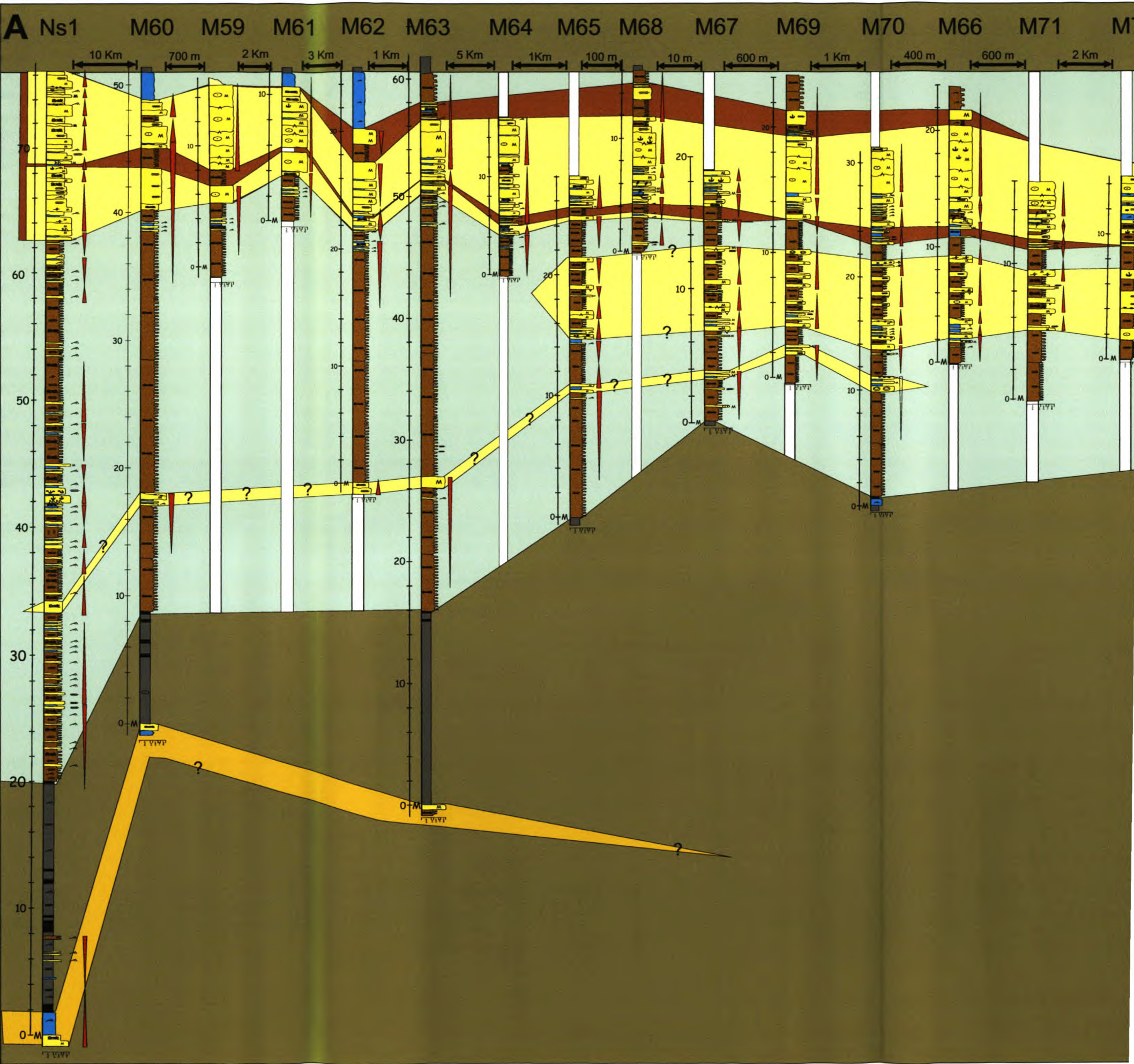
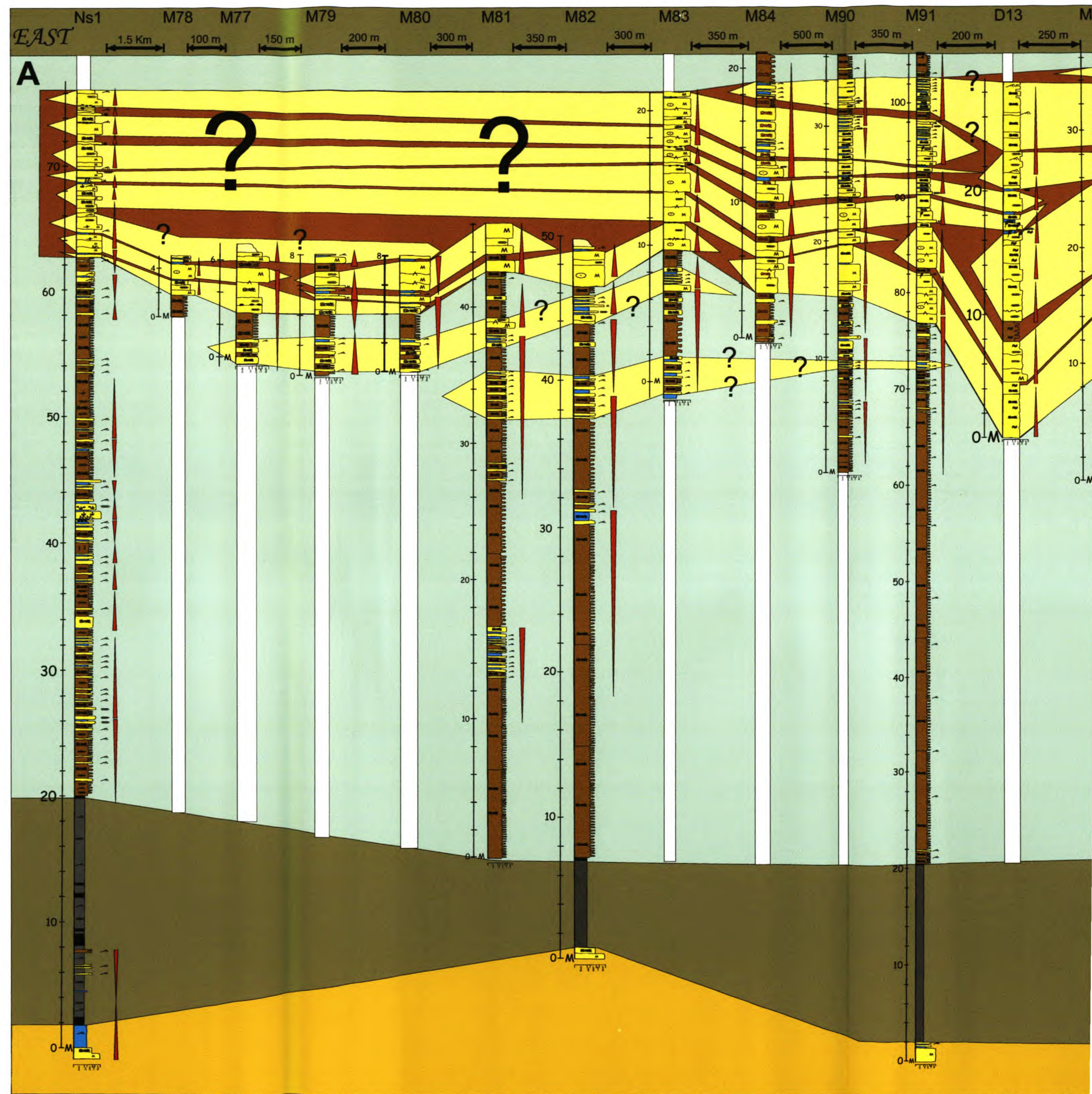
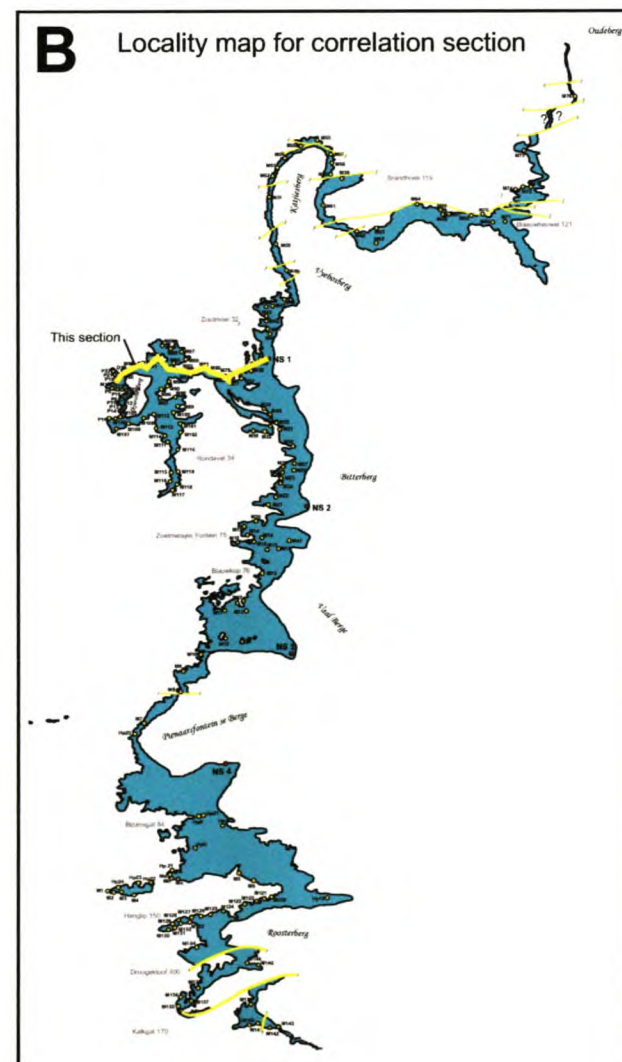
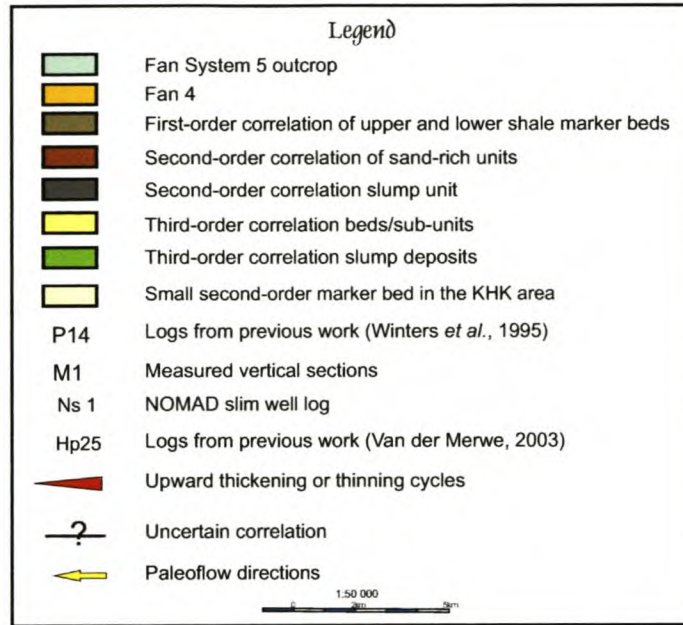


Figure 4.23.2 (A) East-west (oblique dip) correlation of the SB unit. This section was hung from the top of FS 5. Correlation of these units was difficult due to the wedging nature of the channel-fill sands. This section also represents the transition from the channel environment to the depositional sheet sands. A thinning of the section is noted. The last outcrop of the Blauwkop sand-rich unit, before it pinches out, occurs in the lower part of some of the sections. **(B)** Locality map for this section.



NORTH

Figure 4.23.5 (A) North-south (oblique strike) correlation of the Katjesberg section in the SB unit. This section is hung from the top of FS 5. It is the most northern outcrop of FS 5 and comprises overflow and sheet sand deposits. Small splay channel-fills occur between the overflow deposits. Palaeoflow varies from north to east. **(B)** Locality map for the Katjesberg section.

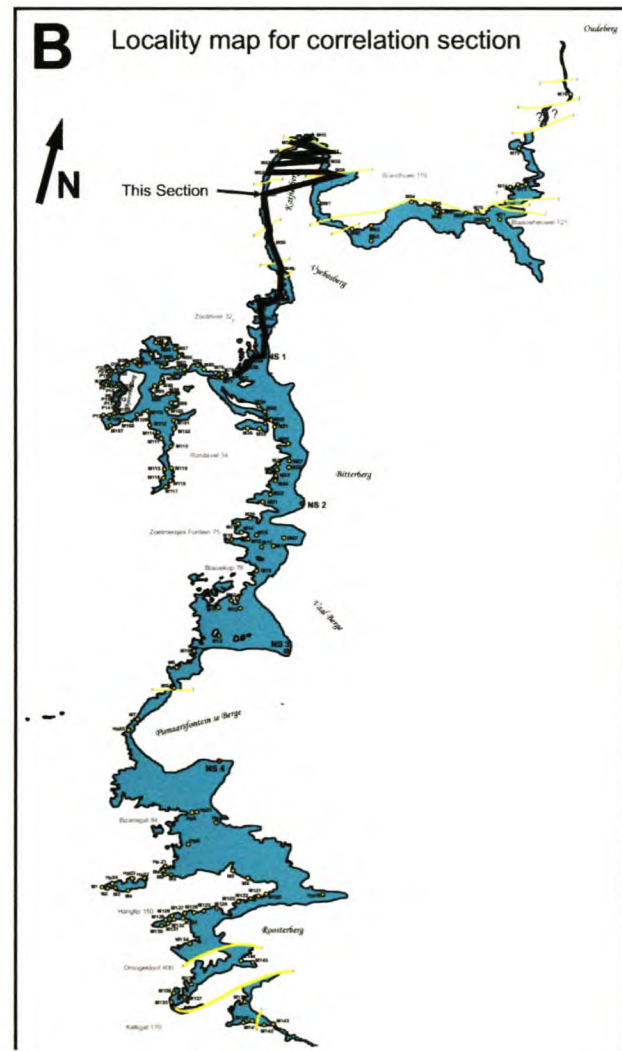
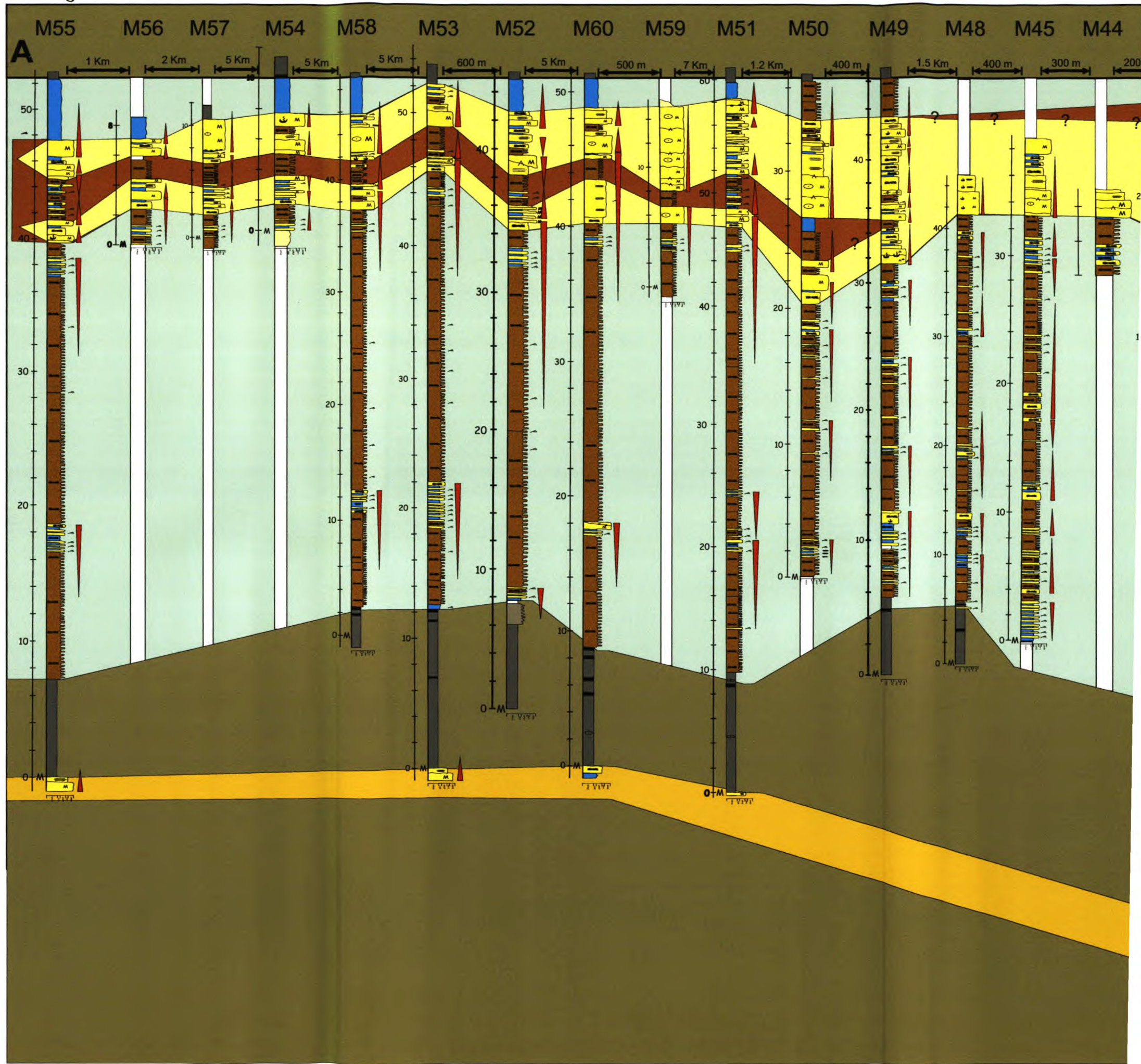
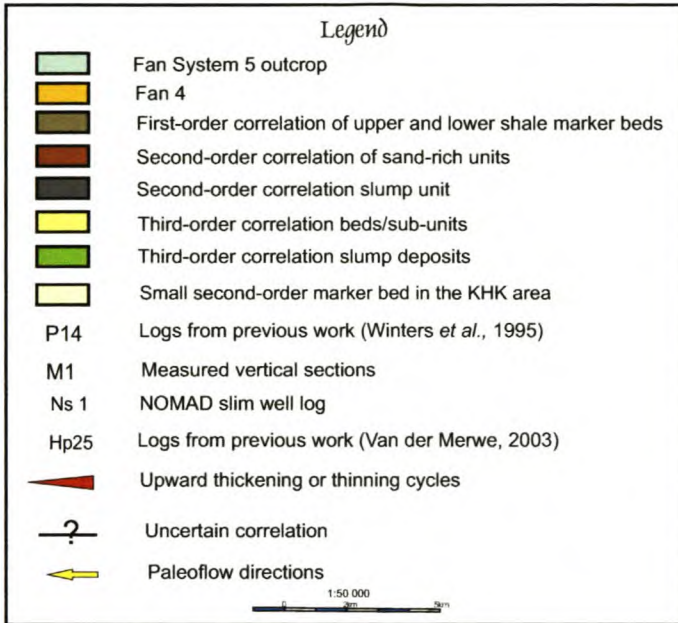


Figure 4.25 (A) Oblique strike profile of the GHK (Groot Hangklip) sand-rich unit. Correlation of this section was extremely difficult due to the variations and wedge-out of beds in the channel-fill environment. This section is characterized by soft-sediment deformation and slump deposits, which belong to a high-energy and unstable environment. Two distinct channel complexes were correlated with numerous smaller channel-fills. These fills pinch out in less than 4 km **(B)** Locality map for the correlation section with the main palaeoflow to the northeast.

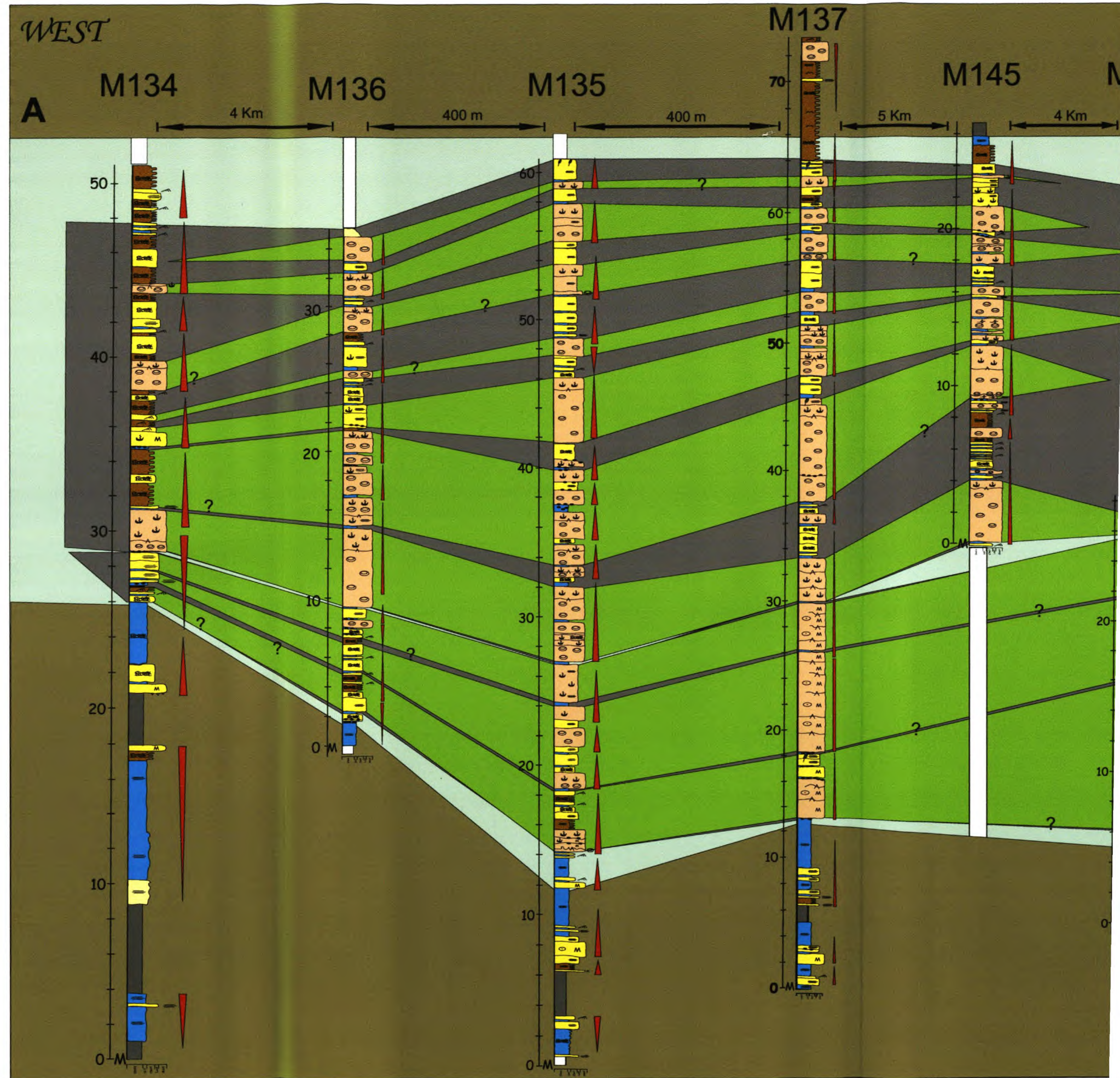
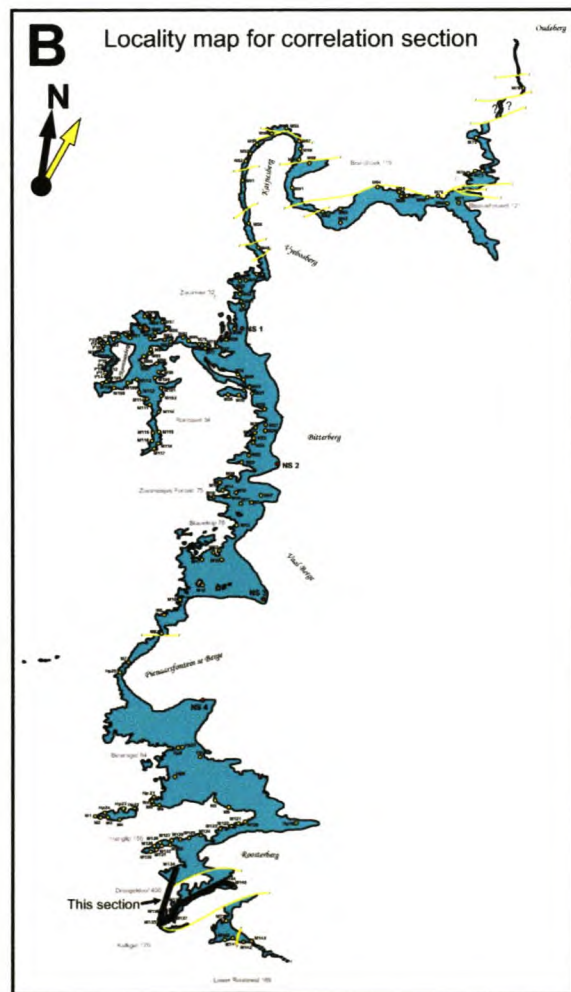
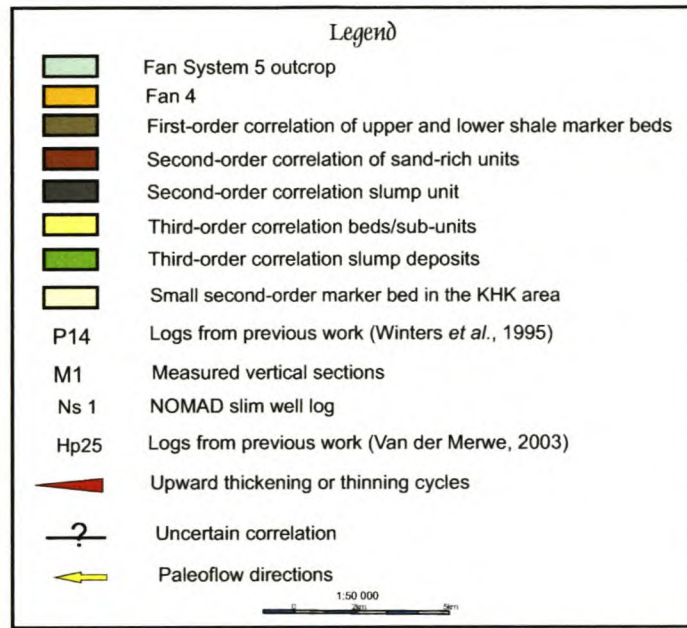


Figure 4.26.1 (A) North-south oblique strike correlation section of the Kalkgat (KG) unit. It comprises numerous channel-fills with massive slump and dewatered sediments. Two channel complexes occur with the lower pinching out to the north of the section. The KG unit pinches out in less than 1 km to the south of M143 outcrop log. **(B)** Locality map for the Kalkgat correlation section. Paleoflow direction mainly to the northeast.

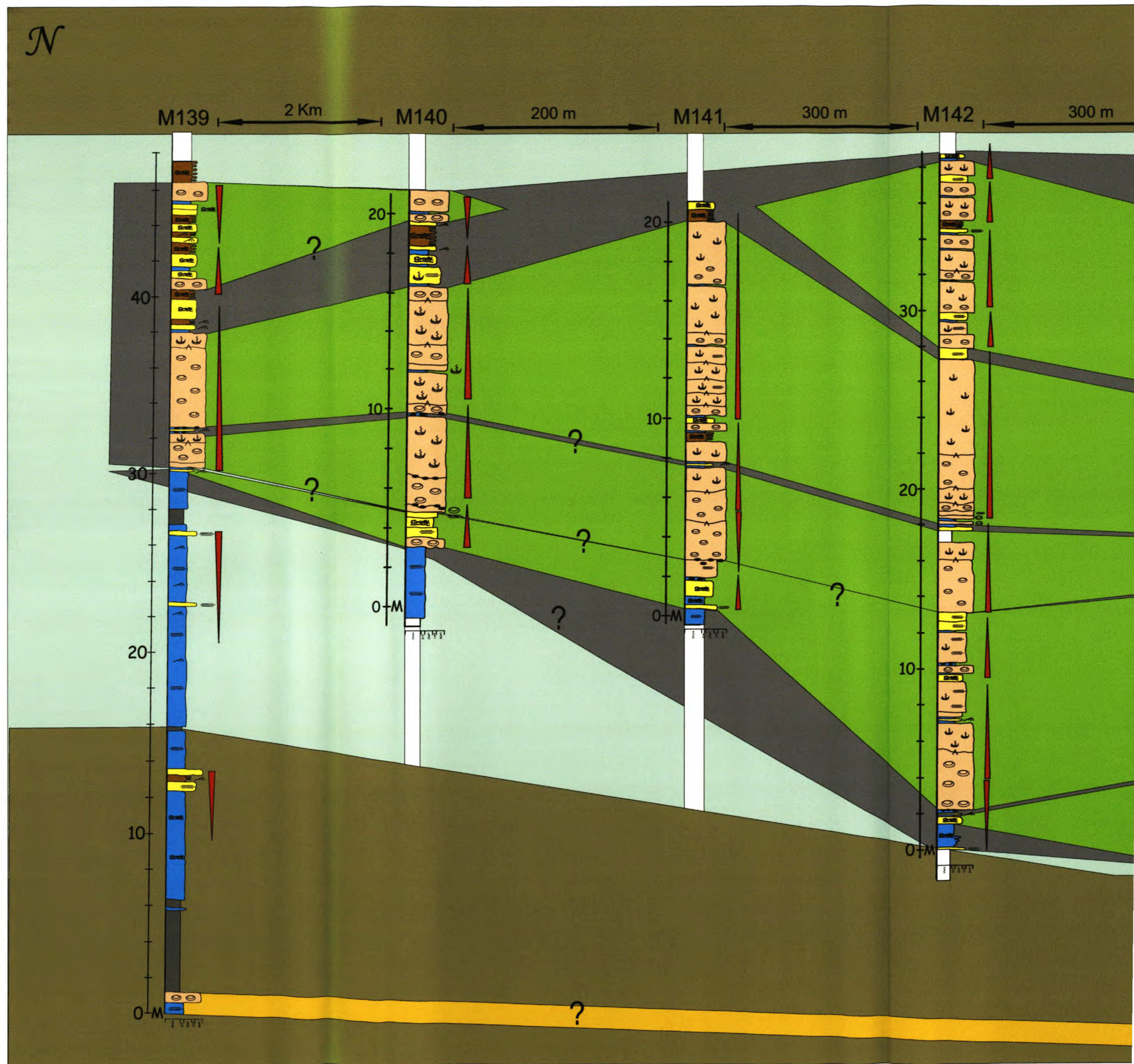
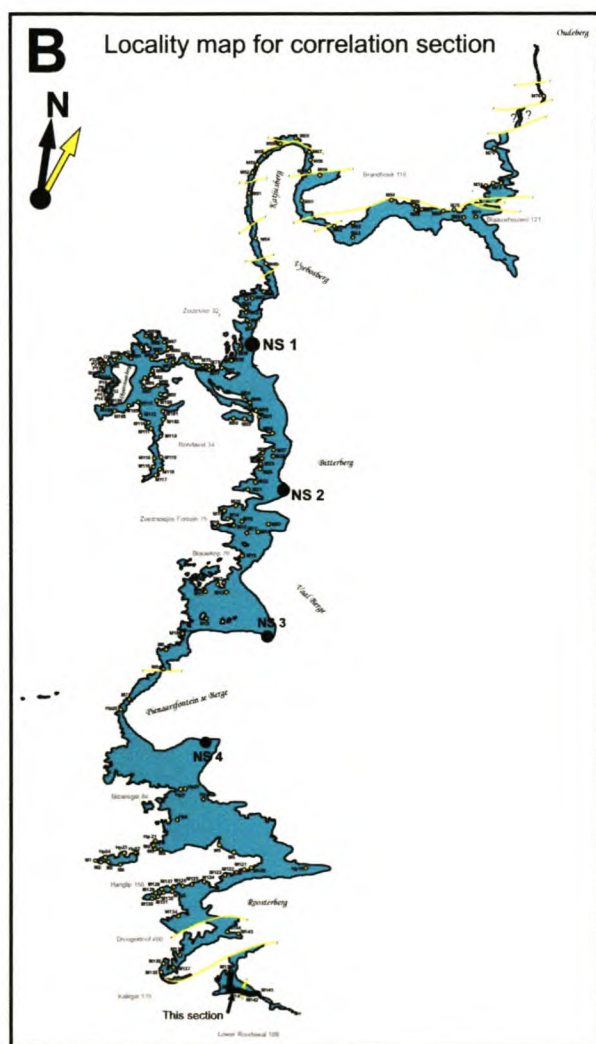
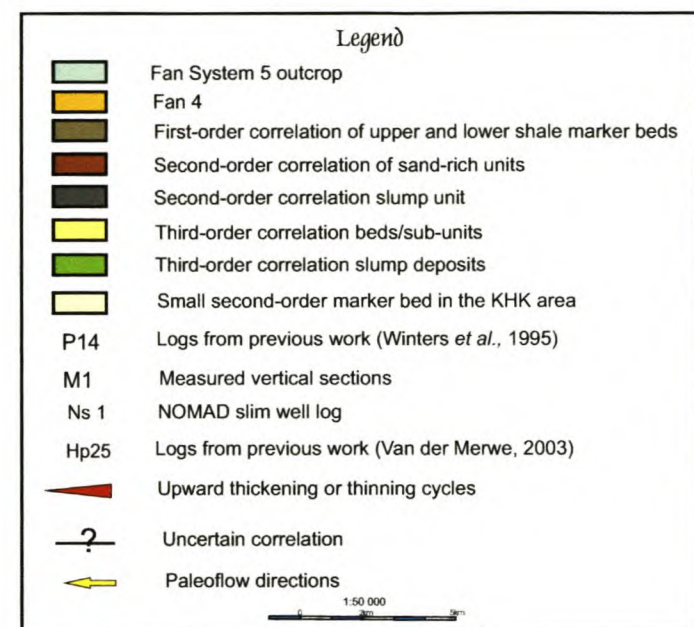
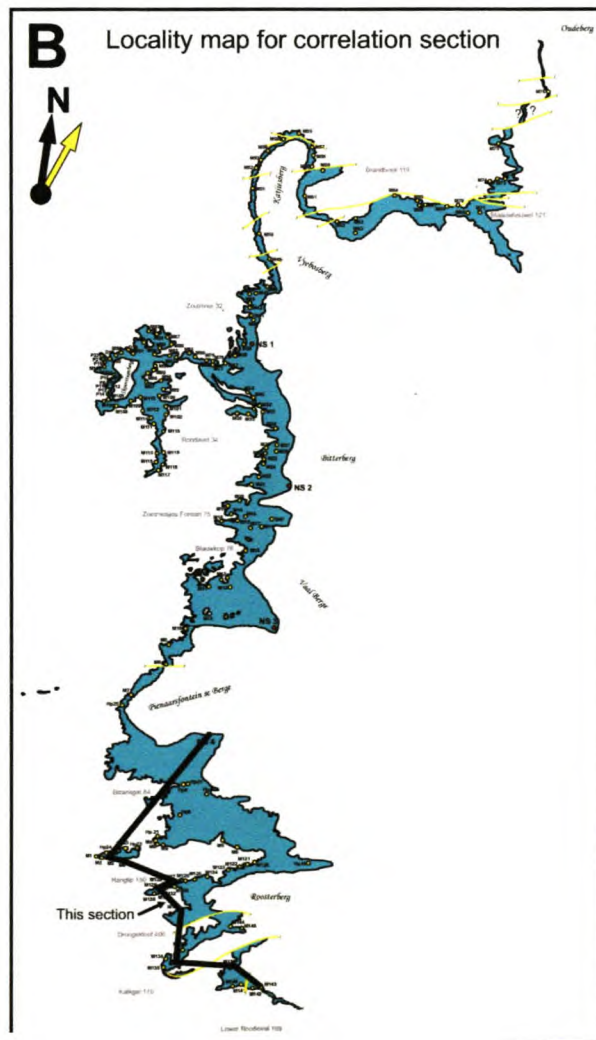
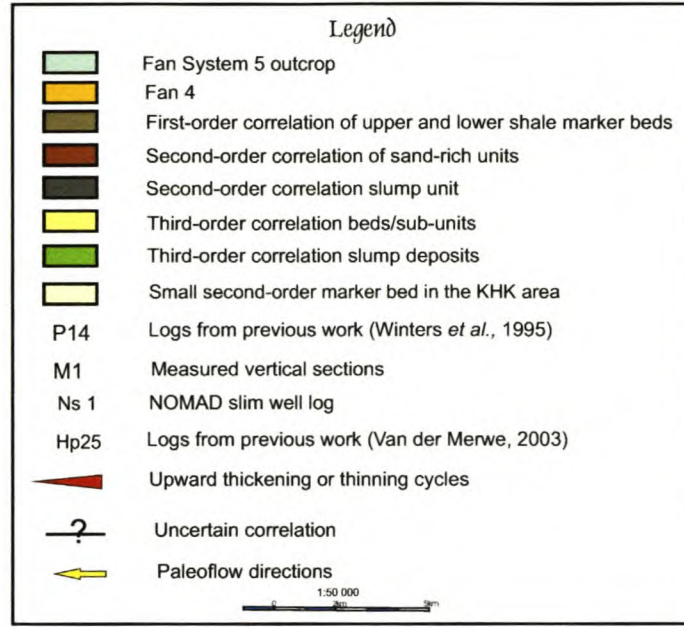
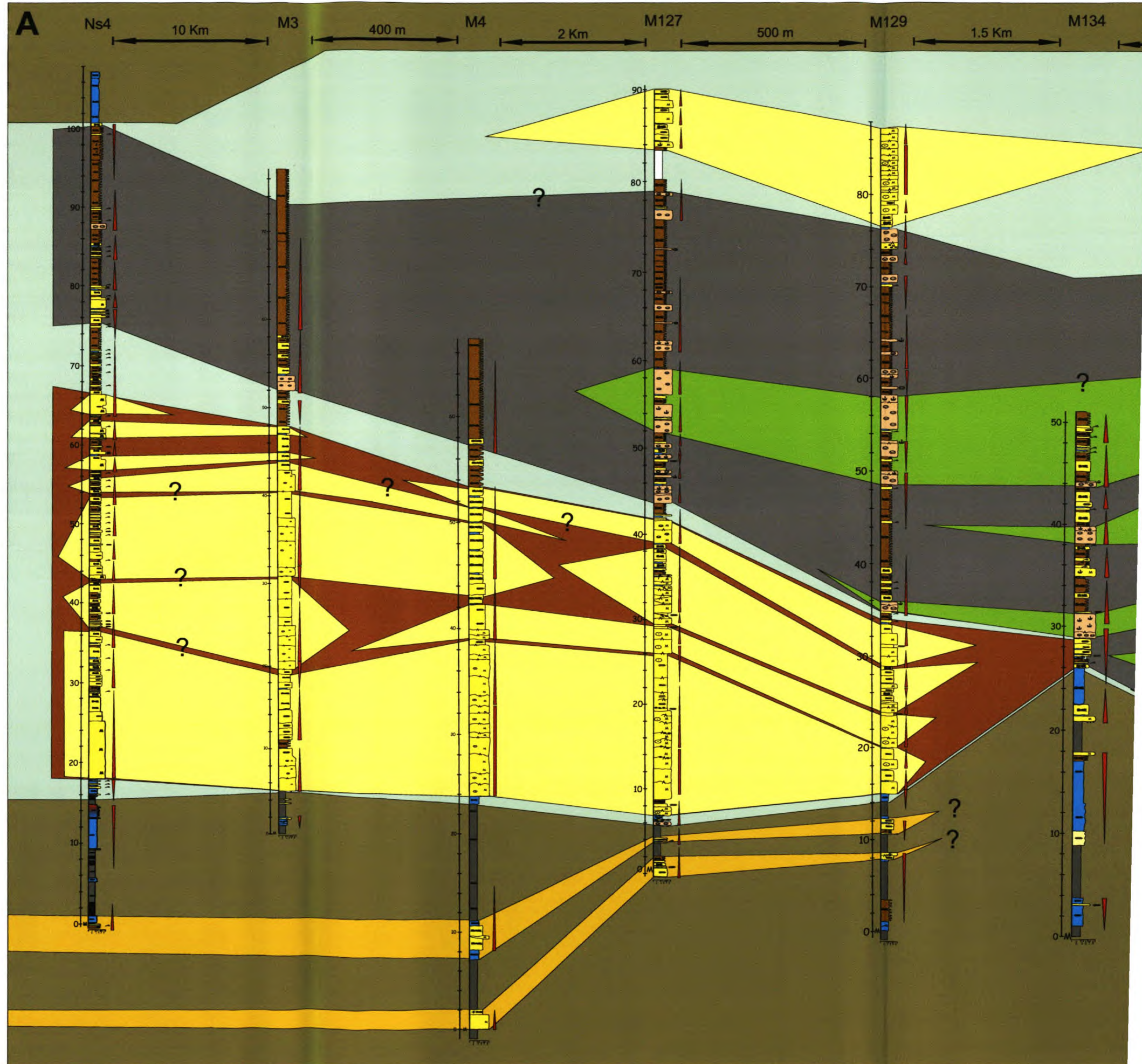


Figure 4.26.2 (A) Oblique strike section through most of the southern outcrop from the NS 4 well in the KHK unit to the last outcrop log M143 in the KG unit. Three major channel units occur, which are overlain by a slump unit. Above this slump occur smaller, undeformed, channel-fills which form part of the last and youngest sand flows of FS 5. Note the transition over the M134 vertical section. **(B)** Locality map for this section. Main paleoflow is to the northeast.



NORTH



4.7 Internal architecture and geometry

The general geometry and distribution of the architectural elements of FS 5, as well as the direction of the main channels and smaller channel complexes have been compiled in an architectural map (Figs E+E1-5). The boundaries of each element and depositional environment have been idealised because of limited field exposure. The distribution and type of architecture for each unit, with reference to the above Figures, will be explained in detail in the following section.

4.7.1 Channel development

4.7.1.1 General

Only general descriptions are provided for the main types of channels and their architecture in Section 3. The next sub-section will only concentrate on the channel complexes and their general characteristics in FS 5.

The channel complexes consist of dozens of amalgamated individual channel-fills. These channel-fills are around 50 – 350 m wide and 6 – 15 m thick. They have erosional basal surfaces and concave-up geometry. They are often asymmetrical and less steep where the channel margins are characterized by interfingering between the channel-fill and sandy levees. The steeper channel margin is an erosional surface, which cuts into the surrounding layered deposits. The basal erosional surface often shows evidence of bypass facies (predominantly Lf 6) development.

Channel-fill deposits consist of massive or graded sandstones (Lithofacies 1) deposited by high-density turbidity currents (parent flow). Individual beds have in some occurrences an erosional base, which mimics the main channel erosional surface. The channel complex presents a multi-story architecture due to multiple phases of incision, fill and spill, similar to numerous examples described in the sedimentological literature. Numerous phases of erosion, in-fill and construction, alternating with periods of abandonment, are the main building stones of the channel complexes (Imperato and Nilsen, 1990).

The basal surfaces of the channel complexes in FS 5 show the following characteristic features (Fig. 4.27):

- 1) a 'step-flat' geometry, which is the result of multiple erosion and infill phases
- 2) deep erosional cut-and-fill surfaces and
- 3) a smooth surface with a sharp contact.

At the scale of the channel complex, the degree of amalgamation of individual channels decreases upward. Erosive processes dominated in the basal part of the channel complex, while aggradational build-up characterises the upper part. Channels located in the basal part of the complex show deep incisions, poorly developed levees and little aggradation whereas channels in the upper half of the complex are more constructive than erosive. This vertical facies evolution at the scale of a channel complex reflects a general back-step pattern through stratigraphical depositional time, indicating a decrease of current energy and sediment supply (Sixsmith *et al.*, 2004). Hemipelagites then draped the whole system during the period of shut-off of clastic supply. This evolution of a channel complex mirrors the higher-order overall back-stepping arrangement of the whole FS 5, from the basin floor fan elements to a more channelized-levee system in a base-of-slope fan system.

The channel morphology in the major primary complexes induced lateral confinement and funnelling of high-density gravity flows but not to the same degree as in the canyon. In some places (KHK and KG), the bypass facies is abundant, since most of the clastic material passed through the channel complex, only to be deposited downstream. Bypass processes occur when the flow velocity is too high to allow sediment deposition. At the scale of an individual channel, lag deposits and 'residual' sediments are deposited in the channel axis (Beaubouef *et al.*, 1999; Gardner and Borer, 2000; Mutti, 1992). Lag deposits (mud clasts) form part of the sediment load that is too heavy to remain in suspension, and are transported by a bed-load mechanism at the base of the gravity flow (Figs 4.28.1+2). In contrast, the 'residual' deposits are fine-grained sediments deposited by traction and fall-out mechanisms in the waning stage of the turbidity flow. They drape the basal erosional surface of the channel (Figs 4.28.1+2). The association of lag deposits with fine-grained 'residual' sediments is diagnostic of bypass processes within the channels. The high current density favoured traction, bed-load and grain-to-grain interactions

over turbulence and suspension fall-out processes. As a result, levee development is limited. They only form when the deep channels are almost filled, and are of limited lateral extent.

Confined channel systems open up in unconfined environments. Levees and overflow deposits are more common and better developed in unconfined settings; their volume and lateral extension are, however, still limited. Spill-over lobes and crevasse splays mostly develop in the area. The slope gradient also decreases from the base-of-slope to the basin-plain, which leads to a rapid decrease of flow-energy and deposition of sediments (Fig. 4.29). The channels also open onto a wide basin-plain, and the flow is no longer confined (Fig. 4.29). A combination of these factors explains the particular characteristics of a channel-lobe complex that develops at the unconfined channelized mouth setting (Sixsmith *et al.*, 1998; Eschard *et al.*, 2003) (Fig. 4.29).

Clark and Pickering (1996) proposed a general model for ancient channel systems. They divided the history of any channel system in three main phases (Fig. 4.30):

- Phase 1 represents the initial phase that involves different stages of erosion, bypass and non-deposition.
- Phase 2 is the main phase of deposition and channel infill.
- Phase 3 is characterized by channel abandonment. It is during this phase that widespread, thin-bedded, fining-upward sequences are deposited over the underlying channel-fills.

All of these are applicable to the channel-fills in the different units of FS 5, but not all of the phases have been preserved. The main types of channel geometries were summarised by Johnson *et al.* (2001) and described in Section 3.

The channel complexes of FS 5 were classified according to the scheme proposed by Abreu *et al.* (2003) namely: two or more channel-fills of similar architectural style are termed a Channel Complex and two or more Channel Complexes, bounded at their base by a basinward shift in facies and at their top by a surface of abandonment, is termed a Channel Complex Set. Genetically related, stacked Channel Complex Sets form a Channel Complex System.

4.7.1.2 Klein Hangklip channel complex

Description:

Highly erosive, stacked channel-fill deposits characterize the northern limb of the Hanglip 150 syncline valley (Fig. A; Image D). The channel-fills are erosive into the lower Tierberg shales and into Fan 4 in some localities (Fig. 4.20.4). The main concentration was found on the southernmost outcrops in the study area, but may extend further southwards (Fig. E). These units, previously known as the Hangklip Fan ('Fan 6'), revealed a direct relationship with FS 5 (Van der Merwe, 2003).

The elongated cliff section on Hanglip 150 and Pienaarsfontein 414 is an approximately 8km wide outcrop belt consisting of multiple erosional-based channel-fill complexes (Fig. E1), very similar to the Fan 3 Ongeluks River channel complexes. The channel-fills in the Klein Hangklip area vary between 20 to 100 m in width, sometimes arranged in vertical to off-set stacking patterns (Fig. 4.31). These channel-fills are comprised of massive, amalgamated, fine- to very fine-grained sandstone units up to 15 m in thickness. They are separated by thinner sandstone/siltstone units of varying thickness, not easily identifiable because of poor exposure. In places, the basal contacts of larger channel-fills are highly erosional with rip-up-clasts and amalgamation associated with scour surfaces (Figs 4.32.1+2). Associated with the channel-fill deposits, but partially eroded due to later channel incision, are thinner-bedded sandstone and siltstone units that display parallel- and ripple cross-lamination (Lf 2 and 5).

An erosional remnant of a channel-fill deposit in plan view has been identified in the southern portion of Pienaarsfontein 414 (Fig. 4.33). The channel-fill unit is \pm 100 m wide, 15 m thick, and 400 – 500 m long. The infill consists of massive, amalgamated, fine-grained sandstone eroded into older channel-fills. The orientation of the channel-fill is clearly visible on the aerial photograph (Fig. 4.33). Palaeoflow is orientated north-easterly. This is the only example of a channel-fill in plan view in the Tanqua sub-basin.

Interpretation:

The KHK channel complex system were described and interpreted by Van der Merwe (2003) and the most eastern section by Wild *et al.* (2005). This channel complex system is interpreted as the primary sediment flow of FS 5 which was deposited, and even eroded in some places, on the

basin shales (Fig. 4.20.4). KHK can be divided into three channel complex sets (Fig. E1). These three sets are genetically related and therefore form a channel complex system. KHK-k is the most eastern complex set and comprises six channel complexes. KHK-l is the middle complex set and comprises 19 single, vertically and laterally stacked channel-fills. KHK-m is the most western channel complex set that can also be correlated with the primary channel complex set of the TB sand-rich unit.

This channel complex system consists of more than 28 vertical and lateral stacked channel-fills. The palaeoflow direction varies for each set; KHK-k's main direction trend was to the east, KHK-l to the northeast and KHK-m also to the northeast (Fig. E1). The channelization displayed by these more proximal outcrops is interpreted to represent an upper middle fan, which was most likely deposited at the base-of-slope. Wild *et al.* (2005) recognised two phases of incision within each channel complex of the KHK-k set and only three complexes. An additional three were recognised by Van der Merwe and Wickens (2004) (Figs 4.34.1+2). The first phase resulted in highly confined channels with no evidence of significant spill whereas the second phase of incision was less deep, and unconfined spill deposits occurred. Lateral accretion occurs on the margin of the upper channel complex (See Section 4.7.2) (Fig. 4.34.5). More than one channel-fill, which comprises massive sandstones, occurs in each complex of KHK-k (Figs 4.34.2+3+4+7). Their erosional contacts are associated with lag deposits and rip-up clay clasts (Figs 4.34.3+6). Palaeoflow indicates a change from an easterly to a more north-easterly direction for this set.

KHK-l has the largest amount of channel-fills. The channels are lens-shaped units consisting of massive amalgamated sandstone deposits, overlain by layered units (if not eroded) (Fig. 4.31). The lenticular channels indicate migration, lateral and vertical, from the west to the east (Fig. 4.35.1). Several down-scouring, erosional surfaces are visible at the bases of the massive sandstones (Figs 4.35.3+4+6). Lateral accretion on the margins of some of these channel-fills is also present (See Section 4.7.2 for detail) (Fig. 4.35.7). In some places, thin siltstone layers and rip-up clasts are associated with these erosional surfaces (Fig. 4.35.6). The channel-fill sandstones vary in thickness laterally and decrease their sand/shale ratio towards the sides (Fig. 4.35.4). The massive units in the axis gradually become thinner-bedded towards the margins and upwards (Fig. 4.35.2). KHK-l gives the impression of a distributary channel system (Fig. E1), but is characterized by bypass, rather than deposition, like the BK distributary channel system.

The KHK-m channel complex set consists of two channel complexes and numerous channel-fills with a palaeoflow direction to the northeast (Fig. E1 + Fig. 4.36.1+3). The channel-fills comprise predominately layered beds and are wide with sharp basal contacts, almost a type of step-down pattern (Figs 4.36.2+4+6+7). The complex consists of numerous small channel-fills eroded into each other (Figs 4.36.5+8). Rip-up clay clasts are abundant in these erosional zones (Fig. 4.36.8). Section 4.6 provides a description of the correlative units between these two units. The KHK-m channel complex set represents confinement and sediment bypass is the main depositional characteristic of this complex set (Fig. E1).

In contrast to the channel-fill deposits in the southern part, ripple cross-laminated overbank deposits with smaller channel-fill units predominate in the north-eastern and western parts of the outcrop area (See Section 4.7.3). This thin-bedded succession, previously mapped as the southern extent of FS 5, is interpreted as a stacked overbank succession, marginal to the KHK channel-fills (Fig. E1). The occasional channel-fill associated with this thin-bedded succession evidently originated from the KHK channels and invaded the overbank area with possible contribution to the overbank deposits as crevasse splays. The most distal deposits of this channel complex set outcrop in the Blauwkoop unit and also show up in the two slim well logs of NS 3 and NS 4 (Fig. E). Thus, the BK unit was not a separate unit but represents a transition from mid fan to lower fan, whereas the KHK unit represents a transition from upper to middle fan.

4.7.1.3 Tongberg channel complex

Description:

The TB sand-rich unit comprises three channel complex sets (Van der Merwe and Wickens, 2004) (Fig. E2). TB-f is the most western complex and underwent two periods of erosional incision (Fig. E2). The palaeoflow direction of these complexes is mainly to the northeast. Facies Lf 1 and 2 sandstones predominate and show soft-sediment deformations and dewatering structures in the upper zones (Lf 8). Large slump structures are present in the most western outcrop of this channel complex. One major channel-fill was deposited on the basin shales (Figs 4.37.1+2). Four smaller channel-fills occur above this larger channel-fill (Fig. 4.37.1). Palaeoflow directions are predominantly towards the east. TB-e forms the most eastern outcrop of the unit and hosts two smaller channel-fills (Fig. E2). The latter consist of massive Lf 1 and 2 sandstones and pinch-out in thin overflow units to the east and west in less than 150 m (Fig.

4.22). Palaeoflow directions are to the northeast. The geometry of the TB-e channel-fills is wide with a small indication of an erosional down-cutting towards the west. The TB-g channel complex intersects the uppermost deposits of FS 5 in the TB unit (Fig. E2 + Fig. 4.22). Two 12-17 m thick channel-fills outcrop in the TB-g complex (Figs 4.37.1+2+3). It comprises thick-bedded, parallel and ripple-laminated sandstones (Lf 2) (Table 2) (Figs 4.37.3+4+5). In some places, deformation of the sediment occurs (Lf 8). Plant fragments (Lf 10) are also abundant in these sandstones. The channel-fills have low width:depth ratio geometries and form sharp and erosional basal contacts with underlying thin-bedded units (Fig. 4.37.6). The palaeoflow directions for TB-g are to the north and indicate the last stage of sediment input in the southern part of the basin in FS 5.

The succession above TB-f and below TB-g (more or less 46 m) is dominated by sandstone and siltstone (Lf 4, 5, 7 and 8, Table 2) displaying parallel- and climbing-ripple lamination, and forming coarsening- and thickening upward packages (Fig. 4.37.7). Symmetrical wave ripples were also preserved at the top of these beds (Fig. 4.37.8). These deposits are interbedded with sandstone beds of 2 m or more in thickness, which display ball-and-pillow and large-scale dewatering structures (Figs 4.37.9+10). These deformed bodies could be traced towards the eastern outcrop into non-deformed strata where deformation ceases gradually but relatively abruptly.

Interpretation:

The package of thin-bedded units and slump layers is interpreted to form part of the KG and GHK sand-rich units (Figs E+E2). The two lower channel complex sets, TB-f and TB-e, were deposited in the primary depositional period of FS 5 and correlate with the KHK complex system (Fig. E). The TB-f channel complex set gives the impression of being the proximal part of the KHK-m complex set. The western complex set TB-e could be interpreted as crevasse channel-fills and splays, which originated from the main primary channel complex set of TB-f. The upper channel complex set TB-g differs from the lower channel complex set TB-f in a number of ways - the fill is much thinner-bedded and parallel-laminated. It also contains layers, which are bedded with rip-up clay clasts, plant material and ball-and-pillow structures (Fig. 4.37.11). TB-g is interpreted as the uppermost channel complex of FS 5 in the southern part of the basin. The palaeoflow indicates a northerly flow direction (Fig. E2). The depositional slope gradient for TB-

g was probably at its lowest before basinwide flooding of FS 5 occurred for the deposition of the first-order upper marker bed silty-shales.

The channel-fill geometries for the TB units display low width:depth ratio. No evidence for erosional truncation of the lower units was found. Thus, this part of the unit also reflects a mid-fan setting, but in a more unstable area, compared to the KHK sand-rich unit.

4.7.1.4 Skoorsteenberg channel complex

Description:

The SB unit is characterized by numerous channel-fills in the proximal area, west of Skoorsteenberg, which have provided an immense amount of sediment in the sheet sand lobes area (Fig. E3, see also the model from Fig. D). The SB unit represents the final large-scale sediment input event before flooding and deposition of deep-marine shales, interbedded with high-angle slope sediments of deltaic origin. The channel-fills are composed of large-scale amalgamated sandstone beds, which form a sheet geometry (Winters *et al.*, 1995) (Figs 4.38.1+2). There is a clear vertical partitioning of channel-fills in the Skoorsteenberg locality of the SB unit. The lower part comprises large channel-fills with up to 2 m of basal erosion, filled mainly by massive to structured sandstone with minor amounts of thin- to medium-bedded sandstone (Figs 4.38.1+8). The abandonment facies at the top of these channels developed into a 10 m thick succession of alternating very fine sandstone, siltstone and shale layers (Lithofacies 5) which contain symmetrical ripples in places (Fig. 4.38.4). This lithofacies is overlain by a silty-shale facies (Lf 9) which forms the upper regional marker bed (Fig. 4.38.5). Large-scale internal scours and smaller scour-and-fill bedforms are common in the lower part of the unit (Figs 4.38.7+9+10). Laterally offset-stacked depositional channels with heterolithic fills dominate the upper part of the unit (Figs 4.38.3+6).

Interpretation:

The SB unit consists of two major low width:depth channel complexes (Fig. E3). Winters *et al.* (1995) determined the aspect ratios for the channels to be between 33 (the lowest) and 188 (highest). This represents two phases of deposition. The SB-v represents the lower phase and SB-w the upper phase. The palaeoflow direction of these two phases varies from ENE for SB-v and NE for SB-w. The SB-v channel complex eroded in the thin-bedded underlying overflow deposits

and SB-w complex eroded in to the SB-v complex (Figs 4.38.1+8). Bypass and deposition of sediment is the main characteristic of these channel complexes. The channel complexes comprise numerous small-scale channel-fills, which show different palaeoflow directions (Fig. E3). Erosion is minimal and the amount of amalgamation is very high due to rapid deposition from high-density flows. Basal erosion displays a step-down pattern from the margin to the centre of the channel-fill (Figs 4.38.8+11+12). This suggests concentration of flows in the central part of the channel with numerous flows filling up the channel. Johnson *et al.* (2001) interpreted this change in architecture as a deep-water equivalent of a backfilling depositional system, where there is a decrease in the volume and density of the turbidity current.

The smaller, more erosive channel-fills occur as single flow sub-units inside the larger channel complex (Fig. E3). Most of these sub-units pinch out in less than 50 m down-current (See correlation of the dip section in Fig. 4.23.3). The two main channel complexes developed in less than 1km in a set of 12 different smaller channel-fills; they spread out as frontal lobes and sheet sands, in less than 2.5 km from the confined channelized deposits (Figs D+E3). The SB unit thus forms part of the transition from a mid-fan environment to a lower-fan environment (Fig. E3). The lateral extent of the SB unit was examined as far as borehole NS 2, 15 km to the southeast of the main axis of the SB unit (Fig. 4.24.1). The pinch out of the SB unit near Ouberg Pass is characterized by sheet sand deposits (Fig. E3 + Fig. 4.23.2).

4.7.1.5 Blauwkop channel complex

Description:

This complex is exposed in a dry riverbed on the farm Blauwkop 76. It was the main feeder system for the Blauwkop unit (Figs E+E4). It consists of Lf 1 amalgamated sandstone beds, closely associated with well-bedded overflow, levee, and sheet sand deposits, spread over 60 km² (Fig. 4.39.1). Kirschner and Bouma (2000) identified seven channel-fills, which they grouped into two types. Identification was based on aspect ratios, basal down-cutting patterns, and internal architecture. A narrow channel that cut into the underlying marginal deposits (Figs 4.39.2 +3+5; Fig. 4.27.B) characterizes the Type-1 channel-fills. The channel-fill is composed of amalgamated massive Lf 1 sandstones (Table 2) (Figs 4.39.4+5). The Type-1 channel-fills comprise erosive flows that scoured a narrow conduit into the underlying marginal deposits. The only remnants of these flows are silt layers along the channel margins (Fig. 4.39.7). These deep erosive channels

were filled up by successive turbidity currents that deposited the amalgamated sheets of Lf 1 sandstones beds (Figs 4.39.1+6). These channels shallow progressively which led to the deposition of overflow deposits and eventually sheet sands. The Type-2 channel differs from the Type-1 due to higher sand:shale ratio and different depth in erosional surfaces. The channels expose a step-wise down-cutting pattern into the underlying sediments (Fig. 4.27.A). This suggests less erosive power from the initial turbidity currents (Kirschner and Bouma, 2000).

Kirschner and Bouma (2000) also interpreted two depositional sub-environments within the Type-2 channels: channel axis deposits and channel margin deposits. The channel axis deposits consist of amalgamated sheets of Lf 1 and Lf 2 sandstones (Figs 4.39.1+6+7), comparable with the channel-fill of Type-1 channels. The channel margin deposits are very similar to the inner levee or X-type deposits comprising Lf 2 and Lf 3 (Table 2). The only difference is the higher sedimentation rate for these marginal deposits. Evidence for this observation was that the average thicknesses for the channel margin beds in the Lf 2 are 108 cm, compared to the 35 cm beds in the inner levee or X-type overflow deposits (Figs 4.39.1+6+7). The angle of climb of the climbing ripples is also steeper. Kirchner and Bouma (2000) suggested an environment of deposition within the channel rather than beyond the levee crest. Small crevasse splay channel-fills are also present in the overflow and sheet lobe deposits. Y- and Z-type overflow deposits occur on the fringes of the main channel-conduit (Fig. 4.39.8).

Interpretation:

It is apparent that the internal architecture of this distributary channel system does not consist of a single, backfilled feeder channel, as depicted in the model shown in Bouma (2000) (see Section 3 for detail on the Bouma fine-grained model). It could be described more accurately as a channel sequence that comprises seven individual channel-fills in the BK unit (Fig. E4). The palaeoflow direction of these seven channels varies from northwest to northeast (Fig. E4). This means that there was a shift in the channel depocentre, which would have caused a lateral shift in the depositional sheet lobes (Fig. 4.39.3). This shift was associated with the formation of new feeder channels. Type-1 and Type-2 channels are interpreted to reflect the down-dip morphologic changes within a feeder channel. As the turbidity currents started to spread out toward the lower fan, the Type-1 morphology was gradually replaced by the Type-2 channel morphology (Fig. 4.39.3). Kirschner and Bouma (2000) concluded that the close vertical association of Type-1 and Type-2 channels reflects the updip/down dip shift of the depocentre in the sheet sand lobes. The

degree of connectivity among the channel deposits is high, although it is moderate between channel and levee-overbank deposits.

The origin of the BK unit was briefly discussed in Section 4.6. Most of FS 5 directly to the south of Blauwkoop is in the subsurface. Outcrops to the west thin out into overflow deposits whereas outcrops to the east are mostly covered. The well log NS 3 provides detail of FS 5 and the BK unit in the Brakke Rivier area (Fig. 4.24.1). The lower thin-bedded overflow beds in NS 3 can be correlated to the lower KHK channel-fills. The middle unit consists of more massive sandstones, which is an indication of channel activity that could correlate with the upper channel-fill units of the KHK and the BK units (Fig. 4.24.1). A representative section for more detail information in the proximal areas of the unit, is log NS 4. It reveals a very sandy package over the lower 60 m and a massive channel-fill above the base of FS 5, eroded by successive smaller, scour-and-fill channels. These channel-fills could correlate directly to the KHK complex (Fig. C). The only problem with this interpretation is the uncertainty whether the NS 4 channels are major crevasse channels or part of the main axis of the channelized units in KHK and TB.

4.7.1.6 Groot Hangklip channel complex

Description:

The GHK unit consists of one complex set of channels (Fig. E5). It comprises two complexes, which had recently been named GHK-A and GHK-B by Wild *et al.* (2005) (Figs 4.40.1+11). These comprise thick-bedded soft-sediment deformed and dewatered, fine- to very fine-grained sandstones, typical units forming part of slump deposits. The lower GHK-A comprise two large channel-fills, GHK-A1 and GHK-A2.

GHK-A1 comprises predominantly massive Lf 1 amalgamated sandstones, which contain abundant dewatering structures in most of the beds (Fig. 4.40.2). It outcrops 200m south of the main Groot Hangklip cliffs and could be traced for more than 2 km in a NE direction before it disappears in the subsurface (Fig. E5 + Fig. 4.40.3). The thickness of this channel is about 35 m and its width 140 m (Figs 4.40.3+4+5). The base of the channel comprises a sharp, loaded, and in places, erosional surface (Figs 4.40.6+7). Groove and prod marks occur on the base of the first massive sandstones deposited on the erosional surfaces. The underlying units consist of silt-shale layers (Fig. 4.40.7). The layers overlying GHK-A1 exhibit a wide range of soft-sediment

deformation structures such as convoluted lamination, dish and pillar structures, loaded bed bases, large (>1.5m) flame structures and ball-and-pillow structures (Fig. 4.42.8). GHK-A2 channel-fill consists predominantly of massive chaotic and deformed amalgamated sandstone beds (Fig. 4.40.9). The thickness of this channel-fill is 15 m with 2-3 m deep erosion at the base (Fig. 4.40.10). The degree of amalgamation and dewatering decreases towards the margins of these erosional surfaces (Wild *et al.*, 2005).

The upper GHK-B channel complex is bound at the base by composite erosion surface with 1.5 m of incision into thin-bedded units, comprising numerous scour surfaces with rip-up clay clasts. This thin-bedded sub-unit indicates the break between GHK-A and B (Fig. 4.40.11). Bed thickness rarely exceeds 1.5 m. The upper beds of GHK-B display soft-sediment deformation structures, which include convolute lamination (Lf 7), dewatering structures and ball-and-pillow structures (Lf 8) (Fig. 4.40.12). These beds are interbedded with thin, ripple cross-laminated sand- and siltstone layers (Lf 5) (Fig. 4.40.13).

Interpretation:

Wild *et al.* (2005) interpreted the GHK-A and GHK-B complexes as a channel complex set. The channel complexes are vertically stacked with numerous small erosional channel-fills. The composite nature of the basal incision surface reflects successive phases of channel aggradation and erosive flushing of the conduit, suggesting bypass of sediment into the deeper basin to the NE (Fig. E5). The palaeoflow directions for the two complexes vary from NE for GHK-B to N for GHK-A. The geometries of the GHK-A1 and GHK-A2 channel-fills comprise a typical erosive, multiple-event channel with a complex fill of massive Lf 1 sandstones and thinner beds at the top. The margins of these channels comprise unstable slumped deposits.

The GHK unit comprised very unstable sediments, which were deposited on a base-of-slope or lower slope area. Bypass facies seems to dominate in these types of channels, especially in the lower GHK-A complex. The thinner slump units above the TB primary channels correlate with these channel-fills of the GHK-B complex. These units of TB could be interpreted as overflow or lobe deposits from the GHK unit (Figs E+E5).

4.7.1.7 Kalkgat channel complex

Description:

The KG unit comprise six channel-fills in two complexes within one complex set (Fig. E5 + Fig. 4.41.1). The sediment characteristics are very similar to the GHK slump layers. The basal, underlying units comprise 15 m thick packages of thin alternating sandy siltstones and shale layers (Lf 5) (Fig. 4.41.2). Erosional surfaces cut the underlying units by > 7 m in some places (Figs 4.41.3+4). The lower complex, KG-h, consists of three channel-fills, which pinch out to the NE (Figs 4.41.1+5). The channel-fills of KG-h comprise predominately dewatered massive (Lf 1) and layered parallel-laminated sandstones (Figs 4.41.5+6+7). The base of this complex consists of a multiple erosional surface and clusters (1 m thick) of rip-up clay clasts (Figs 4.41.4+8). The upper complex, KG-j also comprises three channel-fills. The channel-fills consist predominantly of chaotic sediments with soft-sediment deformation structures, for example ball-and-pillow, dewatering, convoluted lamination and large flame structures (Lf 7 and 8, see Table 2) (Figs 4.41.9+10). These units thin out into thin-bedded ripple-laminated sand- and siltstone. Symmetrical wave ripples and bioturbation (Lf 3 and 10) characterize the upper 10 m. The regional silty shale marker bed of the first-order correlation zone (Lf 9) overlies this complex.

Interpretation:

The KG unit is the most southern outcrop preservation of FS 5. It pinches out in less than 500 m to the south. The palaeoflow directions for the lower Kg-h are to the NNE and for the upper channel complex, KG-j, to the NE. The lower KG-h complex pinches out less than 3 km to the NE of the main conduit (Fig. E5 + Fig. 4.26.1). The upper KG-j complex maintains a constant thickness throughout the area. The channels of this complex could be classified as erosional multiple event channels, following the scheme of Johnson *et al.* (2001). The only difference is that the north-western channel margins have eroded very sharply and will fit more appropriately in the deep erosional scour surface model in Figure. 4.27.1.B. This indicates active bypass of sediment to the lower fan region and due to the abundant slump deposits, this area can be interpreted as a highly unstable area with a higher than normal slope gradient (Surlyk, 1987). The KG unit is correlated with the GHK unit (see Section 4.6 for more detail) and interpreted as having being deposited in the most proximal part of the Fan 5 system. A lower to middle upper fan position is the most likely depositional setting for the KG unit.

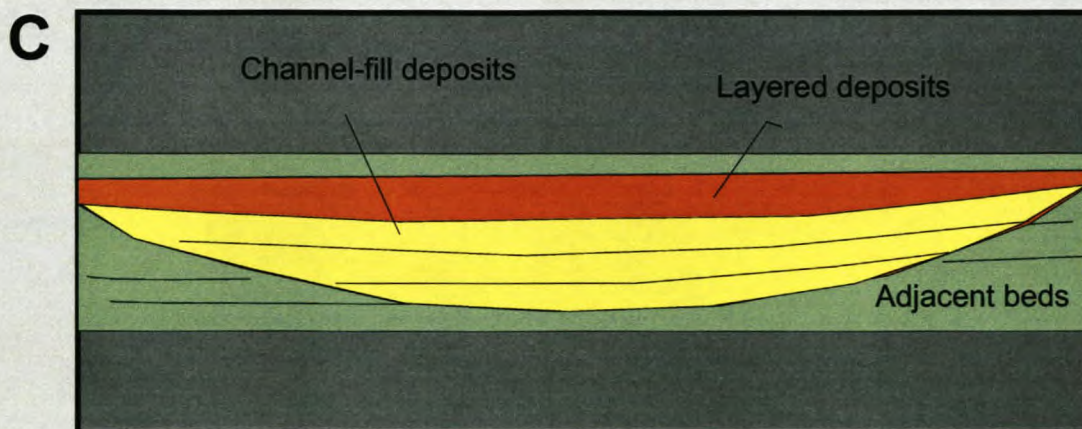
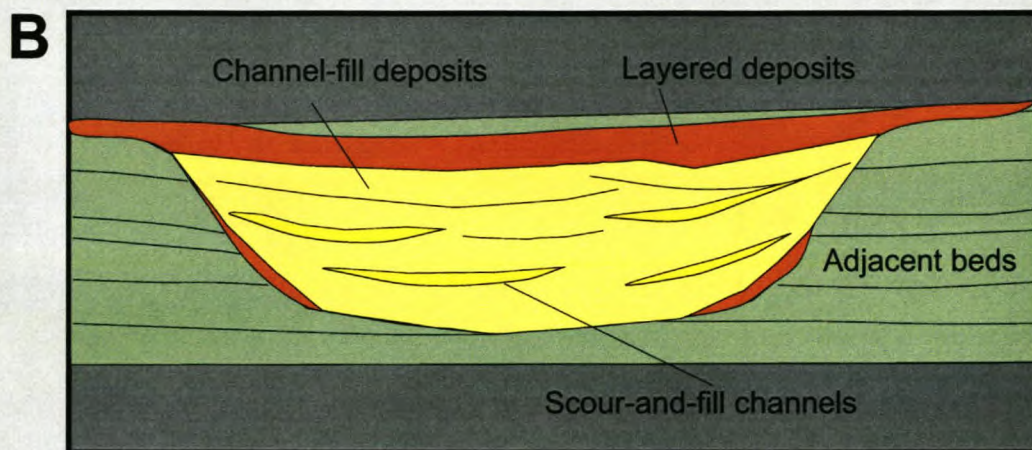
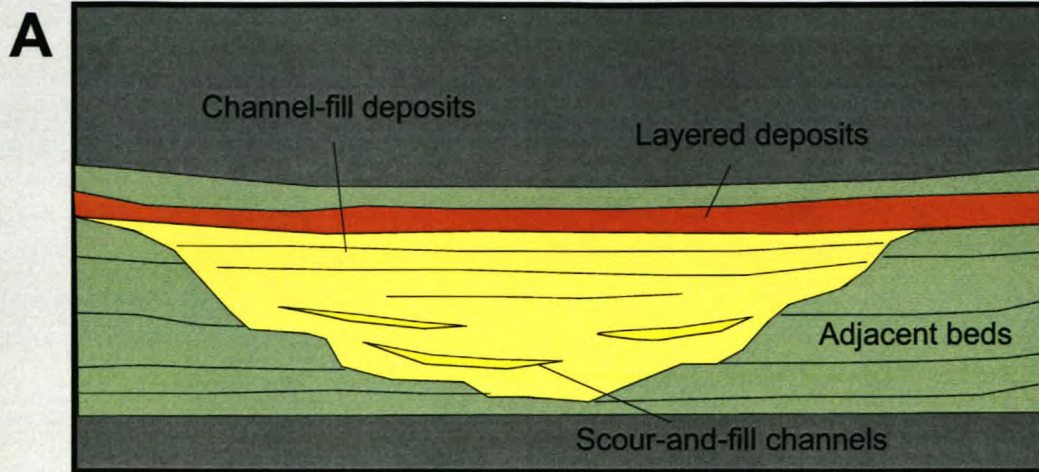


Figure 4.27 Three types of basal erosional surfaces for channels. (A) step-flat geometry, (B) deep erosional cut and (C) smooth erosional contact.



Figure 4.28.1 Lag deposits or “remnants” of successive channeling in a channel complex. These lag deposits comprise predominantly clay clasts. The upper and lower channel-fills are indicated by the dashed line. Pencil (15 cm) for scale. Skoorsteenbergr locality.

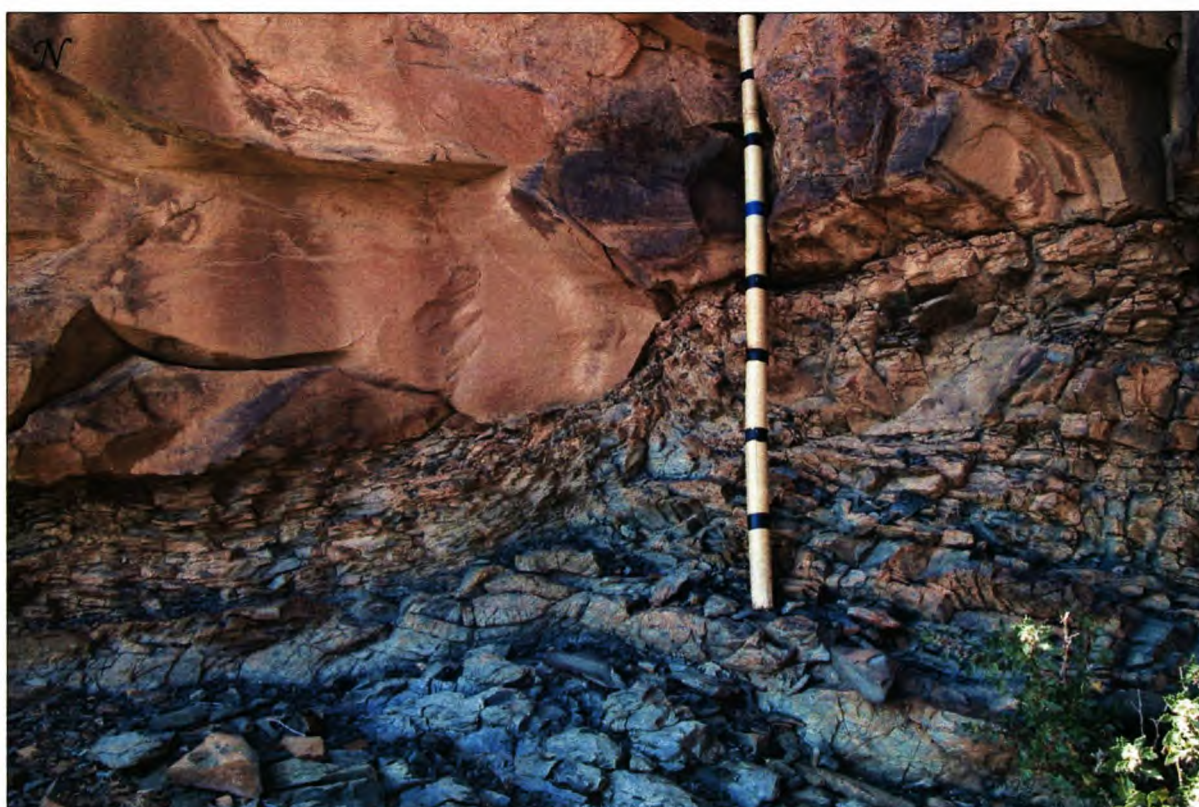


Figure 4.28.2 Erosional channel-fill base with lag deposits consisting predominantly of rip-up clay and silt clasts. Tongberg locality.

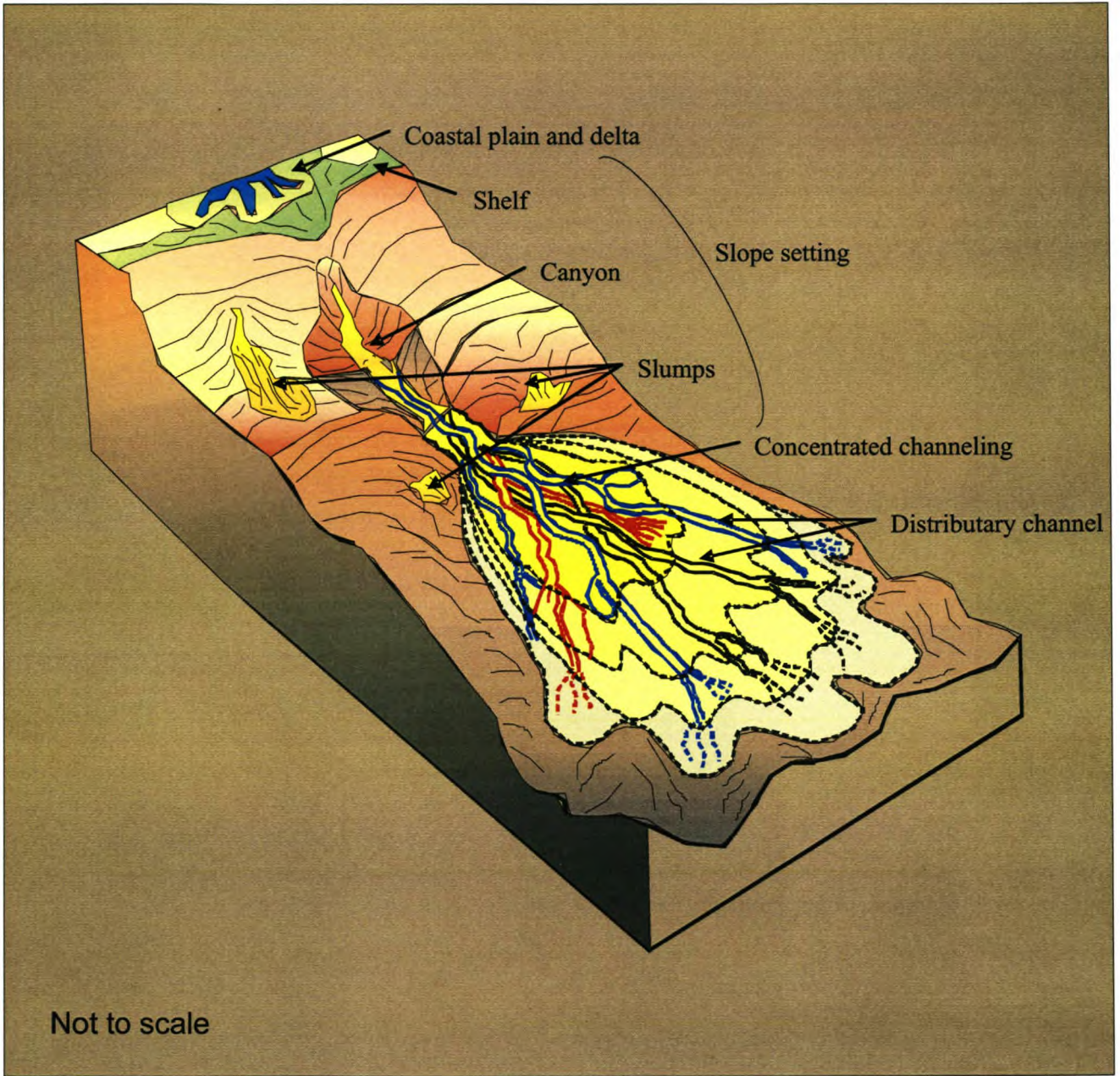


Figure 4.29 Depositional model proposed for the development of a channelized system from a confined canyon environment into an unconfined mid-fan to lower fan on the basin floor. Note the spreading of the distributary channels. Sketch modified from Johnson *et al.* (2001) and Van der Merwe (2003).

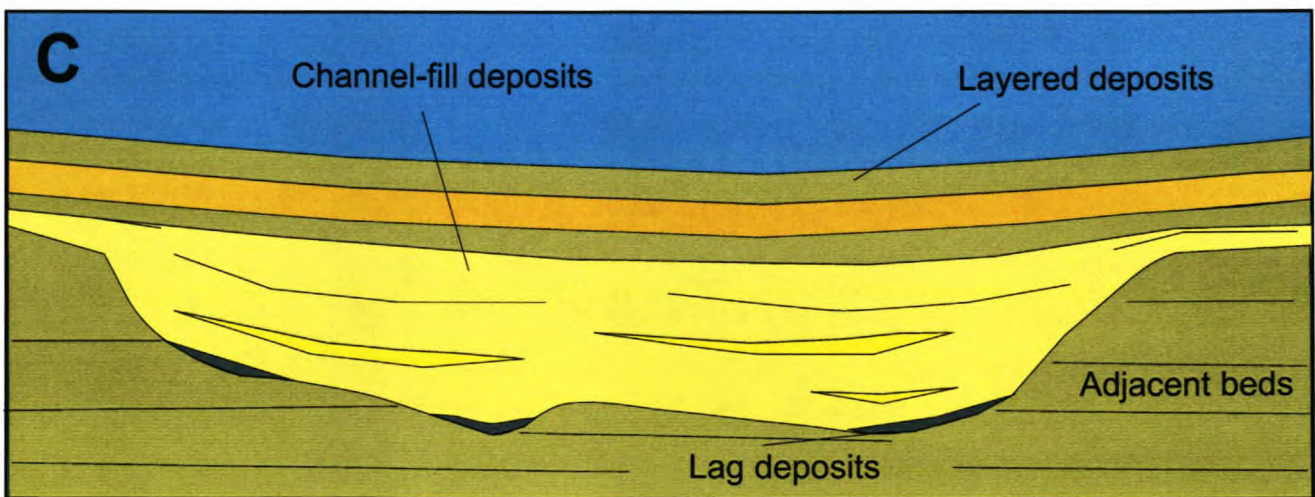
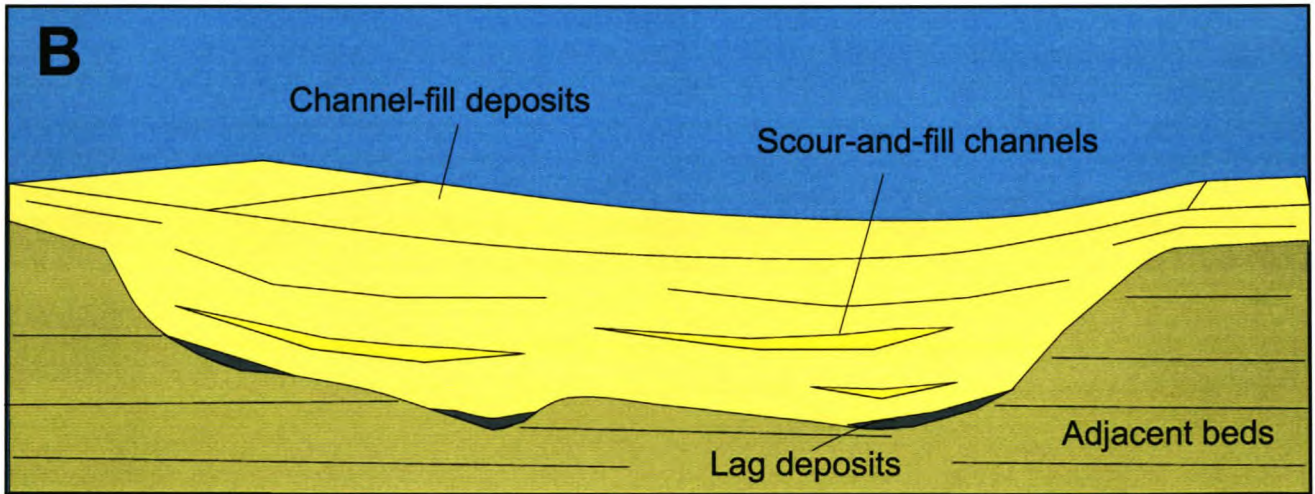
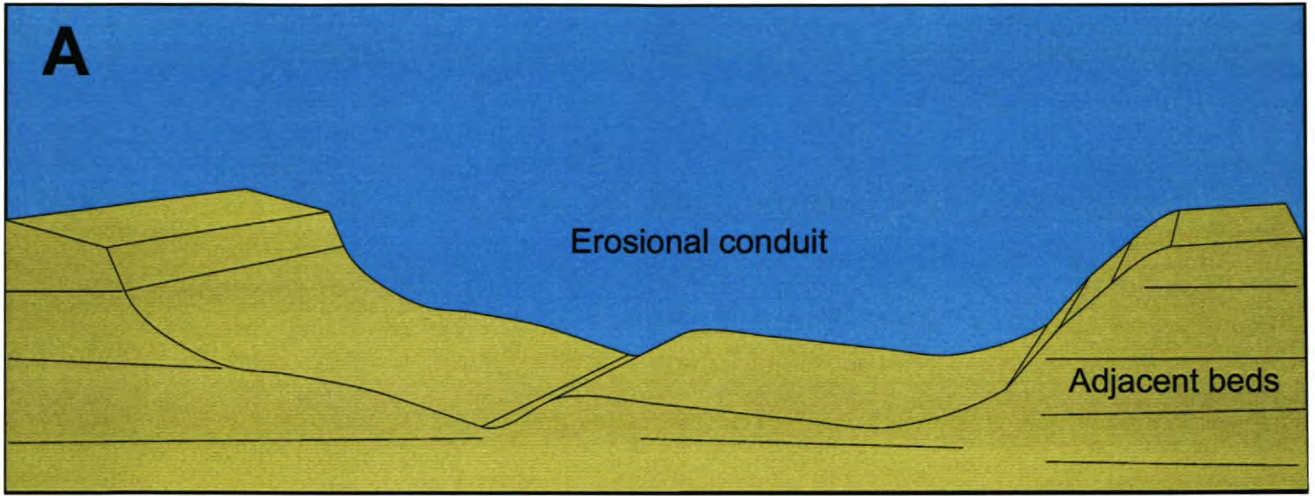
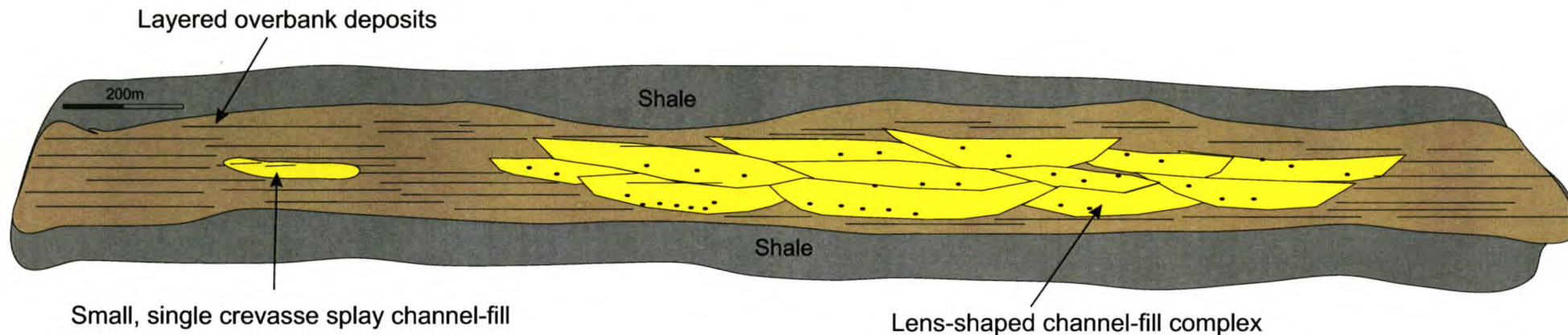


Figure 4.30 Evolution model for ancient channel systems by Clark and Pickering (1996). They propose a three phase development: **A**) Erosional phase, **B**) Depositional phase and **C**) fining-upward and abandonment deposits.

Figure 4.31 Cross-section through the channel-fill complex in KHK. Variable architecture consisting of channel-fills which stack in a lateral and vertical offset arrangement. Erosional bases, and in some places mud drapes, are characteristic in the KHK unit. Associated with channel-fills are the layered overbank deposits with small crevasse channels.



118



Figure 4.32.1 Erosional contact in-between two channel-fills. Rip-up clay clasts are abundant in these contact zones. Located on Hanglip 150.



Figure 4.32.2 Very steep erosional scour forming the base of a channel-fill. Dashed line indicates the steep (47°) angle. Located on Pienaarsfontein 414.

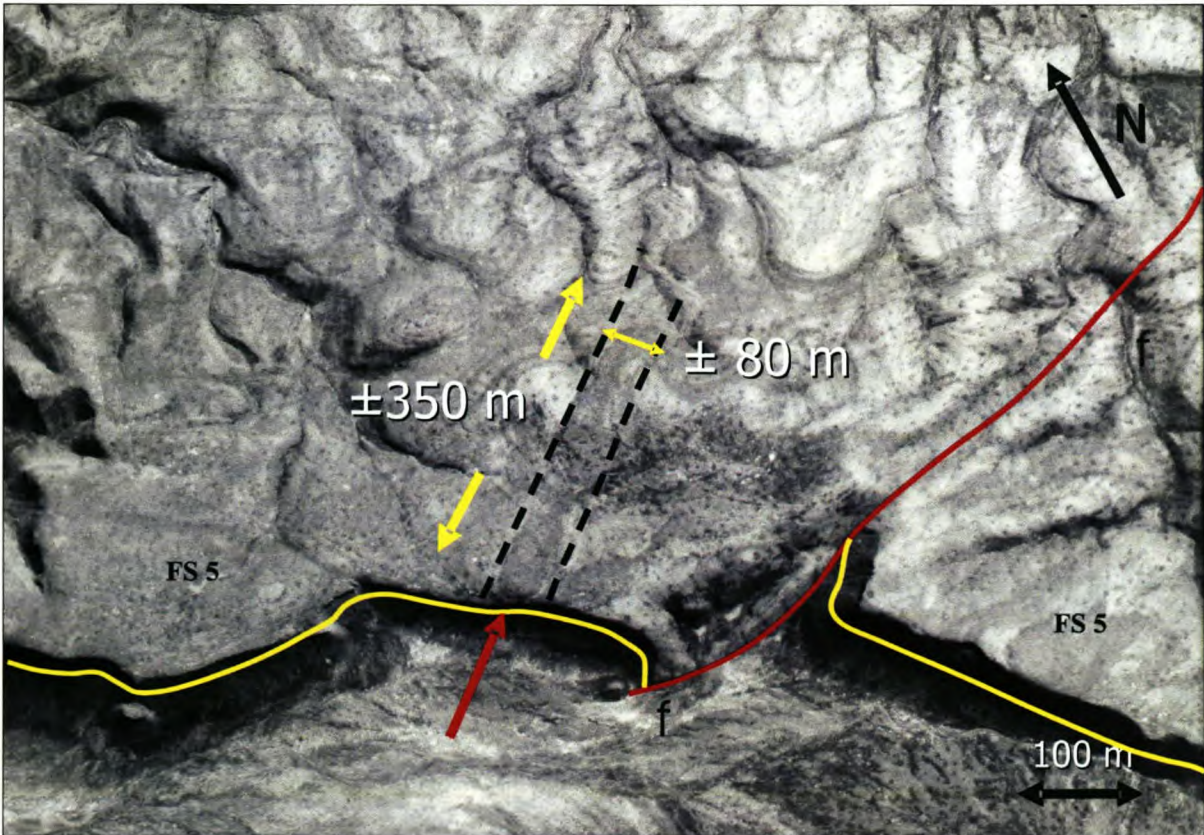
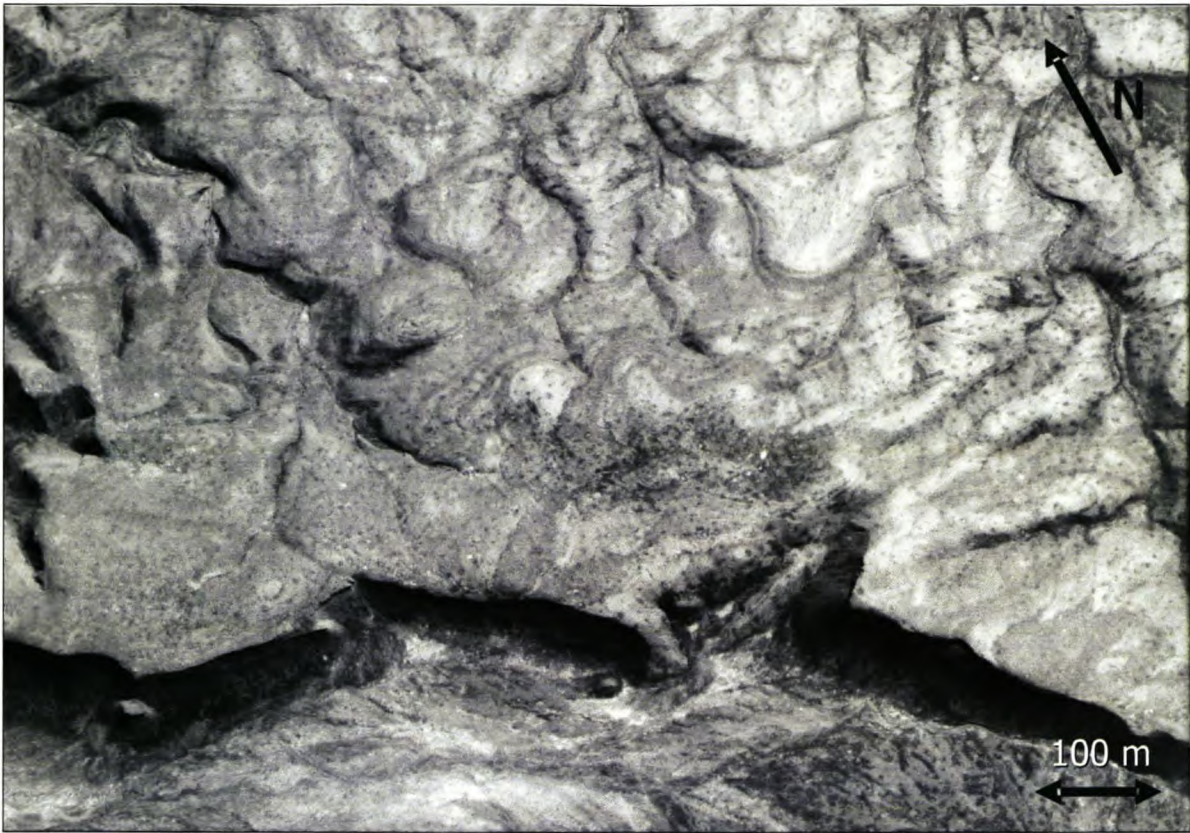


Figure 4.33 Aerial photograph showing erosional remnant of a channel-fill in FS 5 on the farm Pienaarsfontein 414. This channel-fill forms part of the KHK-I channel complex.

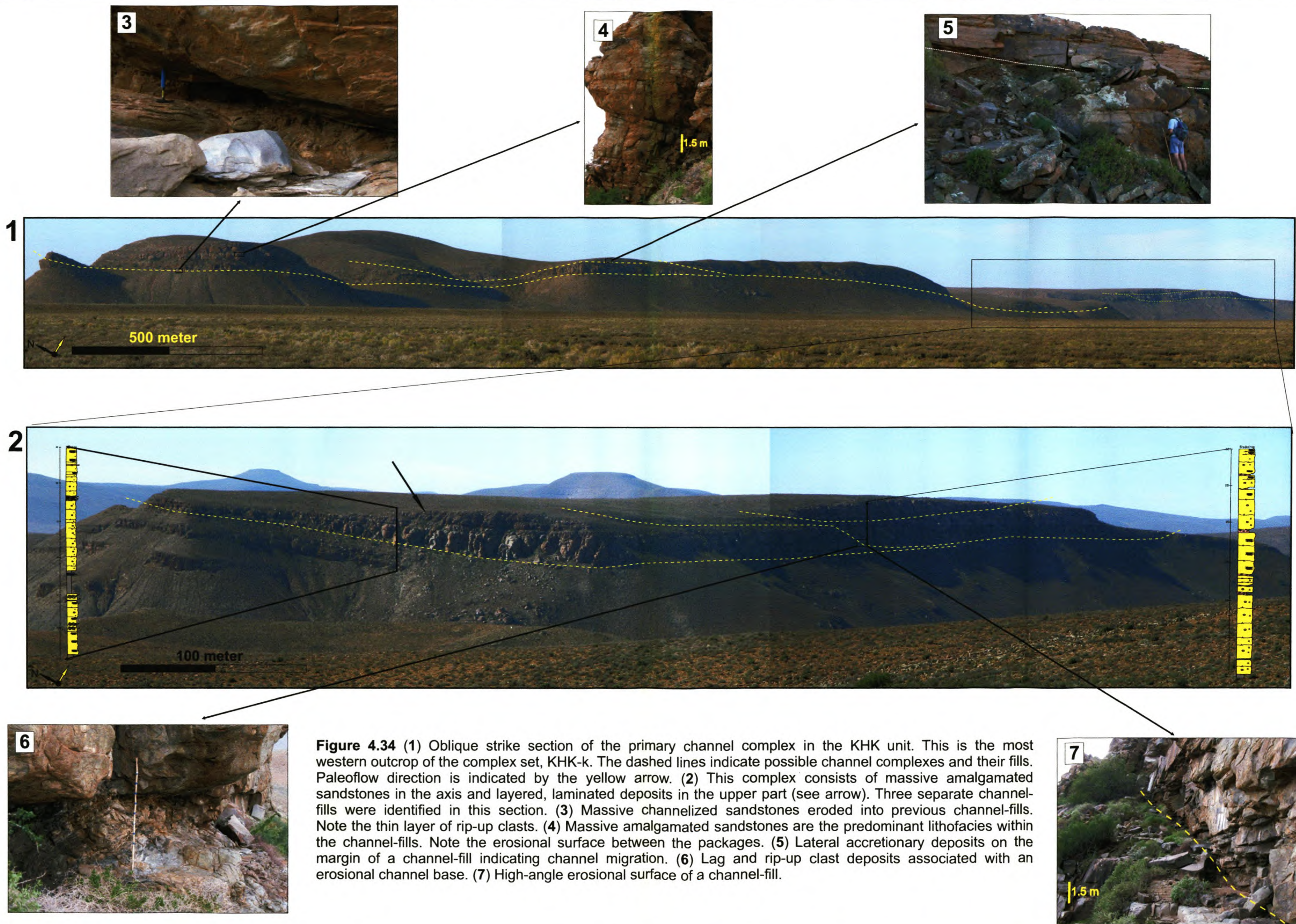


Figure 4.34 (1) Oblique strike section of the primary channel complex in the KHK unit. This is the most western outcrop of the complex set, KHK-k. The dashed lines indicate possible channel complexes and their fills. Paleoflow direction is indicated by the yellow arrow. (2) This complex consists of massive amalgamated sandstones in the axis and layered, laminated deposits in the upper part (see arrow). Three separate channel-fills were identified in this section. (3) Massive channelized sandstones eroded into previous channel-fills. Note the thin layer of rip-up clasts. (4) Massive amalgamated sandstones are the predominant lithofacies within the channel-fills. Note the erosional surface between the packages. (5) Lateral accretionary deposits on the margin of a channel-fill indicating channel migration. (6) Lag and rip-up clast deposits associated with an erosional channel base. (7) High-angle erosional surface of a channel-fill.

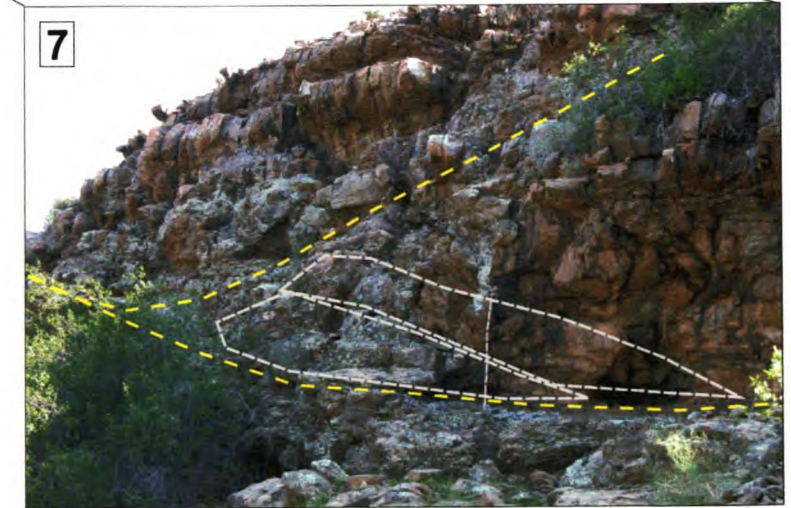
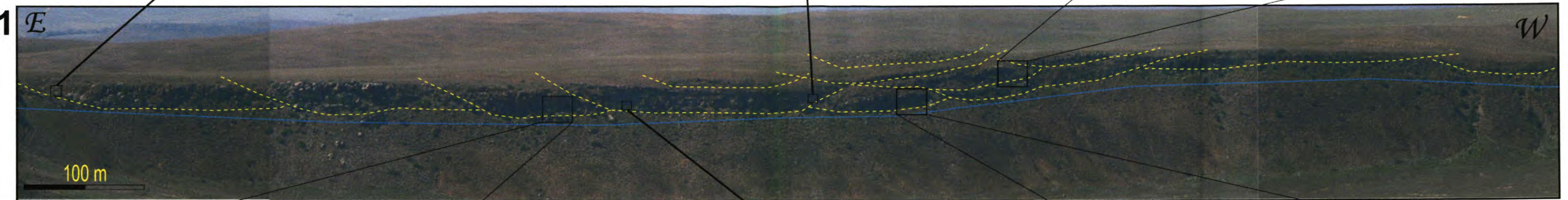
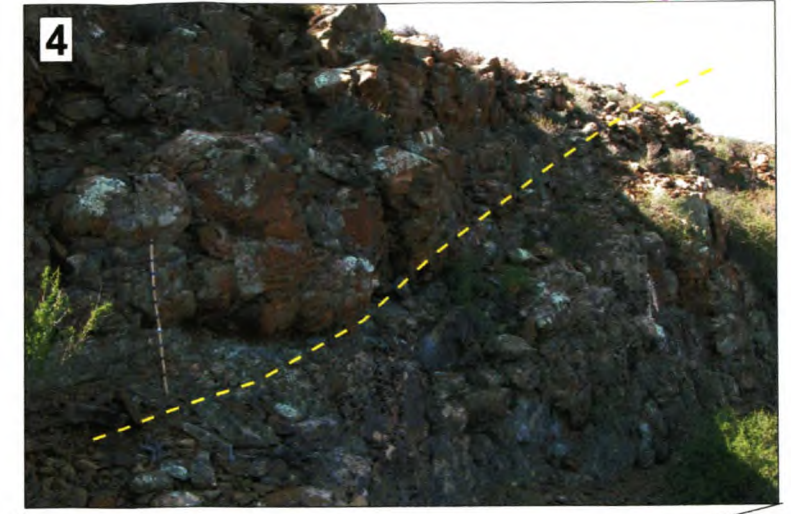
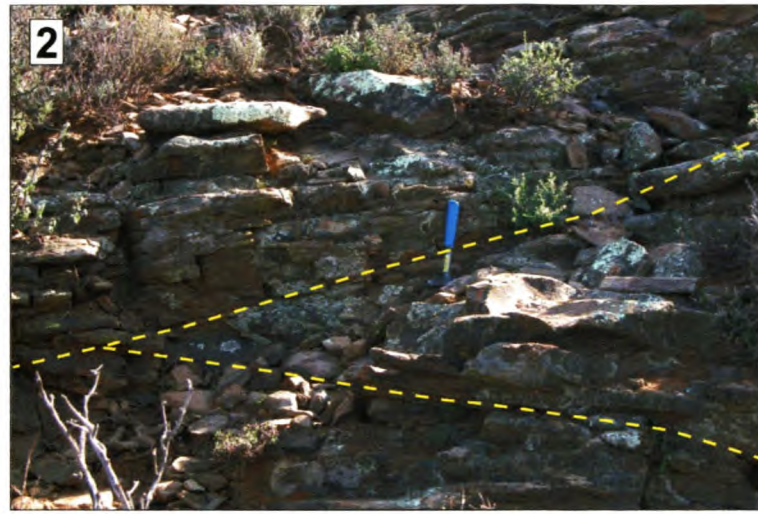


Figure 4.35 (1) KHK-I forms the middle channel complex set of the KHK sand-rich unit where 19 channel-fills were identified. Note the vertical and laterally stacked pattern of these fills. Also note that the central area of this photo section contains numerous channel-fills which eroded into each other. Note the occurrence of LADs in this area. This area represents the axis where the primary conduits were concentrated. Numerous smaller fills occur also in this section. (2) Layered levee deposits of channel margin and inter-channel areas. (3) Erosional surface with abundant rip-up clasts (4) Erosional contact between channel-fills. (5) Massive amalgamated sandstones are the main lithofacies. Note the sharp erosional base and chaotic sediment fill. (6) Large rip-up clay clasts associated with an erosional surface. (7) Lateral accretionary deposits (LADs) resulted from channel migration.

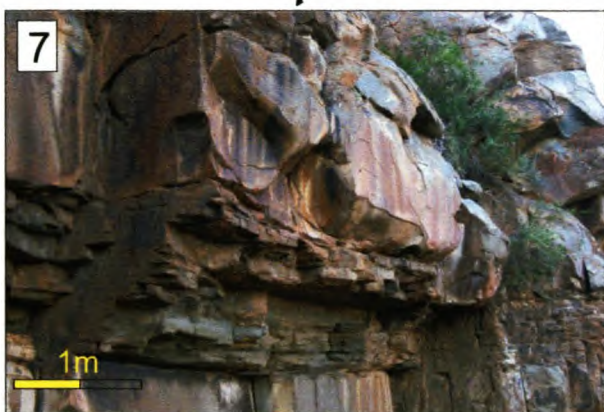
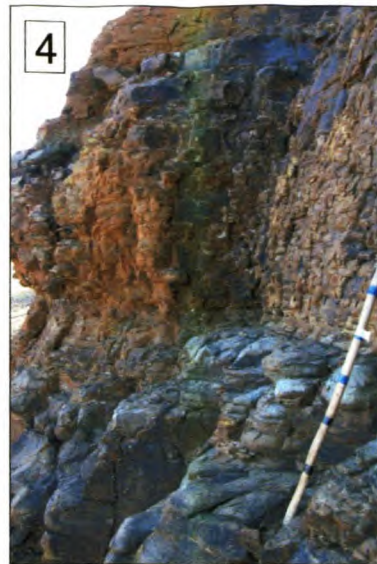


Figure 4.36 (1) KHK-m is the easternmost outcrop of the KHK unit. It comprises two large open channel complexes with numerous channels and in contrast to KHK-k and KHK-l, more layered channel-fill deposits. The paleoflow direction is ENE. These units could correlate with the TB units. (2) Thick, amalgamated layered deposits. (3) Close-up of the channel complex. Note the thick-bedded massive amalgamated sandstones. (4) Massive sandstones overlain by T_b layered beds. (5) Scour-and-fill within the larger complex. (6) Sharp basal contact of the complex. Note the thick succession (25m) of layered beds with amalgamated contacts. Note also the absence of siltstone and shale intra-beds. (7) Massive, amalgamated sandstones with dewatering structures, interbedded with laminated sandstones. (8) Thick package of rip-up clay clasts associated with scour surface.

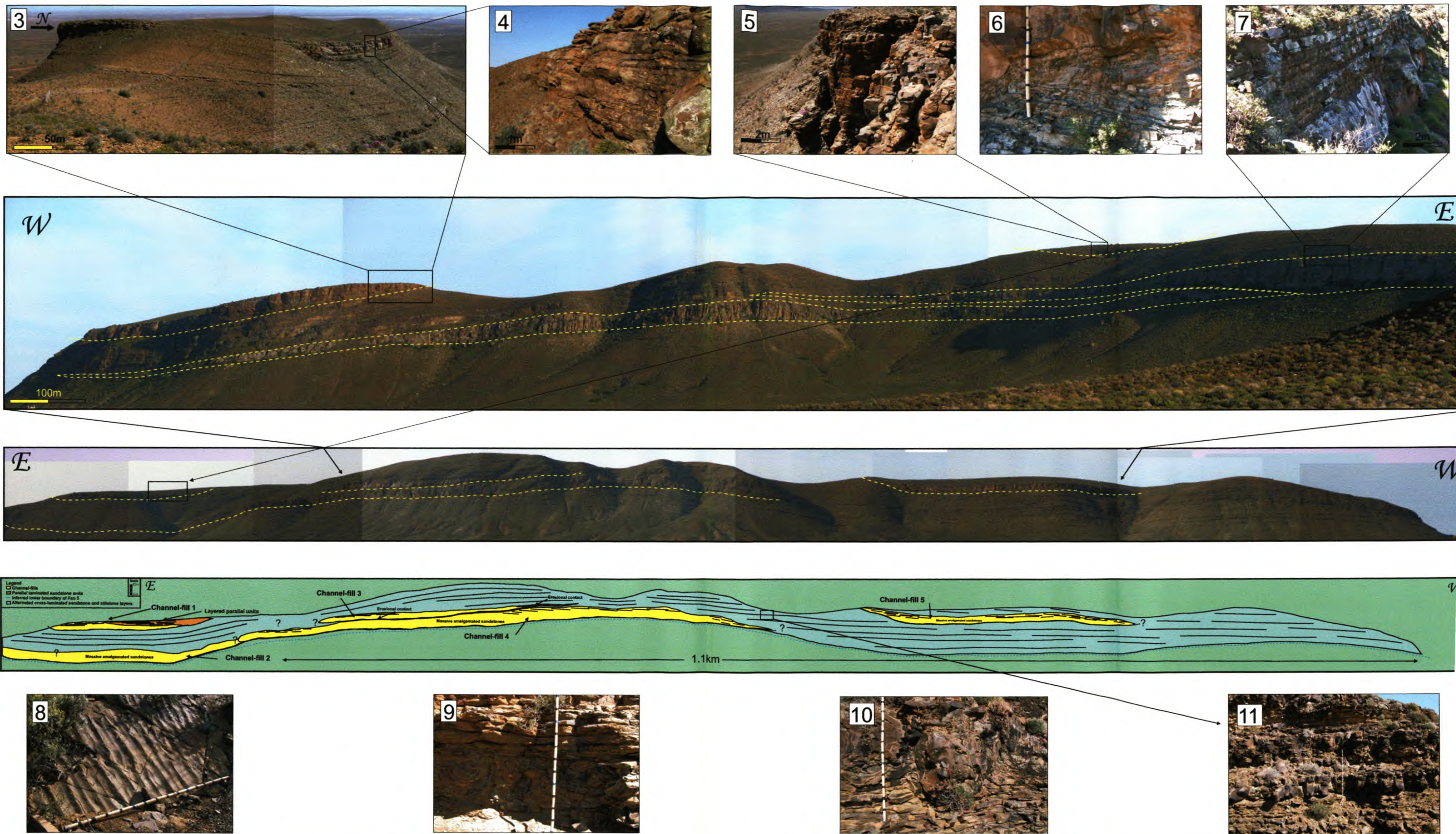


Figure 4.37 (1)+(2) The Tongberg unit reflects four different periods of sediment input. This oblique dip section displays channel-fills associated with thin-bedded overflow deposits. The two photo panels 1 and 2 are back to back; 1 faces south and 2 faces north. Two large channel complexes are indicated by the dashed lines; they form part of the TB-f complex. The upper two channel-fills form the TB-g sub-unit. The main paleoflow direction was to the NE. A thin-bedded 40m thick interval occurs between the TB-f and TB-g channels. It comprises predominantly slump beds with thicknesses of 2-3m. These deformation beds are correlated with the slump channel-fills of GHK. (3)+(4)+(5) The upper TB-g channel-fills comprise layered deposits interbedded with overflow sediments. Plant fragments are abundant. Note the amalgamation of beds. These channels have low depth:width ratio geometries and erosion is minimal. (6) Erosional channel-fill contacts with associated lag and rip-up clast deposits. (7) Massive channelized sands overlain by layered beds, which form the abandonment facies of the channel-fill. (8) Wave ripples in the upper 10 m of the FS 5 succession. (9)+(10) Ball-and-pillow structures associated with the thin-bedded unit between TB-f and TB-g. (11) The thin-bedded package above TB-f consists of thin, ripple cross-laminated sandstone and siltstones. These beds are interbedded with thicker (2m) slump units.

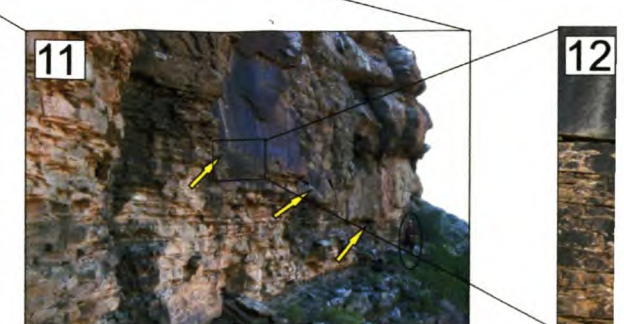
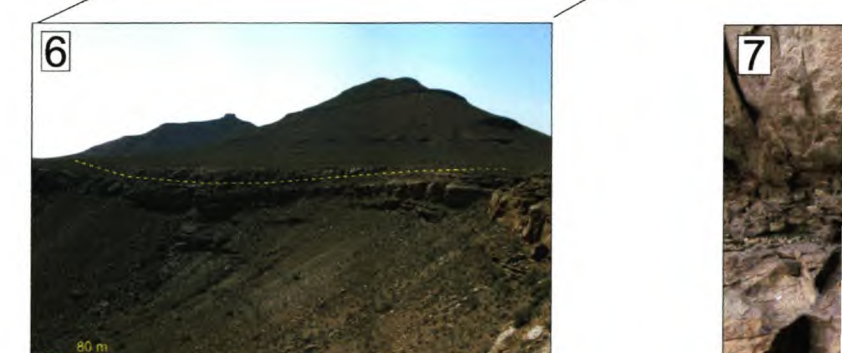
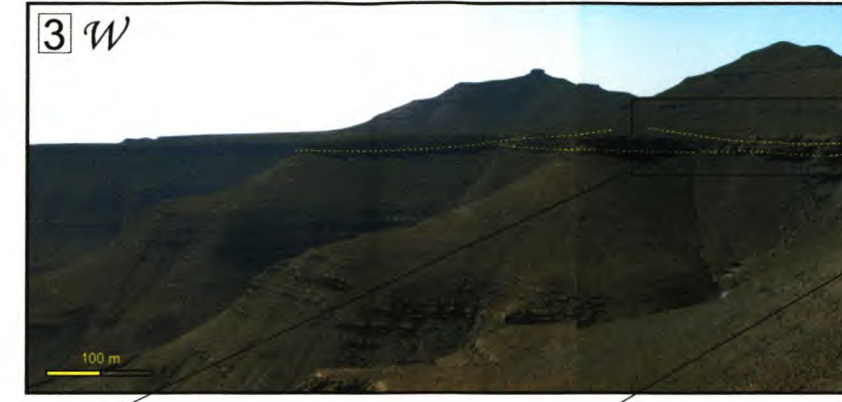
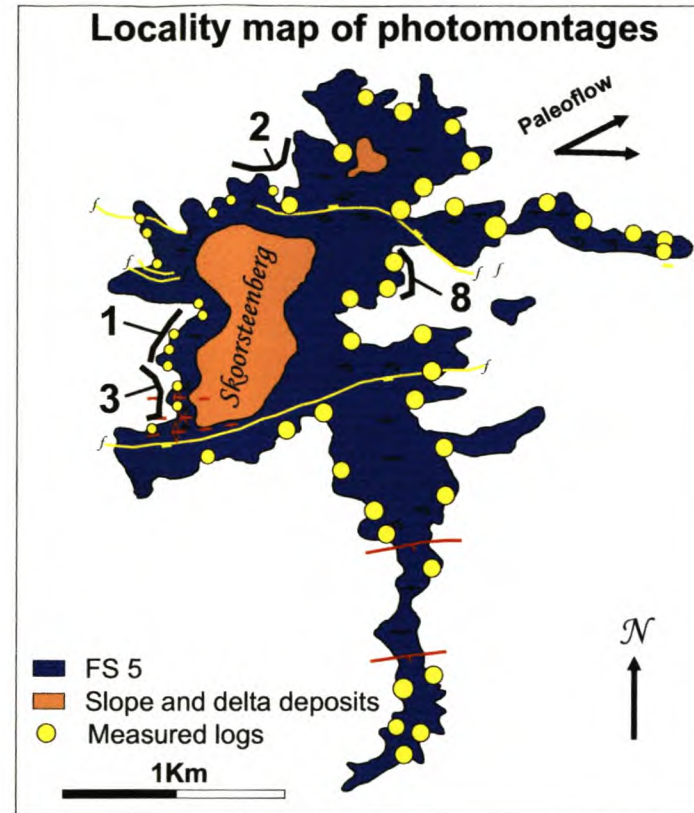
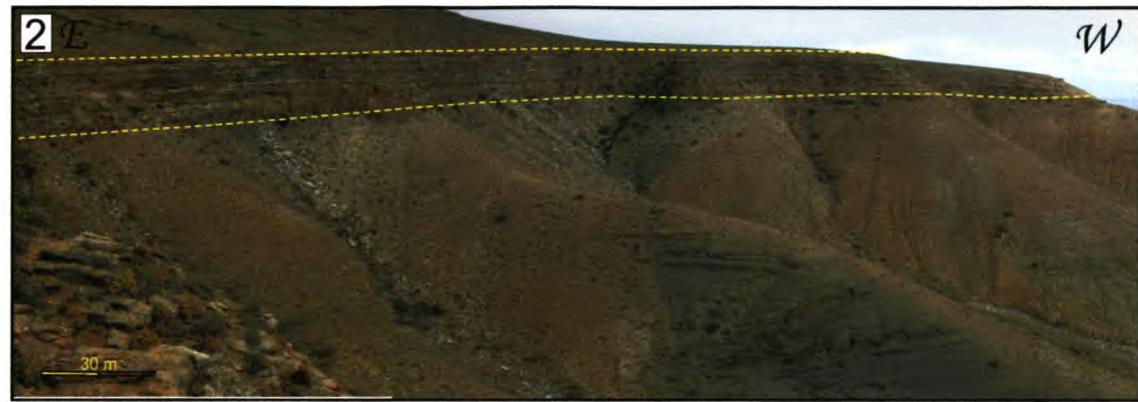
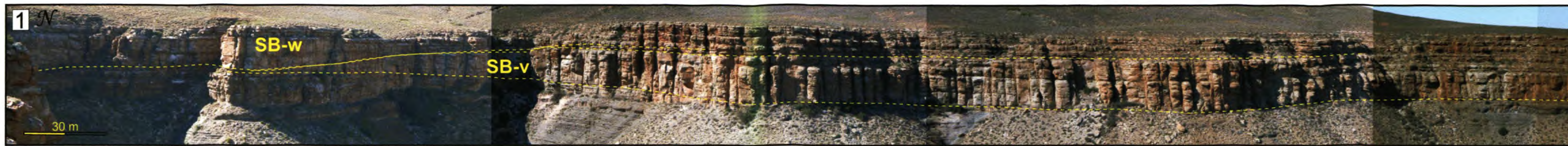


Figure 4.38 (1) The SB unit consists of channel-fills with large-scale amalgamated beds displaying a sheet geometry. This is an oblique strike section of the two (SB-w and SB-v) large channel complexes. Numerous smaller channel-fills occur within these channel complexes. (2) Laterally extensive, amalgamated massive sandstones on the margin of the SB channel complexes. (3) Numerous smaller channel-fills eroded into the lower SB-v channel complex. (4) Symmetrical wave bedding in the upper thin-bedded units of SB. (5) Silty-shale deposits overlying FS 5, indicating a period of low-energy and background sedimentation. (6) Laterally offset-stacked depositional channel-fills in the upper deposits of the SB unit. (7)+(9)+(10) Erosional contacts associated with lag and rip-up clast deposits are abundant in the channelized environment. (8) The lower SB-v complex eroded by a channel-fill. Note the step-down erosional surfaces of these fills in (11) and (12), indicated by arrows. The paleoflow of these channels are to the ENE-NE.



Figure 4.39 (1) The Blauwkop unit comprises several channel-fills that form part of a distributary channel complex. Thick-bedded, amalgamated sandstones are associated with the channels and form part of the inner levee or X-type overflow deposits. Note the channel-fill (A) associated with these beds. (2) Type 1 channel-fill embedded and eroded into layered deposits. (3) Schematic diagram illustrating possible depositional areas for the different types of channels. (4) Massive amalgamated sandstones associated with the channel-fills. (5) The margin of a Type 1 channel-fill. Note the step-down incision and the abrupt truncation of the layered deposits. (6) Inner levee marginal deposits consist of massive, amalgamated bedded sandstone units with loading at the base. (7) Layered deposits form part of the inner levees and comprise ripple cross-laminated sand and siltstones. (8) Thin-bedded units consisting of siltstone and shales. These form part of the outer levee deposits or Z-type overflow deposits and were deposited along the fringes of the channel conduit systems.

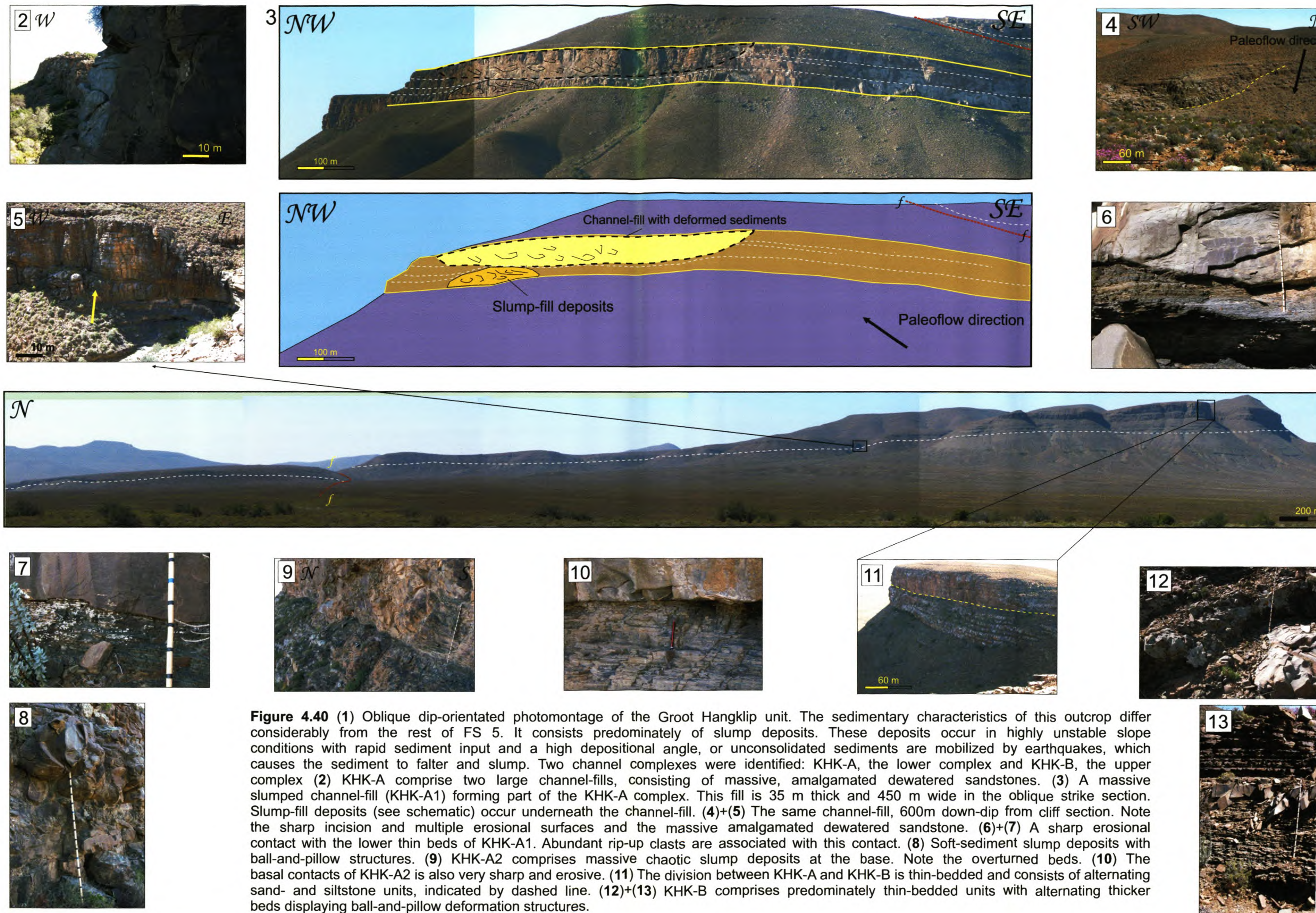


Figure 4.40 (1) Oblique dip-orientated photomontage of the Groot Hangklip unit. The sedimentary characteristics of this outcrop differ considerably from the rest of FS 5. It consists predominately of slump deposits. These deposits occur in highly unstable slope conditions with rapid sediment input and a high depositional angle, or unconsolidated sediments are mobilized by earthquakes, which causes the sediment to falter and slump. Two channel complexes were identified: KHK-A, the lower complex and KHK-B, the upper complex (2) KHK-A comprise two large channel-fills, consisting of massive, amalgamated dewatered sandstones. (3) A massive slumped channel-fill (KHK-A1) forming part of the KHK-A complex. This fill is 35 m thick and 450 m wide in the oblique strike section. Slump-fill deposits (see schematic) occur underneath the channel-fill. (4)+(5) The same channel-fill, 600m down-dip from cliff section. Note the sharp incision and multiple erosional surfaces and the massive amalgamated dewatered sandstone. (6)+(7) A sharp erosional contact with the lower thin beds of KHK-A1. Abundant rip-up clasts are associated with this contact. (8) Soft-sediment slump deposits with ball-and-pillow structures. (9) KHK-A2 comprises massive chaotic slump deposits at the base. Note the overturned beds. (10) The basal contacts of KHK-A2 is also very sharp and erosive. (11) The division between KHK-A and KHK-B is thin-bedded and consists of alternating sand- and siltstone units, indicated by dashed line. (12)+(13) KHK-B comprises predominately thin-bedded units with alternating thicker beds displaying ball-and-pillow deformation structures.

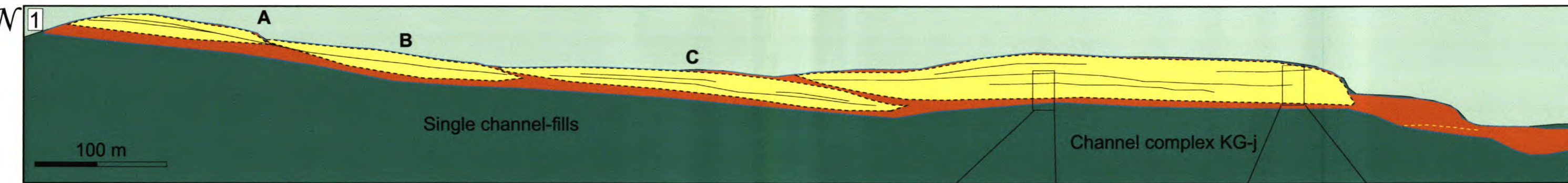
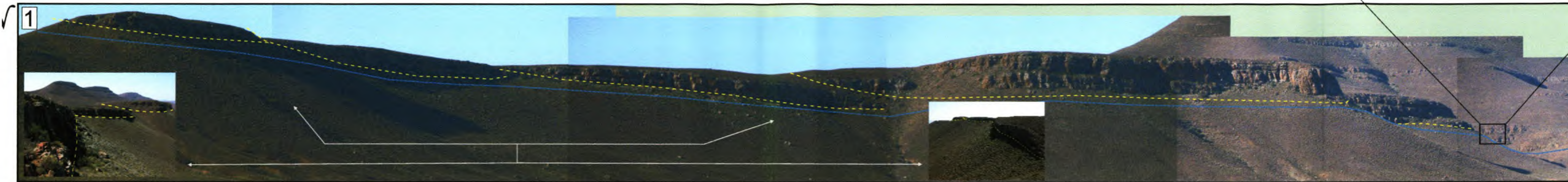


Figure 4.41 (1) Kalkgat complex, the most southern unit of FS 5 before it pinches out. Two large channel complexes, KG-h and KG-j, were identified. They contain numerous scour-and-fill channels comprising predominately masses of dewatered and chaotic slump deposits. Three channel-fills in the KG-j complex are indicated on the photomontage and line drawing. Main paleoflow direction is to the NE. (2) Underlying the channel-fills is a 15m package of thin-bedded ripple-laminated deposits. (3) Erosional incisions are common in the basal parts of the smaller channel-fills, indicating a high-energy environment. (4) Multiple erosional surfaces in the KG-h complex. Note the abrupt incisions of the smaller channel-fills in this complex. (5)+(6) KG-h comprises predominately massive, dewatered, amalgamated sandstones and numerous smaller scour-and-fill channels. (7) KG-j forms an outcrop of 45 m thick with dewatered and slumped amalgamated massive sandstones. The upper part of the channel complex consists of more layered deposits which show ripple cross-lamination. (8) Rip-up clay clasts as lag deposits associated with erosional incisions. (9)+(10) The dominant lithofacies in these channels are slumps. Note the sharp contact with the underlying units.



4.7.2 Lateral accretion deposits (LADs)

Description:

The only known occurrence of LADs is on the farms Hanglip 150, Pienaars Fontein 400 and Rondavel 34 near Skoorsteenberg. LADs are present in the KHK and SB units and are located along the margins of some of the channel-fills in the channel complex (Fig. E). LADs are composed of non-amalgamated, shingled, inclined, lenticular sand bodies associated with shale rip-up clasts (Fig. 4.42.1). The net-to-gross (percentage sand to shale) in the packages concerned is between 50 – 75 %. The inclined beds dip up to 18° and are orientated more or less perpendicular to the palaeoflow (Fig. 4.42.1). The KHK channel complex containing the LADs is approximately 500 – 650 m wide and up to 45 m thick (Fig. E1 + Fig. 4.34). Individual sand bodies have a flattened lens shape that tapers both in a down-dip and up-dip direction (Fig. 4.42.1). The underlying surfaces of some of these lens-shaped sand bodies show very peculiar flute marks and micro faulting (Van der Merwe, 2003) (Fig. 4.42.2). These marks might be good palaeo-migration indicators for the channels. The LADs were exposed to a period of erosion prior to deposition of successive channel sands (Fig. 4.42.3). The Skoorsteenberg LADs are associated with slump structures, which were caused by unstable channel margins (Figs 4.42.4+5).

Interpretation:

Lateral accretion represents a gradual and/or constant lateral shift in the position of a channel (Abreu *et al.*, 2003). LADs tend to occur in the upper part of channel complex sets in confined channel systems, reflecting an increase in sinuosity and thickness of single channel-fills through the evolution of a channel complex set. This may be due to changes in gradient and sediment supply as the system evolves. Elliott (2000) ascribed the lateral accretion units in channels of the Ross Formation (Ireland) to periods of lowered sea level, when sedimentation rate was so high that sediment could have been derived from quasi-continuous hyperpycnal currents from the delta mouth. According to Elliott (2000), the lateral accretion deposits seen in many of the submarine-channel outcrops in the Ross Formation, could be explained by a steady sediment supply process rather than by an ignitive (rapid deposition) event process. The depositional model of Abreu *et al.* (2003) suggests that the accretion surfaces would form by relatively continuous and gradual lateral sweep of channel bends by systematic erosion of the outer banks and deposition along

inner banks. This is similar to the classic fluvial point-bar model of Galloway and Hobday (1983).

The KHK and SB channels do not reveal any form of meandering. Most of the channel flow patterns in KHK, SB, and in the rest of FS 5, are straight lines, although small bends in channel flow pattern were noted in places (Fig. E).



Figure 4.42.2 Peculiar flute marks at the base of some LAD units. This is a good indication of the direction of channel migration.



Figure.4.42.1 Lateral accretion deposits underlying the KHK channel-fills. Note the lensoid geometry of these units. Underlying this is the presumed channel margin with slump deposits which originate during marginal bank-collapse. An erosive channel-fill with a paleoflow direction to the NE overlies the LADs.



Figure 4.42.3 The upper channel-fill forms a sharp angular unconformity on the lower LADs. Note hammer for scale.



Figure 4.42.4 Plan-view of the stacked lateral accretions in the SB unit. The environment in which these deposits form is highly unstable and slumping along the margins occurs frequently.

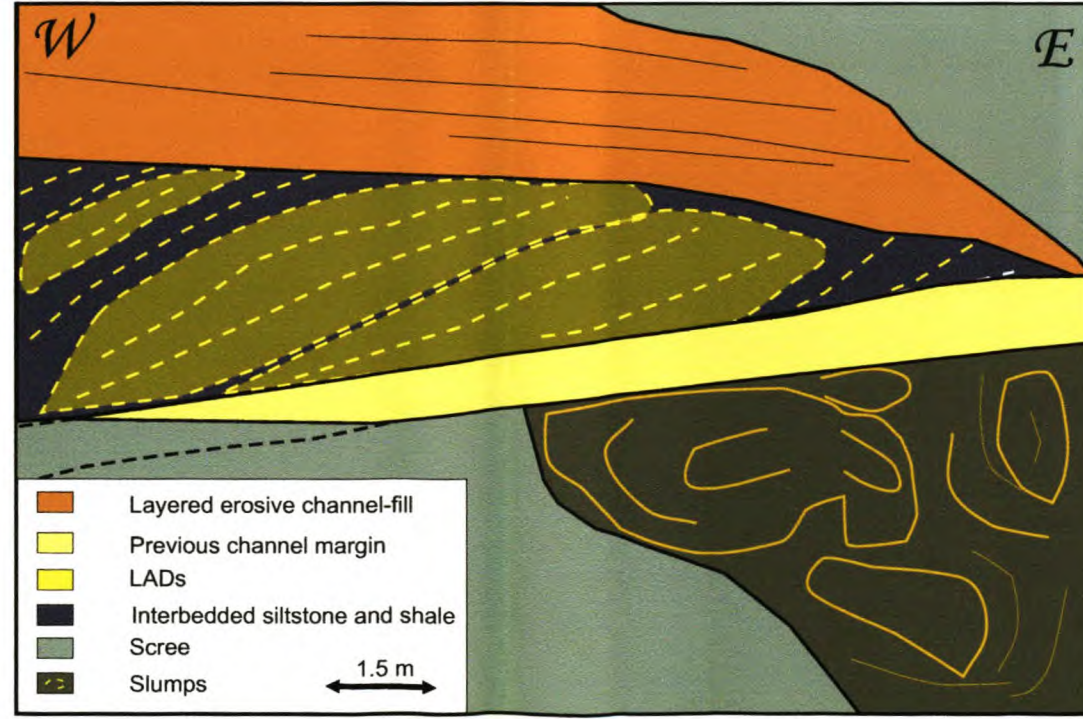


Figure 4.42.5 Channel-fill deposited on LADs and slump deposits. The latter likely being caused by bank collapse. It is very sensitive that these deposits are preserved because most of it is taken by successive flows.

4.7.3 Overflow deposits (overbanks)

Description:

The term ‘overbank’ defines the area of active deposition adjacent to and beyond the channel banks or channel margins (Boggs, 2001). Thus, as the main body of the turbidity current flows through the channel, the less dense fraction can spill over the channel margins into the overbank area. Because it is difficult to identify channel banks or build-up levees, the term “overflow deposits” is suggested for FS 5. These deposits are dominated by packages of ripple-laminated sandstone and siltstone layers, interbedded with finer-grained deposits (typical Lf 2, 4 and 5) (Table 2). These packages are commonly stacked and often attain thicknesses of 20 – 30 m. Three types of overflow deposits have been observed in the outcrops of FS 5 (Fig. 4.43.7):

- X-type, comprising predominantly stacked, discrete beds of 20-100 cm in thickness, dominated by ripple cross-, climbing ripple- and sigmoidal lamination (Figs 4.43.1+2). These units are interbedded with thin beds of parallel-laminated siltstones.
- Y-type deposits consist of an alternations of thinner sandstone (10 - 20 cm) and siltstone beds. The sandstone units are mostly ripple cross-laminated and the siltstone units also indicate ripple laminations (Figs 4.43.3+4). Thin, less than 5 cm thick shale beds, are also interbedded with these deposits. Palaeoflow directions in this facies can vary considerably (up to 20°) from the main channel flow directions.
- Z-type deposits are very fine and consist of thin, parallel-laminated sandy/silty units, less than 10 cm in thickness (Figs 4.43.5+6). The siltstone and shale units form a major part (60%) of these deposits.

Some of the best outcrops of the Y-type overflows occur on the western side of Pienaars Fontein se Berg, logs Hp 25 and M7 (Fig. 4.44.1). Medium-bedded ripple cross-laminated sandstone, interbedded with thin rippled units of siltstone, are the main characteristics of these outcrops. A few small crevasse splay channels occur in the overflow deposits on Bizansgat 85 with palaeoflow direction to the northeast. Similar channel-fills occur in the upper section of the TB unit, where smaller crevasse splay channels are located in the overflow outcrops (Fig. 4.6.2).

The continuity of these deposits is often interrupted by the presence of crevasse splay channel-fill deposits (Fig. E). The Y and Z-type deposits are most continuous whereas the X-type deposits are less continuous and correlate more easily with the main channel-fill or levee deposits.

Interpretation:

The proportion of overflow facies in FS 5 varies between the different types of overflow deposits. However, about 65% of the outcrop is estimated to consist of overflow deposits. X-type deposits occur close to the major channelized units, i.e. in the more proximal depositional areas of the fan (Fig. 4.43.7). These deposits could genetically be connected directly to the levee deposits, if any levees were constructed. The X-type deposits are located close to the channel margins of TB, KHK, and SK units in FS 5 (Figs E1+E2). One of the characteristics for this type of overflow deposits is the sigmoidal lamination (Figs 4.43.1+2). The Y-type deposits occur in association with the X-type deposits but are further away from the main channel axis (Fig. 4.43.7). The palaeoflow directions of the Y-type deposits are also much more variable than the X-type deposits; the latter flowing more or less in the same direction as the channel. The X- and Y-type deposits indicate trends of upward-thickening and thinning patterns (Fig. 4.44.1). The thickening-upward overflow deposits would represent an increase in channel activity, whereas a thinning-upward trend would indicate a decrease in channel activity.

The Z-type overflow deposits predominate in the northern outcrops below the Skoorsteenberg and Blauwkoop units (Fig. E). These very finely laminated alternations of sandstone, siltstone and shale are the distal low-energy equivalent of turbidite currents, which have bypassed the main channel axial systems. In the Skoorsteenberg area, these deposits attain a thickness of almost 45m below the channel-fill sandstones (Fig. 4.44.2). This unit eventually thins out towards the most eastern outcrops where FS 5 pinches out. These deposits could also be interpreted to represent flow stripping of turbidity currents - as the sand-rich portion of the flow continuous along the channel, the finer-grained portion separates from the main flow and overflows the channel margins.

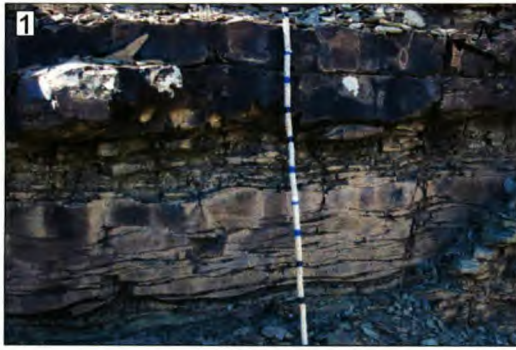


Figure 4.43.1+2 X-type deposits comprise stacked, discrete beds of 40-50 cm, dominated by ripple cross-, climbing and sigmoidal laminations.

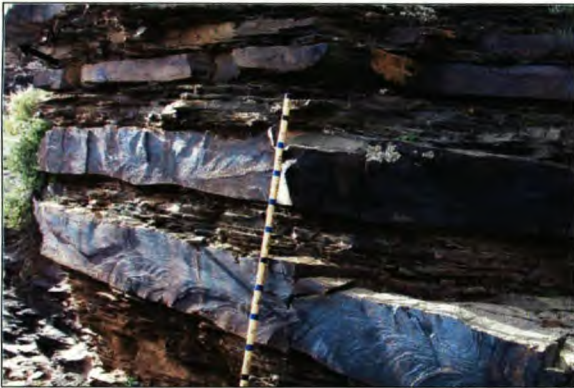


Figure 4.43.3 Y-type deposits occur in the middle depositional environment from the main sediment conduits. These units consist predominantly of 10-15 cm thick ripple cross-laminated sandstone beds.

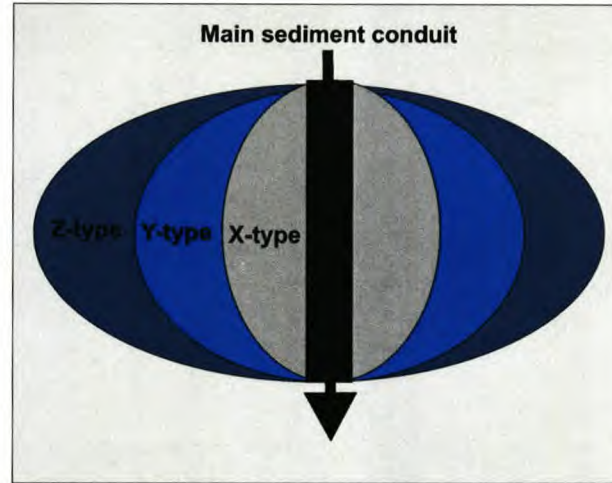


Figure 4.43.7 Areal distribution of three types of overflow deposits away from the main sediment conduit.

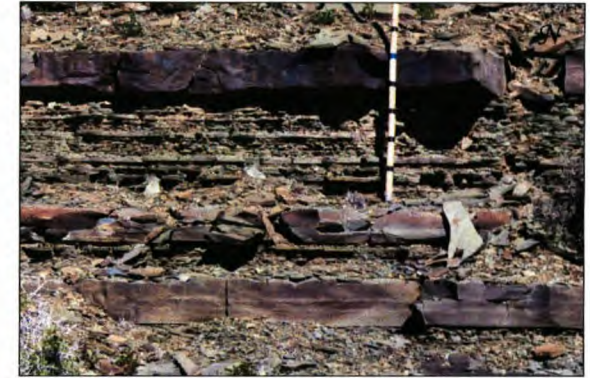


Figure 4.43.4 Thin siltstone layers interbedded with Y-type deposits. Climbing ripple lamination predominates in the sand-rich units.

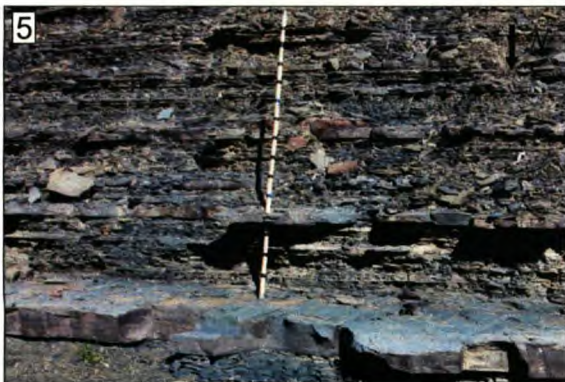


Figure 4.43.5+6 Z-type deposits are very finely laminated units with beds never exceeding 5 cm in thickness. Siltstone and shale intervals are abundant. This type of overflow occurs in the most distal depositional environment of a turbidite flow, i.e. a very low-energy environment with minor traction currents to rework the sediments.



M7

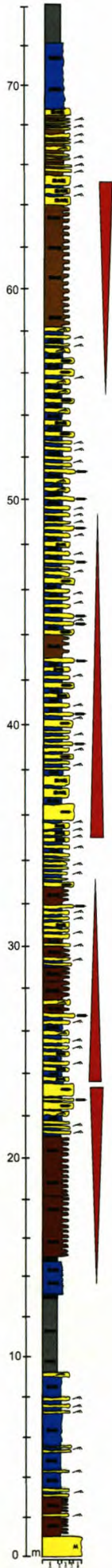


Figure 4.44.1 Vertical section M7 logged on the farm Krantzkraal. It also forms part of the Krantzkraal and KHK correlation sections. Four upward thickening/thinning cycles could be identified, which indicate different flow conditions within the main channel conduits. M7 comprises predominantly Y-type deposits. The paleoflow directions determined in these deposits varies considerably because of the 30° deviation from the main conduit directions.

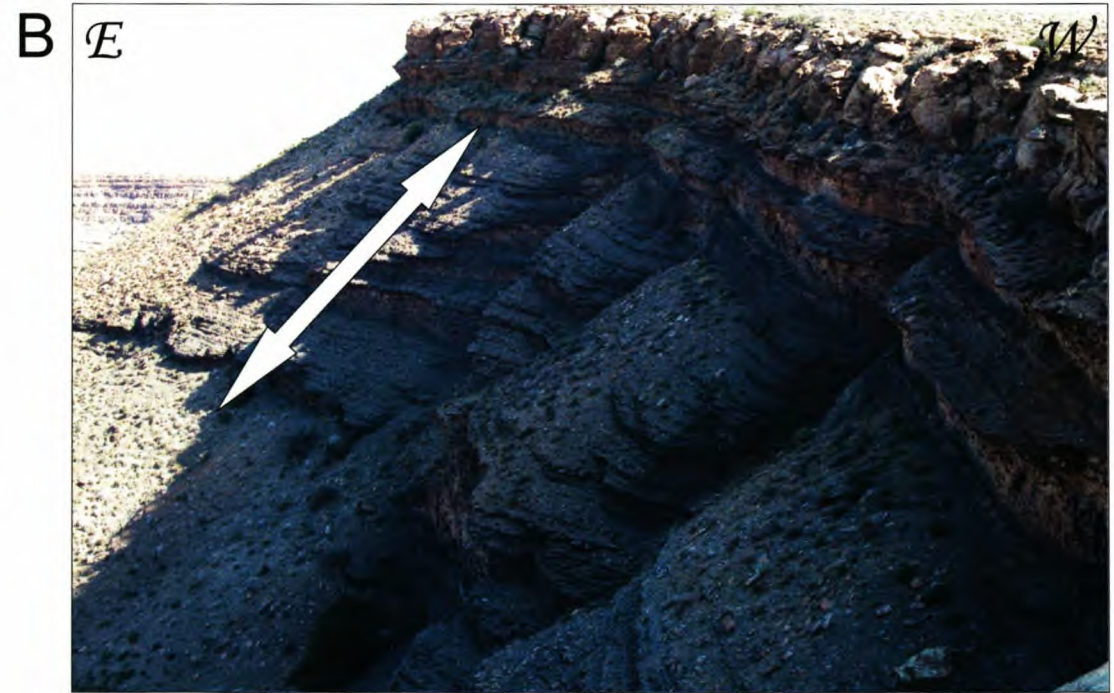


Figure 4.44.2 A+B This 45 m thick, thin-bedded succession forms part of the SB unit. It comprises predominantly Z-type overflow deposits. These deposits record the density and the amount of depositional flows through a conduit in a nearby locality. Laminated siltstone is the predominant facies type. Note the SB unit's massive amalgamated sandstones deposited onto the thin, underlying overflows.

4.7.4 Levee deposits

Description:

Mutti and Normark (1987) first introduced the term levee for the explanation of the sediments, which are deposited on the channel margins of submarine sediments. Levee deposits in their typical architectural form were not very well preserved in the FS 5 channel complex environments. The interpretation of the existence of true levee deposits and true overflow deposits varies in FS 5. Kirschner and Bouma (2000) interpreted part of the overflow area that borders the channel proper in the Blauwkoop unit as levee deposits, even though no positive relief of levee crests could be observed in the field. Levee deposits stem from spilling of sediment from the body and wake of turbidity currents into the interchannel area as they pass through the channel (Fig. 4.45.1). They consist of a laterally continuous sequence of interbedded sandstones and siltstones with lithofacies 4 and 5 predominant (Table 2). Away from the channel, a decrease in the sandstone bed-thickness, percentage of amalgamation, number of sandstone beds, angle of climbing ripple contacts, grain size of the sandstones, and net:gross sand ratio was observed, which was interpreted to reflect the decrease in the strength of overflows. Kirschner and Bouma (2000) also regard the true overflow deposits as the lateral continuation of levee deposits, that indicate a decrease in energy and density of the turbidity flows away from the channel. These form a series of thinly interbedded fine-grained siltstone, which exhibits extreme lateral continuity over hundreds of metres.

Interpretation:

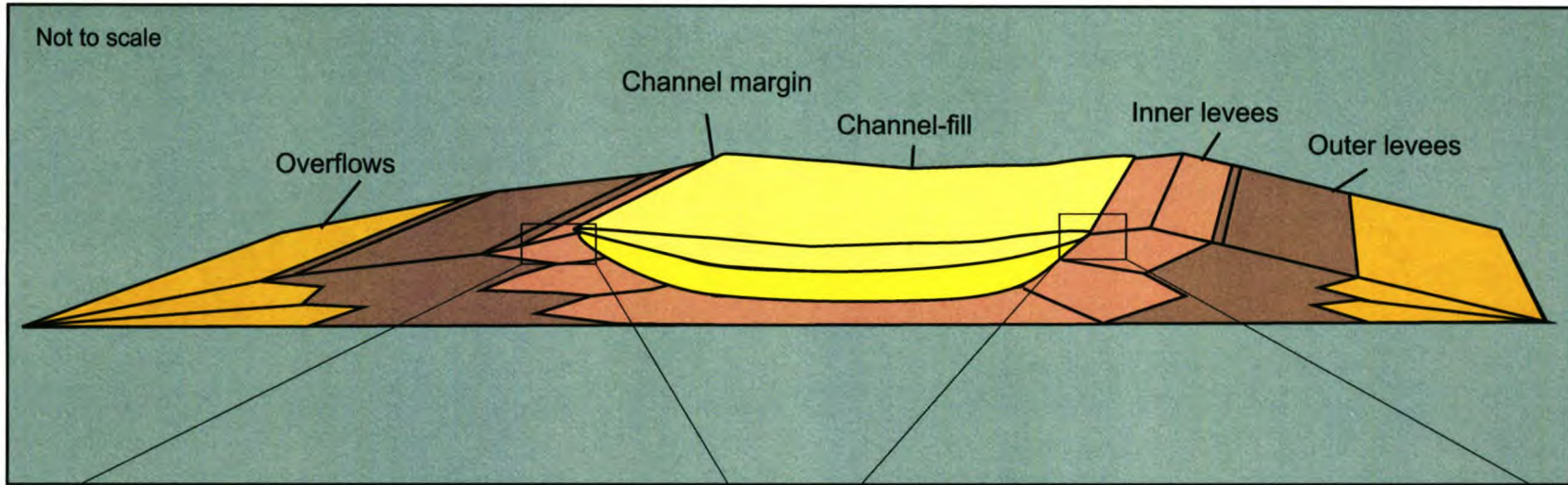
Channel levees are formed from the overspill of channelized turbidity currents. Seen in plan view in modern deep-marine depositional environments, channel levee architecture can generally be characterized by irregular or mounded geometry (Fig. 4.45.1). Ancient levee deposits possess a high potential for subsequent sediment modification, e.g. differential compaction, faulting, inter- and intrastratal slip, and are difficult to distinguish from other basin slope deposits. Because it is virtually impossible to preserve and recognize the positive relief morphology of levees in ancient channel complexes, ancient levee deposits are grouped into the more general facies-association term “overbank” deposits, as described by Mutti and Normark (1987) (overflows in this thesis). Levee architectural elements may exist within overbank deposits, but it is generally difficult to apply the architectural element scheme to such sequences. The description of typical levee

deposits refers to large-scale bundling of beds, wedging out over hundreds of metres to a few kilometres, as seen on the high-resolution seismic sections of the Mississippi channel levee deposits (Weimer, 1990).

Deptuck *et al.* (2003) divided overflow units into an outer levee element and an inner levee element. The outer levee deposits consist predominantly of fine-grained sediments, which were deposited furthest from the main channels (Fig. 4.45.1). The inner levee deposits occur directly adjacent to within the channel-fill environments and consist mainly of vertically stacked thick sandstone beds with ripple-cross lamination. The inner levees are subject to bank collapse and erosion by successive parent flows in the channels (Figs 4.45.2+3).

The X-type overflow deposits, which are deposited very close to the channel margins, could be interpreted as inner levee deposits, following the scheme of Deptuck *et al.* (2003). The Y- and Z – type overflow deposits will then occur in the outer levee environments. In this thesis, the terms for overflow and the three types of overflow deposits are perhaps now acceptable because the exact boundary between true levees and true overflow deposits is very unclear. Thus, the occurrence and locations of these outcrops are concentrated close to the channel complex environments of TB, KHK, BK and Skoorsteenbergr. Bank collapse as slumps is present in the SB unit (Figs 4.45.2+3).

Figure 4.45.1 A idealize schematic diagram of levee deposits that occur along the margins of the erosive channel-fills. They are deposited during the periods of active sediment bypass within the channel. Inner levees are deposited very close to the margin and comprise thick, ripple cross-laminated units amalgamated with previously deposited beds. Outer levees are deposited further away from the margin and consist of thick-bedded units, alternating with thinner beds. A levee system is characterized by a mounded geometry, but these mounds are very seldom preserved in ancient systems.



137

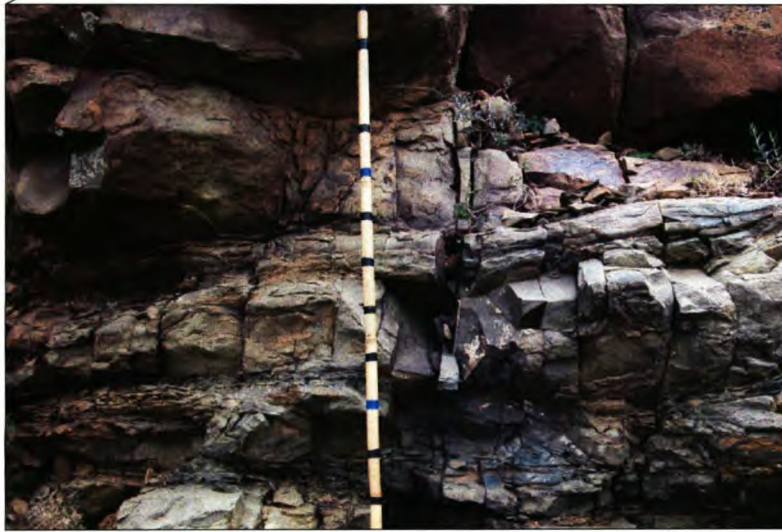


Figure 4.45.2 Inner levee deposits along the margin of a channel-fill. Note the amalgamated surfaces. Skoorsteenberg locality.



Figure 4.45.3 Marginal collapse of the inner levees during successive erosional flows within the channel. Occurs within the SB unit.

4.7.5 Frontal splays (sheet sands)

Description:

A general description of “sheet sand” or “spreading sand” deposits is provided in Section 3. Almost 40% of the FS 5 outcrops consist of this architectural element with Lf 1, 5 and 10 as the main lithofacies (Table 2). The sheet sands are parallel-sided, laterally extensive and exhibit coarsening/thickening upward or fining/thinning upward trends. Sheet sandstones are commonly stacked, but separated by finer-grained intervals (Fig. 4.46.1). The latter are typically traceable over distances up to a few kilometres. Large sheet sand deposits occur in the Blauwkop and Skoorsteenbergrug units on the farms Zoetmeisjes Fontein 75, Hoogevlakte 33, Theronshoek, Brandhoek 119 and Blaauwheuwel 121 (Figs E+E3+E4). The sheet sand deposits could be divided into three types (Fig. 4.47.4):

- The O-type deposits occur close to the mid-fan distributary channels. The beds are thick (1-2m), massive, sandstones with a strong erosive nature and abundance of rip-up clasts and dewatering structures (Figs 4.46.2+3).
- The P-type deposits are medium to thick-bedded (20-100 cm), fine-grained sandstone beds that commonly exhibit sole structures (Figs 4.47.1+2). These beds are amalgamated into fine, upward-siltier deposits. The sandier portion of these deposits typically displays T_{abc} divisions. Small rip-up clay clasts were also observed.
- The Q-type deposits consist of thinner-bedded sandstones (5-15 cm) with rare sole structures, but well-developed intrastratal sedimentary structures (T_b , T_c and T_d) throughout the beds. Beds are separated from each other by thin siltstone/mudstone intervals (Fig. 4.47.3). Lf 5 is the main lithofacies in the Q-type sheet deposits. Sheet sandstone packages reach a maximum thickness of 30 m.

Interpretation:

The term “frontal splay”, as defined and discussed by Posamentier and Kolla (2003) and Posamentier (2003), refers to channel termination lobe and sheet sand deposits. The frontal splays are similar to crevasse splays with one significant distinction; frontal splays form at the termini of channels, whereas crevasse splays form in close proximity to breaches in a levee. Sedimentary structures such as climbing ripples, which are commonly associated with rapid

sedimentation from suspension, would characterize deposits from rapid flow expansion, and therefore may be more common to crevasse splays than frontal splays.

As turbidity currents become unconfined at the channel mouth, they spread laterally across the basin floor (Fig. 4.29). The velocity decrease causes deposition of the coarser components of the flow close to the channel mouth, while the finer materials are carried further away across the fan (Saito and Ito, 2002). The sheet deposits that make up the fan could therefore be defined as inner lobe and outer lobe facies. The inner lobe facies consists of deposits described under the O-type, whereas the middle lobe facies comprises the P-type and the outer lobes consist of the Q-type deposits (Fig. 4.47.4).

The sheet sand deposits from the BK and SB sand-rich units were deposited directly from the frontal splays of the mid-fan environment. This is evident in the fluctuations of channels and reduction in flow energy. The architectural facies maps of the BK and SB units indicate the evolution (from O-type to pinch out) of these sheet sands and lobes from the distributary channel mouths (Figs E3 + E4). The main difference between sheet sands or frontal splays and overflow deposits lies in their depositional patterns vis-à-vis those from the main channel complexes and their internal structures. Overflow deposits are associated with the marginal environments of the FS 5 units, whereas the sheet sands are associated with the terminations of these units. Sheet sands are mostly uniform and massive with rip-up clay clasts, whereas ripple cross-lamination is the most common internal sedimentary structure in overflow deposits.



Figure 4.46.1 A package of laterally extensive sheet sandstones in the BK unit on Zoetmeisjes Fontein 75. Note the vertically stacked pattern with finer-grained intervals. This is the typical O-type sheet deposits near the channel-lobe transition zone.



Figure 4.46.2 The O-type deposits are characterized by high-energy sand flows. These high-velocity flows cause erosion and deposition rip-up clay clasts.



Figure 4.46.3 Dewatering dish/pillar structures are common features in the sheet sand deposits, especially in rapidly deposited massive sandstones. Note the unique dish structures in this photo. Scale is 10 cm for upper section of staff. Located at Blaauwheuwel 121.



Figure 4.47.1 P-type sheet deposits are medium- to thick-bedded with sole structures. These beds occur in the middle zone of sheet deposition. Located at Blaauwheuwel 121.

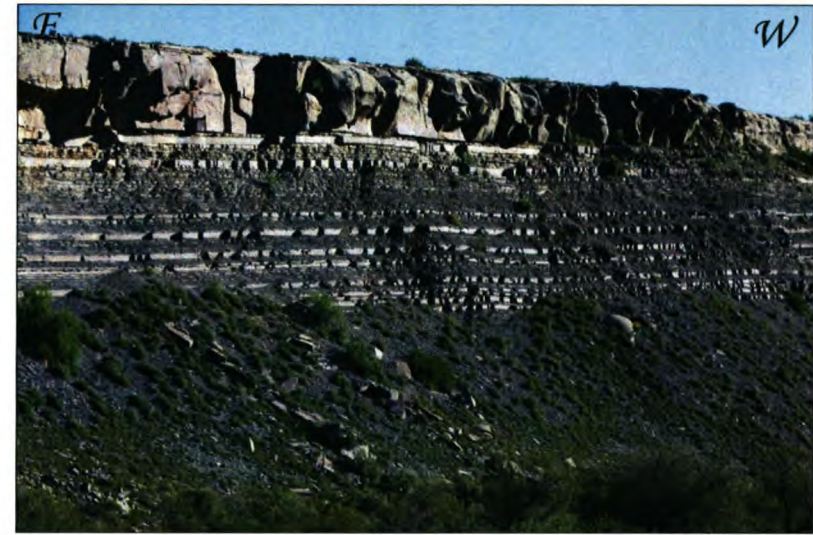


Figure 4.47.2 P-type sheet deposits of the SB unit at Blaauwheuwel. Note the upward thickening pattern in the upper part of the succession.

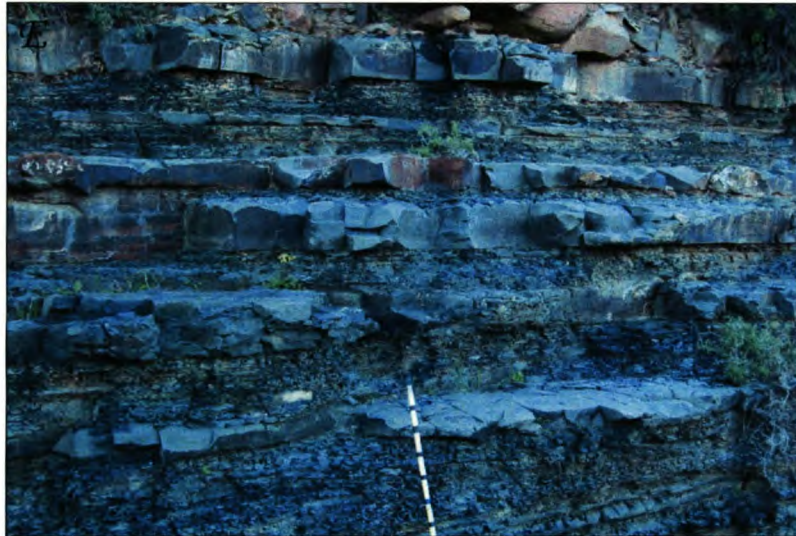


Figure 4.47.3 Q-type sheet deposits comprise thin sandstone beds interbedded with siltstone and shale. These deposits are associated with fan termination. Located at Rondavel 34.

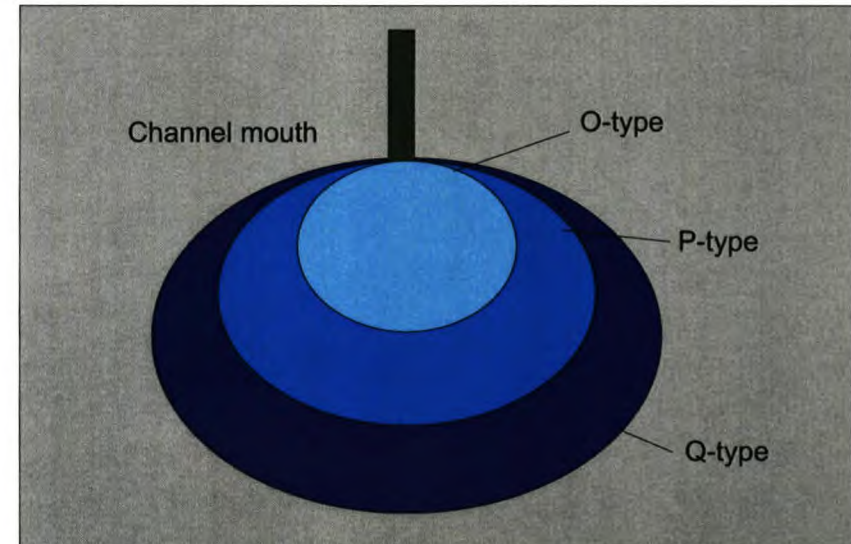


Figure 4.47.4 Schematic drawing illustrating the position of sheet deposits relative to the channel mouth.

4.7.6 Slump elements

Description:

The slump deposits of Kalkgat, Groot Hangklip and Tongberg display a combination of ball-and-pillow, dewatering and chaotic soft-sediment deformation structures, with Lf 8 and 7 being the predominant lithofacies (Table 2). The palaeoflow directions of this facies are the same as the turbidite flows of FS 5. The ball-and-pillow structures are spherical sandstone balls surrounded by a convoluted shale matrix (Table 2). The chaotic sandstone and siltstone deposits comprise predominantly structureless massive slump units displaying dewatering structures (Fig. 4.48.1). These units were deposited in the erosive thalwegs of the channels.

Interpretation:

The slump deposits of Groot Hangklip have been known for many years. The present interpretation for these units is that they formed within the base-of-slope environment as part of a slope fan (Wild *et al.*, 2004). Correlation of the Kalkgat complex with the GHK complex suggests a new interpretation for deposition of these units. Due to the chaotic nature of these deposits, it was difficult to interpret and divide them into architectural elements. Channels filled with chaotic sediments are the main element of the Kalkgat and GHK slump deposits but are absent in the TB region (Fig. 4.48.2). The thin beds with ball-and-pillow and dewatering structures in the TB region are interpreted as deformed sheet-slump deposits that correlate with the GHK and Kalkgat channels (Fig. E5 + Fig. 4.48.3).

The slump units do not correlate with the rest of FS 5 turbidite units. They were initiated by the release of sediment in great quantities on the mid- to upper slope environment (Fig. E5). Evidence from the Kalkgat and GHK region indicates that the slump deposits were deposited at a later stage during the FS 5 development. The presence of wave ripples and bioturbation in the upper units indicates a shallow basinal environment and highly unstable conditions with continuous input of sediment from the delta mouth into the shallow basin.



Figure 4.48.1 Slump deposits in the TB unit, displaying ball-and-pillow deformation structures. They are overlain by bedded sandstone layers (above dashed line). Located at Hanglip 150.

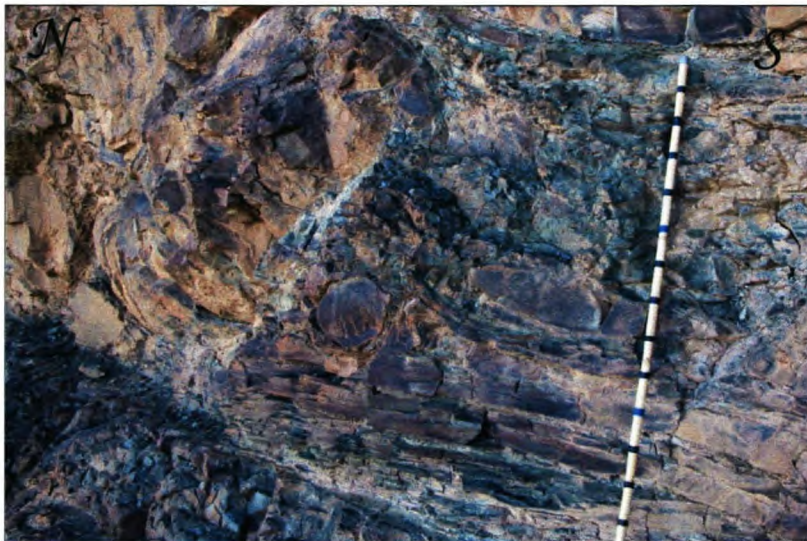


Figure 4.48.2 Massive, chaotic slump deposits constitute the predominant facies type in the GHK and KG channel-fills



Figure 4.48.3 Ball-and-pillow structures are common in the TB depositional environment.

4.8 Influence of basin floor topography on deposition

Small variations in topography of the sea floor, especially near the source, may cause large changes in the sediment transport paths to their depositional basins. The alternation of sand deposition and the switching of palaeocurrent directions between the fans in the Tanqua sub-basin were probably related to minor tectonic activities which resulted in changes in the sea floor topography and were responsible for deltaic switching (Scott *et al.*, 2000).

The distribution of channel-fill deposits in the southern part of the study area (Fig. E) indicates that subtle basin floor topography could have influenced the depositional pattern and concentration of channels. Associated with this area are two large synclinal and anticlinal structures (Fig. B) that possibly could have caused subtle basin floor expression during deposition of the fans. The abrupt termination of Fans 3 and 4, the facies variation north and south of the KHK channels and the transport orientation of these channels could serve as evidence for basin floor control or gravity flow deposition. The occurrence of slump deposits associated with channel deposits also indicates that this part of the fan experienced a very unstable environment. The flow path directions of the BK and SB units do not indicate any influence by basin floor topography. There is no evidence of any early mass transport systems which could have caused slumping in the basinal shales with the resultant formation of basinal topography structures underlying FS 5.

Chapter 5

Sequence Stratigraphy

Chapter 5

Sequence Stratigraphy

5.1 General

Sequence stratigraphy have been defined as “the study of rock relationships within a chronostratigraphic framework of repetitive, genetically related strata bounded by surfaces of erosion or non-deposition, or their correlative conformities” (Posamentier *et al.*, 1988; Van Wagoner, 1995). The terminology and specific definitions of a cycle, depositional sequence, composite sequence, etc. as described by Vail (1975), Vail *et al.* (1977, 1984), Mitchum (1977), Posamentier *et al.* (1988, 1991), Posamentier and Vail (1988), Galloway (1989), Van Wagoner *et al.* (1988, 1990), Weimer (1990), Mitchum and Van Wagoner (1991), Weimer *et al.* (1994, 1998) and Burgess *et al.* (2000) are preferred throughout this section and the reader is redirected to these authors for more detail.

Various research and application models were compiled for the depositional sequences of the Tanqua sub-basin in Bouma and Wickens (1991), Brink (1992), Wickens (1994), Goldhammer *et al.* (2000) and Johnson *et al.* (2001). They concluded the following sequence hierarchy (Fig. 5.1):

- That the entire sedimentary fill of the Karoo Basin is identified as a first-order sequence, with its internal stratigraphic architecture closely controlled by orogenic cycles of loading and unloading in the Cape Fold Belt (CFB).
- The tectonic paroxysms dated in the CFB (Hälbich *et al.*, 1983) further provide the basic subdivision of the foreland stratigraphy and are regarded as of second-order cyclicity (Catuneanu *et al.*, 1998).
- The time-span for the total Ecca basin-fill succession equates with third-order duration of sea-level cyclicity, which may be subdivided into two ‘third order’ (1-10 My) depositional sequences with several superimposed high-frequency, ‘fourth-order’ (0.1 – 1 My) depositional sequences.

Thus, the high-stand conditions of the third-order duration prevailed until a fall in relative sea level, of fourth-order duration, initiated the first submarine fan to be deposited in the Tanqua sub-basin (Wickens, 1994) (Fig. 5.1), each third-order sequence consists of higher-frequency fourth-order (0.1-1 m.y. duration) sequences. In this hierarchical scheme, the fourth-order sequences are the fundamental building blocks of the larger seismic-scale sequences (Fig. 5.2). The individual fan systems, interpreted here as fourth-order lowstand deposits, each genetically tie to one high-frequency sequence. Fan 1 was assigned to the lowstand systems tract of fourth-order sequence 1. Fan 2 to fourth-order sequence 2, and so on. Fan systems 1 through 5 form a progradational stack revealed mainly by their spatial distribution and regional facies variation (Fig. 5.1). This long-term progradational pattern is interpreted here as depicting the third-order high-stand systems tract of sequence 1 and records a combination of reduced accommodation space and/ or increased sediment supply (Abreu and Anderson, 1998; Goldhammer *et al.*, 2000).

The fourth-order sequence boundaries are placed at the base of the major sand-rich fan packages, which are interpreted as lowstand deposits, and the recessive-weathering interfan shale intervals are seen as the fourth-order transgressive and high-stand systems tract of each high-frequency sequence (Fig. 5.1). Although these interfan units comprise silty shale in general, especially in the up-dip position, they contain one or more dark shale horizons associated with carbonaceous concretions or layers (Fig. 5.3). The latter are of early diagenetic origin and indicate periods of starvation in the basin. These horizons were interpreted as condensed sections representing maximum flooding of the fourth-order high-stand (Goldhammer *et al.*, 2000).

5.2 Fan System 5

The prime objective of this section is to illustrate how the concepts and principles of sequence stratigraphy could be applied to Fan System 5 in order to derive a chronostratigraphic framework into which the various depositional events of FS 5 can be placed.

5.2.1 Sequence framework

The increase in sediment volume, sand:shale ratio, and change from low- to high-concentration deposition at any given point on the fan, are associated with renewed active fan growth, and

therefore are interpreted as an abrupt increase in sediment supply to the basin floor. This increase in sediment supply over the whole fan system relates to a decrease in accommodation space on the coeval shelf and the generation of an up-dip sequence boundary (Fig. 5.1). Episodes of fan growth occurred at a high-frequency intrafan scale, marked by abrupt increases in sand deposition immediately above Type 2 condensed sections, and also on the lower frequency scale for the five complete fans (Johnson *et al.*, 2001; Johnson and Hadler-Jacobsen, 2001) (Fig. 5.1).

Sequence boundaries were interpreted at the bases of the low-frequency five fans of the Tanqua sub-basin, based on a clear surface that marks a fan-wide abrupt increase in sediment supply (Fig. 5.1). The change is marked by either the erosive base of a channel complex overlying distal basin plain or fan fringe deposits, or the planar base of an amalgamated sheet sandstone overlying more distal turbidite deposits.

5.2.2 Key surfaces

The key surfaces used in the sequence stratigraphic framework for FS 5 are fan flooding surfaces and sequence boundaries. Type 1 sequence boundaries are inferred to occur at the bases of the regionally extensive sandstone-rich fan successions. FS 5 is therefore underlain by a fourth-order sequence boundary and overlain by a third-order sequence boundary (Figs 5.1+2). In deep-marine systems, the sediments between the initial flooding surface and the next sequence boundary represent a condensed interval that records the basinal equivalent of the late lowstand, transgressive and early high-stand systems tracts. The late high-stand systems tract may be represented by a thin, mud-dominated turbidite succession. This is evident in the section between the last sandy flows of Fan 4 (LST) and the first sandy flows of FS 5 (ELST). Sequence boundaries of fifth- and sixth- order sequences are also evident in FS 5.

5.2.3 Condensed intervals

The condensed section intervals represent the most reliable correlation markers in the Tanqua Fan Complex. Three types of condensed sections have been identified, based on their facies type and distribution (Johnson *et al.*, 2001).

- Type 1 horizons represent relatively long-duration breaks in sedimentation that allowed the development of distinct diagenetic processes. They are associated with the 20- to 60 m thick, fine-grained basinal shale packages that developed between fans (Figs 5.4.1+2). These shale packages are interpreted as transgressive and high-stand systems tracts of low-frequency sequences (Fig. 5.1).
- Type 2 horizons comprise 20 cm to 3 m thick intrafan packages of predominantly shale to silty-shale beds (Fig. 5.5.1). These deposits are traceable for more than 20 km laterally within the fan system and therefore represent significant periods of condensation. Type 2 condensed horizons are most common between amalgamated sheets or above channel-fills. Because of their lateral extent in the intrafan setting, Type 2 horizons are interpreted as higher order (shorter duration) condensed sections than Type 1 horizons. An alternative interpretation is that these sand-poor zones relate to autocyclic avulsion of channels within the fan. For example, avulsion of up-dip channels may cause the development of intersheet/sheet fringe deposits above an older sheet, producing a succession with the characteristics of a Type 2 horizon (Fig. 5.5.2). With this interpretation, a less highly ordered vertical and lateral stratigraphic signature might be expected within a fan than those observed herein. Johnson *et al.* (2001) interpreted the Type 2 horizons as being related to relative sea-level rises on the shelf and representing transgressive and high-stand systems tracts of high-frequency sequences.
- Type 3 horizons are <30 cm thick and occur within individual amalgamated sheets or within channel complexes (Figs 5.6.1+2). They have limited lateral extent (<5 km) and are interpreted to represent a shorter duration of more localized sediment starvation than Type 2 horizons. The origin of Type 3 horizons could be autocyclic and related to compensation cycles, or it could relate to very high-frequency parasequence-scale, shelf-flooding events.

5.2.4 Flooding surfaces

Most of the major flooding surfaces, i.e. initial flooding surfaces (IFS) and maximum flooding surfaces (MFS) form part of the shallow marine sequence stratigraphy and are not recorded in the

deep marine setting. The MFS, for example, would only be recorded within the condensed shale succession of the deep marine deposits, but it would be very difficult to recognise.

Sixsmith (2000) suggested two new flooding surfaces, which were recognized and applied in the Laingsburg Fan Complex. These surfaces were referred to as the Initial Fan Flooding Surface (IFFS) and the Maximum Fan Flooding Surface (MFFS) (Fig. 5.7). Both of these surfaces have been recognised within FS 5.

The IFFS is the first surface that recorded the onset of cessation of a fan system. The IFFS vertically separates a sandstone-rich succession from a retrogradational thinning and fining upward package of sandstones (a transgression package) that culminate in shale (Fig. 5.8.1). The IFFS represents the surface at which there is evidence of the creation of up-dip accommodation space due to relative sea level rise.

The MFFS is characterised by the change from the transgressive package to background deposition of hemipelagic shales, above which only hemipelagic shale was recorded in the deep basin. The MFFS therefore marks the base of a hemipelagic shale succession and occurs between the IFFS and the base of the transgressive systems tract on the rising limb of the relative sea level curve (Fig. 5.8.2).

This terminology requires a subdivision of the lowstand systems tract into the early, middle and late LST (Sixsmith, 2000). The early LST (ELST) records deposition of the entire basin floor fan complex, and correlates in time to the sequence boundary on the shelf (Fig. 5.9). The middle LST (MLST) records a retrogradational package above the basin floor fan, representing a reduction in sand supply to the deep basin because of up-dip increases in accommodation space (Fig. 5.9). This occurs during late, slow relative sea-level fall when the rate of relative sea-level fall is decreasing and during early, slow relative sea-level rise. This would lead to preferential sand storage on the slope, in the slope fan and lowstand wedge. The base of MLST marks the position of the IFFS. The late LST (LLST) records further accommodation space increase on the early rising limb of the relative sea-level curve where sedimentation is restricted to shelf edge deltas and incised valleys, and no sediment is transported to the deep basin. The LLST is bounded at its base by the MFFS, and its upper surface corresponds with the IFS and the base of the shelfal TST (Fig. 5.9).

5.2.5 Systems tract

The systems tract, to which the deposition of the different units of FS 5 belong, is the lowstand systems tract (LST). The transgressive (TST) and high-stand systems tract (HST) were very weakly recorded in the system. The LST stratigraphically forms the oldest part of a sequence and represents a period of relative sea-level fall and early relative sea-level rise. The low-frequency transgressive and high-stand systems tracts represent the intervals of fines between the fans. The interfan sandstone cycles are tentatively interpreted as parasequences within the low-frequency high-stand systems tracts (Van Wagoner *et al.*, 1988).

Sixsmith (2000) identify two types of transgressive packages in the turbidite environment:

- Type-A transgressive package infers a relatively long break in sediment supply, and therefore a relative sea-level rise, allowing development of an IFFS and MFFS and subsequent deposition of hemipelagic shales (Fig. 5.10.1). The Type-A transgressive package was recorded very weakly or is absent within FS 5.
- Type-B transgressive package comprises predominantly alternating siltstones and shales (Fig. 5.10.2). It is interpreted to occur when sedimentation has moved to another depocenter because of large-scale autocyclic processes. The Type-B package corresponds to the Type 2 and 3 condensed sections of Johnson *et al.* (2001). It predominates between the different units of FS 5, which is a good indication and supportive evidence for the autocyclic nature of these units.

5.2.6 A sequence stratigraphic model for FS 5

FS 5 is the last depositional sand-rich system of the first, third-order sequence cycle and comprises six depositional sand-rich units. These six, genetically related and unrelated units, are interpreted as fourth-order lowstand events that can be correlated between sections, using the criteria for identifying transgressive packages and condensed intervals described above (Fig. 5.11). These units occur on different stratigraphic levels within FS 5 (see Section 4 for detailed sedimentological descriptions of these units) and are separated by Type 2 and 3 intervals, which occur only locally and not regionally throughout the basin (Fig. 5.11). This is good supportive

evidence for autocyclic deposition of the sand-rich units within a lowstand systems tract. Numerous correlation panels were compiled in strike and dip directions (south to north) of FS 5, and hung on a datum horizon, mostly the base of FS 5 (See Section 4).

The section between the top of Fan 4 and the first flows of FS 5 comprises typical Type 1 and 2 condensed sections. The Type 1 condensed sections are very thin (30-60 cm) and only two of these beds occur in the section (Figs 5.12.1+2). Between these condensed units are predominately Type 2 silty-shale beds, which indicate a late HST period, causing initial muddy turbidites, followed by a marine flooding surface (Fig. 5.12.3). The latter also forms the Type 1 sequence boundary for the first turbidite sand flows of FS 5 during a forced lowstand regression.

The Klein Hangklip (KHK) and Tongberg (TB) channel complexes formed the conduits for the first sand-rich deposits in the basin, which could have been initiated by a forced regression during the drop of sea-level (Hunt and Tucker, 1992). This erosive sand package was deposited on a fourth-order sequence boundary and indicates the start of the first ELST (Fig. 5.13). Genetically related to KHK and TB is the Blauwkop (BK) unit, which indicates a progradational trend deeper into the basin (Fig. 5.13). The Groot Hangklip (GHK) and Kalkgat (KG) units are also genetically related, and form part of the mid-stratigraphic deposits of FS 5 (Fig. 5.13). These units occur in the most proximal part of FS 5 and are genetically unrelated to the lower depositional units (Fig. 5.13); they predominantly comprise slump sediments with Type 2 condensed sections at the top and bottom (see Section 4 for detail). These units were deposited in a stage of renewed regression during a relative sea-level fall. This caused a large amount of unstable sediment input into the basin.

Shortly after deposition of the GHK and KG units, a short period of Type B transgression occurred, followed by deposition of the Skoorsteenberg (SB) and upper Tongberg (TB) units (Figs 5.11+13). It is unclear whether these two phases of deposition are genetically related, although seemingly deposited on the same stratigraphical level (Figs 5.11+13). These are the uppermost deposits of the FS 5 sequence, before regional transgression and maximum flooding, that resulted in the HST upper slope and deltaic deposits (Brink, 1992; Wickens, 1994) (Fig. 5.1). The SB unit constitutes the northernmost part of FS 5, and indicates evolution from a progradational and aggradational to a retrogradational pattern of deposition (Figs 5.13+14).

The six units of FS 5 could be linked genetically into three unrelated sand-rich units, which are under- and overlain by Type 2 condensed sections or B-type transgression packages (Fig. 5.13). The overall stacking pattern of these three major combined phases of deposition can be divided into a progradational stacking pattern (first phase, KHK, TB, BK), a retrogradational stacking pattern (second phase, GHK, KG), and a progradational pattern again (third and final phase, upper TB, SB) (Fig. 5.14). The different depositional patterns of these three phases could be ascribed to autocyclicity, due to a lack of regional sequence boundaries within FS 5.

Within individual fan systems, however, autocyclic (intra-basinal) processes, such as channel and lobe-type deposition, as well as other random phenomena (local topography) appear to dominate facies architecture, resulting in unpredictable arrangement of reservoir-scale elements (individual sheet sand bodies) (Fig. 5.13). Such autocyclic drivers result in the formation of even higher-frequency cycles (e.g. fifth-order). Thus, at the higher-frequency scale, there is less predictability within individual fan systems, suggesting that their reservoir-scale architecture was driven mostly by autocyclic processes, which were more random (Goldhammer *et al.*, 2000). The sequence hierarchy of each of the submarine fans in the Tanqua sub-basin is ascribed to the high-resolution fourth-order lowstand systems tract (Brink, 1992; Wickens, 1994). Thus, FS 5 forms a fourth-order depositional sequence and each of the sand-rich units a high-resolution fifth-order sequence (Figs 5.1+2+13). The FS 5 units are comprised of several different sub-units, which in this case, could be described as sixth-order units with minor marine flooding surfaces. These extra high-resolution sixth-order sequences comprise even smaller local events that relate to ultra high-frequency seventh-order depositional sequence cycles (Fig. 5.14).

The time intervals for fifth-order sequences are estimated between 0.01 - 0.02 My (10 000 – 20 000 y), but for the ultra high sequence orders the time estimate could be in days, months, years or hundreds of years. The absence of a high-resolution chronostratigraphic framework and a lack of outcrop between the fan complex and the foreland thrust belt, do not allow the discrimination of the principal driving mechanism of fan evolution.

5.2.7 Summary

The following is a short interpretation of the evolution of FS 5, from the top of Fan 4 through FS 5 until shut-down of the system in the first third-order sequence cycle. This interpretation is based on Fig. 5.14.

The top of Fan 4 comprises a MLST with an underlying IFFS, which is in turn overlain by the MFFS boundary and the LLST (Fig. 5.14). The TST and HST form part of the Type 1 condensed section above the LLST. The IFS and MFS will be recorded within the condensed section. The Type 1 condensed section is covered by a silty-shale bed of 4 m, which could have been caused by the late HST before maximum flooding occurred above this package (Fig. 5.14). Three periods of LSTs developed during a fall and rise of sea-level in FS 5:

- The first sand-rich turbidite flows of FS 5 were deposited directly on the maximum flooding surface, i.e. the Type 1 sequence boundary. The ELST deposits comprise massive erosional sandstones and channel-fills (KHK, TB, and BK) (Fig. 5.14). Several flows were recorded before a Type B transgressive package was formed during a rise in the sea-level. However, before a significant TST and HST could develop, the sea-level fell again.
- Forced regression, caused high-energy unstable sediment deposition in the most proximal part of FS 5 (GHK and KG), this forms the second fifth-order ELST (Fig. 5.14). This ELST developed into a MLST and LLST. The LLST is overlain by the second Type B transgressive package (Type 2 condensed section), which also never developed into a HST, before sea-level falls again.
- During the gradual fall of the sea-level, deposition of the third ELST (TB and SB units) took place (Fig. 5.14). This ELST developed also into a MLST and a LLST. A major TST represents the upper 10 m of FS 5 with clear evidence for the development of the IFFS and MFFS. This latter surface is overlain by a Type 1 condensed section, which was deposited before and during the early HST. This surface represents the close-down of the system and lower third-order and fourth-order sequence package (Fig. 5.14).

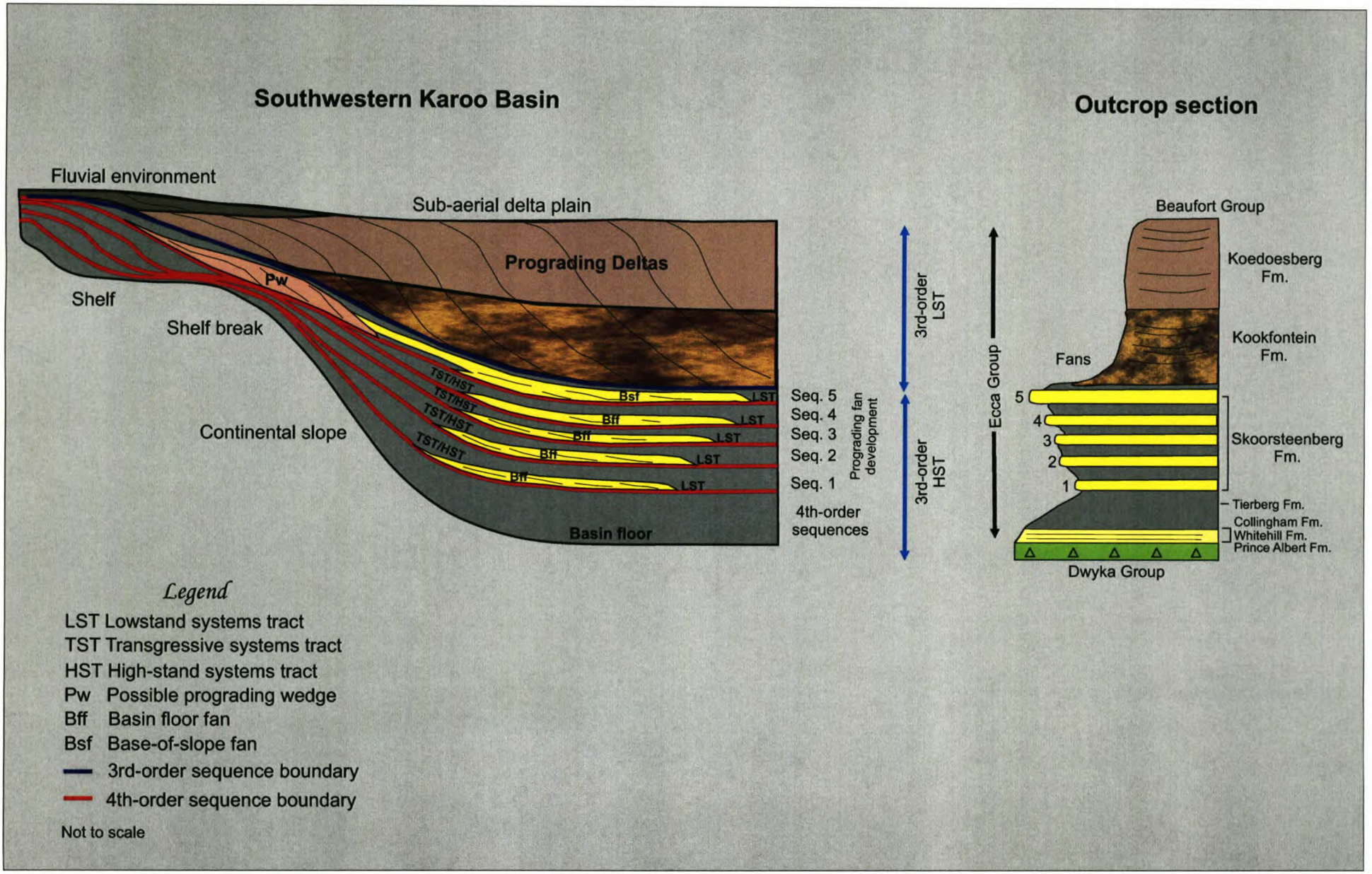


Figure 5.1 Diagram illustrating the application of sequence stratigraphy and deposition of the fan systems in the Tanqua sub-basin (modified and redrawn from Wickens, 1994).

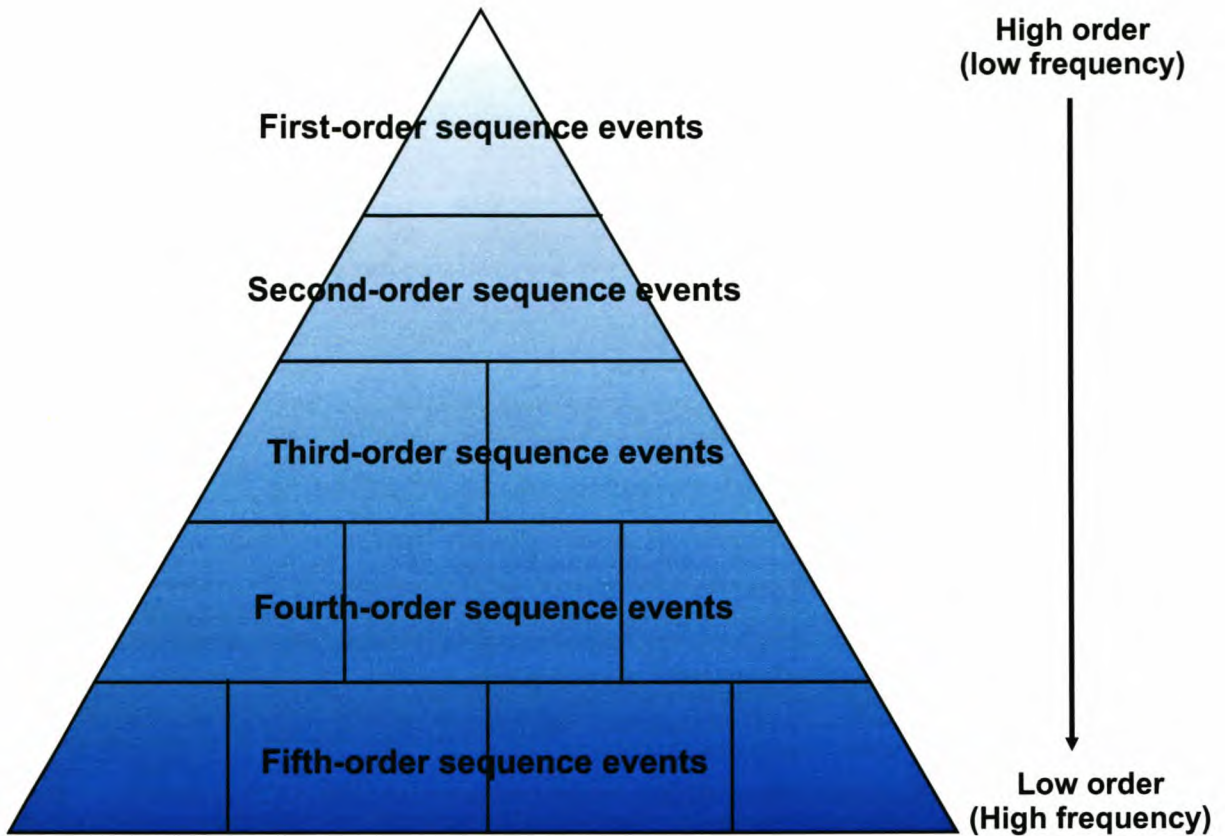


Figure 5.2 Diagrammatic illustration of the concept of hierarchy. First-order events are associated with large-scale events and fifth-order sequences are associated with relatively short-lived, geological events (modified from Catuneanu, 2002).



Figure 5.3 Interfan unit, between Fans 3 and 4, consisting of silty-shale and dark shale horizons, representing periods of starvation in the basin. These horizons are interpreted as condensed sections representing maximum flooding. Located on the farm Rondavel 34.



Figure 5.4.1 Very fine hemipelagic shales. Distinct diagenetic processes characterize Type 1 condensed sections. They indicate periods of starvation in clastic supply to the basin. Located at Klipfontein 31.



Figure 5.4.2 Very fine, dark hemipelagic shales between the basin floor fans, representing a Type 1 condensed section. Located at Brandhoek 119.

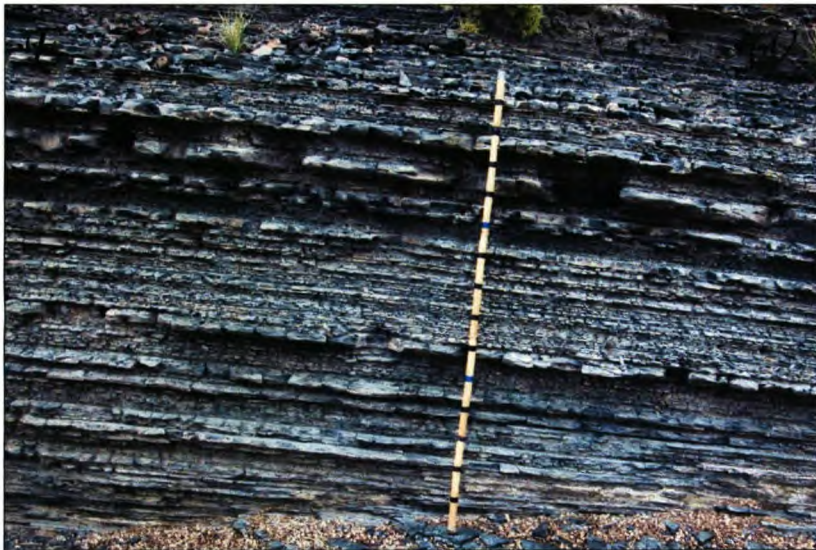


Figure 5.5.1 Type 2 horizons comprise 20 cm- to 3 m-thick intrafan packages of predominantly shale to silty-shale beds. Predominant between the units in FS 5. Located at Rondavel 34.

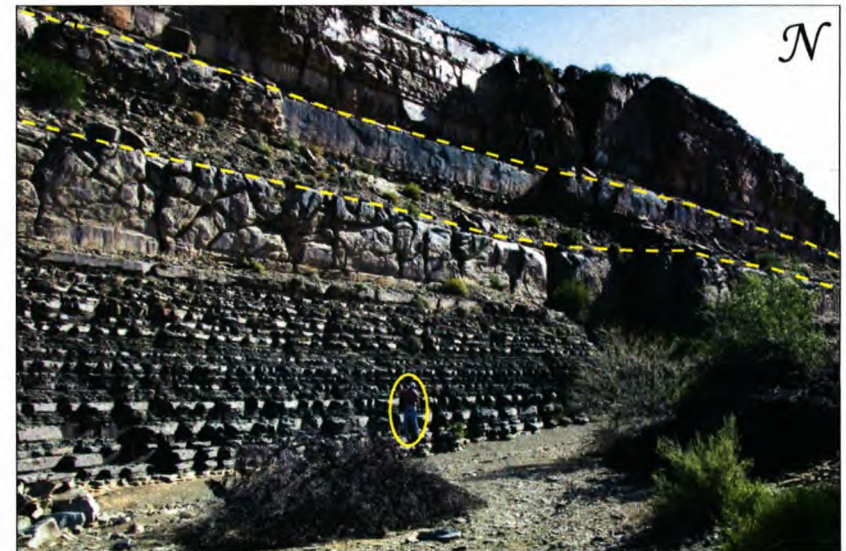


Figure 5.5.2 Up-dip channel switching may cause development of intersheet/sheet fringe deposits, producing a succession with characteristics of a Type 2 horizon (Indicated by dashed line). Note person for scale. Located at Zoetmeisjes Fontein 75.



Figure 5.6.1 Type 3 horizons occur above or within channel and amalgamated environments. The origin of Type 3 horizons could be autocyclic switching within the fans. Dashed line indicates the horizon above a channel-fill. Located at Droogekloof 400.

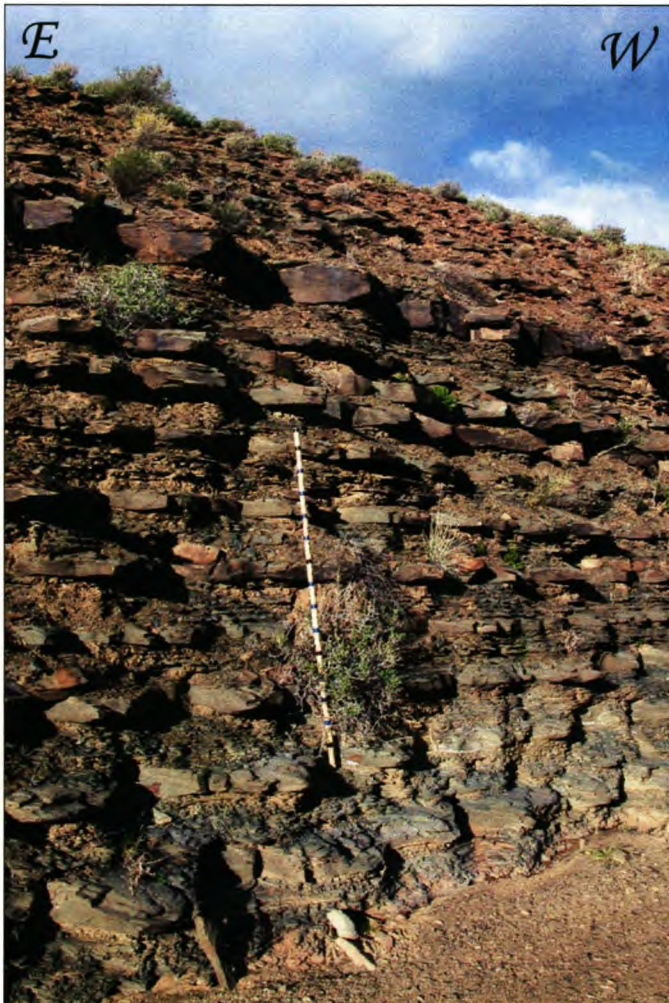


Figure 5.6.2 Type 3 horizons have limited lateral extent (<5 km) and are interpreted to represent a shorter duration of more localized sediment starvation than Type 2 horizons. The thicknesses of the layers is 30 cm to 40 cm. Located at Kookfontein 78.

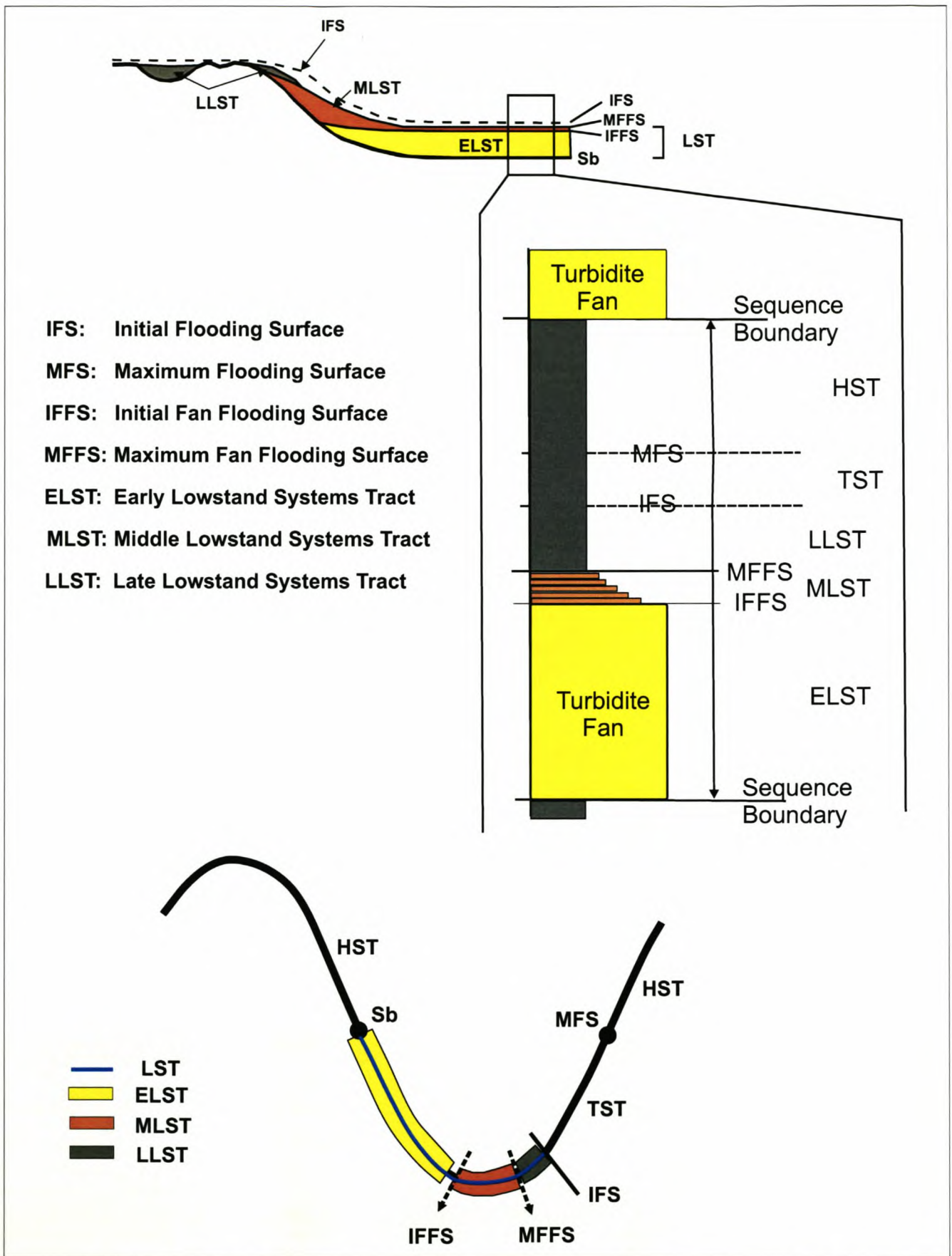
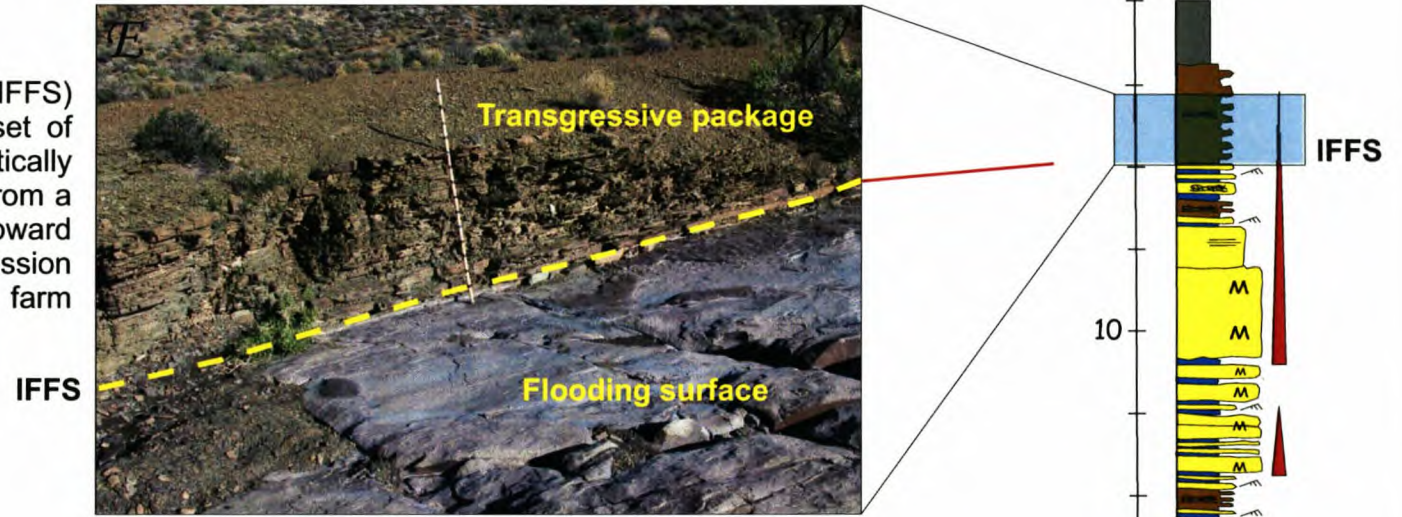


Figure 5.7 Diagram for a deep basin profile. Lowstand sedimentary responses split into the early, middle and late lowstand systems tract. The initial and maximum fan flooding surfaces mark periods of distinct increases in landward accommodation space and are recorded in the basin (redrawn from Sixsmith, 2000).

Figure 5.8.1 Initial fan flooding surfaces (IFFS) is the first surface that records the onset of cessation of a fan system. The IFFS vertically separates a sandstone-rich succession from a retrogradational thinning- and fining-upward package of thin sandstones (a transgression package). Example from M62 on the farm Brandhoek 119.



159

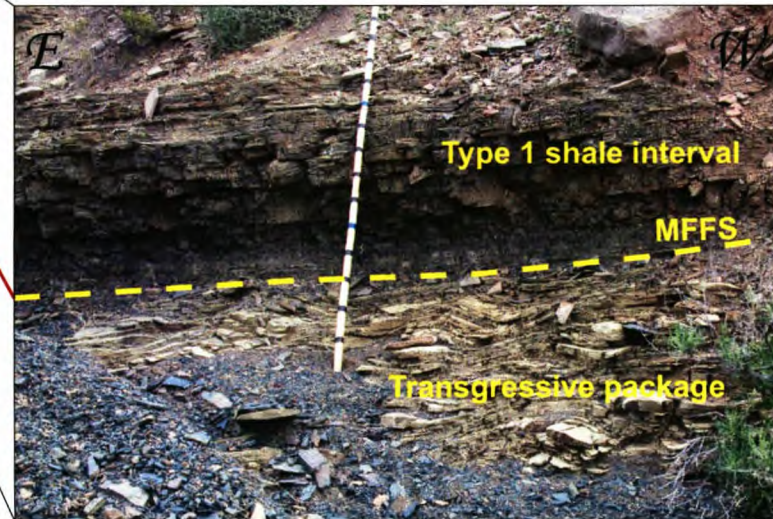
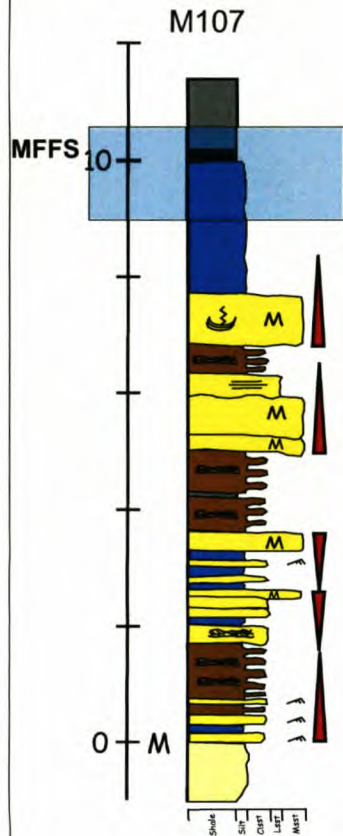


Figure 5.8.2 Maximum fan flooding surface (MFFS) is characterised by the change from the transgressive package to background deposition of hemipelagic shales. The MFFS therefore marks the base of a hemipelagic shale succession. Example from M107 in the Skoorsteenberg area.

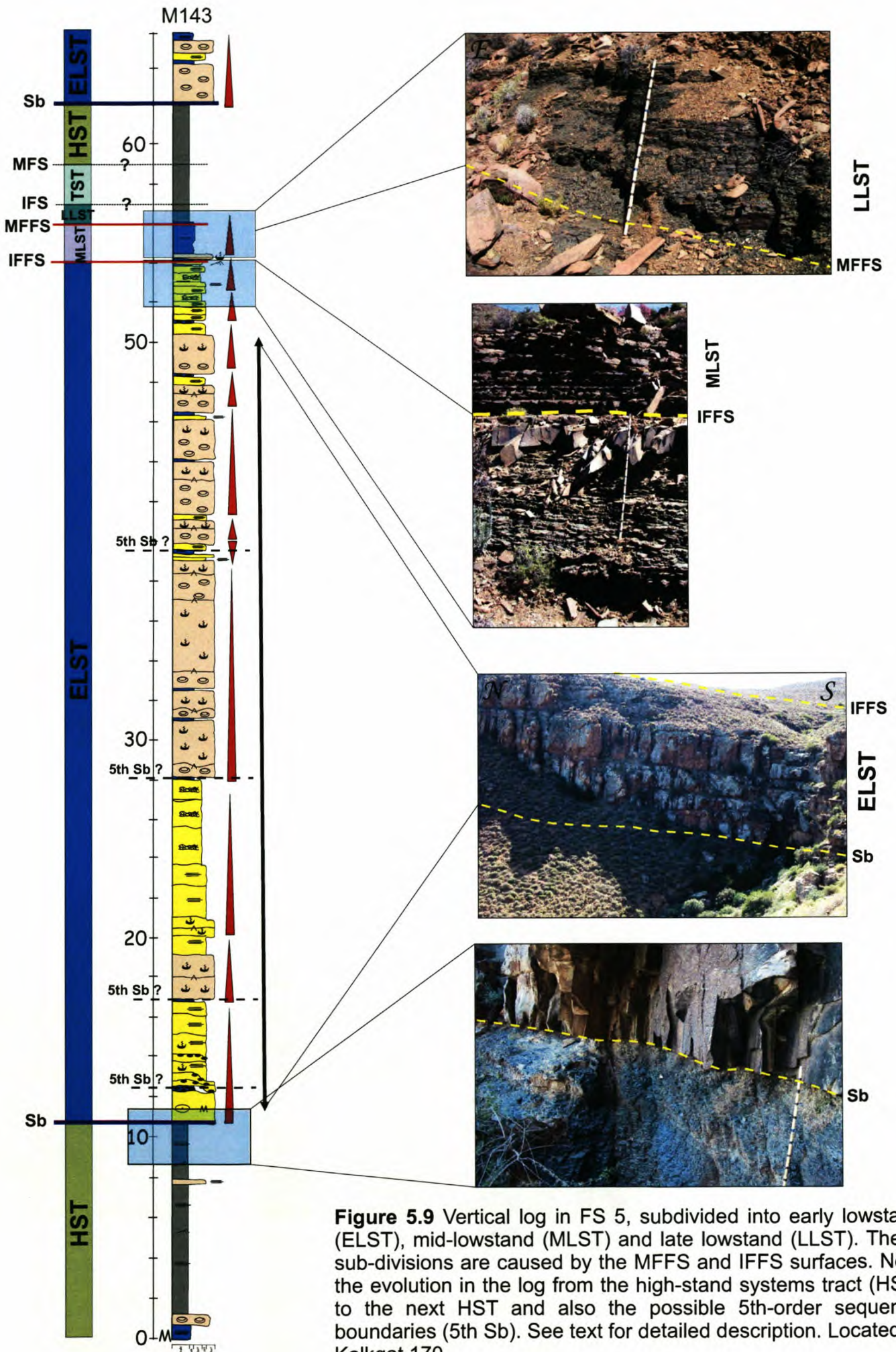


Figure 5.9 Vertical log in FS 5, subdivided into early lowstand (ELST), mid-lowstand (MLST) and late lowstand (LLST). These sub-divisions are caused by the MFFS and IFFS surfaces. Note the evolution in the log from the high-stand systems tract (HST) to the next HST and also the possible 5th-order sequence boundaries (5th Sb). See text for detailed description. Located at Kalkgat 170.

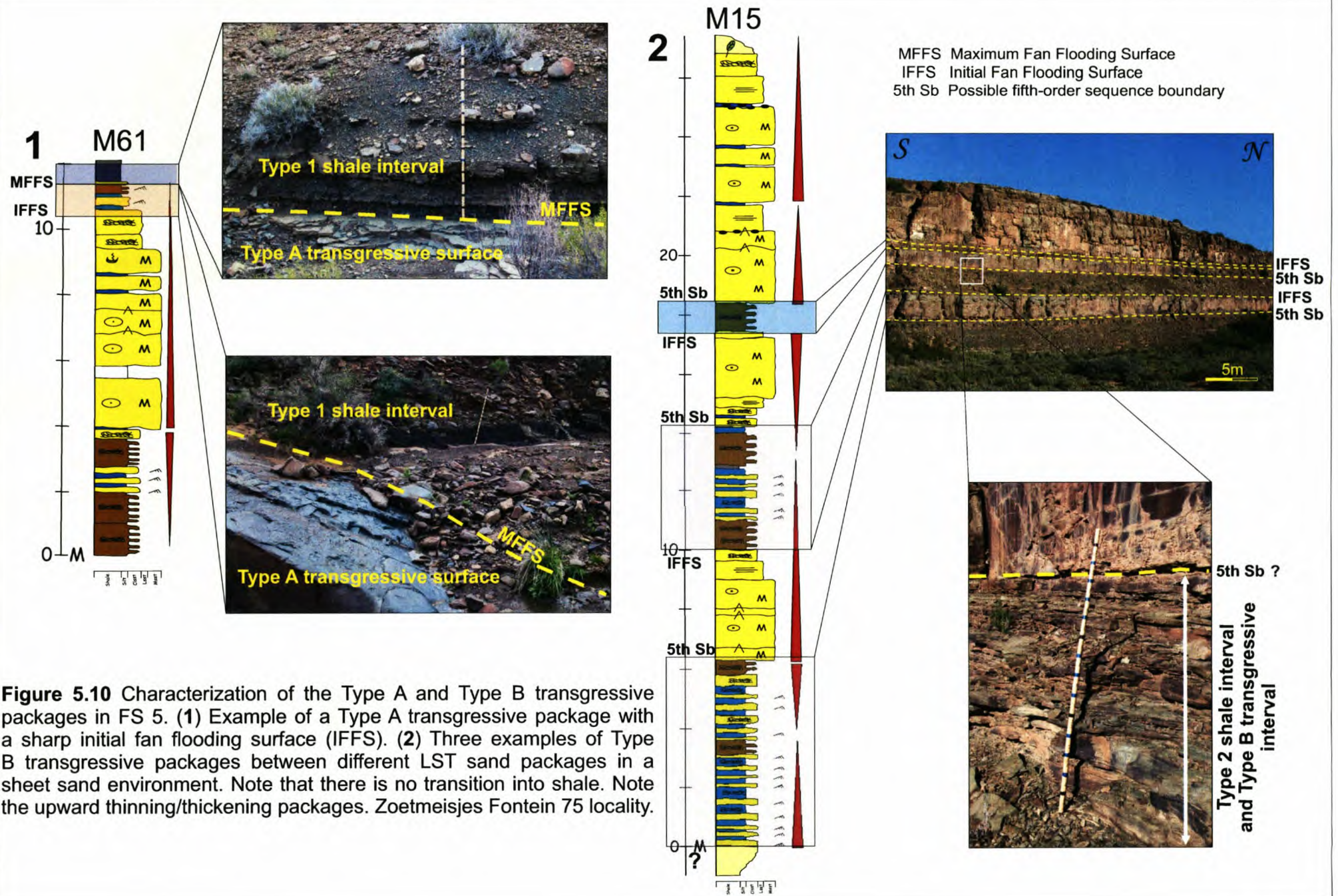


Figure 5.10 Characterization of the Type A and Type B transgressive packages in FS 5. (1) Example of a Type A transgressive package with a sharp initial fan flooding surface (IFFS). (2) Three examples of Type B transgressive packages between different LST sand packages in a sheet sand environment. Note that there is no transition into shale. Note the upward thinning/thickening packages. Zoetmeisjes Fontein 75 locality.

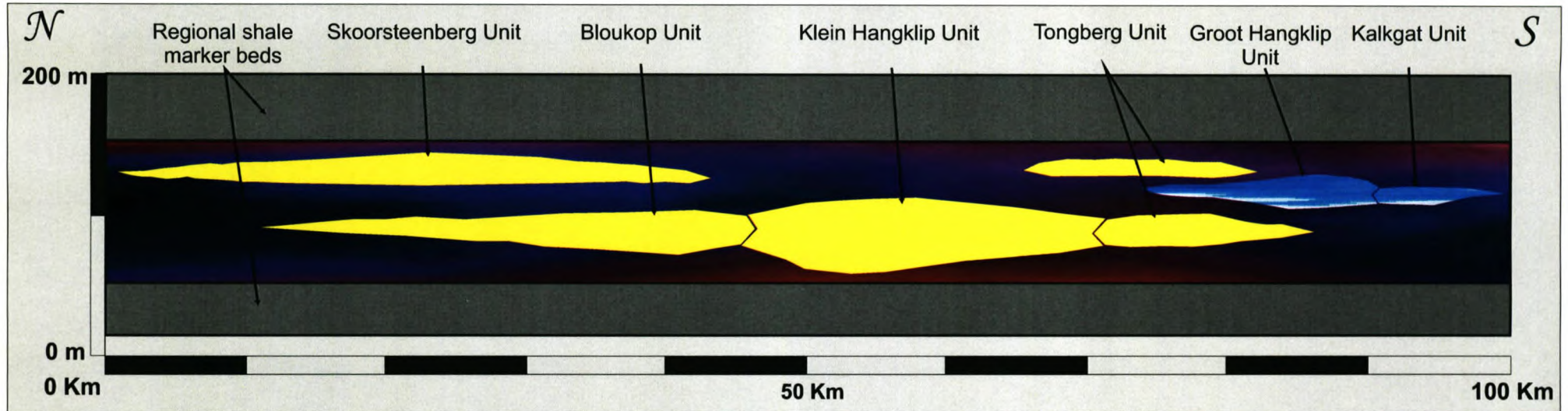


Figure 5.11 Idealized diagram of the six sand-rich units of FS 5. It is clearly evident that some of the units form part of the same depositional event. The units are vertically separated by the Type 2 or Type B transgressive packages. Regional Type 1 condensed section encloses FS 5. FS 5 is interpreted as a fourth-order sequence event and each of the sand-rich units would then be fifth-order, high-resolution sequence events.

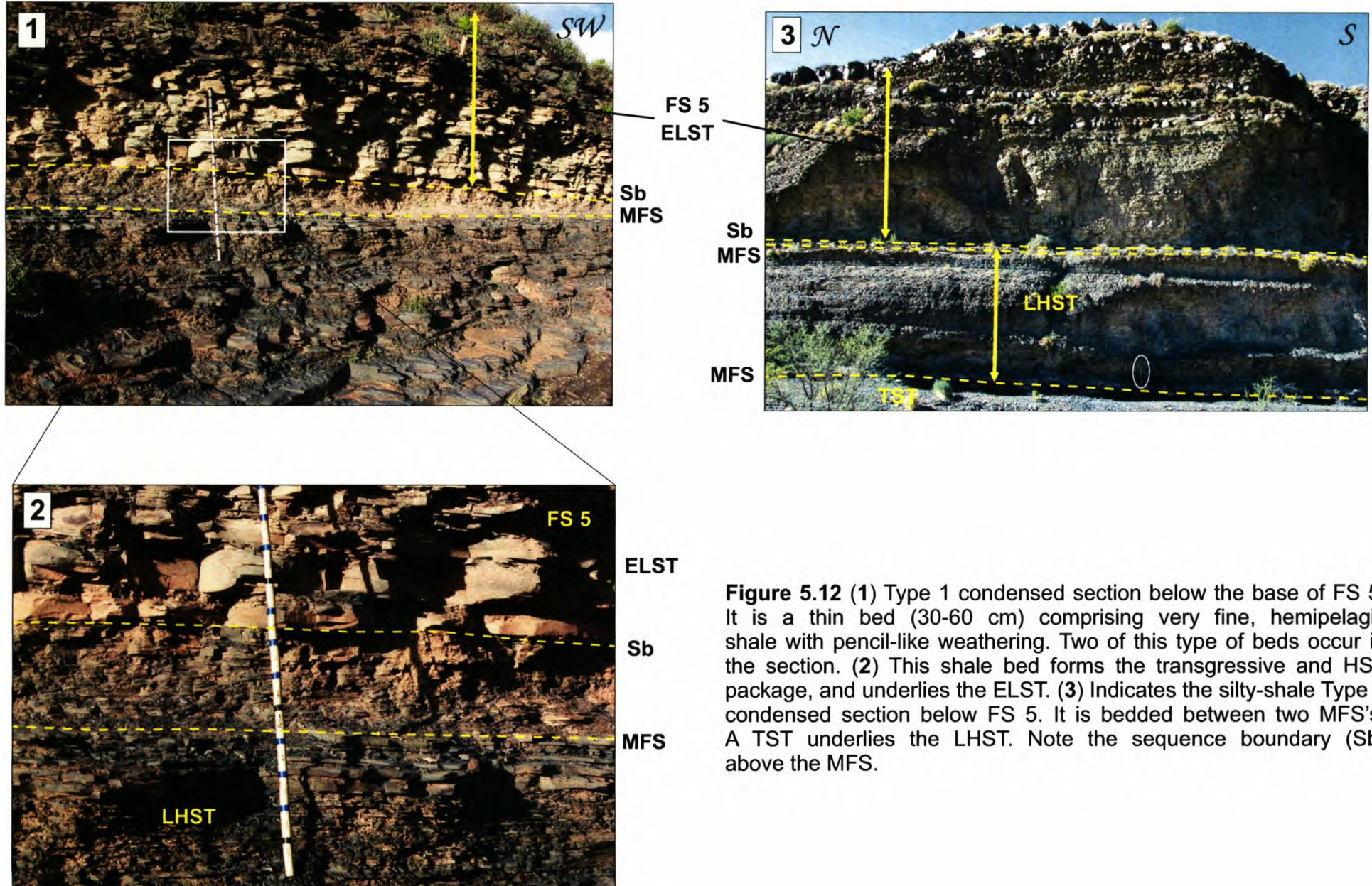
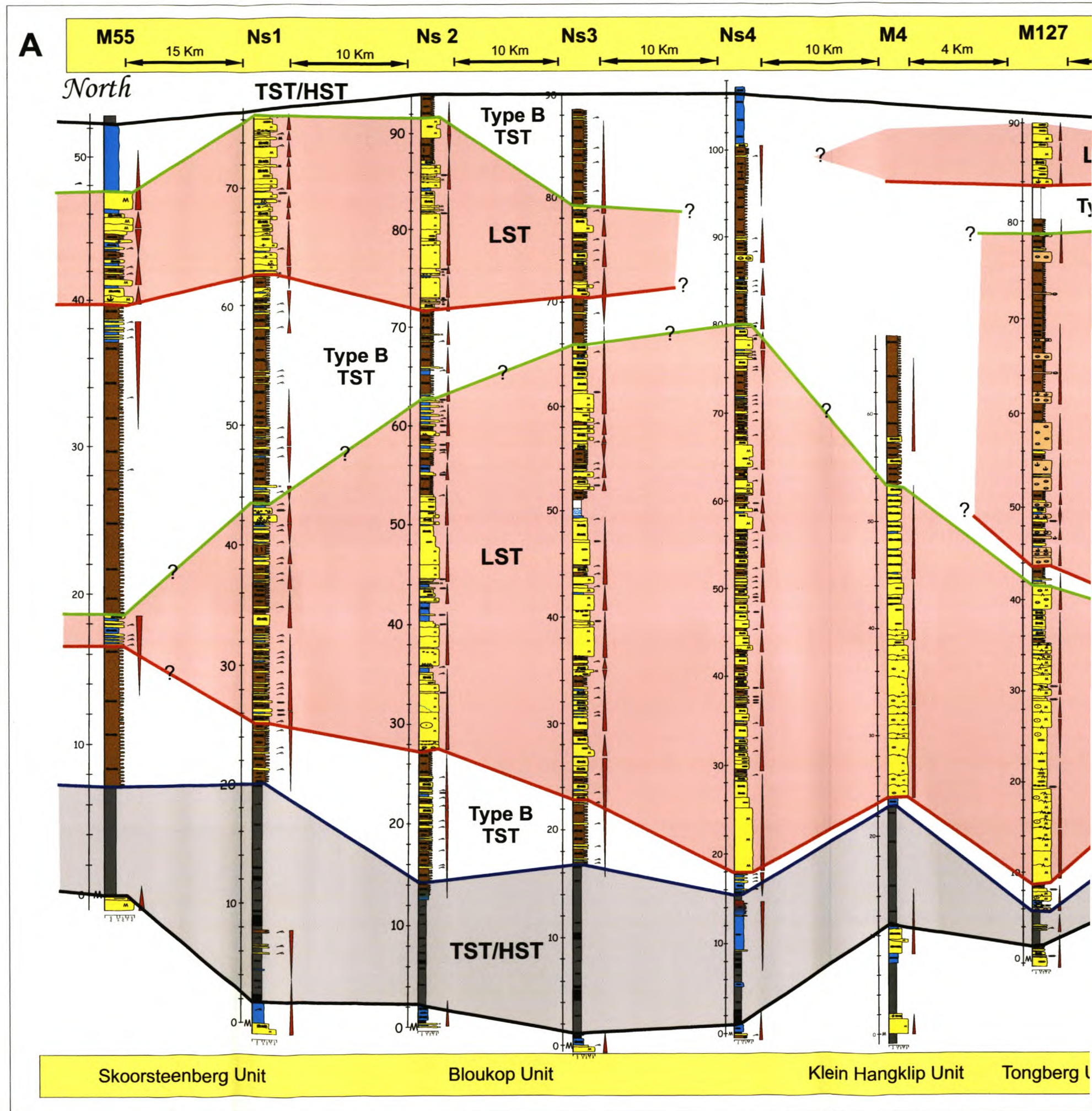
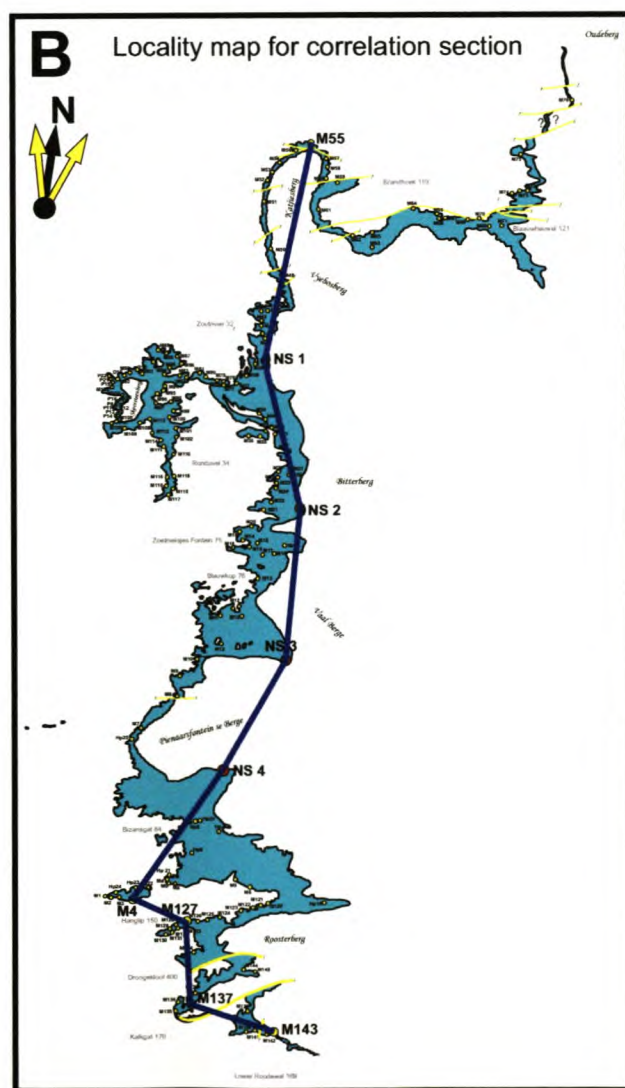
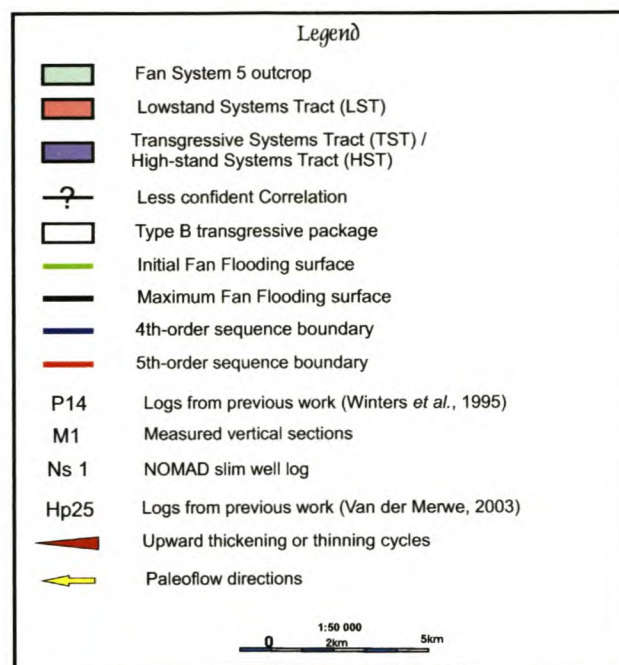


Figure 5.12 (1) Type 1 condensed section below the base of FS 5. It is a thin bed (30-60 cm) comprising very fine, hemipelagic shale with pencil-like weathering. Two of this type of beds occur in the section. (2) This shale bed forms the transgressive and HST package, and underlies the ELST. (3) Indicates the silty-shale Type 2 condensed section below FS 5. It is bedded between two MFS's. A TST underlies the LHST. Note the sequence boundary (Sb) above the MFS.

Figure 5.13 (A) Sequence stratigraphic interpretation for FS 5 across oblique depositional strike. All high-order sequence boundaries and flooding surfaces are shown, as well as systems tract interpretations. The six depositional units are also indicated. **(B)** Locality map for the correlations section.



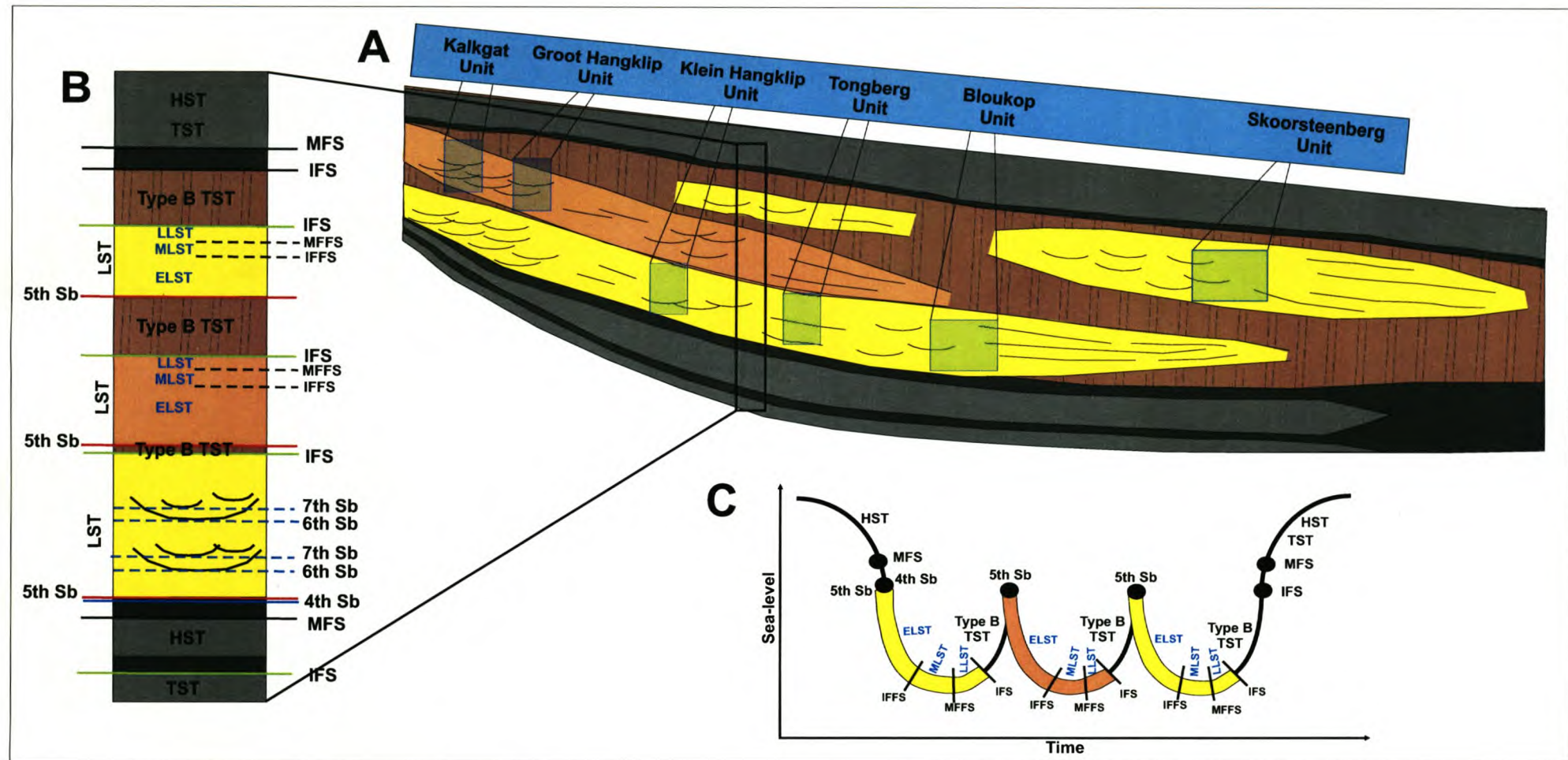


Figure 5.14 (A) Schematic diagram illustrating the evolution of the units in FS 5. Depositional dip direction. (B) Sequence stratigraphical evolution of FS 5. (C) Interpretation of sea-level fluctuations during deposition.

Legend

Turbidite Sand-rich Unit
 Channel-fills
 Slump Unit
 Layered deposits
 Silty-shale Unit
 Hemipelagic Shale
HST Highstand Systems Tract
LST Lowstand Systems Tract

ELST Early Lowstand Systems Tract
MLST Middle Lowstand Systems Tract
LLST Late Lowstand Systems Tract
TST Transgressive Systems Tract
Type B TST Type B Transgressive Systems Tract (TST)
MFS Maximum Flooding Surface
IFS Initial Flooding Surface
MFFS Maximum Fan Flooding Surface

IFFS Initial Fan Flooding Surface
4th-order Sequence boundary (Sb)
5th-order Sequence boundary (Sb)
 Possible **6th-order** Sequence boundary (Sb)
 Possible **7th-order** Sequence boundary (Sb)

Chapter 6

Discussion

Chapter 6

Discussion

This section provides a discussion on the most important findings regarding the evolution of Fan System 5 in a base-of-slope to basin floor depositional setting. A depositional model was compiled to illustrate the depositional setting and the basic elements of deposition. These form the building blocks of the fan system.

6.1 Architectural elements

FS 5 was deposited in a base-of-slope to upper basin-floor environment. The internal architecture of the fan system comprises channelized, transitional and sheet elements. Channels concentrated in the proximal areas, are commonly wide and shallow in most of the sand-rich units, and filled with amalgamated, thick massive bedded sandstones. Deep, erosional-based channels are less frequent and only concentrated in the more proximal outcrop areas. The channel-fills typically show a high degree of vertical and lateral off-set stacking patterns with a gradual change to adjacent transitional and sheet-like overflow elements in the more proximal outcrops. The more distal outcrops, i.e. the lower mid-fan and lower fan environments comprise low width:depth ratio channel-fills and sheet sands. Most of the sand is concentrated in the turbidite units with a net:gross (sand-to-shale ratio) of 65% - 90%. The units are separated by shale and siltstone intervals. Three types of erosional surfaces were identified in the channelized environments:

- 1) Steep concave erosional surfaces associated with high-energy, bypass environments,
- 2) Step-down erosional surfaces associated with a lower energy but still a bypass environment and
- 3) smooth, low-angle erosional surfaces associated with areas where deposition is the focus.

Flow patterns of the channels indicate braided and very low-sinuosity patterns, but more straight for single channels. This is a very good indication that turbidite flows were not influenced by any basin floor topography. However, the higher angle base-of-slope setting for proximal FS 5 caused

the turbidite flows to be more confined in an undeviated channelized environment. The channel-fills at the base of initial flows comprise massive sandstone units, which suggest rapid invasion of the basin floor by high-energy turbidity flows, followed by a gradual reduction in the volume of flows. These successions commonly display upward-thinning trends, suggesting a retrogradational mode of fan building. Small crevasse type channel-fills are associated with thin-bedded overflow and sheet deposits.

Deposition of sands along the channel margins at a Palaeoflow angle of 45° – 80° is interpreted as overflow deposits. Levee deposits are very difficult to identify in the field and in most cases presumed to be absent, because the channel-fills indicate a gradual lateral transition into overflow deposits. Three types of overflow deposits are recognized in FS 5:

- 1) X-type, which comprise thick, ripple cross-laminated sandstones alternating with very thin layers of siltstones near the channel margin (10 - 400 m),
- 2) Y-type overflow deposits comprising thinner sandstone beds with thicker siltstone layers further away from the channel margin (500 – 3 km) and
- 3) Z-type deposits most distal from the channel margin (3 - 10 km) representing the transition of thin sandstone units into basin shales. The Z-type overflow units comprise predominantly very thin-bedded, ripple cross-laminated sandstones and silty-shale layers. The overflow deposits occur predominantly in the mid-fan and upper fan environment.

The sheet sand deposits constitute 30% of the outcrop area in FS 5. The two main sheet sand and sheet lobes occur in the Blaauwheuwel 121 and Zoetmeisjes Fontein 75 areas. Three types of sheet sandstones were identified in the field:

- 1) O-type sheet sandstones comprising thick, massive structureless beds (2-4m), close to the channel mouth (10 – 1km),
- 2) P-type sheet deposits comprising thinner sandstone beds (30 cm – 1 m), further away from the O-type deposits (1km – 8 km) and
- 3) Q-type sheet deposits furthest away from the depositional channel mouth. The latter comprise very thin-bedded, parallel-laminated sand-silt-shale layers that eventually change into basin shales, indicating gradual fan termination.

Overflow and sheet deposits are distinguished on the basis of thickness and internal structural development, which directly relate to the distance from the channel margins. This makes the interpretation for the location of sheet or overflow deposits more precise in terms of distance from the channel margin or channel mouth.

Massive slump deposits occur in the most proximal outcrops of FS 5. These outcrops (Groot Hangklip and Kalkgat areas) comprise steep concave erosional channels, chiefly filled with massive chaotic slump and dewatered sandstone and siltstone deposits. The slumps display soft-sediment deformation and dewatering structures, which are indicative of very unstable and high-energy conditions. These deposits do not correlate with the adjacent turbidite flows of FS 5, which indicates a separate slope unit within the FS 5 succession. Thick-bedded overflow deposits, which comprise ball-and-pillow and dewatered sandstones, occur along the margins of these slump channels. They thin out in less than 6 km from the channel margins.

6.2 Stages of fan development

Exposures of FS 5 indicate lateral and vertical development of six depositional sandstone units. Three of these sand-rich units, namely lower-Tongberg, Klein Hangklip and Blauwkop, form the lower initial conduits of fan deposition. The lower-Tongberg and Klein Hangklip outcrops are characterized by confined channel systems, which are divided into three channel complexes. This division in the channelized environment indicates a mid-fan depositional setting, which hosts both confined and unconfined channels. The variation in Palaeoflow directions within the channel-fills suggests deposition from confined to less-confined flows. The Blauwkop outcrops are characterized by a distributary channel system, comprising amalgamated sandstone packages. This system developed into a depositional sheet lobe and sheet deposits in the down-dip direction. The Blauwkop unit forms part of the lower fan environment where deposition from unconfined flows predominated. The sheet sands gradually thin out until they terminate within the basin shales.

The lower-Tongberg, Klein Hangklip and Blauwkop units (TKB) represent a typical prograding system, which developed from the initial Klein Hangklip conduits into the lower fan distributary channel and sheet sand systems of Blauwkop. The GHK and KG units, which correlate with each

other, are interpreted as the same sand-rich unit, deposited in a base-of-slope to lower slope environment. The Palaeoflow direction is similar to the main flow direction of FS 5, which indicates a similar source area as for the TKB units. Deposition of this slump-dominated unit suggests a period of tectonic instability caused by the proximity of the syntaxial structures.

The uppermost and final sand-rich turbidites of FS 5 constitute part of the Skoorsteenbergs unit and the upper Tongberg unit. The Skoorsteenbergs (SB) unit forms the northernmost outcrops of FS 5. It consists of amalgamated, massive sandstone packages within a channelized system comprising low width:depth ratio channel-fills. The channelized deposits change downstream, over a very short distance, into depositional sheet lobes and sheet deposits with single small splay channels. This transition indicates that the channelized area of the SB unit forms part of a lower mid-fan environment, which developed into a lower fan and eventually into a gradual fan pinch out. The depositional pattern of the SB unit indicates progradation into the basin, and was characterized by three distinct constructional phases. Erosional surfaces into the underlying units characterize the initial phase, progradation and aggradation of massive amalgamated sandstone units characterize the second phase, whereas the final phase is characterized by abandonment and retrogradation in the upper part of the unit. It is in this final phase that small splay channel-fills might still have developed within the thin-bedded upper units.

The upper Tongberg unit consists of two small channel-fills, which were deposited within thin-bedded overflow units. The fills comprise layered beds, which could have been deposited during the retrogradational phases of deposition within FS 5. These deposits occur on the same stratigraphic level within FS 5 as the SB unit, but direct correlation could not be demonstrated.

Thus, four stages of unit development could be identified within FS 5. Each of these units was deposited within a different stratigraphic time frame. The upper 5 – 10 m of FS 5 contains thin beds, with bioturbation and small wave-ripple structures with amplitudes of 0.5-2 cm and wavelengths of 15 – 30 cm. This might reflect shallow, wave base conditions, but more research needs to be done on this subject, because similar symmetrical ripples were noted, but not interpreted, at a water depth of nearly 3 km from the Yap Ridge, east of the Philippines (Fujioka *et al.*, 1989). These beds are overlain by a condensed section, which indicates a subsequent rise in sea-level.

6.3 Depositional model

6.3.1 Type of slope setting

The zone where the slope meets the basin plain is called the base-of-slope or toe-of-slope (Prather, 2003). The erosional conduit (upper fan channel) that runs downs the slope becomes depositional in this part. The base-of-slope area is an important depositional zone that aggrades at a depositional angle of $0.2 - 1.2^\circ$. Once the upper fan channel is formed by a massive slide/slump, it is normally too wide for the density currents that follow, especially in the down-dip part. The result is a complex of channel-fills with erosion between succeeding major currents, resulting in amalgamated sand-on-sand contacts. Channels act as conduits for a long time before they eventually fill up. The initial flows are strongly erosional, the following flows somewhat less erosional and more depositional. Final infill takes place during the abandonment phase. Amalgamated contacts result and overflows can be constructed during the active phase of sediment transport and deposition. Currents commonly shift laterally to make use of a more favourable gradient, thereby eroding a significant part of the earlier channel and its X-type overflow deposits. Interaction of strong and weaker density currents of different sizes produces a rich variety in the size of channel-fills with amalgamated contacts.

Deposition that took place up-dip from the GHK and TKB section was removed by modern day erosion. The interpretation of a base-of-slope depositional position is therefore considered a strong possibility. The majority of the sediment, however, would have bypassed this region. In the base-of-slope area, often some widening and shoaling of the conduit can be observed, such as the Klein Hangklip and Tongberg units. This, together with the fact that the sediment transport energy decreases, will result in the formation and filling of channels that are very wide and shallow, but seldom reach from one side of the conduit to the other. Thus, the TKB, GHK and KG units were deposited in a base-of-slope area and the SB unit was deposited in a mid- to lower-fan environment.

6.3.2 Multi-source versus Point-source deposition

Most present day depositional models are constructed for basin floor- and slope fan systems, deposited from a single point source feeder system. The fine-grained depositional model of Bouma (2000) has been compiled for a basin floor-fan environment with the lower four fans of the Tanqua sub-basin as analogue. The variation in stratigraphical position and Palaeoflow directions of the different units of FS 5 suggest the possibility of more than one feeder system. The Bouma fine-grained model therefore remains a good analogue for the individual units of FS 5. However, the various depositional patterns of these units within FS 5 require a new model or an upgrade from the existing one. Both a point-source and multi-source model could be used to explain the deposition of FS 5.

Heller and Dickinson (1985) propose a multi-entry source model for a ramp, delta-fed, sand-rich turbidite system (Section 3, Fig. 3.5). However, due to the lack of outcrop and modern examples for this model, it has been overwhelmed by the point-source models. The sedimentary characteristics of each unit in FS 5 differ from one another and the layered deposits between the sand-rich units comprise overflow and sheet deposits of previous flows from neighbouring localities. In addition, the absence of any significant major basin floor structures, which could have caused deviations of turbidite flows in different directions, led to the conclusion that more than one entry point delivered sediments onto the base-of-slope (Fig. 6.1). The GHK and KG units suggests the most southerly entry point whereas the TKB and SB units suggest medial and westerly entry points respectively (Fig. 6.1). The upper Tongberg channel-fills might be associated with renewed sediment bypass and deposition from the original TKB entry point (Fig. 6.1). The multi-source model could explain the autocyclic depositional patterns and the down-lapping nature of the GHK+KG unit onto the lower TKB unit from the south.

The Palaeoflow directions of all the FS 5 units indicate a mean value towards the northeast. This evidence suggests a possible point source model for FS 5 (Fig. 6.2). Possible avulsion events during deposition of the units of FS 5 would suggest that fundamental changes in flow parameters must have occurred from the point source to the base-of-slope (Fig. 6.2). The most likely cause was increased flow discharge at times. Such increased discharge would have resulted in enhanced overspill associated with the confined channel margins (Fig. 6.2). This would explain the depositional changes from the TBK to the GHK+KG and SB units (Fig. 6.2). The SB

unit almost gives the impression of an oversize crevasse splay development. Increased flow discharge probably led to increased delivery of sediment volumes from the deltaic source systems to the shelf edge. This increased sediment flux could perhaps be compared to the Mississippi River discharge spikes caused by abrupt draining of Pleistocene pro-glacial lakes or abrupt shifts of drainage divides resulting in glacial melt water being directed down the Mississippi system (Hall and Link, 1990; Teller, 1990; Licciardi *et al.*, 1999; Blum *et al.*, 2000).

Both these models could explain the depositional history of FS 5. However, due to modern day erosion of the proximal outcrops of this fan system, both these models are inconclusive and at this stage only hypothetical.

6.3.3 Sequence stratigraphy

Sea-level fluctuation has played a fundamental role in the deposition of the FS 5. Each of the basin floor fans in the Tanqua sub-basin represents a fourth-order lowstand sequence, whereas the units within FS 5 represent fifth-order sequences. Individual sub units within these units would then be a high-resolution sixth-order sequence. The condensed sections represent the most reliable correlation markers within FS 5. Three types were identified based on their facies and distribution (Johnson *et al.* 2001). Type 1 condensed sections only occur in the lower interfan unit between Fan 4 and FS 5 and the upper succession overlying FS 5. This type of condensed section occurs regionally and forms part of the TST and HST during sea-level rise. Type 2 condensed sections form the intervals between the successive units in FS 5 and represents a Type B transgressive surface (Sixsmith, 2000). Type 3 condensed sections have limited extent and only occur in small localities between the sixth-order sequence packages.

The TKB system was deposited during the first lowstand fifth-order cycle. This cycle could be divided into numerous small sub-cycles, which formed sixth-order and possibly seventh-order sequences. A short period of sea-level rise, which caused the deposition of a Type 2 condensed section, ended abruptly with sea-level fall. This caused deposition of the high-energy slump unit of GHK and KG in a lowstand fifth-order sequence. After a second period of sea-level rise and deposition of a Type 2 condensed section, an immediate, but more gradual sea-level fall caused the formation of the SB and upper Tongberg lowstand fifth-order sequence packages. The uppermost 10 m succession of wavy bedded units in FS 5 forms part of the LLST of the SB unit,

overlain by a MFFS and dark hemipelagic shale, which was deposited during the TST and HST of sea-level rise.

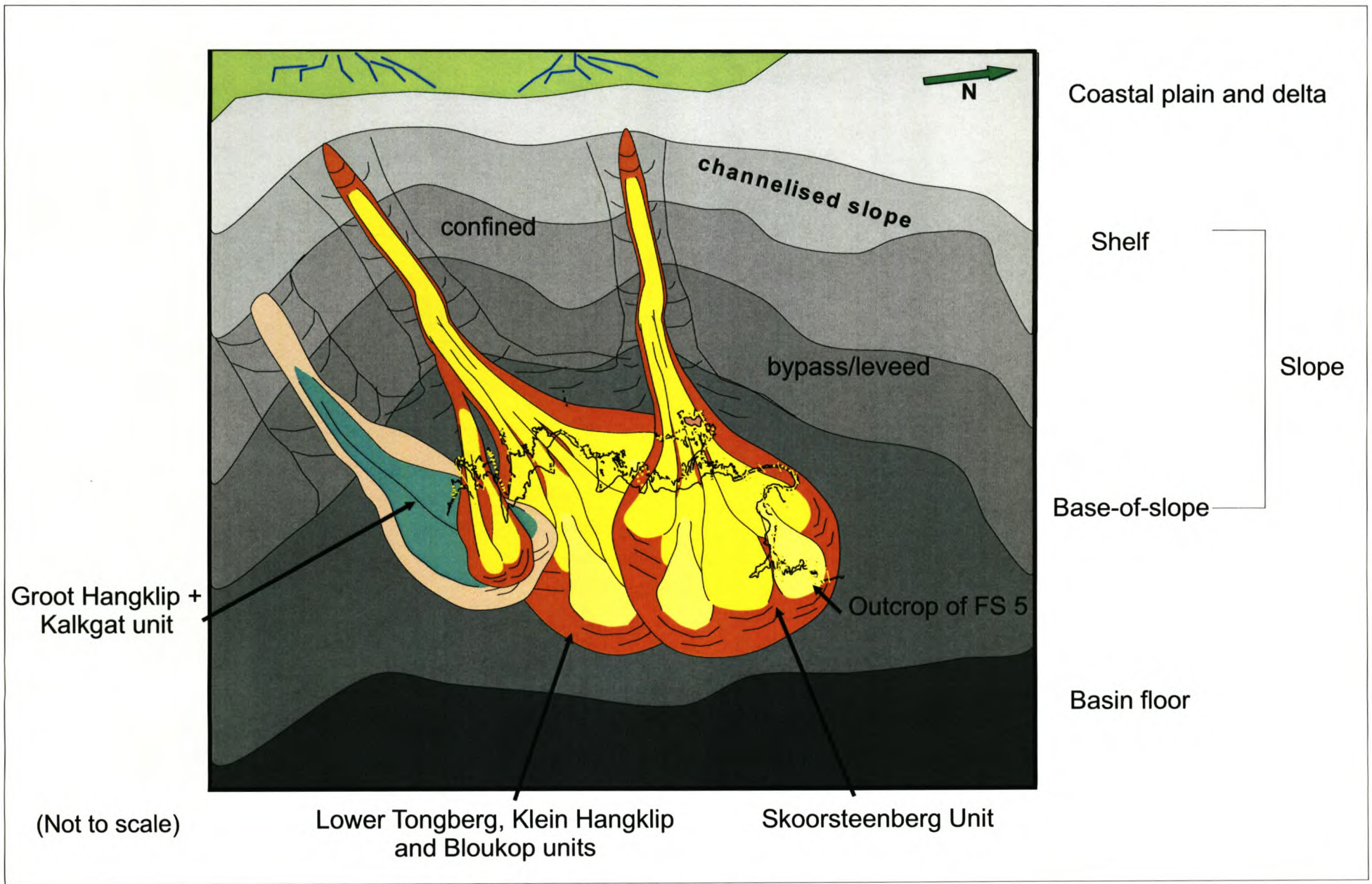


Figure 6.1 Possible multi-source model for FS 5. Note the outcrop map of FS 5.

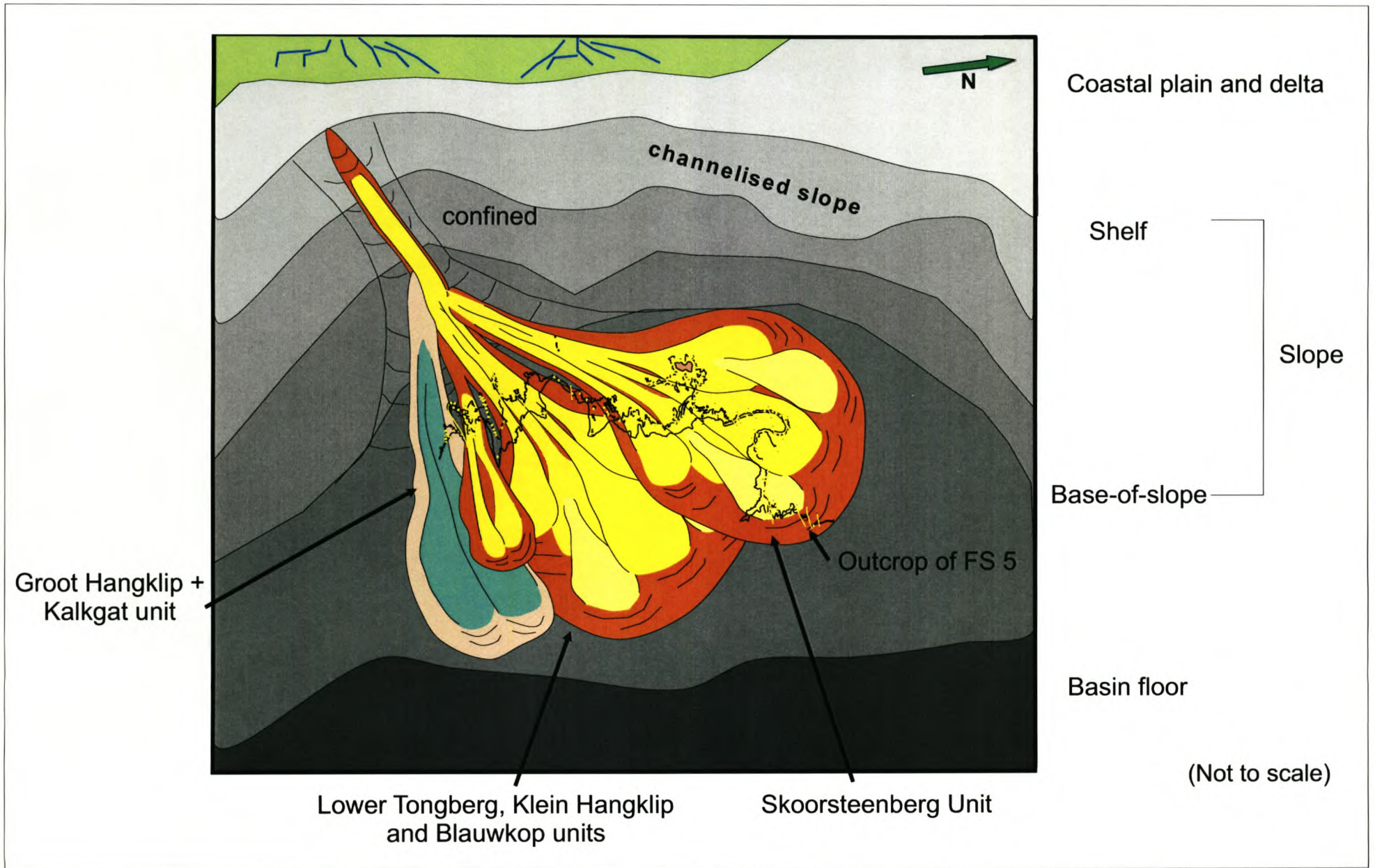


Figure 6.2 Possible point-source model for FS 5. Note the outcrop map of FS 5.

Chapter 7

Conclusions

Chapter 7

Conclusions

1. Three post-depositional structural domains were identified in the outcrop of FS 5, namely the Droogekloof, Brakke Rivier and Brandhoek provinces. They were caused by late-stage post-depositional structural movement within the CFB. The Droogekloof province was the most active structural province, because this area is closely associated with the mega-Baviaanshoek anticlinal structure to the south. The channel complexes of the Klein Hangklip, Groot Hangklip, Tongberg and Kalkgat units were deposited in this structural province. The distribution and concentration of the channel-complexes within the Klein Hangklip unit seem to have been dictated by syn-depositional folding.
2. Ten lithofacies associations were identified within FS 5. These include massive structureless sandstones and bypass lag deposits, which are characteristic in the channel-fill environment. Thin, sheet-like ripple cross-laminated sandstones and siltstones constitute the overflow facies. Massive and thin-bedded sheet sandstones form the down-dip extensions in the spreading depositional environments. Wavy and sigmoidal ripple-laminated sand- and siltstones are abundant in the upper abandonment facies of FS 5. Thinly bedded sandstone and siltstone intercalated with frequent mudstone intervals, record the most distal expressions of the turbidites. Chaotic slumps with abundant soft-sediment deformation structures occur in the unstable channelized environment of GHK and KG. Dark hemipelagic shales occur at the base and top of the FS 5 succession.
3. The main architectural elements are channel complexes that consist of vertically and laterally stacked channel-fills. Lateral accretion deposits are associated with the channelized and bypass facies environments and prove lateral migration of low-sinuosity channels. The X, Y and Z type of overflow deposits occur along the channel margins. The X-type overflows were deposited closest to the channel margins, comprise thick, ripple cross-laminated layers, whereas the Z-type overflows were deposited furthest from the margins, and comprise very thin ripple cross-laminated layers of sandstone/siltstone. O, P and Q-type deposits form the sheet-sand deposits. The O-type comprise massive, thick

sandstone units closest to the channel mouth, whereas the Q-type were deposited in the distal-fan environment and consist of thin sand-silt layers, which eventually pinch out. The unstable slump deposits consist of sandstone beds displaying ball-and-pillow and dewatered structures and indicate a highly unstable depositional area.

4. Fan System 5 is the uppermost and final submarine fan system in the Tanqua sub-basin. This 107 m thick succession represents six depositional units, which were deposited on different stratigraphic time-levels within the FS 5 succession. The TKB unit was deposited first. It developed confined channel complexes in the most proximal setting, followed by a distributary mid-fan channel complex and a lower-fan sheet sand in a down-fan direction. The GHK and KG units record the second phase of deposition and comprise highly unstable slump sediments, which originated from a lower slope environment. The SB unit represents the final and uppermost turbidite deposits of the FS 5 succession. The outcrops reflect deposition in a lower-mid fan distributary channel complex, which developed into a lower and distal-fan sheet sand depositional environment. The upper Tongberg channel-fills represent late stage crevasse splay channels.
5. Three types of condensed intervals have been recognised within FS 5. They are divided into three types, based on lithofacies association and thickness. The Type 1 condensed section intervals (hemipelagic shale intervals) could be interpreted as TSTs and HSTs of third- and fourth-order sea-level cycles. The Type 2 condensed intervals (thin-bedded sand and siltstones) are interpreted as Type B transgressive units of fifth-order sea-level cycles. The different units within FS 5 are interpreted as LSTs of these fifth-order cycles. Type 3 condensed intervals, which were deposited more locally and on small scale, subdivide the depositional units into ultra-high sequences, which represent possible sixth- and seventh-order lowstand sea level cycles.
6. Two possible depositional models have been compiled for deposition of FS 5 in a base-of-slope environment. The multi-source model suggests the possibility of three entry points, which deposited the TKB, upper Tongberg, SB and GHK + KG as separate units. The point-source model suggests a single entry point with deposition of the units in the transition zone from lower slope to base-of-slope. Both these models work for the

sequence stratigraphic interpretations, but the multi-source model indicates direct relationship to sea-level fluctuations and the point source model to autocyclic processes.

7. Termination of FS 5 is characterized in the north by a gradual transition from sand-rich beds into siltstone beds and eventually into basin plain shales. This occurred in both the TKB and SB units. The termination of FS 5 in the south of the outcrop area is abrupt and associated with the highly erosive Kalkgat slump-filled channels.
8. The occurrence and distribution of clastic sandstone dykes in the south of the study area seems to reflect tectonic instability during deposition of FS 5. This instability was probably related to the growth of the syntaxis anticlinoria structures, i.e. the Hex River and Baviaanshoek, south of the Tanqua sub-basin.

References

References

Abreu, V.S. and Anderson, J.B. (1998) Glacial eustasy during the Cenozoic: Sequence stratigraphic implications. *AAPG Bulletin*, Vol. **82** (7), pp. 1385-1400

Abreu, V.S., Sullivan, M., Pirmez, C. and Mohrig, D. (2003) Lateral accretion packages (LAPs): an important reservoir element in deep-water sinuous channels. *Marine and Petroleum Geology*. Vol. **20**, pp. 631-648

Allen, J.R.L. (1982) *Sedimentary Structures: Their character and physical basis*. Amsterdam, Elsevier. Vols. **1&2**

Allen, J.R.L. and Leeder, M.R. (1980) Criteria for the instability of upper-stage plane beds. *Sedimentology*. Vol. **27**, pp. 209-217

Anderson, J.M. and Cruickshank, A.R.I. (1978) The biostratigraphy of the Permian and Triassic. Part 5: A review of the classification and distribution of Permo-Triassic tetrapods. *Palaeontologia Africana*, Vol. **21**, pp. 15-44

Andersson, P.O.D., Johansson, A. and Kumpulainen, R.A. (2003) Sm-Nd isotope evidence for the provenance of the Skoorsteenberg Formation, Karoo Supergroup, South Africa. *Journal of African Earth Sciences*, Vol. **36**, pp. 173-183

Bagnold, R.A. (1956) An approach to the sediment transport problem from general physics. *Professional Papers of the United States Geological Survey*. pp. 442

Bangert, B., Stollhofen, H., Lorenz, V. and Armstrong, R. (1999) The geochronology and significance of ash-fall tuffs in the glaciogenic Carboniferous-Permian Dwyka Group of Namibia and South Africa. *Journal of African Earth Sciences*. Vol. **29** (1), pp. 33-49

Basu, D. (1992) A Channel-Levee/Overbank Deposits at Bloukop: Architecture and Development. *Tanqua Report, Geo-Marine Consultants, inc.* Vol. **2**, pp. 20 1-17

Basu, D. and Bouma, A.H. (2000) Thin-Bedded Turbidites of the Tanqua Karoo: Physical and Depositional Characteristics. In: Bouma, A.H and Stone, C.G. (Eds.). Fine-grained Turbidite Systems. *AAPG Memoir 72/SEPM Special Publication*, **Vol. 68**, pp. 263-278

Beaubouef, R.T., Rossen, C., Zelt, F.B., Sullivan, M.D., Mohrig, D.C. and Jennette, D.C. (1999) Deep-Water Sandstones, Brushy Canyon Formation, West Texas (Field Guide for AAPG Hedberg Field Research Conference – April 15-20, 1999) . *AAPG Continuing Education Course Note Series. AAPG, Tulsa*. **Vol. 40**, pp. 50

Blum, M.D., Guccione, M.J., Wysocki, D.A., Robnett, P.C. and Rutledge, E.M. (2000) Late Pleistocene evolution of the lower Mississippi River Valley, southern Missouri to Arkansas. *GSA Bulletin*. **Vol. 112**, pp. 221-235

Boggs Jr., S. (2001) *Principles of Sedimentology and Stratigraphy*. 3rd ed.: Prentice Hall, New Jersey. pp. 774

Bouma, A.H. (1962) *Sedimentology of some Flysch deposits, a graphic approach to facies interpretation*. Elsevier, Amsterdam. pp. 168

Bouma, A.H. (1995) Review of Fine-Grained Submarine Fans and Turbidite Systems. Tanqua Report, *Geo-Marine Consultants, inc.* pp. 1-73

Bouma, A.H. (2000) Coarse-grained and fine-grained turbidite systems as end member models: applicability and dangers. *Marine and Petroleum Geology*, **Vol. 17**, pp. 137 – 143

Bouma, A.H. and Wickens, H. de V. (1991) Permian passive margin submarine fan complex, Karoo Basin, South Africa: possible model to Gulf of Mexico. *Gulf Coast Association Geological Societies Transactions*, **Vol. 41**, pp. 30 – 42

Bouma, A.H. and Wickens, H. de V. (1992) Photographic mosaics of cliff sections. Tanqua Report, *Geo-Marine Consultants, inc.* **Vol. 2**, pp. 23-1 - 25-5

Bouma, A.H., and Wickens, H. de V. (1994) Tanqua Karoo, ancient analog for fine-grained submarine fans, in P. Weimer, A.H. Bouma, and B.F. Perkins, Eds., Submarine fans and turbidite systems: sequence stratigraphy, reservoir architecture and production characteristics, *Gulf of Mexico and international: Gulf Coast Section SEPM foundation, 15th Annual Research Conference Proceedings* pp. 23 – 34

Bouma, A.H., Wickens, H. de V. and Coleman, J.M. (1995) Architectural characteristics of fine-grained submarine fans: a model applicable to the Gulf of Mexico. *Gulf Coast Association of Geological Societies Transactions*. **Vol. 45**, pp. 71-75

Breitzkreuz, C., Bahlburg, H., Delakowitz, B. and Pichowiak, S. (1989) Palaeozoic volcanic events in the Central Andes. *Journal of South American Earth Sciences*. **Vol. 2**, pp. 171-189

Brink, G.J. (1992) High-frequency sequence stratigraphy of the Ecca Group, Tanqua Sub basin, South Africa. In: Tanqua Karoo Report. *Geo-Marine Consultants, inc.* **Vol. 1**, pp. 14-1 – 14-7

Burgess, P.M., Flint, S. and Johnson, S. (2000) Sequence stratigraphic interpretation of turbidite strata: An example from Jurassic strata of the Neuquén basin, Argentina. *GSA Bulletin*, **Vol. 112** (11), pp. 1650-1666

Castro, I.P. and Snyder, W.H. (1993) Experiments on wave breaking in stratified flow over obstacles. *Journal of Fluid Mechanisms*. **Vol. 255**, pp. 195-211

Catuneanu, O. (2002) Sequence stratigraphy of clastic systems: concepts, merits, and pitfalls. *Journal of African Earth Sciences*. **Vol. 35**, pp. 1-43

Catuneanu, O., Hancox, P.J. and Rubidge, B.S. (1998) Reciprocal flexural behavior and contrasting stratigraphy: a new basin development model for the Karoo retro arc foreland system, South Africa: *Basin Research*. **Vol. 10**, pp. 417 – 439

Clark, J.D. and Pickering, K.T. (1996) Architectural elements and growth patterns of submarine channels: Application to hydrocarbon Exploration. *AAPG Bulletin*. **Vol. 80** (2), pp194-221

Cole, D.I. (1992) Evolution and development of the Karoo Basin. In: de Wit, M.J. and Ransom, I.G.D. (Eds.). *Inversion Tectonics of the Cape Fold Belt, Karoo and Cretaceous Basins of Southern Africa*. A.A. Balkema, Rotterdam. pp. 87-99

Cole, D.I. and McLachlan, I.R. (1991) Oil potential of the Permian Whitehill Shale Formation in the main Karoo Basin, South Africa. In: Ulbrich, H. and Campos, A.R (Eds.) *Gondwana seven proceedings*. Instituto de Geociencias, Univ.de Saõ Paulo, Brazil. pp. 279-390

Collinson, J.D. and Thompson, D.B. (1989) *Sedimentary structures*, 2nd ed.: Chapman and Hall, London. pp. 207

Cromwell, J.C. (1957) Origin of pebbly mudstone. *Geology Society of America Bulletin*. **Vol. 63**, pp. 993-1010

De Beer, C.H. (1990) Simultaneous folding in the western and southern branches of the Cape Fold Belt. *South African Journal of Geology*. **Vol. 93**, pp. 583-591

De Beer, C.H. (1992) Structural evolution of the Cape Fold Belt syntaxis and its influence on syntectonical sedimentation in the SW Karoo Basin. In: De Wit, M.J. and Ransome, I.G.D. (Eds.), *Inversion Tectonics of the Cape Fold Belt, Karoo and Cretaceous Basins of Southern Africa*. A.A. Balkema, Rotterdam. pp. 197-206.

De Beer, C.H. (1995) Fold interference from simultaneous shortening in different directions: the Cape Fold Belt syntaxis. *Journal of African Earth Sciences*. **Vol. 21** (1), pp. 157 – 169

Deptuck, M.E., Steffens, G.S., Barton, M. and Pirmez, C. (2003) Architecture and evolution of upper fan channel-belts on the Niger Delta slope and in the Arabian Sea. *Marine and Petroleum Geology*. **Vol. 20**, pp. 649-676

De Wit, M.J. and Ransome, I.G.D. (1992) Regional inversion tectonics along the southern margin of Gondwana. **In:** De Wit, M.J. and Ransome, I.G.D. (Eds.) *Inversion Tectonics of the Cape Fold Belt, Karoo and Cretaceous Basins of Southern Africa*. A.A. Balkema, Rotterdam. pp. 15-21

Dzulynski, S. and Sanders, J.E. (1962) Current marks on firm mud bottoms. *Transactions of the Connecticut Academy of Arts and Sciences*. **Vol. 42**, pp. 57-96

Elliott, T. (2000) Depositional architecture of a sand-rich, channelized turbidite system: The Upper Carboniferous Ross Sandstone Formation, Western Ireland. **In:** Weimer, P, Slatt, R.M., Bouma, A.H. and Lawrence (Eds.). Deep-water reservoirs of the world. *Gulf Coast Section Society of Economic Paleontologists and Mineralogists Foundation 20th annual research conference*. pp. 342-372

Eschard, R., Albouy, E., Deschamps, R., Euzen, T. and Ayub, A. (2003) Downstream evolution of turbiditic channel complexes in the Pab Range outcrops (Maastrichtian, Pakistan). *Marine and Petroleum Geology*. **Vol. 20**, pp. 691-710

Flood, R.D. (1988) A lee wave model for deep-sea mud wave activity. *Deep Sea Res.* **Vol. 35**, pp. 973-983

Friès, G. and Parize, O. (2003) Anatomy of ancient passive margin slope systems: Aptian gravity-driven deposition on the Vocontian palaeomargin, western Alps, south-east France. *Sedimentology*. **Vol. 50**, pp. 1231-1270

Fujioka, K., Watanabe, M.E. and Kobayashi, K. (1989) Deep-sea photographs of the Northwestern and Central Pacific Ocean – An invitation to deep-sea environment. *Bulletin of the Ocean Research Institute, University of Tokyo*. **Vol. 27**, pp. 1-214

Galloway, W.E (1989) Genetic stratigraphic sequences in basin analysis, I. Architecture and genesis of flooding-surface bounded depositional units. *AAPG Bulletin*. **Vol. 73**, pp. 125-142

Galloway, W.E and Hobday, D.K. (1983) *Terrigenous clastic depositional systems: Applications to petroleum, coal, and uranium exploration*. New York: Springer. pp. 416

Gamundí López, O.R. and Rossello, E.A. (1998) Basin fill evolution and paleotectonic patterns along the Samfrau geosyncline: the Sauce Grande basin – Ventana foldbelt (Argentina) and Karoo basin – Cape Fold Belt (South Africa) revisited. *Geology Rundsch.* **Vol. 86**, pp. 819-834

Gardner, M.H. and Borer, J.M. (2000) Submarine channel architecture along a slope-to-base profile, Brushy Canyon Formation, West Texas. In Bouma A. and Stone, C, (Eds.) Fine-grained turbidite systems. *AAPG Memoir, 72 SEPM Special Publ.* **Vol. 68**, pp. 195-214

Geertsema, H. and Van den Heever, J.A. (1996) A new beetle, *Afrocupes firmae* gen. et sp. nov. (Permocupedidae), from Late Palaeozoic Whitehill Formation of South Africa. *South African Journal of Science.* **Vol. 92**, pp. 497-499

Geertsema, H. and Van den Heever, J.A. (2000) First record of a late Cretaceous-Palaeocene tenebrionid from southern Africa. *South African Journal of Science.* **Vol. 96**, pp. 553-555

Goldhammer, R.K., Wickens, H. De V., Bouma, A.H. and Wach, G. (2000) Sequence Stratigraphic Architecture of the Late Permian Tanqua Submarine Fan Complex, Karoo Basin, South Africa. In: Bouma, A.H and Stone, C.G. (Eds.). Fine-grained Turbidite Systems. *AAPG Memoir 72/SEPM Special Publication*, **Vol. 68**, pp. 165-172

Hälbich, I.W., Fitch, F.J. and Miller, J.A. (1983) Dating the Cape Orogeny. In: Söhnge, A.P.G. and Hälbich, I.W. (Eds.) Geodynamics of the Cape Fold Belt. *Special Publication Geology Society of South Africa.* **Vol. 12**, pp.165-175

Hall, B.A. (1973) Slump folds and the determination of palaeoslope. *Abstract. Progression Geology Society of America. Vol. 5*, pp. 648

Hall, B.R. and Link, M.H. (1990) Reservoir description of a Miocene turbidite sandstone, Midway-Sunset Field, California. In: Barwis, McPherson and Studlick (Eds.). *Sandstone Petroleum Reservoirs: Casebook in Earth Science*. Springer-Verlag, New York. pp. 509-533

Haq, B.U. and Van Eysinga, F.W.B. (1987) *Geological Time Table* (4th edition). Elsevier, Amsterdam.

Heller, P.L. and Dickinson, W.R. (1985) Submarine ramp facies model for delta-fed, sand-rich turbidite systems. *AAPG Bulletin. Vol. 69*, pp. 960-976

Hodgson, D.M., Flint, S.S., Hodgetts, D., Drinkwater, N.J., Johannesson, E.P. and Luthi, S.M. (2006) Stratigraphic evolution of Permian submarine fan systems, Tanqua depocenter, South Africa. *Journal of Sedimentary Research. Vol. 76*, pp. 19-39

Hunt, D. and Tucker, M.E. (1992) Stranded parasquences and the forced regressive wedge systems tract: deposition during base-level fall. *Sedimentary Geology. Vol. 81*, pp. 1-9

Imperato, D.P. and Nilsen, T.H. (1990) Deep-sea-fan channel-levee complexes, Arbuckle Field, Sacramento Basin, California. In: Barwis, McPherson and Studlick (Eds.). *Sandstone Petroleum Reservoirs: Casebook in Earth Science*. Springer-Verlag, New York. pp. 535-555

Johnson, M.R. (1991) Sandstone petrography, provenance and plate tectonic setting in Gondwana context of the southeastern Cape-Karoo Basin. *South African Journal of Geology. Vol. 94*, pp.137-154.

Johnson, S.D. and Hadler-Jacobsen, F. (2001) Field Guide for AAPG Hedberg Field Research Conference: Deep –Water Sandstones, Tanqua Karoo, South Africa. Den Norske Stats Olje Selskap: STATOIL. pp. 69

Johnson, S.D., Flint, S., Hinds, D. and Wickens, H. de V. (2001) Anatomy, geometry and sequence stratigraphy of basin floor to slope turbidite systems, Tanqua Karoo, South Africa. *Sedimentology*. **Vol. 48**, pp. 987-1023

Jopling, A.V. and Walker, R.G. (1968) Morphology and origin of ripple-drift cross-lamination, with examples from the Pleistocene of Massachusetts. *Journal Sedimentary Petrology*. **Vol. 38**, pp. 971-984

Kingsley, C.S. (1977) *Stratigraphy and Sedimentology of the Eccca Group in the Eastern Cape Province, South Africa*. Unpub. Ph.D thesis, Univ. Port Elizabeth. pp. 296

Kirschner, R.H. and Bouma, A.H. (2000) Characteristics of a Distributary Channel-Levee-Overbank System, Tanqua Karoo. In: Bouma, A.H. and Stone, C.G. (Eds.) Fine-grained turbidite systems, *AAPG Memoir 72/SEMP Special Publication*. **Vol. 68**, pp. 233-244

Kneller, B.C. and Branney, M.J. (1995) Sustained high-density turbidity currents and the deposition of thick, massive sands. *Sedimentology*. **Vol. 42**, pp. 607-616

Kuenen, Ph. H. (1953) Graded bedding with observations on Lower Paleozoic rocks of Britain. *Verhandl. Koninkl. Nederlandse Akademiese Wetenschap. Amsterdam, Afdeling Natuur*. **Vol. 20**, pp. 1-47

Kuenen, Ph. H. (1958) Experiments in geology. *Transactions Geology Society of Glasgow*. **Vol. 23**, pp. 1-58

Kuenen, Ph. H. (1967) Emplacement of Flysch-type sand beds. *Sedimentology*. **Vol. 9**, pp. 203-243

Kuenen, Ph. H. and Migliorini, C.I. (1950) Turbidity currents as a cause of graded bedding. *The Journal of Geology*. **Vol. 58** (2), pp.91-127

Licciardi, J.M., Teller, J.T. and Clark, P.U. (1999) Freshwater routing by the Laurentide Ice Sheet during the last deglaciation. **In:** Clark, P.U., Webb, R.S. and Deigwin, L.D. (Eds.) Mechanism of Global Climate Change at Millennial Time Scales, *America Geophysical Union*. pp. 177-201

Lein, T., Walker, R.G. and Martinsen, O.J. (2003) Turbidites in the Upper Carboniferous Ross Formation, western Ireland – reconstruction of a channel and spillover system. *Sedimentology*. **Vol. 50**, pp. 113-148

Lowe, D.R. (1988) Suspended load fallout-rate as an independent variable in the analysis of current structures. *Sedimentology*. **Vol. 35**, pp. 765-776

Marot, J.E.B. (1992) Petrography of selected Tanqua Karoo sandstones. Karoo Field report. *Geo-Marine Consultants, Inc.* **Vol. 1**, pp. 11 1-11

Martinsen, O.J., Lien, T. and Walker, R.W. (2003) Facies and sequential organisation of a mudstone-dominated slope and basin floor succession: The Gull Island Formation, Shannon Basin, Western Island. *Marine and Petroleum Geology*. **Vol. 20**, pp. 131-134

McCave, I.N. and Tucholke, B.E. (1986) Deep-current controlled sedimentation in the western North Atlantic. **In:** Vogt, P.R. and Tucholke, B.E. (Eds.) The Geology of North America, the Western North Atlantic Region. *Geological Society of America*, Boulder. **Vol. M**, pp. 1117-1126

Mitchum, R.M. (1977) Seismic stratigraphy and global changes of sea level, Part 1: Glossary of terms used in seismic stratigraphy. **In:** Payton, C.E. (Ed.) Seismic Stratigraphy – Applications to Hydrocarbon Exploration. *AAPG Memoir*. **Vol.26**, pp. 205-212

Mitchum, Jr. R.M. and Van Wagoner, J.C. (1991) High-frequency sequences and their stacking patterns: sequence-stratigraphic evidence of high-frequency eustatic cycles. *Sedimentary Geology*. Vol. 70, pp. 131-160

Morris, W.R., Scheihing, M.H., and Wickens, H. de V. (2001) *Depositional Environments and Reservoir Architecture of Deepwater Sandstones of the Tanqua Karoo Sub-basin, South Africa: A Field Seminar*. Field guidebook. Kuparuk Geoscience Group, Phillips Alaska Inc. pp. 112

Mutti, E. (1992) *Turbidite Sandstones*. Agip and Instituto di Geologia, Univ. Parma. pp. 275

Mutti, E. and Normark, W.R. (1987) Comparing examples of modern and ancient turbidite systems: Problems and concepts. In: Leggett, J.K. and Zuffa, G.G. (Eds.), *Marine Clastic Sedimentology: Concepts and Case Studies*. Graham and Trotman, London. pp. 1-38

Mutti, E. and Ricci Lucchi, F. (1972) Le torbiditi dell'Appennino Settentrionale: Introduzione all'analisi di facies. *Memorie della Società Geologica Italiana*. Vol. 11 pp. 161-199 (Translated into English by T.H. Nilsen, 1978, *International Geological Review*. Vol. 20, pp. 125-166

Mutti, E. and Ricci Lucchi, F. (1975) Turbidite facies and facies associations. Field Trip Guidebook A-11. 9th *International Sedimentology Congress*, Nice, France. pp. 21-36

Neetling, B.C. (1992) The Depositional characteristics of submarine Fan 6 in the Tanqua sub-basin, Permian Ecca Group, South Africa. Tanqua Karoo Field report. *Geo-Marine Consultants, Inc.* Vol. 2, pp. 21 1 – 31

Normark, W.R. (1970) Growth patterns of deep-sea fans. *AAPG Bulletin*. Vol. 54, pp. 2170-2195

Normark, W.R. (1978) Fan valleys, channels, and depositional lobes on modern submarine fans: characters for recognition of sandy turbidite environments. *AAPG Bulletin*. Vol. 62, pp. 912-931

Pickering, K.T., Stow, D.A.V., Watson, M.P. and Hiscott, R.N. (1986) Deep-Water Facies, Processes and Models: A Review and Classification Scheme for Modern and Ancient Sediments. *Earth Science Review*. Vol. 23, pp. 75-174

Pickering, K.T., Hiscott, R.N. and Hein, F.J. (1989) *Deep Marine Environments: Clastic sedimentation and tectonics*. Unwin Hyman, London. pp. 416

Posamentier, H.W., Jervey, M.T. and Vail, P.R. (1988) Eustatic controls on clastic deposition. I. Conceptual framework. In: Wilgus, C.K., Hastings, B.S., Kendall, C.G.St.C., Posamentier, H.W., Ross, CA. and Van Wagoner, J.C. (Eds.) *Sea Level Changes – An intergrated Approach*, *SEPM Special Publication*. Vol. 42, pp. 110-124

Posamentier, H.W., Erskine, R.D. and Mitchum, R.M. (1991) Models for submarine fan deposition within a sequence stratigraphic framework. In: Weimer, P. and Link, M.H (Ed.) *Seismic Facies and Sedimentary Processes of Modern and Ancient Submarine Fans and Turbidite Systems*. Springer-Verlag. New York. pp. 127-136

Posamentier, H.W. and Vail, P.R. (1988) Eustatic controls on clastic deposition. II. Conceptual framework. In: Wilgus, C.K., Hastings, B.S., Kendall, C.G.St.C., Posamentier, H.W., Ross, CA. and Van Wagoner, J.C. (Eds.) *Sea Level Changes – An integrated Approach*, *SEPM Special Publication*,. Vol. 42, pp. 125-154

Posamentier, H.W. and Kolla, V. (2003) Seismic geomorphology and stratigraphy of depositional elements in deep-water settings. *Journal of Sedimentary Research*. Vol. 73, pp. 367-388

Posamentier, H.W. (2003) Depositional elements associated with a basin floor channel-levee system: case study from the Gulf of Mexico. *Marine and Petroleum Geology*. Vol. 20, pp. 677-690

Potter, P.E. and Pettijohn, F.J. (1977) *Paleocurrents and Basin analysis*, 2nd ed.: Springer-Verlag, New York. pp. 460

Prather, B.E. (2003) Controls on reservoir distribution, architecture and stratigraphic trapping in slope settings. *Marine and Petroleum Geology*. **Vol. 20**, pp. 529-545

Raiswell, R. (1987) Non-steady state microbiological diagenesis and the origin of concretions and nodular limestones. In: Marshall, J.D. *Diagenesis of Sedimentary Sequences*. *Geology Society of London Special Publication*. **Vol. 36**, pp. 41-54

Reading, H.G. and Richards, M. (1994) Turbidite systems in deep-water basin margins classified by grain size and feeder system. *AAPG Bulletin*. **Vol. 78**, pp. 792-822

Remacha, E. and Fernández, L.P. (2003) High-resolution correlation patterns in the turbidite system of the Hecho Group (South-Central Pyrenees, Spain). *Marine and Petroleum Geology*. **Vol. 20**, pp. 711-726

Remacha, E., Fernández, L.P., Maestro, E., Oms, O., Estrada, R. and Teixell, A. (1998) Excursion A1. *The Upper Hecho Group turbidites and their vertical evolution to deltas (Eocene, South-central Pyrenees)*. IAS 15th International Sedimentological Congress, Alicante, Spain, Field Trip Guidebook. pp. 1-25

Rubidge, B.S. (1991) A new primitive dinocephalian mammal-like reptile from the Permian of Southern Africa. *Palaeontology*. **Vol. 34**, pp. 547-559

Saito, T. and Ito, M. (2002) Deposition of sheet-like turbidite packets and migration of channel-overbank systems on a sandy submarine fan: an example from the late Miocene – early Pliocene fore arc basin, Boso Peninsula, Japan. *Sedimentary Geology*. **Vol. 149**, pp. 265-277

Scott, E.D., Bouma A.H., and Wickens, H. de V. (2000) Influence of Tectonics on Submarine Fan Deposition, Tanqua and Laingsburg Sub basins, South Africa, in A.H.

Bouma and C. G. Stone, Eds., Fine-grained turbidite systems, *AAPG Memoir 72/SEPM Special Publication*. Vol. 68, pp. 47-56

Scott, E.D. (1997) *Tectonics and sedimentation: evolution, tectonic influences and correlation of the Tanqua and Laingsburg sub-basins, southwest Karoo Basin, South Africa*. Unpublished Ph.D. thesis, Louisiana State University. pp. 234

Shanmugam, G. and Moiola, R.J. (1988) Submarine Fans: Characteristics, Models, Classification, and Reservoir Potential. *Earth-Science Reviews*. Vol. 24, pp. 383-428

Simons, D.B. Richardson, E.V. and Nordin, C.F. (1965) Sedimentary structures generated by flow in alluvial channels. In: Middleton, G.V. (Ed.) *Primary Sedimentary Structures and Their Hydrodynamic Interpretation*. *SEMP Special Publication*. Vol. 12, pp. 34-52

Sixsmith, P.J. (2000) *Stratigraphic Development of a Permian Turbidite System on a Deforming Basin Floor: Laingsburg Formation, Karoo Basin, South Africa*. unpubl. Ph.D. thesis. University of Liverpool. pp. 229

Sixsmith, P.J., Flint, S.S., Johnson, S.D. and Wickens, H. de V. (1998) Anatomy of an elongated, Permian turbidite fan complex, an example from the Karoo Basin of South Africa. *Extended Abstracts Volume, 1998 AAPG International Conference and Exhibition, Rio de Janeiro, 1998* pp.760

Sixsmith, P.J., Flint, S.S., Wickens, H. de V. and Johnson, S.D. (2004) Anatomy and stratigraphic development of a Basin floor turbidite system in the Laingsburg Formation, Main Karoo Basin, South Africa. *Journal of Sedimentary Research*. Vol. 74 (2), pp. 239 - 254

Skipper, K. (1971) Antidune cross-stratification in turbidite sequence, Cloridorme Formation, Gaspe, Quebec. *Sedimentology*. Vol. 17, pp. 51-68

Skipper, K. and Bhattacharjee, S.B. (1978) Backset bedding in turbidites: a further example from the Cloridorme Formation (Middle Ordovician), Gaspé, Quebec. *Journal of Sedimentary Petrology*. **Vol. 48**, pp. 193-202

Suppe, J. (1985) *Principles of structural geology*. Prentice-Hall, Englewood Cliffs, New Jersey. pp. 537

Surlyk, E. (1987) Slope and deep shelf gully Sandstones, Upper Jurassic, East Greenland. *AAPG Bulletin*. **Vol. 71** (4), pp. 464-475

Teller, J.T. (1990) Volume and routing of late-glacial runoff from the southern Laurentide Ice Sheet: *Quaternary Research*. **Vol. 34**, pp. 12-23

Theron, J.C. (1973) Sedimentological evidence for the extension of the African continent southwards during the Late Permian-Early Triassic times. Proc. Pap., 3rd *Gondwana Symposium*., Canberra, Australia. pp. 61-71.

Truswell, J.F. (1970) *An introduction to the Historical Geology of South Africa*. Purnell & sons. Cape Town. pp. 167

Turner, B.R. (1999) Tectonostratigraphical development of the Upper Karoo foreland basin: orogenic unloading versus thermally-induced Gondwana rifting. *Journal of African Earth Sciences*. **Vol. 28**(1), pp. 215-238

Vail, P.R. (1975) Eustatic cycles from seismic data for global stratigraphic analysis (abstract) *AAPG Bulletin*. **Vol. 59**, pp. 2198-2199

Vail, P.R., Mitchum Jr. R.M., Thompson III, S. (1977) Seismic stratigraphy and global changes of sea level. Part 3: relative changes of sea level from coastal onlap. In: Payton, C.E. (Ed.) *Seismic Stratigraphy – Applications to Hydrocarbon Exploration*. *AAPG Memoir*. **Vol. 26**, pp. 63-81

Vail, P.R., Hardenbol, J. and Todd, R.G. (1984) Jurassic unconformities, chronostratigraphy and sea-level changes from seismic stratigraphy and biostratigraphy. In: Schlee, J.S. (Ed.) *Interregional Unconformities and Hydrocarbon Accumulation. AAPG Memoir. Vol. 36*, pp. 129-144

Van Antwerpen, O. (1992) *Ongeluks River channel-fills, Skoorsteenberg Formation*. Unpubl. Honours thesis. Univ. Port Elizabeth. pp. 69

Van der Merwe, W.C. (2003) *Facies architecture and variation of the Hangklip Fan in the Bizansgat and Klein Hangklip area, Tanqua Sub-basin, South Africa*. Unpubl. Honours thesis. Univ. of Stellenbosch. pp. 119

Van der Merwe, W.C. and Wickens, H. de V. (2004) From fan axis to fan margin: Example from a slope setting, South-Western Karoo Basin, South Africa. Abstract-poster. Regional West-Africa Deepwater Conference and Exhibition. Nigeria. *AAPG*. pp. A47-A48

Van Lente, B. (2004) *Chemostratigraphic trends and provenance of the Permian Tanqua and Laingsburg depocentres, southwestern Karoo basin, South Africa*. Unpubl. Ph.D. thesis, University of Stellenbosch. pp. 339

Van Wagoner, J.C. (1995) Overview of sequence stratigraphy of foreland basin deposits: terminology, summary of papers, and glossary of sequence stratigraphy. In: Van Wagoner, J.C. and Bertram, G.T. (Eds.) *Sequence Stratigraphy of Foreland Basin Deposits. AAPG Memoir. Vol. 64*, pp. ix-xxi

Van Wagoner, J.C., Posamentier, H.W., Mitchum, R.M., Vail, P.R., Sarg, J.F., Loutit, T.S. and Hardenbol, J. (1988) An overview of sequence stratigraphy and key definitions. In: Wilgus, C.K., Hastings, B.S., Kendall, C.G.St., Posamentier, H.W., Ross, C.A. and Van Wagoner, J.C. (Eds.) *Sea level changes – An integrated approach. SEMP Special Publication. Vol. 42*, pp. 39-45

Van Wagoner, J.C., Mitchum, Jr.R.M., Campion, K.M. and Rahmanian, V.D. (1990) Siliciclastic sequence stratigraphy in well logs, core, and outcrops: concepts for high-resolution correlation of time and facies. *AAPG Methods in Exploration Series*. Vol. 7, pp. 55

Veevers, J.J., Cole, D.I. and Cowan, E.J. (1994) Southern Africa: Karoo Basin and Cape Fold Belt. In: Veevers, J.J. and Powell, C. McA. (Eds.) Permian-Triassic Pangean Basins and Fold belts along the Panthalassan Margin of Gondwanaland. *Geology Society of America Memoir*. Vol. 184, pp. 223-279.

Visser, J.N.J. (1990) The age of the late Palaeozoic glaciogene deposits in southern Africa. *South African Journal of Geology*. Vol. 93, pp. 366-375

Visser, J.N.J. (1992) Basin tectonics in southwestern Gondwana during the Carboniferous and Permian. In: De Wit, M.J. and Ransome, I.G.D. (Eds.), *Inversion Tectonics of the Cape Fold Belt, Karoo and Cretaceous Basins of Southern Africa*. A.A. Balkema, Rotterdam. pp. 109-115

Visser, J.N.J. (1993) Sea-level changes in a back-arc-foreland transition: the late Carboniferous-Permian Karoo Basin of South Africa. *Sedimentary Geology*. Vol. 83, pp. 115-131

Visser, J.N.J. (1997) Deglaciation sequences in the Permo-Carboniferous Karoo and Kalahari basins of southern Africa: a tool in the analysis of cyclic glaciomarine basin fills. *Sedimentology*. Vol. 44, pp. 507-521

Visser, J.N.J., Looock, J.C. (1978) Water depth in the main Karoo Basin, South Africa, during Ecca (Permian) sedimentation. *Transactions Geology Society of South Africa*. Vol.81, pp. 185-191

Visser, J.N.J., Looock, J.C. and Jordaan, M.J. (1980) Permian deltaic sedimentation in the western half of the Karoo Basin, South Africa. *Transactions Geology Society of South Africa*. Vol. 83, pp. 415-424.

Wach, G.D., Lucas, T.C., Goldhammer, R.K., Wickens, H. de V., and Bouma, A.H. (2000) Submarine fan through slope to deltaic transition basin-fill succession, Tanqua Karoo, South Africa. In: Bouma, A.H. and Stone, C.G. (Eds.). *Fine-grained Turbidite Systems. AAPG Memoir 72/SEPM Special Publication. Vol. 68*, pp. 173-180

Walker, R.G. (1978) Deep-water sandstones facies and ancient submarine fans: models for exploration for stratigraphic traps. *AAPG Bulletin. Vol. 62*, pp. 932-966

Weimer, P. (1990) Sequence stratigraphy, facies geometries and depositional history of the Mississippi Fan, Gulf of Mexico. *AAPG Bulletin. Vol. 74*, pp. 425-453

Weimer, P., Varnai, P., Acosta, Z.M., Budhijanto, F.M., Martinez, R.E., Navarro, A.F., Rowan, M.G., McBride, B.C., and Villamil, T. (1994) Sequence Stratigraphy of Neogene Turbidite Systems, Northern Green Canyon and Ewing Bank, northern Gulf of Mexico. In: Weimer, P., Bouma, A.H. and Perkins, B.F. (Ed.) *Submarine Fans and Turbidite Systems*. GCSSEPM Foundation 15th Annual Research Conference. pp. 383-399

Weimer, P., Varnai, P., Budhijanto, F.M., Acosta, Z.M., Martinez, R.E., Navarro, A.F., Rowan, M.G., McBride, B.C., Villamil, T., Arango, C., Crews, J.R. and Pulham, A.J. (1998) Sequence Stratigraphy of Pliocene and Pleistocene Turbidite Systems, Northern Green Canyon and Ewing Bank (Offshore Louisiana), Northern Gulf of Mexico. *AAPG Bull. Vol. 82 (5b)*, pp.918-960

Wickens, H. de V. (1984) *Die stratigrafie en sedimentologie van die Groep Ecca wes van Sutherland*. M.Sc. thesis (unpubl.), Univ. Port Elizabeth. pp. 84

Wickens, H. de V. (1992) Submarine fans of the Permian Ecca group in the SW Karoo Basin: Their origin and reflection on the tectonic evolution of the basin and its source areas; De Wit, M.J & Ransomem, I.G.D (Eds.) *Inversion tectonics of the Cape Fold Belt, Karoo and Cretaceous Basins of Southern Africa*. A.A. Balkena, Rotterdam. pp. 117-125

Wickens, H. de V. (1994) *Basin Floor Fan building Turbidites of the South-western Karoo Basin, Permian Ecca Group, South Africa*. Unpub. Ph.D. thesis, Univ. Port Elizabeth. pp. 233

Wickens, H. de V. (2001) Turbidites of the southwestern Karoo Basin: Facies architecture, heterogeneity distribution and Reservoir applications. *DONG-Field excursion Guidebook*. pp. 78

Wickens, H. de V. and Bouma, A.H. (1998) *The Tanqua Karoo Turbidites: facies architecture, heterogeneity, distribution and reservoir applications*, Unpub. Field excursion guidebook, Tanqua Consortium, Louisiana State University. pp. 73

Wickens, H. de V. and Bouma, A.H. (2000) The Tanqua Fan Complex, Karoo Basin, South Africa - Outcrop Analog for Fine-Grained, Deepwater Deposits In: Bouma, A.H and Stone, C.G. (Eds.). Fine-grained Turbidite Systems. *AAPG Memoir 72/SEPM Special Publication*. Vol. 68, pp. 173-180

Wickens, H. de V., Brink, G.J., Basson, W.A. and Van Rooyen, W. (1990) *The sedimentology of the Skoorsteenberg Formation and its applicability as a model for submarine fan turbidite deposits in the Bredarsdorp Basin*. Unpub. Report, Soekor, Parow, South Africa. pp. 47

Wickens, H. de V., Brink, G.J. and van Rooyen, W. (1990) *The sedimentology of the Skoorsteenberg Formation and its applicability as a model for submarine fan turbidite deposits in the Bredasdorp Basin*. Unpubl. Rep. Soekor, Parow. pp. 47

Wickens, H. de V., Brink, G.J., Van Rooyen, W., Bouma, A.H. and Brown, L.F. Jr. (1992) The Tanqua Turbidite and Deltaic Complexes: Depositional Models, Reservoir Realities and the Application of Sequence Stratigraphy. *AAPG Field Seminar Guidebook*, SOEKOR, Parow. pp. 180

Wild, R., King, R., Van Lente, B., Flint, S., Hodgson, D., Potts, G. and Wickens, H de V. (2004) *Slope Project: First year report and field guide. Strat Group.* University of Liverpool and University of Stellenbosch. Part A. pp. 65

Wild, R.J., Hodgson, D.M. and Flint, S.S. (2005) Architecture and stratigraphic evolution of multiple, vertically-stacked slope channel complexes, Tanqua depocenter, Karoo Basin, South Africa, *in: Hodgson, D.M. and Flint, S.S., Eds., Submarine Slope Systems, Processes and Products: Geological Society, London, Special Publications. Vol. 244*, pp. 89-112

Winters, S., Grobber, N. and Wickens, H de V. (1995) Architectural geometries of Fan 5 in the Skoorsteenbergrivier area, Tanqua Sub-basin, Permian Ecca Group, South Africa. Fieldwork Report for Phase 2. *GeoMarine Consultants, Inc.* pp. 7-1 – 7-14

Woodcock, N.H. (1979) The use of slump structures as palaeoslope orientation estimators. *Sedimentology. Vol. 26*, pp. 83-99

Appendix

Appendix

List of GPS positions for the measured vertical sections, which are presented in this thesis.

M1	S 32° 52.750 ¹ E 019° 58.316 ¹	M14	S 32° 40.662 ¹ E 020° 04.178 ¹
M2	S 32° 52.803 ¹ E 019° 58.419 ¹	M15	S 32° 40.873 ¹ E 020° 04.352 ¹
M3	S 32° 52.779 ¹ E 019° 58.753 ¹	M16	S 32° 40.891 ¹ E 020° 04.604 ¹
M4	S 32° 52.874 ¹ E 019° 59.441 ¹	M17	S 32° 41.095 ¹ E 020° 04.739 ¹
M5	S 32° 52.159 ¹ E 020° 03.635 ¹	M18	S 32° 40.875 ¹ E 020° 03.528 ¹
M6	S 32° 52.410 ¹ E 020° 04.101 ¹	M19	S 32° 40.393 ¹ E 020° 03.848 ¹
M7	S 32° 46.831 ¹ E 019° 59.572 ¹	M20	S 32° 40.025 ¹ E 020° 04.474 ¹
M8	S 32° 46.002 ¹ E 020° 00.947 ¹	M21	S 32° 39.626 ¹ E 020° 04.914 ¹
M9	S 32° 45.074 ¹ E 020° 01.240 ¹	M22	S 32° 39.196 ¹ E 020° 05.151 ¹
M10	S 32° 44.690 ¹ E 020° 01.832 ¹	M23	S 32° 38.719 ¹ E 020° 05.440 ¹
M11	S 32° 43.076 ¹ E 020° 02.841 ¹	M24	S 32° 36.835 ¹ E 020° 05.444 ¹
M12	S 32° 42.540 ¹ E 020° 03.925 ¹	M25	S 32° 38.444 ¹ E 020° 05.435 ¹
M13	S 32° 41.844 ¹ E 020° 04.380 ¹	M26	S 32° 38.428 ¹ E 020° 05.937 ¹

M27	S 32° 38.206 ¹ E 020° 05.977 ¹	M43	S 32° 33.190 ¹ E 020° 04.708 ¹
M28	S 32° 38.340 ¹ E 020° 05.681 ¹	M44	S 32° 32.904 ¹ E 020° 04.835 ¹
M29	S 32° 38.162 ¹ E 020° 05.458 ¹	M45	S 32° 32.824 ¹ E 020° 05.070 ¹
M30	S 32° 37.546 ¹ E 020° 05.898 ¹	M46	S 32° 36.617 ¹ E 020° 05.055 ¹
M31	S 32° 36.942 ¹ E 020° 05.342 ¹	M47	S 32° 40.772 ¹ E 020° 05.769 ¹
M32	S 32° 36.857 ¹ E 020° 05.258 ¹	M48	S 32° 32.405 ¹ E 020° 05.564 ¹
M33	S 32° 36.851 ¹ E 020° 05.067 ¹	M49	S 32° 31.763 ¹ E 020° 05.447 ¹
M35	S 32° 37.066 ¹ E 020° 04.789 ¹	M50	S 32° 30.752 ¹ E 020° 05.205 ¹
M36	S 32° 37.053 ¹ E 020° 04.366 ¹	M51	S 32° 29.452 ¹ E 020° 04.919 ¹
M37	S 32° 35.198 ¹ E 020° 03.807 ¹	M52	S 32° 28.740 ¹ E 020° 04.851 ¹
M38	S 32° 35.034 ¹ E 020° 04.287 ¹	M53	S 32° 28.332 ¹ E 020° 05.099 ¹
M39	S 32° 34.404 ¹ E 020° 04.655 ¹	M54	S 32° 27.914 ¹ E 020° 05.595 ¹
M40	S 32° 33.734 ¹ E 020° 05.005 ¹	M55	S 32° 27.345 ¹ E 020° 07.072 ¹
M41	S 32° 33.635 ¹ E 020° 04.897 ¹	M56	S 32° 27.617 ¹ E 020° 06.277 ¹
M42	S 32° 33.272 ¹ E 020° 04.902 ¹	M57	S 32° 27.379 ¹ E 020° 06.489 ¹

M58	S 32° 27.946 ¹ E 020° 07.618 ¹	M74	S 32° 29.046 ¹ E 020° 14.835 ¹
M59	S 32° 28.608 ¹ E 020° 07.870 ¹	M75	S 32° 27.666 ¹ E 020° 15.196 ¹
M60	S 32° 28.517 ¹ E 020° 07.478 ¹	M76	S 32° 25.614 ¹ E 020° 17.380 ¹
M61	S 32° 29.888 ¹ E 020° 07.927 ¹	M77	S 32° 35.281 ¹ E 020° 03.510 ¹
M62	S 32° 30.315 ¹ E 020° 07.856 ¹	M78	S 32° 35.281 ¹ E 020° 03.510 ¹
M63	S 32° 30.163 ¹ E 020° 09.140 ¹	M79	S 32° 35.005 ¹ E 020° 02.578 ¹
M64	S 32° 29.384 ¹ E 020° 10.989 ¹	M80	S 32° 34.891 ¹ E 020° 02.475 ¹
M65	S 32° 29.656 ¹ E 020° 11.793 ¹	M81	S 32° 34.839 ¹ E 020° 02.179 ¹
M66	S 32° 30.082 ¹ E 020° 13.987 ¹	M82	S 32° 34.817 ¹ E 020° 01.975 ¹
M67	S 32° 29.987 ¹ E 020° 12.018 ¹	M83	S 32° 34.985 ¹ E 020° 01.462 ¹
M69	S 32° 29.833 ¹ E 020° 13.058 ¹	M84	S 32° 34.818 ¹ E 020° 00.817 ¹
M70	S 32° 29.789 ¹ E 020° 13.365 ¹	M86	S 32° 34.566 ¹ E 020° 01.697 ¹
M71	S 32° 30.044 ¹ E 020° 14.514 ¹	M91	S 32° 34.886 ¹ E 019° 59.898 ¹
M72	S 32° 28.926 ¹ E 020° 15.893 ¹	M92	S 32° 34.989 ¹ E 019° 59.517 ¹
M73	S 32° 29.018 ¹ E 020° 15.125 ¹	M93	S 32° 35.176 ¹ E 019° 59.120 ¹

M94	S 32° 35.332 ¹ E 020° 00.853 ¹	M109	S 32° 36.599 ¹ E 019° 59.837 ¹
M95	S 32° 35.547 ¹ E 020° 00.830 ¹	M110	S 32° 37.773 ¹ E 020° 01.146 ¹
M96	S 32° 35.629 ¹ E 020° 00.479 ¹	M111	S 32° 37.310 ¹ E 020° 00.779 ¹
M97	S 32° 35.907 ¹ E 020° 00.473 ¹	M112	S 32° 36.852 ¹ E 020° 00.462 ¹
M98	S 32° 35.839 ¹ E 020° 01.051 ¹	M113	S 32° 36.403 ¹ E 020° 00.331 ¹
M99	S 32° 36.237 ¹ E 020° 01.281 ¹	M114	S 32° 37.231 ¹ E 020° 00.675 ¹
M100	S 32° 36.390 ¹ E 020° 01.008 ¹	M115	S 32° 38.494 ¹ E 020° 00.893 ¹
M101	S 32° 36.771 ¹ E 020° 01.258 ¹	M116	S 32° 39.000 ¹ E 020° 00.799 ¹
M102	S 32° 37.186 ¹ E 020° 01.327 ¹	M117	S 32° 39.036 ¹ E 020° 00.890 ¹
M103	S 32° 35.344 ¹ E 019° 58.804 ¹	M118	S 32° 38.918 ¹ E 020° 01.127 ¹
M104	S 32° 35.586 ¹ E 019° 59.176 ¹	M119	S 32° 38.494 ¹ E 020° 01.166 ¹
M105	S 32° 36.397 ¹ E 019° 59.000 ¹	M120	S 32° 52.975 ¹ E 020° 04.856 ¹
M106	S 32° 36.650 ¹ E 019° 58.748 ¹	M121	S 32° 52.999 ¹ E 020° 04.773 ¹
M107	S 32° 36.879 ¹ E 019° 58.701 ¹	M122	S 32° 53.066 ¹ E 020° 04.250 ¹
M108	S 32° 36.856 ¹ E 019° 59.154 ¹	M123	S 32° 53.177 ¹ E 020° 03.878 ¹

M124	S 32° 53.414 ¹ E 020° 02.931 ¹	M139	S 32° 56.484 ¹ E 020° 03.976 ¹
M125	S 32° 53.536 ¹ E 020° 02.405 ¹	M140	S 32° 57.122 ¹ E 020° 04.151 ¹
M126	S 32° 53.559 ¹ E 020° 01.989 ¹	M141	S 32° 57.104 ¹ E 020° 04.301 ¹
M127	S 32° 53.583 ¹ E 020° 01.536 ¹	M142	S 32° 37.211 ¹ E 020° 04.757 ¹
M128	S 32° 53.690 ¹ E 020° 01.074 ¹	M143	S 32° 57.164 ¹ E 020° 05.224 ¹
M129	S 32° 53.815 ¹ E 020° 00.791 ¹	M144	S 32° 55.016 ¹ E 020° 03.475 ¹
M130	S 32° 54.017 ¹ E 020° 00.699 ¹	M145	S 32° 55.149 ¹ E 020° 03.873 ¹
M131	S 32° 53.915 ¹ E 020° 00.978 ¹		
M132	S 32° 53.786 ¹ E 020° 01.106 ¹		
M133	S 32° 53.750 ¹ E 020° 01.572 ¹		
M134	S 32° 54.534 ¹ E 020° 01.771 ¹		
M135	S 32° 56.516 ¹ E 020° 01.094 ¹		
M136	S 32° 56.150 ¹ E 020° 01.8198 ¹		
M137	S 32° 56.261 ¹ E 020° 01.575 ¹		
M138	S 32° 55.981 ¹ E 020° 01.906 ¹		